MECHANISTIC STUDIES ON EFFERVESCENT-INDUCED PERMEABILITY ENHANCEMENT

by

Jonathan D. Eichman

A dissertation submitted in partial fulfillment
of the requirements for the degree of

Doctor of Philosophy
(Pharmacy)

at the

UNIVERSITY OF WISCONSIN-MADISON

1997

AW
EE3

To my parents for all their
love and support

ACKNOWLEDGMENTS

I would like to thank my parents for all their encouragement, support, and unconditional love. I would have never been able to obtain by doctorate degree if they had not believed in my abilities as a person. I know they have waited a long time for this moment, and am happy that I could fulfill their deepest wishes.

I would also like to acknowledge the most important person in my life, Kelly Frye. Meeting her approximately five years ago and has changed my life forever (for the best, of course!!). Her intelligence, motivation, and determination inspired me and without it, I probably would still be thinking of starting my first experiment.

My labmates during my graduate career have also been a great help with theoretical discussions on my data or just going to the Union terrace to relax and enjoy the atmosphere instead of being frustrated over bad results.

I also appreciate the work done by Albert Ntambi and Annisa Johnson, who were two undergraduate students who performed some of the in-vitro permeability studies.

Last but certainly not least, I would like to like to thank Dr. Joseph R. Robinson for his mentorship over the last twelve years of my life. I first met Dr. Robinson when I visited Madison as a potential undergraduate. Ever since then, he has had confidence and has supported me even during times when everybody else had given up hope for me. His enthusiasm and scientific excellence has propelled me to levels I thought I would never achieve. I can never overstate may deepest appreciation for all he has taught me as a scientist and a person.

Mechanistic Studies on Effervescent Induced Permeability Enhancement

Jonathan D. Eichman
Under the supervision of Professor Joseph R. Robinson
At the University of Wisconsin-Madison

Recently, interest in applying effervescent technology to advanced drug delivery systems has emerged due to a greater understanding of its biological effects. Studies have revealed that effervescence can: (1) create a "pseudo-fed" state in the stomach; (2) thin or strip the mucus layer lining the stomach and intestine; and (3) enhance intestinal drug absorption. The latter point has never been closely studied and is usually assumed to be attributed to a pH buffering effect and/or increased dissolution rates imparted by carbon dioxide (CO_2) evolution. In order to optimize drug permeability across intestinal epithelium, it is necessary to have a detailed understanding as to the effervescent penetration enhancement mechanism(s).

Results indicated that effervescence induced penetration enhancement for a variety of drug compounds across rat and rabbit intestinal tissue. Absorption enhancement was greatest for hydrophilic drugs (e.g. mannitol, tetracycline) with decreased effects for compounds with a greater hydrophobicity (e.g. diazepam). In addition, enhancement also declined with reduction in the CO_2 bubbling rate. Nitrogen bubbling induced equivalent permeability enhancement when compared to CO_2. This indicated that the enhancement mechanism is not unique

to the chemical entity CO_2, but to epithelial disruption as verified by reduced transepithelial electrical resistance (TEER) values. Epithelial cell enzyme (5'-ND and LDH) and protein release assays failed to show membrane perturbation or damage while the MTT cell viability assay indicated that CO_2 did not induce cell toxicity. Therefore, it is concluded that the reduction in TEER is associated with an opening of the paracellular pathway. Tissue recovery was relatively rapid (20 min.) after CO_2 exposure. Other potential enhancement mechanism(s) may also include theories on increased fluid flow (i.e. solvent drag) and membrane hydrophobicity.

Table of Contents

Chapter 1: INTRODUCTION

I. Anatomical Properties of the Gastrointestinal Tract

The alimentary canal begins at the oral cavity and sequentially proceeds to the pharynx, esophagus, stomach, small intestine and large intestine. The main focus of this review will examine the gastrointestinal tract in detail, analyzing the segments of interest for oral effervescent drug delivery, namely the stomach and intestines.

The stomach is an enlarged J-shaped sac situated between the esophagus and small intestine. It functions as a storage site for consumed food while it chemically and physically breaks down the food for absorption in the small intestine. The stomach is the most distensible portion of the gastrointestinal tract in which its shape, position, and size vary depending upon the quantity of food and/or liquid contained within the organ. The average adult stomach can hold between 1.0 and 1.5 liters of food or liquid (Carola, 1992). When empty, the stomach interior contains large longitudinal folds called rugae, which gradually flatten as the stomach fills, thus providing a greater holding capacity (Marieb, 1997). Ingested food enters the stomach from the esophagus through the cardiac orifice and leaves via the pyloric opening into the uppermost region of the small intestine, the duodenum (Bannister, 1995). The diameter of the pyloric aperture is regulated by contractions of a ring of smooth muscle called the pyloric sphincter.

As food passes through the sphincter into the intestine, the sphincter closes, preventing reflux of food particles into the stomach.

The stomach (Figure 1.1) is divided into four main regions: the cardia, fundus, body, and pylorus. The cardia is a ring-shaped portion of the stomach surrounding the cardiac orifice. The proximal portion of the stomach is referred to as the fundus region, which has a characteristic dome-shaped appearance, located above the gastroesophageal junction, and is typically in direct contact with the diaphragm (Van de Graaff, 1995). The fundus functions as a food reservoir and secretes a large capacity of the stomach mucus. The body is the largest region of the stomach and is centrally located. As it curves to the right, it forms the side of greater curvature to its left and lesser curvature to its right. The body leads into the final region of the stomach, the pylorus, which has a characteristic funnel shape narrowing as it leads towards the pyloric sphincter.

The gastric wall (Figure 1.2) consists of four major layers commonly found throughout the gastrointestinal tract: the mucosa, submucosa, muscularis externa, and serosa.

The mucosa is folded into rugae, which tend to be more numerous towards the pyloric region and near the area of greater curvature (Bannister, 1995). The mucosa (Figure 1.3) can be further segmented into three separate layers: the epithelium, lamina propria, and muscularis mucosae.

The stomach epithelium consists of millions of 0.2 mm diameter "slit-like" depressions called gastric pits, which open into tubular gastric glands (Bannister, 1995). A single layer of mucus-secreting columnar epithelial goblet cells line the surface of the stomach and gastric pits, providing a protective and lubricating layer to the gastric wall (Marieb, 1997).

There are three types of gastric glands differentiated by their location within the

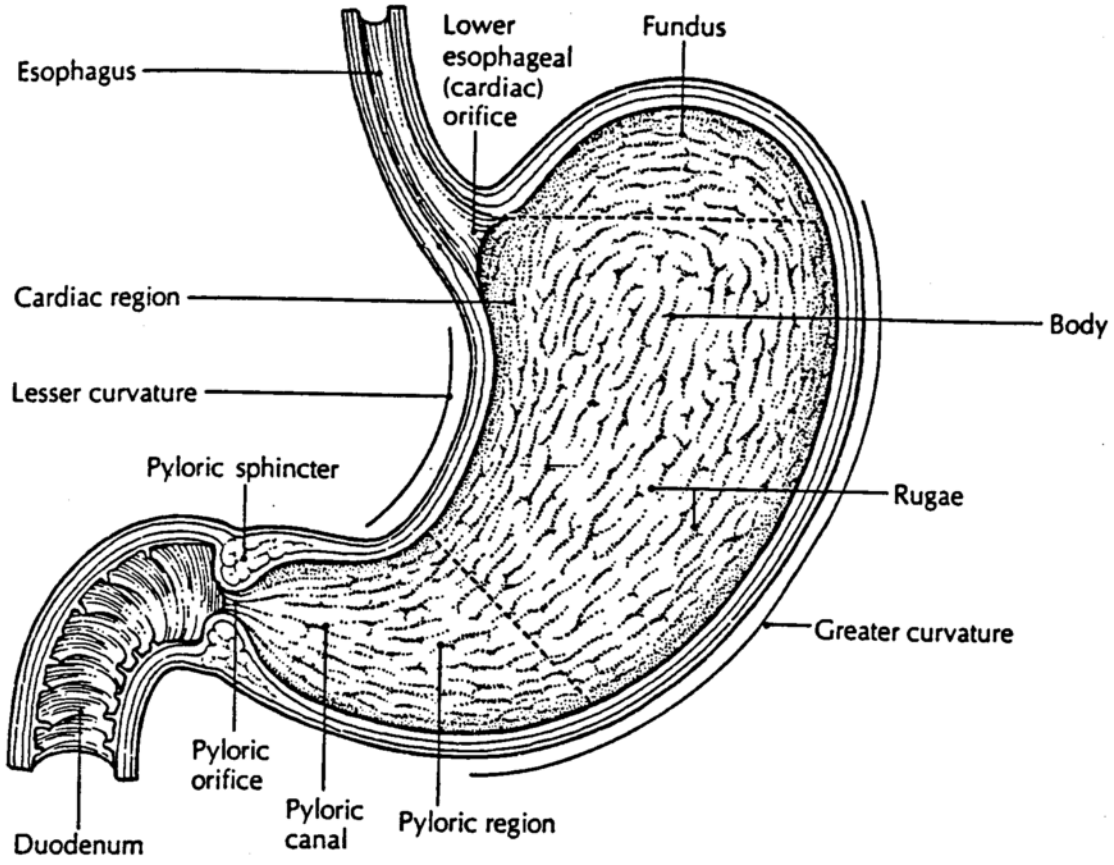

Figure 1.1: Longitudinal section of the stomach showing the four major regions of the stomach and the sphinctors. (Reproduced from Carola, R., et. al., 1992).

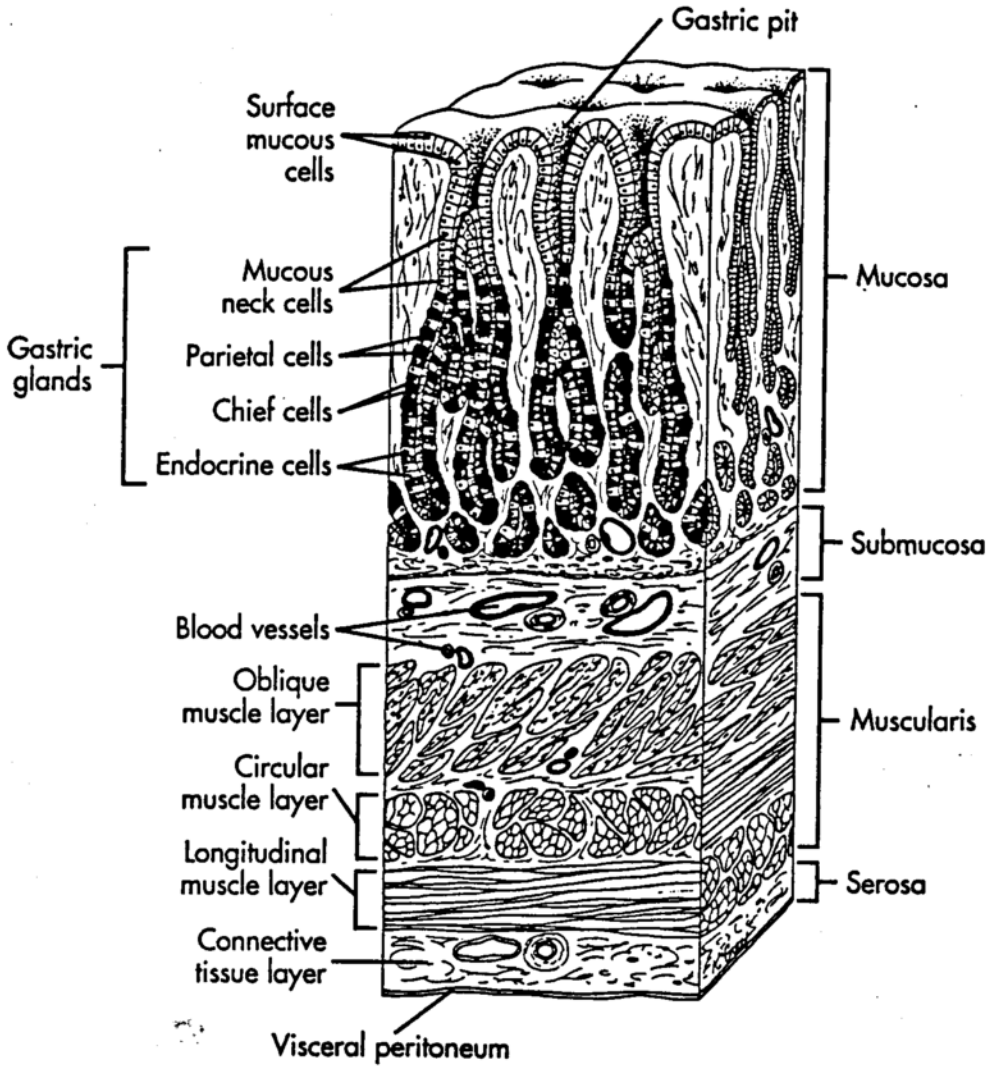

Figure 1.2: A sectional view of the stomach wall illustrating the four major layers: the mucosa, submucosa, muscularis externa, and serosa. (Modified from Seeley, R.R. et. al., 1996).

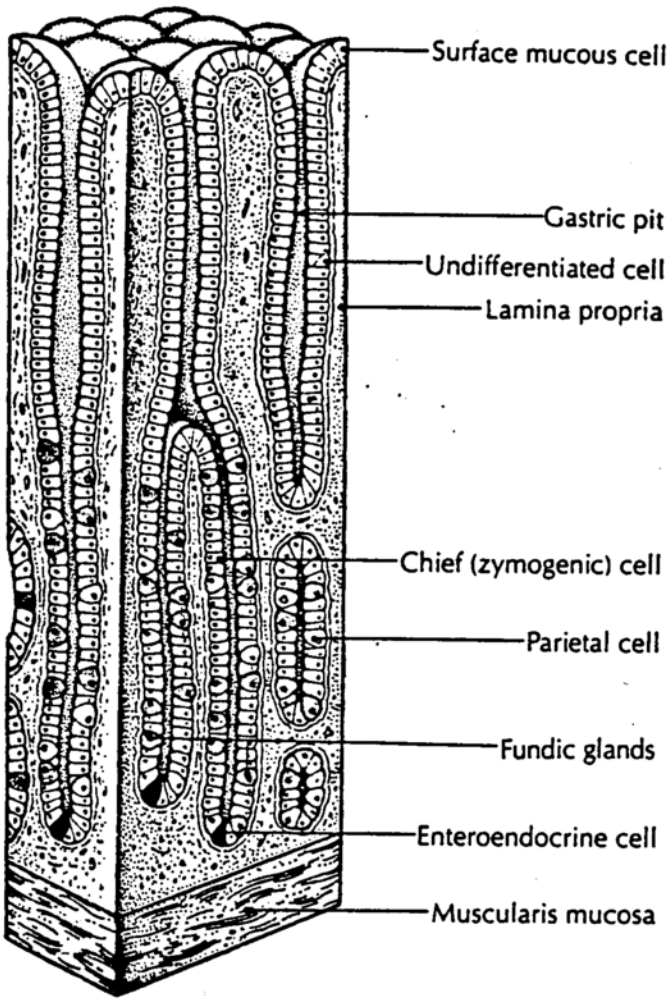

Figure 1.3: Magnification of the stomach mucosa illustrating three separate layers: the epithelium, lamina propria, and muscularis mucosae. (Modified from Carola, R. et. al., 1992).

stomach and also by the population of specialized cells within the glands. The principal glands are the most abundant and are found within the fundus and body regions. The stomach contains several types of secreting cells: (1) chief (zymogenic) cells, which secrete pepsinogen and renin; (2) parietal cells, which produce hydrochloric acid and intrinsic factor; (3) goblet cells; (4) stem cells; and (5) enteroendocrine cells, which secrete gastrin and somatostatin (Marieb, 1997).

Cardiac glands are localized near the cardiac orifice and contain mostly goblet and chief cells. Pyloric glands are heavily populated within the pylorus and contain a high number of goblet and enteroendocrine cells (Bannister, 1995).

The lamina propria is the next region of the mucosa and is situated distal to the epithelium and between gastric glands. It contains a layer of connective tissue in association with immunological lymphoid tissue. The third and final layer of the mucosa, the muscularis mucosae, is a thin layer of smooth muscle.

The second major layer of the gastric wall , the submucosa, consists of loose connective tissue functioning as an attachment zone for the upper mucosa and lower muscular layers.

The muscularis externa consists of three muscle layers: (1) longitudinal, (2) circular, and (3) oblique (Frick, 1991). These three layers intertwine, forming a crisscross pattern which allows the stomach wall to strongly contract in numerous angles and directions. The musculature within the upper regions of the stomach wall provide a constant tonic contractile state while the stomach contains food. The lower musculature provides a mixing motion via peristaltic waves when the pressure receptor within the stomach is activated by food or large volumes of liquid (Bannister, 1995). The peristaltic waves provide a mechanism in which the stomach is able to grind and disintegrate large food particles to smaller more digestible ones. As each wave moves from the body to the pyloric orifice, the

pyloric sphincter contracts so as to let very small particles of food pass through the aperture and into the upper portion of the small intestine. Larger particles are thrown back into the body for further reduction.

The serosal layer consists of peritoneum covering the entire stomach surface except for a small area along the greater and lesser curvatures. The exposed area allows nutrient vessels and nerves to pass to the stomach (Lindner, 1989).

The intestines can be divided into two anatomical divisions, the small intestine and large intestine. The small intestine can be further broken down into three segments: the duodenum, jejunum, and ileum. The shortest and widest of these segments, the duodenum, begins at the pylorus and connects to the jejunum at the ligament of Treitz (Rubin, 1987). The jejunum, the longest segment, attaches to the ileum, which in turn connects to the large intestine via the ileo-caecal junction.

The small intestine wall includes the mucosa, submucosa, muscular, and serous layers (Gray, 1989) as shown in Figure 1.4. The innermost layer, the mucosa, is important to digestion and absorption of material from the luminal cavity. It is highly perfused via capillaries and anatomically wide at the start of the duodenal cap but gradually decreases in thickness and blood supply to the distal end of the ileum (Gray, 1989). Its absorptive efficiency is maximized due to an enormous increase in surface area by circular folds (i.e., folds of Kerckring or plicae circulares) and numerous villi (Carr, 1984; Haeberlin, 1992). The folds of Kerckring may be large or small and project into the luminal space of the duodenum and the first half of the jejunum. From the latter half of the jejunum, the circular folds diminish in size and density until they almost disappear at the distal ileum (Gray, 1989). The villi increase the surface area of the small intestine by 7 to 14-fold (Allen, 1994). The surface area of the intestine declines from the

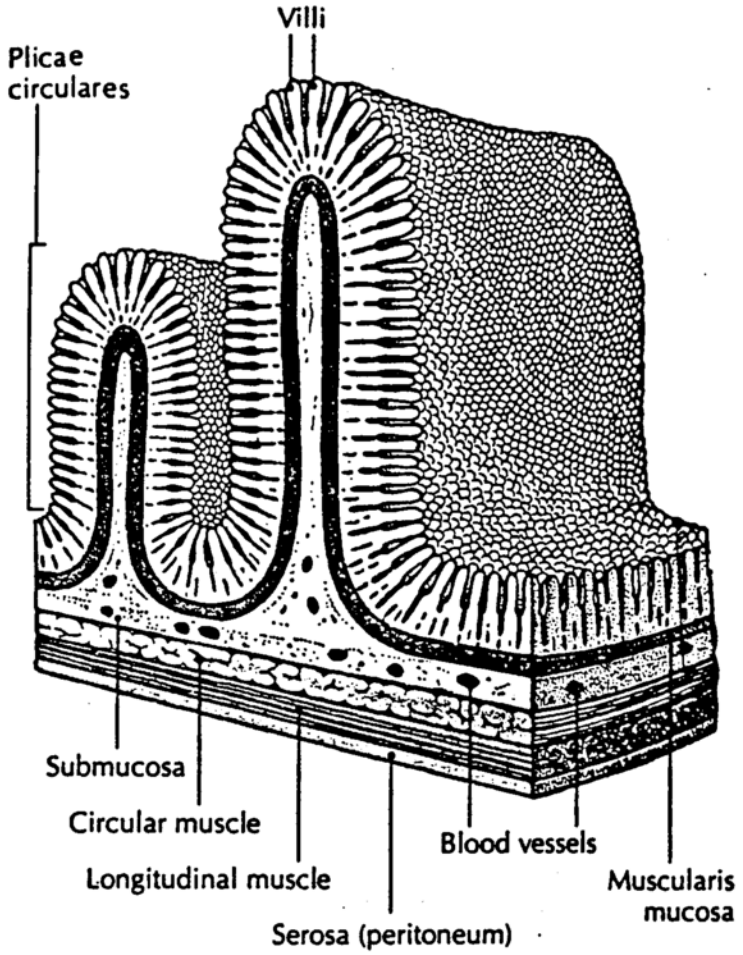

Figure 1.4: General structure of the small intestine depicting the mucosa, submucosa, muscular, and serosal layers. (Reproduced from Carola, R., et.al., 1992).

proximal to the distal end of the segment. The small intestinal mucosa consists of principally three distinct layers, the epithelium, the underlying connective tissue (i.e. lamina propria), and the smooth muscle (i.e. muscularis mucosa). These layers are shown diagramatically in Figure 1.5. The epithelium is a continuous single cell layer which lines the intestine (i.e. the villi and folds) and comes into direct contact with the contents of the lumen. This single layer of epithelium is a heterogeneous assortment of cells which include absorptive cells (i.e. enterocytes), entero-endocrine cells, goblet cells, Paneth cells, tuft cells, M cells, and undifferentiated crypt cells (Carr, 1984; Haeberlin, 1992; McMinn, 1974). The undifferentiated cells originate in the crypts of Lieberkuhn, maintaining the integrity of the mucosa via supplementation of new cell populations. The new cells take the place of older cells, which are continuously displaced from the villus tip due to injury or are at the end of their life span (Carr, 1984; Rubin, 1987). The turnover rate for epithelial cells in the small intestine is 2 days (Kleinman, 1989).

Absorptive cells are the most numerous cell type in the intestine and are characteristically columnar, polarized, and granular in nature. The lateral intercellular spaces of mucosal epithelial cells are attached by tight junctions located at the apical end of adjacent cell membranes (Martinez-Palomo, 1975). The tight junctional complex, which includes the tight junction (i.e. zonula occludens), the intermediate junction (i.e. zonula adhaerens), and a series of desmosomes (i.e. macula adherens) that underlie the intermediate junction, plays an important role in the regulation of paracellular permeability. The epithelial cell apical surface contains a striated or brush border consisting of "finger-like" microvilli (1 μm long and 0.1 μm wide) that increase the intestinal surface area by a factor of 15 to 40 (Brown, 1962). The brush border is coated with a carbohydrate rich glycoprotein structure called the glycocalyx, which confers a net

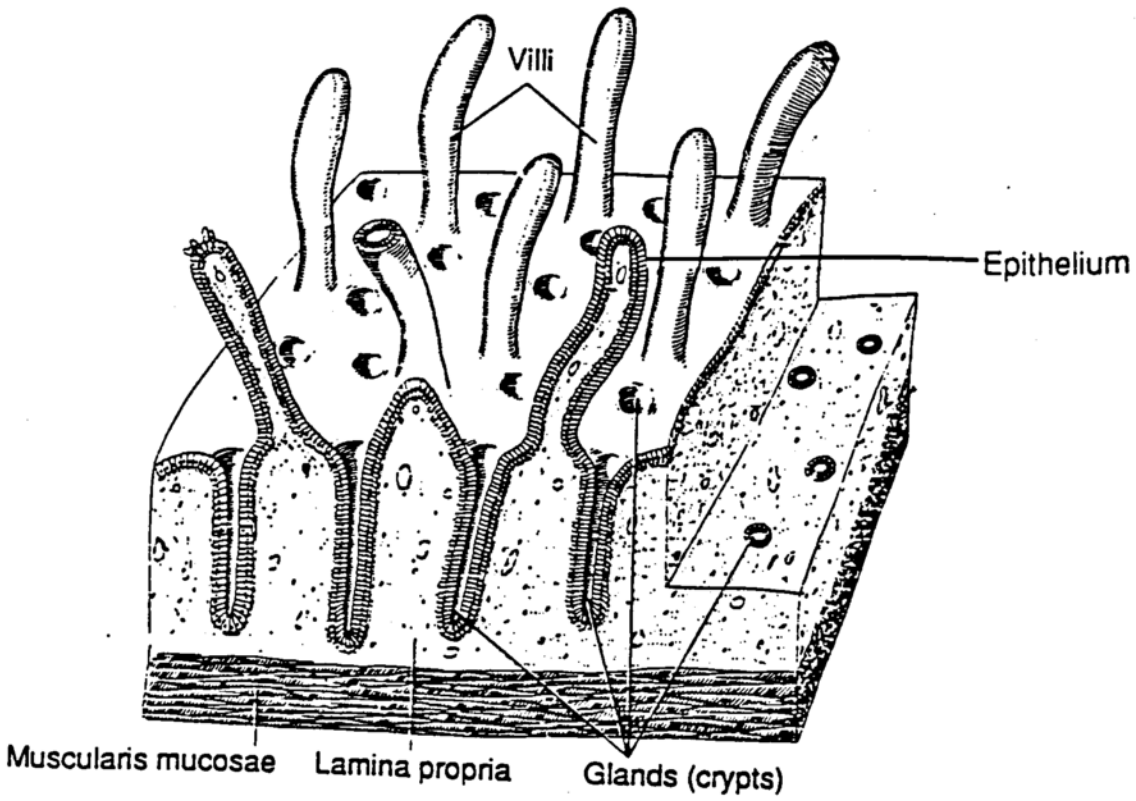

Figure 1.5: General structure of the small intestinal mucosa illustrating the epithelium, lamina propria, and muscularis mucosae. (Modified from Junqueira, et.al., 1989).

negative charge to the border. Mucus is a viscoelastic gel that is closely associated with the mucosa. Mucus production occurs through the entire length of the gastrointestinal tract. Brunner's glands are the main source of mucus in the duodenum along with goblet cells (Allen, 1994). Goblet cells are found in both the small and large intestines and produce mucus in both of these segments (Allen, 1994). The density of goblet cells in the small intestine increases from the jejunum to the latter part of the ileum (Madara, 1994). The primary function of mucus is to create a barrier which protects the epithelium from disruption by luminal contents (i.e. mechanical damage by food, etc.). The epithelium is separated from its adjacent layer, the lamina propria, by a continuous basement membrane. The lamina propria is a layer of connective tissue containing a rich supply of blood and lymph vessels. The highest cell populations are those of immunological nature including plasma cells, macrophages, and lymphocytes, as well as less populated mast cells, fibroblasts, eosinophils, and nerve fibers (Madara, 1994). The lamina propria also contains aggregated lymphoid follicles within the small intestine called Peyer's patches. These round immunological structures are quite large and of highest quantity within the ileum (Gray, 1989; Madara, 1994). The patches are also found in the duodenum and jejunum but are smaller in size and in less abundance (Gray, 1989; Madara, 1994). A main feature of the intestinal tract, the villi, are absent from these structures. The lamina propria provides functions such as (1) support for the epithelium, (2) epithelium nourishment, (3) material transport after epithelium absorption via blood and lymphatic vessels, and (4) immunological functions (Madara, 1994).

The third layer of the mucosa, the muscularis mucosa, is a smooth muscle region which separates the mucosa from the submucosa. Potential functions of

this layer include control of the stagnant diffusion layer next to the epithelium and control of villi movement.

The layer just below the mucosa is the submucosa, which consists of blood and lymph vessels, nerves, fat cells, and connective tissue (Carr, 1984). Brunner's glands are also embedded within the submucosa and are mainly found in the duodenum and proximal jejunum. These glands can penetrate the mucosa and secrete an alkaline glycoprotein (i.e. mucinous) fluid into the intestinal lumen.

The muscularis externa is the next most outward layer from the submucosa and has an uppermost region of circular muscle and a distal layer of longitudinal muscle. This layer decreases in thickness from the proximal to the distal part of the small intestine. The serosal layer consists of flat mesothelial cells with an underlying coat of loose connective tissue (Carr, 1984; Gray, 1989).

The large intestine connects from the small intestine at the ileo-cecal junction and includes the cecum, colon, rectum, and the anal canal. The major functions of the large intestine are fluid resorption and elimination of undigested substances (Gray, 1989; Mrsny, 1992).

The large intestine, unlike the small intestine, does not have villi but does contain *plica semilunares* (i.e. cresentric folds) (Haeberlin, 1992). The composition of the cecum, colon, and rectum consists of four layers (Figure 1.6): the serosa, muscularis externa, submucosa, and mucosa. The serosal layer consists of squameous epithelia and is found only in regions of the large intestine where there is contact with the peritoneum (McMinn, 1974; Mrsny, 1992). The serosa is connected to the muscularis externa via loose connective tissue. As in the small intestine, there are two layers of muscle, an inner circular layer and an outer longitudinal muscle layer. However, the longitudinal muscle fibers form assembled muscle bands called taenie coli. The cecum and colon contain three

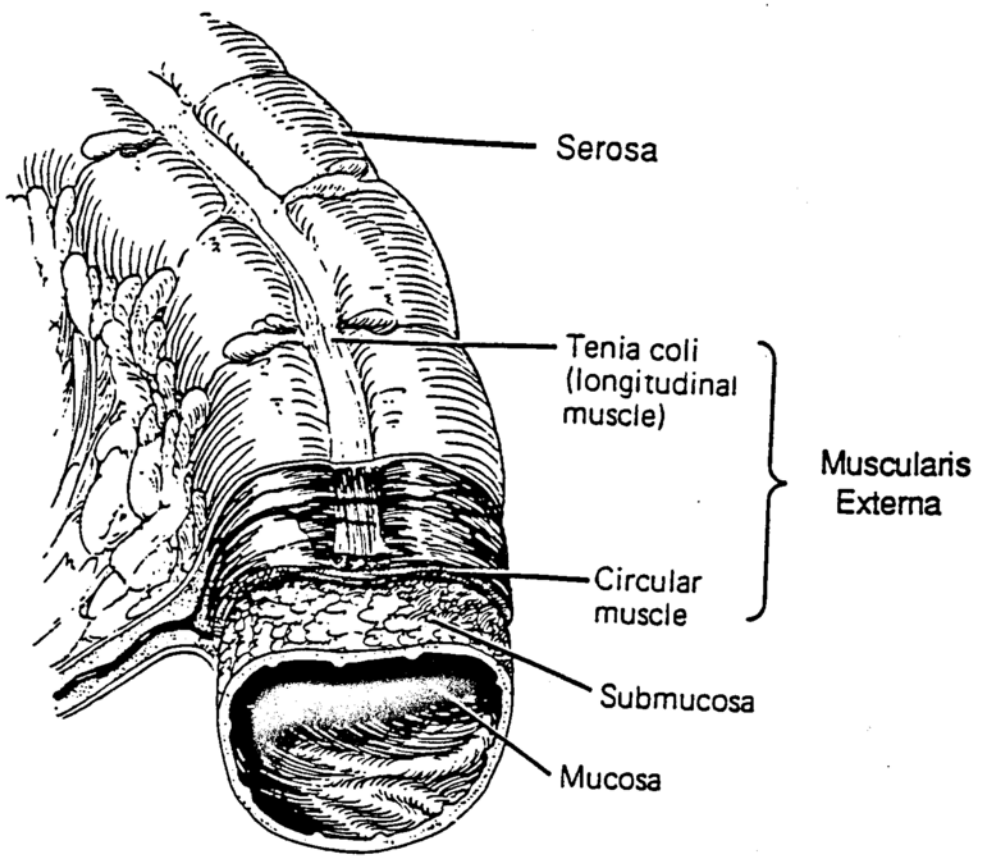

Figure 1.6: Cross-sectional diagram of the large intestine. (Modified from Junqueira, L.C., et. al., 1989).

of these bands, which individually are referred to as the taenia libera, taenia mesocolica, and taenia omentalis (Gray, 1989). Contractions of the taenie coli form pouches within the cecum and colon referred to as haustra or sacculi. Therefore, as chyme enters the large intestine, churning and peristalsis of the intestinal wall is due to these muscular contractions (Mrsny, 1992). At the start of the rectum, the three taeniae spread and join to create a single uniform layer of longitudinal muscle covering the entire rectum (Christensen, 1994; McMinn, 1974).

The submucosa histology is equivalent to that previously mentioned in the small bowel section. The adjacent and innermost layer is the mucosa. The mucosa is similarly divided into three layers, i.e. the epithelium, lamina propria, and muscularis mucosa. The cells of the epithelium have brush borders on the apical surface and include columnar epithelial cells, goblet cells, entero-endocrine cells, and M cells. Unlike the small intestine, there are no Paneth cells present and many more goblet cells are present, especially towards the distal part of the large intestine (McMinn, 1974; Mrsny, 1992). The lamina propria and the muscularis mucosa layers are similar to the small intestine in that the lamina propria contains blood and lymph vessels, macrophages, lymphocytes, neutrophils, plasma cells, and eosinophils (McMinn, 1974). The muscularis mucosa has similar layers of smooth muscle as the small bowel. In general, the main differences between the large and small intestines include: (1) the absence of circular folds (plicae circulares); (2) the cecum and colon have taeniae coli; and (3) the absence of villi throughout the large intestine (McMinn, 1974).

The final section of the large intestine, the anal canal (Figure 1.7), is somewhat different than the previous regions. The lining of the anal canal is divided into two parts; (1) the upper mucosal lining and (2) the lower cutaneous lining. The line

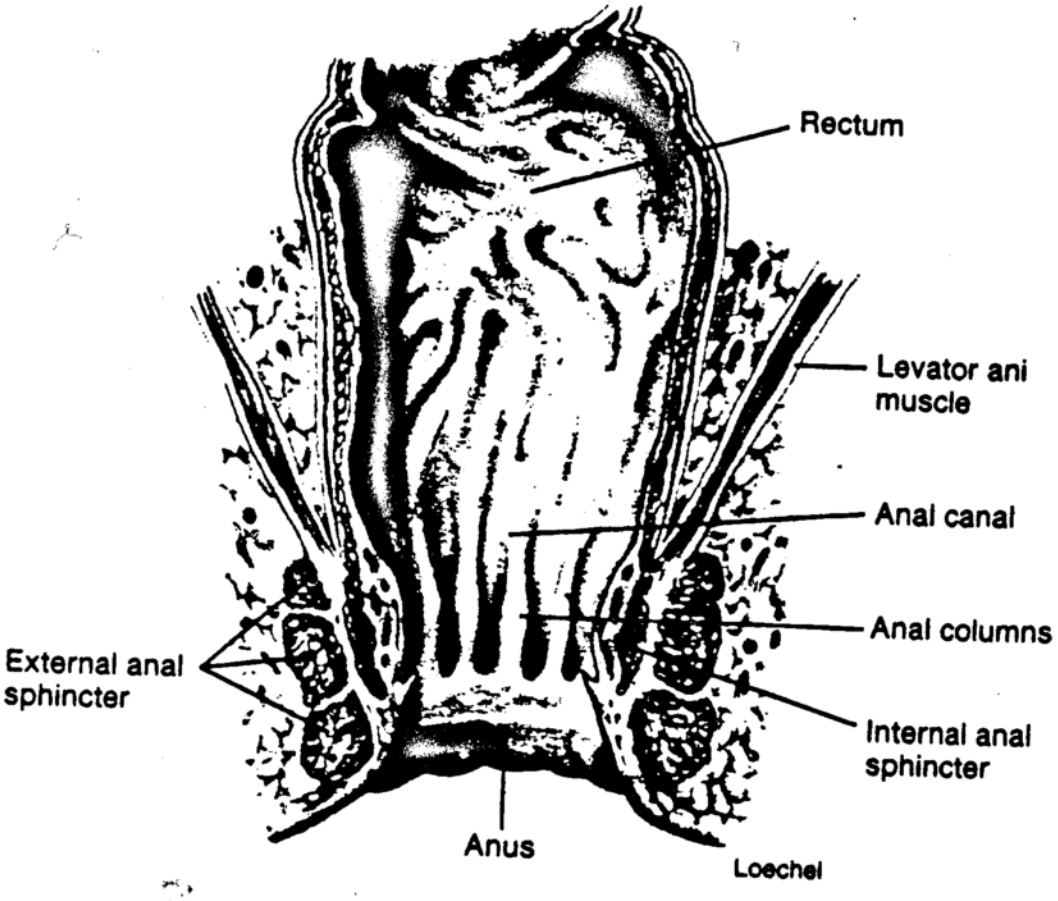

Figure 1.7: Longitudinal section of the anal canal illustrating the major anatomical regions. (Modified from Hole Jr., 1990)

separating these two sections is called the pectinate line (Bacon, 1962; Goligher, 1984). The upper third of the anal canal is similar to the rectum, where the epithelium consists of columnar absorptive cells, goblet cells, and the existence of tubular crypts extending into the submucosa. The lower two-thirds of the canal, the pectin region, consists of stratified squamous epithelium (i.e.. skin-like). Sweat glands, hair follicles, and sebaceous glands are not characteristically found in this region. The pecten regional submucosa is a dense connective tissue firmly holding the "skin-like" epithelium in place. Below the pecten region and near the anal orifice, the lining resembles normal skin, where hair follicles, sweat glands, and sebaceous glands are present (Bacon, 1962; Goligher, 1984). This region is separated from the pecten area via an indentation referred to as the white line.

The musculature of the anal canal is complex and will be covered in brief detail. The uniform layer of longitudinal muscle proceeds from the rectum and fuses with skeletal muscle fibers which connect to the anal external sphincter. The external sphincter completely surrounds the anal canal and consists of three sections: the subcutaneous part, the superficial part, and the deep part (Christensen, 1994).

The circular muscle layer also proceeds from the rectum into the anal canal, becomes thickened, and forms the internal anal sphincter (Christensen, 1994; McMinn, 1974). The internal sphincter covers the upper three-fourths of the anal canal until ending at the white line (Gray, 1989). Muscles of the internal and external sphincters provide the tone in which the anus is normally closed and upon defecation, the muscles relax and the anal canal opens (Gray, 1989). The anal canal does not have a serosal layer due to the absence of a peritoneal covering.

II. Gastrointestinal Drug Delivery

The gastrointestinal tract is by far the most convenient and commonly used route for administration of therapeutic compounds. The main advantages of gastrointestinal delivery are its large absorptive surface area, relatively high permeability, and successful patient compliance due to ease of administration. During the decade of the 1980's, greater than two-thirds of the dosage forms marketed were for orally administered drugs (Ranade, 1991). Other routes of administration available include: (1) parenteral injections (i.e., intramuscular, intravenous, subcutaneous, etc.); (2) transdermal; (3) vaginal; (4) nasal; (5) ocular; and (6) rectal. These alternate routes have been useful in delivering therapeutic levels of a wide number of drugs which have not achieved absorption across the intestinal barrier. However, they have not gained as high a rate of acceptance or compliance from the general public due to the stigmatism associated with delivery system insertion into certain body cavities (e.g., rectal, vaginal), discomfort upon drug delivery (e.g., injections), and/or the complexity associated with the delivery device.

The epithelium of the gastrointestinal tract directly interfaces the intestinal lumen with a 200 μm thick mucus layer separating the two surfaces. The primary function of the epithelium is to provide a barrier which limits and controls the passage of substances from the lumen to the blood capillaries. Therefore, in order for successful gastrointestinal delivery, the drug must be released from the oral dosage form and cross the intestinal epithelium into the circulation with sufficient concentration in order to obtain the desired therapeutic response.

This process can be described in four steps: (1) drug delivery to a specific region for maximal absorption; (2) drug dissolution; (3) transport of the drug across the epithelial barrier; and (4) drug transport from the cell basement membrane into the blood capillaries (Hoener, 1996).

In delivering therapeutic agents to the gastrointestinal tract, there are numerous factors which may alter the rate and extent of drug absorption as it undergoes this sequence. These include: (1) physicochemical factors such as: partition coefficient, molecular size, solubility/dispersibility, chemical degradation, and thermodynamics; (2) physiological variables, such as: gastrointestinal pH, blood flow, membrane permeability, gastric emptying, and intestinal transit; (3) biological barriers, such as bacterial degradation, hepatic first pass effect, gastrointestinal associated immunities, and enzymatic degradation; and (4) dosage form factors, such as disintegration time, residence time, and release rate (Bassett, 1996). Therefore, one must be sensitive to all underlying issues when formulating oral drug delivery systems.

In the early years of oral drug delivery, a drug was formulated for delivery to the gastrointestinal tract via a tablet, capsule, or solution/suspension. In most cases, these dosage forms often released the drug quickly by disintegrating within the gastric environment. The major prerequisite was to obtain efficient and substantial drug absorption, thereby providing an efficient means for curative therapy. In recent years, an increased emphasis has been on developing new and exciting delivery systems which utilize unique gastrointestinal tract characteristics in order to target drug delivery to specific regions of the tract and/or obtain controlled drug release to decrease dosing frequency.

Targeting of drugs in the gastrointestinal tract may be accomplished by chemical conjugation of the drug to polysaccharides or polymers. In order for

successful site-specific delivery, the linkage between the two molecules needs to be sensitive to a unique environmental factor (e.g., pH, enzymes) within a certain segment of the gastrointestinal tract. 5-Aminosalicylic acid conjugation provided specific release within the upper small intestine through degradation of the linkage by brush border enzymes (Pellicciari, 1993). Steroids attached to glycosides were targeted to the colon, where the conjugate was released due to cleavage by bacterial enzymes specific to that region (Haeberlin, 1993).

Polymer systems may also be utilized for regional drug delivery by taking into consideration the pH variations within the gastrointestinal fluids (Table 1.1). As one proceeds from the stomach to the colon, there is a general increase in pH. Previous studies have shown an increase from the stomach to rectum, but more recent studies contradict these claims, showing a slight fall in pH from the ileum to colon (Evans, 1988). Some polymers will swell, shrink, or degrade in certain pH environments (Dong, 1991; Kim, 1994). Drugs incorporated within these polymer systems have the potential for controlled release at specific sites of the gastrointestinal tract, depending upon the pH sensitivity of the polymer. Copolymers of (dimethylamine)ethylmethacrylate combined with different methacrylates are very sensitive to pH changes in which they swell and release drug at pH values of the upper intestine (Bassett, 1996). A methylvinyl ether-maleic anhydride copolymer system is completely soluble or insoluble depending upon the size of the alkyl group on the copolymer ester (Ranade, 1996). Therefore, a drug incorporated within this copolymer could potentially be released anywhere in the gastrointestinal tract by simple formulation of the copolymer components.

Hydrogel polymers crosslinked with azo bonds have been formulated with the intention to provide site-specific delivery to the colon. In addition, these polymers

Table 1.1: pH of gastrointestinal fluids.

Gastrointestinal Region	pH
stomach	1.0 - 3.5 [a]
duodenum	5.0 - 6.8 [a]
jejenum	6.0 - 7.0 [a]
ileum	6.5 - 7.5 [b]
colon	6.4 - 7.5 [b]

(a) (Gruber, P., et. al., 1987)

(b) (Parr, A., 1997)

are also pH sensitive so as to swell as they travel down the gastrointestinal tract without releasing the drug due to the interlocking azo bonds. By the time the delivery system reaches the colon, it is fully hydrated and the localized azoreductases slowly degrade the crosslinks, providing controlled release of the drug (Brondsted, 1992; Kopecek, 1992). Pectin, a heterogeneous polysaccharide, is also degraded by colonic bacterial enzymes. It is useful as a non-toxic polymeric carrier for release in the colon (Ashford, 1994). Other types of polymeric systems include erosion-controlled devices, which are susceptible to pH and/or temperature degradation, and bioadhesive polymers, which can enhance drug absorption by prolonging intestinal transit time through polymer attachment to mucus and/or the epithelial monolayer.

Oral osmotic pump devices are formulated in a unique fashion to utilize the gastrointestinal fluid osmolarity to provide controlled release. In the elementary osmotic pump, the drug is released from a single chamber membrane-reservoir device, in which a semi-permeable membrane is used to regulate the osmotic flux of water into the tablet. The rate of drug release is dependent upon the rate of water influx into the system. An over-the-counter appetite suppressant, Accutrim®, is a controlled release formulation that utilizes the OROS® osmotic tablet system. It releases phenylpropanolamine for over 16 hours (Bassett, 1996). Other OROS® products include indomethacin, metoprolol, and acetazolamide. Additional drugs under current investigation for utilization with the OROS® system include albuterol, prazosin, and nifedipine (Bassett, 1996).

One of the new and more complex challenges facing intestinal drug delivery is the recent development of peptide and protein therapeutics. For the majority of these compounds, parenteral administration is the primary route to obtain substantial concentrations in order to produce a therapeutic response. The lack

of success in oral delivery of proteins and peptides is mainly due to : (1) enzymatic hydrolysis by intestinal proteases and peptidases; (2) aggregation and adsorption to physical and biological surfaces; (3) high molecular weight; (4) rapid clearance after absorption; and (5) hydrophilicity (Fix, 1996). The permeabilities of a number of these agents have been demonstrated by both in-vivo and in-vitro experimental methods (Table 1.2). Some of the approaches utilized to improve oral delivery have included site-specific delivery, chemical modification, bioadhesive polymer inclusion, penetration enhancers, enzyme inhibitors, and carrier systems (e.g., portenoids, liposomes, nanoparticles). Each of these approaches envelopes various technologies in which they protect peptides from enzymatic cleavage, alter the hydrophilicity, and/or deliver the protein/peptide to a specific region of the gastrointestinal tract. Chemical modification has shown promise by improving a peptide's enzymatic stability and/ or membrane permeability. Absorption enhancement was seen by increasing the lipid solubility of thyrotropin-releasing hormone (TRH), tetragastrin, insulin, and lysozyme by addition of a fatty acid acyl group to the amino terminus (Muranishi, 1991).

Enzyme inhibitors have also showed varied success when administered in combination with peptides. Puromycin, an aminopeptidase inhibitor, was able to enhance the absorption of metkephamed across rat intestinal tissue. In the absence of puromycin, the peptide was quickly degraded (Banga, 1995). The protease inhibitors, sodium glycocholate, bacitracin, and camostat mesilate, all provided increased insulin absorption within rat small intestine and colon (Yamamato, 1994). Other researchers have also showed similar success with insulin and protease inhibitors (Fuiji, 1985; Lee, 1991b).

Since proteolytic enzymes are a major contributor for inhibiting protein/peptide

Table 1.2: List of a representative sample of proteins and peptides that have been investigated for oral delivery with resultant effects. (Modified from Smith, P.L., et al., 1992).

Protein/Peptide	Species	Tissue	Extent of Absorption
Insulin	rat	duodenum	< 5%
B-Lactoglobulin	rabbit	ileum	< 5%
Alfosfalin	human, baboon	small intestine	5 - 50%
Renin Inhibitor	rabbit	jejunum	< 5%
BSA	rat	intestinal	< 5%
Tetragastrin	dog, rat	intestinal	< 5%
Cyclosporin	human	intestinal	5 - 50%
Empedopeptin	mouse	intestinal	< 5%
Leuceptins	rabbit	intestinal	> 25%
TRH analogs	dog	intestinal	3 - 13%

absorption, the concept of protection within a controlled release system would seem favorable for a method to increase absorption. These systems could protect the peptide/protein from deactivation within the low pH of the stomach, deliver to the colon in order to minimize proteolytic inactivation, deliver a high localized concentration, and/or include other substances (i.e., penetration enhancers, protease inhibitors) to improve absorption.

All the methods mentioned above have showed some success for enhancing peptide/protein agents under in-vitro and in-vivo experimental conditions. When administered alone, less than 1-5% of most proteins and peptides are absorbed in the intestinal tract. Due to the high potency of most proteins and peptides, all that is required for human delivery is to slightly improve the bioavailabilty to 10-30%. The approaches above continue to move in the right direction, but until systems are developed that limit protein and peptide inactivation, gastrointestinal delivery will not be the major route for administration.

III. Biological Barriers and Current Solutions to Drug Delivery through the Gastrointestinal Tract

A. Permeability

The luminal barrier consists of two components: (1) the physical barrier and (2) an immunological barrier. The physical barrier includes a variety of factors which may effect drug permeability including a monolayer of epithelium, the mucusal layer lining the epithelial surface, proteolytic enzymes, pH, and intestinal motility (Kleinman, 1989). Permeation of molecules across the epithelium may proceed through simple diffusion, specific transport mechanisms (e.g., active transport, endocytosis), or penetration through gaps created by cellular turnover at the villus tips (Loehry, 1973).

The most common route for absorption of drug molecules is by simple diffusion across the mucus and intestinal epithelium. There are two pathways (Figure 1.8) associated with simple diffusion, paracellular and transcellular.

The paracellular pathway is the primary route for hydrophilic substances (log $K_{o/w} < -0.01$) in which solutes diffuse into the intercellular space between epithelial cells. The solute must first traverse the tight junctional complex located at the apical surface between adjacent cells. This junction appears to fuse opposing cell membranes, closing off the pathway to solute flux. However, the tight junction has a small opening which allows diffusion of smaller molecules (3-10 Å), such as water and electrolytes, but acts as a barrier to larger molecules. Solutes entering the paracellular space diffuse through the junction and past the

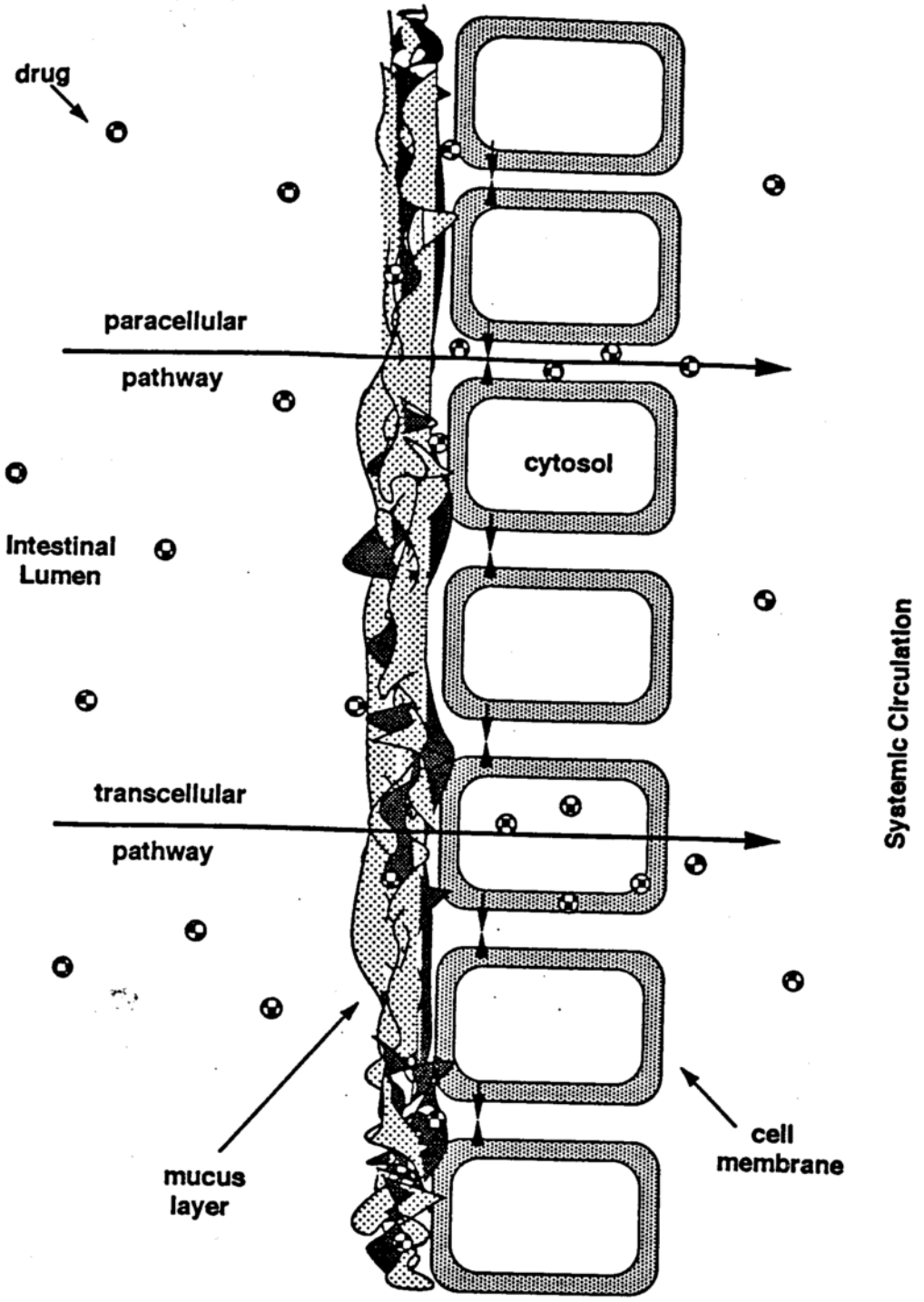

Figure 1.8: The two major absorption routes for drugs undergoing passive diffusion from the lumenal cavity, across the intestinal epithelial monolayer, and into the circulation.

basement membrane into a capillary rich layer of tissue.

Permeation of solutes across the intestinal epithelium has been mainly studied through quantitative passive diffusion studies utilizing metabolically inert hydrophilic molecules of varying molecular weight. Typical molecules studied include polyethylene glycol (PEG), mannitol, inulin, EDTA, lanthanum, and horseradish peroxidase (Hollander, 1992). The results indicate that hydrophilic marker permeability differs between segments of the intestinal tract. The tendency is of decreasing permeability as one moves sequentially down the tract, with the highest permeability in the duodenum and the lowest in the colon (Artursson, 1993; Chadwick, 1977). This reduction in permeability has been observed with compounds ranging from 60 to 40,000 Da (Loehry, 1973). Due to the hydrophilic nature of these markers, they would be expected to traverse the epithelium through the paracellular space and not the hydrophobic cell membrane. Therefore, one may conclude that the pores between the cells are becoming smaller in diameter and/or the number of pores decreasing when moving toward the distal portion of the intestine.

Intestinal permeability of hydrophilic probes has been demonstrated to be molecular weight dependent. Smaller molecules typically have higher permeability coefficients than their larger counterparts. When examining a series of homologous compounds, e.g. PEG, it was found that their permeabilities were inversely proportional to their molecular weight (Chadwick, 1977). The molecular weight dependence is in agreement up to a certain point, at which linearity no longer exists. For PEG compounds, this breakoff molecular weight is $\approx$ 400 (Artursson, 1993). Heterogeneous polar molecules have a molecular weight dependence except for some unusual results which indicate that some low molecular weight compounds have decreased permeability coefficients when

compared to their higher molecular weight counterparts. This is indicative for other factors contributing to epithelial permeation rates. Recently, results from studies suggest that properties such as structural flexibility, molecular geometry, charge, and molecular stability play significant roles (Ghandehari, 1997; Lane, 1996). One study showed that intestinal permeability correlated to the cross-sectional diameter of the probe molecule (Ma, 1992). Another showed the importance of the molecule's hydrodynamic radius (HR) to permeability in which inulin (MW ≈ 5000, HR = 10 Å) showed a greater permeability across rabbit colon tissue than PEG 4000 (MW ≈ 4000, HR = 15.9 Å) (Ghandehari, 1997).

The transcellular pathway is the primary route for hydrophobic substances (log $K_{o/w} \geq -0.01$) in which the solute partitions into the cell membrane. Biological membranes are hydrophobic bilayers of phospholipids in which cholesterol and proteins are randomly inserted (Stein, 1986). There are two potential pathways for lipophilic solutes to be absorbed: (1) the solute partitions into the cell membrane and diffuses to the basolateral side while remaining within the membrane; or (2) the solute partitions from the membrane into the cell cytoplasm and then back into the basement membrane. Lipophilic compounds (e.g., diazepam, hydrocortisone, progesterone) tend to have high permeability across intestinal epithelium due to the large surface area available for membrane partitioning where they rapidly partition into the cell membrane from the luminal fluid and are usually completely absorbed.

The immunological barrier is composed of gut-associated lymphoid tissue (GALT) which is often aggregated into specialized regions called Peyer's patches (Rubas, 1991). Peyer's patches are associated with cell-mediated immunity and IgA antibody development. These two constituents prohibit viruses, antigens, microorganisms, and other toxic materials from entering the body (Van Elburg,

1992). Drug permeability across Peyer's patches into the lymph system has been shown whereby transport occurs by endocytosis and passive diffusion across cell membranes or through the paracellular space (Rubas, 1991). Horseradish peroxidase (HRP) is absorbed by fluid phase endocytosis into Peyer's patch tissue at a 3-fold increase over tissue absent of Peyer's patches (Bockman, 1973; Keljo, 1983). Bovine serum albumin, IgG, and immunomodulating compound have also shown permeability enhancement across Peyer's patch tissue (DeBoer, 1994).

Small microparticles < 5 μm in size are capable of traversing Peyer's patches and undergo phagocytosis by macrophages. Larger particles, > 5 μm but not exceeding 35 μm, accumulate within Peyer's patches. Examples include carbon, pollens, latex, and liposomes (DeBoer, 1994).

Surface properties of drugs or particles influence Peyer's patch permeability, where absorption is greater with hydrophobic materials than hydrophilic. When examining paracellular marker diffusion of mannitol, PEG 400, and PEG 4000, no difference in absorption is found between tissue with or without Peyer's patches (Rubas, 1991).

1. Transepithelial Electrical Resistance (TEER)

Intestinal epithelium acts as a barrier with two distinct properties; permeability and permselectivity. Permeability may be measured by electrical resistance across the epithelium while permselectivity of the barrier is qualitatively measured by the selectivity of transport between anions and cations (Powell, 1981).

Membrane permeability is a quantitative measure in which the epithelium is depicted as an electrical circuit of capacitors and resistances (Figure 1.9). The intercellular resistances include those relating to the tight junction and the intercellular space, R_J and R_I, respectively. There are also contributions to the total resistance from the apical membrane, R_a, and the basolateral membrane, R_b, as well (Powell, 1981).

The epithelium may be categorized into two classifications depending upon the value of its TEER across a specified surface area. The small intestine is classified as "leaky" due to its relatively low area resistance values, ranging from 50 to 100 $\Omega \times cm^2$. The colon is considered "tight" with tissue resistance values of $\approx 300\ \Omega \times cm^2$ (Powell, 1981). Various tissue TEER values are listed in Table 1.3.

TEER reflects both the total paracellular and transcellular ion flow across an area of tissue. In tight epithelia, the ion flow across the paracellular space is significantly reduced when compared to transcellular ion flow. Therefore, in "tight" tissues, TEER is significantly influenced by changes in the transcellular ion flow. In "leaky" epithelium, the reverse is true. The paracellular space has significant ion flow compared to diminished flow across the cell membrane. Therefore, it is believed that the transcellular ion flow may be neglected (Artursson, 1993). A number of experiments have been conducted showing that a simultaneous decrease in TEER is associated with an alteration in integrity of the tight junction (Atisook, 1991; Madara, 1985; Munck, 1977; Pappenheimer, 1987) and an increase in solute permeability by the paracellular route (Artursson, 1990; Artursson, 1993; Rubas, 1996). However, a decrease in TEER has also been associated with protein release from cell membranes (Hosoya, 1994).

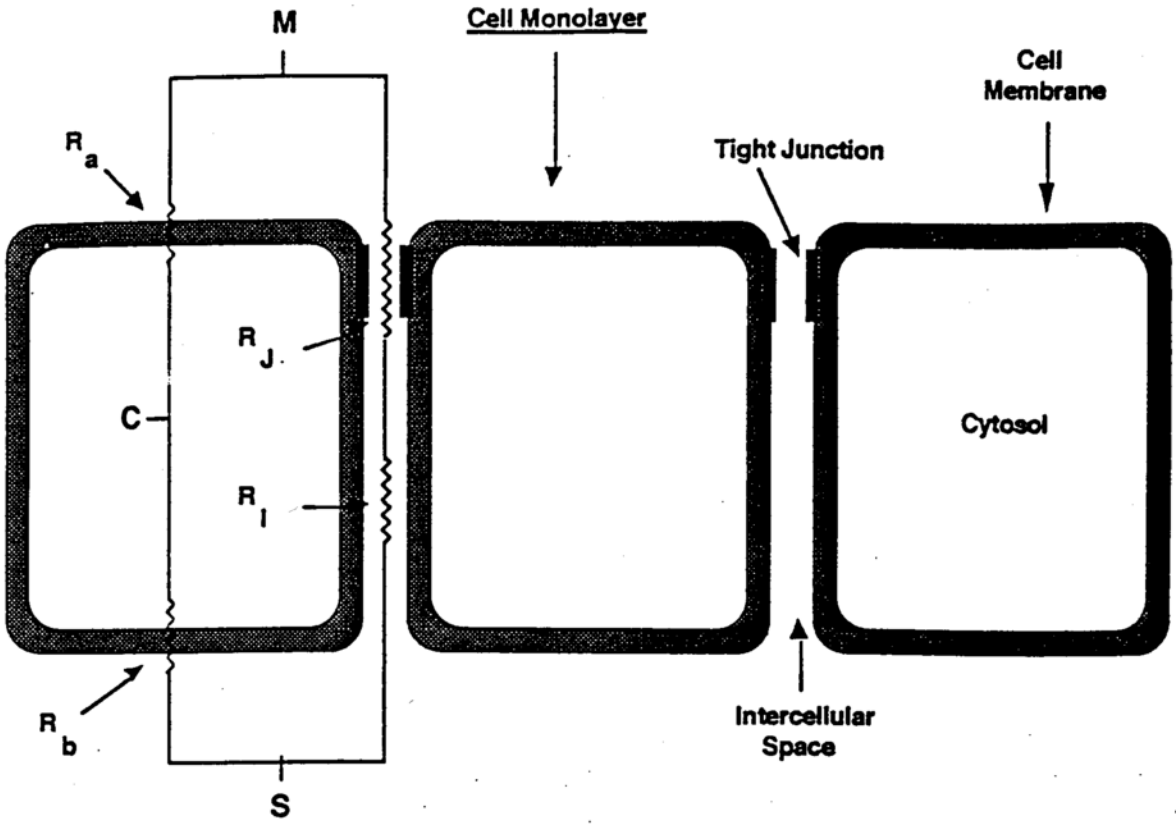

Figure 1.9: Paracellular and transcellular resistances. R_a, the apical membrane resistance, R_b, the basolateral membrane resistance, comprise the transcellular resistance. The paracellular resistance is comprised of R_J and R_I, the tight junctional and intercellular resistances, respectively. M, S, and C depict the serosal, mucosal, and cellular solutions, respectively. (Modified from Powell, D.W., 1981).

Table 1.3: Transepithelial electrical resistances for various epithelia. Modified from (Powell, 1981)

Tissue	Species	Tissue Resistance ($\Omega \times cm^2$)
Gastric Mucosa		
Antrum	necturus	1,730
Fundus	necturus	2,230
Small Intestine		
Duodenum	rat	98
Jejunum	rat	51
Ileum	rabbit	100
Colon	rabbit	385
Gallbladder	rabbit	20
Urinary Bladder	toad	3,755
Proximal Renal Tubule	dog	6 - 7
Amphibian Skin	toad	763
	frog	8,700

2. Penetration Enhancers

Penetration enhancers are typically low molecular weight compounds which enhance drug absorption across the epithelium of the gastrointestinal tract. They are thought to increase drug permeability through the intestine and other epithelial barriers (i.e. nasal, vaginal, etc.) by affecting the membrane transport pathways (i.e. paracellular and transcellular) and/or reducing the barrier effect of the mucosal lining. The ultimate acceptance of these agents for systemic delivery with drugs is based on the concern for their potential toxicity due to extensive local tissue damage and the time to tissue recovery.

Enhancers are comprised of five major categories: (1) bile salts and their derivatives (e.g., sodium taurocholate, sodium deoxycholate, and sodium glycocholate, STDHF, etc), (2) chelators (e.g., citric acid, enamines, EDTA, etc.), (3) fatty acids and their derivatives (e.g., arachidonic acid, oleic acid, sodium caprylate, monoolein, etc.), (4) surfactants (e.g., SDS, polyoxyethylene-20-cetylether, etc.), and (5) non-surfactants (e.g., 1-alkylazacycloalkanone, unsaturated cyclic ureas, β-cyclodextrin, etc.) (Lee, 1990).

At high concentrations, bile salts are capable of reducing the viscosity of the mucus layer and thus decreasing its barrier properties (Martin, 1989). It has been shown experimentally that sodium taurocholate increases the absorption of sulfanilic acid in the rat small intestine (Muranishi, 1990). Sodium tauro-24,25 dihydrofusidate (STDHF) has been shown to increase rectal absorption of cefoxitin. Other bile salts have demonstrated ability to increase the permeabilities of growth hormone, fosfomycin, and various other drugs (Muranishi, 1990). The damage to the intestinal epithelium induced by bile salts is a major concern for

incorporation of these compounds into drug delivery systems. Some of the bile salts (i.e. sodium deoxycholate) have caused extensive microvilli damage in the rectum (Nakanishi, 1983).

The rate limiting structure for paracellular permeation is the tight junction, which is highly dependent on extracellular calcium (Ca^{2+}) for maintenance of its structural integrity. Ca^{2+} indirectly affects the tight junction by binding to uvomorulin, a cell adhesion molecule, causing secondary effects such as movement of actin microfilaments to the tight junctional region (Lee, 1990). Chelators bind to extracellular Ca^{2+}, preventing attachment of Ca^{2+} to uvomorulin. This action precipitates a sequence of events leading to an eventual opening of the intercellular space and consequently increased paracellular drug diffusion. Chelators may also lower the viscosity of mucus due to the important role Ca^{2+} plays in maintaining mucosal structure (Lee, 1990).

Fatty acids have also been shown to favorably alter the pore size of the intercellular channel. Colonic absorption of cefmetazole in rat studies was increased in the presence of certain penetration enhancers. The mechanism was suggested to be pore enlargement, in which sodium laurate and sodium caprate opened the pore size from 8-9 Å to 14-16 Å, while sodium caprylate and sodium taurocholate opened the pore to 11-12 Å (Muranishi, 1990).

Surfactants have been reviewed as effective enhancers for intestinal delivery (Swenson, 1994; van Hoogdalen, 1989). They have been shown to affect the epithelial membrane and at times to cause extensive damage (Swenson, 1994). However, this damage is reversible and recovery occurs within a short period of time (Swenson, 1994).

Mixed micelles are composed of fusogenic lipid (e.g., dodecanoic acid, linoleic acid), which is solubilized by incorporation of a surfactant or bile salt. The

permeability enhancement effect follows the order: large intestine > small intestine > stomach (Muranishi, 1985). Mixed micelles have enhanced absorption of human calcitonin nine-fold across rat colon without acute tissue damage using a combination of 40 mM monoolein : 40 MM sodium taurocholate (Hastwell, 1994). By using various mixed micellar combinations, aminoglycosides, heparin, carboxyfluorecein, and other drugs have shown permeability enhancement, especially within the large intestine (Hashida, 1984; Muranishi, 1985; Muranishi, 1979; Thompson, 1997).

Cyclodextrins are cyclic carbohydrates which complex with hydrophobic drugs and thus improve their water solubility. Methylated β-cyclodextrin has also been shown to have high surface activity and to destabilize cell membranes by extracting cholesterol from the membrane structure (Thompson, 1997). These properties have combined to enhance absorption of a number of compounds including: indomethacin, progesterone, human growth hormone, and ketoprofen (Thompson, 1997).

All categories of penetration enhancers have the potential to disrupt the phospholipid portion and/or cause protein leaching from the cell membrane. These effects would substantially increase membrane fluidity and thereby reduce the capacity of the membrane to act as a barrier to transcellular drug movement. It has been shown that fatty acids (i.e. monoolein, oleic acid, etc.) interact with the hydrophobic lipid bilayer and the polar head groups of the phospholipids. These interactions affect the overall stability of membrane structure, causing enhanced drug permeation (Muranishi, 1990). Chelators, surfactants, and fatty acids have shown a tendency to cause protein leaching (Lee, 1990). Sodium caprylate has a dual tendency to affect membrane fluidity via protein leaching and lipid interactions.

3. Partition Coefficient

The oil/water partition coefficient ($K_{o/w}$) is an important physiocochemical property of a drug which influences the rate and extent of absorption across intestinal epithelium. As previously mentioned, the cell membrane is highly lipid in nature. For drug movement into this environment from the aqueous luminal cavity, the solute must balance the intermolecular forces acting upon it between the aqueous and lipid phases. If the intermolecular attractive forces are greatest between the solute-water rather than solute-lipid interactions, the energetics will favor localization within the lumen. Membrane permeability will be insubstantial with the paracellular pathway being the major route of absorption. However, if the solute-lipid interaction is favorable, the drug will partition into the membrane and absorption rapid.

$K_{o/w}$ is an indicator of the lipophilic or hydrophilic nature of a drug and is often correlated with drug permeability. Overton was the original investigator implicating the importance between a drug's lipid solubility and the extent of absorption (Stewart, 1990). It has been shown by various studies that as $K_{o/w}$ increases, the rate of absorption across the epithelium also increases (Mayersohn, 1996; Schoenwald, 1978). A decrease in permeability is noted if a drug compound becomes to lipid in nature and is explained by a lack of water concentration (e.g. mineral oil) (Stewart, 1990).

Two exceptions to this theory exist: very small polar molecules showing high absorption rates with low $K_{o/w}$ values, and highly branched compounds having high $K_{o/w}$ but low permeability (Mayersohn, 1996). Small polar molecules such as methanol and urea are able to penetrate the cell membrane through tiny pores incorporated within the membrane created by localized polar regions (e.g.,

proteins). It has been postulated that highly branched compounds have lower than expected permeability due to the fact that they need to disrupt the constrained orientation of membrane lipids. Therefore, they encounter an increased steric hindrance in comparison to linear molecules (Mayersohn, 1996).

4. Permeability Correlation

The correlation of intestinal drug permeabilities between in-vivo and in-vitro animal and human permeability experiments is necessary for validation of the experimental methodology. Until recently, these comparisons were not available due to an inability for obtaining human intestinal permeability values. Lennernäs has recently developed an in-vivo single-pass perfusion technique that is capable of studying membrane transport and obtaining drug permeabilities for regionalized segments of the human gastrointestinal tract (Fagerholm, 1996). Therefore, interspecies comparison between human and animal permeability is now possible.

Lennernäs, et. al., determined the in-vitro permeability coefficients for nine compounds traversing the rat jejunum via passive diffusion using Ussing permeability chambers (Lennernäs, 1997). When comparing human permeability values, there was a high correlation ($r^2 = 0.951$) between the two methodologies in terms of permeability coefficient values. Also, the rank order for the permeability magnitude for each compound was similar in both rat and human tissue (Lennernäs, 1997). The permeability coefficients were approximately 5 to 6 times greater for human than rat jejunum tissue, which may be explained by

differences in surface area, tissue viability, blood flow, unstirred water layer, and tissue thickness (Lennernäs, 1997).

Other studies comparing human permeability to rat jejunum, colon and ileum tissue have shown similar and even higher correlation between the two methods (Artursson, 1993; Fagerholm, 1996). The high correlation between the two methodologies validate the Ussing chamber technique as a useful guide for human absorption prediction.

B. Residence Time

A desirable feature in oral drug delivery is for a delivery system to release a therapeutic compound within a specified region of the gastrointestinal tract for an extended period of time. Since a number of drugs are mainly absorbed within the upper portions of the small intestine, it would be advantageous to localize the system within the stomach or duodenum in order to improve the extent of drug absorption. The small intestinal transit time is between 1 to 3 hours, allowing limited time for slightly permeable drugs to be absorbed across the intestinal epithelium (e.g. proteins, peptides). Within the past two decades, considerable attention has focused on developing new systems which specifically increase residence times at major absorption sites within the gastrointestinal tract.

In the forefront of this development are bioadhesive polymers, which interact with the mucus and/or underlying epithelial layer within the intestinal tract. Mucus is a thin gel-like substance whose thickness ranges from 50 - 450 μm and constitutes an unstirred water layer and thus a diffusive barrier for drug absorption

(Ahuja, 1997). The degree of diffusion across mucus depends upon the molecular weight, capability of hydrogen bond formation, hydration radius, and molecular charge of a drug compound (Ahuja, 1997). The major component of mucus consists of glycoproteins which form a continuous network imparting a gel-like character and conferring a net negative surface charge at physiological pH.

The interaction between a bioadhesive and its biological substrate leads to intimate chain interpenetration and bond formation preventing easy detachment. Therefore, bioadhesive polymers may be utilized to develop controlled release systems which promote increased residence time, localization of the delivery system, and prolonged intimate contact with the absorptive surface. The average mucosal residence time for delivery systems at various administration sites with or without inclusion of a bioadhesive polymer is shown in Table 1.4. The bioadhesive systems show superior residence times at all delivery sites including the small intestine. This illustrates the point that bioadhesives are retained at the site of attachment and the transit/motility patterns of the stomach and intestine are not causing a significant weakening of bond strength which would lead to subsequent detachment.

The duration of bioadhesive attachment to the mucus layer is limited by the mucus turnover rate, which is ≈ 6 to 12 hours. If the bioadhesive attaches directly onto the epithelial cell surface, significantly longer contact times may be achieved in which the residence time is ultimately controlled by the rate of epithelial cell turnover (≈ 24 hours). This may be achieved through chemical incorporation of mucolytic agents (e.g. acetylcysteine) or by stripping off the mucus layer through disruptive mechanical mechanisms (e.g. gas bubbling). In addition to increased residence time, a bioadhesive system may incorporate other additives, such as penetration enhancers, to increase the absorption of drug compounds.

Bioadhesion may also improve protein and peptide absorption by decreasing the diffusional path to the absorption surface, inducing a high concentration at the absorption site, protection from the luminal environment, and/or incorporating

Table 1.4: Typical mucosal tissue contact time for a suspension/solution delivery system with or without a bioadhesive.

Tissue	Contact Time without Bioadhesive	Contact Time with Bioadhesive (1)
Ocular (2)	1 - 2 minutes	12 -15 hours
Buccal (2)	2 - 30 minutes	6 - 12 hours
Nasal (2)	2 - 60 minutes	6 - 12 hours
Small Intestine (3)	1 - 3 hours	6 - 10 hours
Vaginal (2)	30 - 90 minutes	3 - 4 days

(1) Polycarbophil,
(2) Human
(3) Dog

enzyme inhibitors (Lehr, 1992). The bioadhesive polymer polycarbophil was shown to enhance the uptake of the peptide DGAVP in-vivo through increased retention, rapid release, and inhibition of enzyme degradation (Lehr, 1992).

C. Enzymatic Degradation

The enzymatic barrier is considered to be the primary biological barrier which limits the absorption of protein and peptide drugs from the gastrointestinal tract. It is due to the high susceptibility of these compounds for enzymatic degradation that significantly reduces their potential for oral delivery.

Within the gastrointestinal tract, proteins and peptides are hydrolyzed by proteases and peptidases located in the luminal cavity, at the brush border, and within the cell cytosol. Proteases are separated into four distinct classes based upon their mode of action: aspartic, serine, cysteine, and metallo- proteases (Wang, 1996). The stomach environment poses the initial challenge to protein stability, not only due to the acidic pH, but also its high concentration of aspartic proteases, referred to as pepsins (Lee, 1991a). Pepsins are most active at pH 2 to 3 and become inactive at pH values above 5. Pepsin hydrolyses proteins before they enter the small intestine, at which time digestion is continued via pancreatic protease activity. These enzymes are secreted by the pancreas into the intestinal lumen and are commonly categorized into endopeptidases such as trypsin, elastase, and chymotrypsin; and exopeptidases such as carboxypeptidase. The pancreatic peptidases are very efficient in cleaving proteins and polypeptides into smaller peptides. Within 10 minutes, 60-70% of ingested dietary proteins are degraded to small peptides ranging between 2 to 6 amino acid residues (Lee, 1991a). Although highly efficient, their activity towards smaller peptides is greatly diminished. Small peptides containing 4 or more residues are further hydrolyzed by brush border aminopeptidases and aminooligopeptidases (Wang, 1996).

Amino acids and peptides consisting of two to three amino acid residues are absorbed by the intestinal enterocytes into the cytosol, where di- and tripeptidases further reduce the peptides to amino acids. However, some peptides do avoid inactivation and are absorbed intact into the bloodstream.

The distribution of protease activity varies according to regions within the gastrointestinal tract. In several studies, protease activity within the small intestine was shown to be greatest in the ileum, lowest within the duodenum, and intermediate in the jejunum (Stratford, 1985; Stratford, 1986). Therefore, it seems that successful delivery of macromolecules to the small intestine has the greatest opportunity if the delivery system is targeted for protein release within the upper small intestine.

The source of enzyme production within the colon is synthesis and secretion by a large population of resident bacteria (Knuth, 1993). However, the enzymatic activity is substantially lower when compared to that of the small intestine. In rat intestinal tissue, the colon was demonstrated to contain 80% less enzymatic activity than the small intestine (Woodley, 1992). Epithelial cells contain virtually no enzymatic activity. Therefore, developing delivery systems which are formulated to have a dual purpose of protecting proteins and peptides from the small intestine luminal environment and releasing the drug within the large intestine have a greater potential for obtaining optimal absorption profiles.

In addition to site-specific delivery, other approaches to improve oral absorption of proteins and peptides include: chemical modification, inclusion of penetration enhancers and/or protease inhibitors, carrier systems (e.g. liposomes, microspheres, erythrocytes), and inclusion within bioadhesives. A recent concept studied by Irons, et. al., (unpublished data) looked at inhibiting enzyme activity through physical agitation via gas bubble production within the gastrointestinal

tract. Leucine-aminopeptidase activity in-vitro was reduced after bubbling carbon dioxide into an enzyme solution for 15 minutes. This suggests the potential for another method to enhance the bioavailability of these compounds in-vivo.

IV. Statement of the Problem

The discovery that carbon dioxide gas is liberated via an interaction between solubilized components of bicarbonate and acidic powders led to the development of effervescent drug delivery systems. These products date back to the 18th century, when effervescence was primarily used as a masking agent for unpleasant tasting drugs due to its palatable saline taste. Today, this is still the most common application, however, effervescent components are primarily combined within tablets or capsules and dissolved in a glass of water prior to ingestion. Effervescence has been and continues to be an underutilized technology, being used mainly as an adjunct for increasing patient acceptance and compliance rather than for uncovering potentially new applications from its unique qualities.

To date, the current emphasis on biological effects of effervescence has been focused primarily on its buffering action within the stomach. While this is of significant importance in treatments of ulcer and aspiration pneumonitis, other potential effects have gone almost completely unnoticed. These are: (1) increase in drug dissolution rate; (2) alteration of the pH tissue gradient; (3) mucosal stripping; (4) changes in fluid flow; (5) increase in stomach emptying; (6) increase in membrane hydrophobicity; and (7) tissue membrane alteration.

Studies have indicated the potential for effervescence in influencing oral drug absorption. A classic example is comparison of caffeine absorption from hot, cold, or an effervescent solution. The latter produced a shorter time (t_{max}) to maximum blood concentration (C_{max}) in comparison to the other solutions. So, the underlying question remaining to be answered is: what is the effervescent

mechanism(s) which provide faster and/or greater drug absorption? More specifically, the issues that will be examined in detail are: (1) the effervescence influence on drug permeation across intestinal epithelium; (2) insight into the mechanism(s) of drug enhancement; (3) effervescent effect on tissue viability; and (4) the ability for tissue recovery after effervescent exposure. Each of these points will be examined and scrutinized in detail within the subsequent sections.

A complete understanding of the mechanism(s) of effervescent drug absorption enhancement will allow greater potential for development of new and exciting delivery systems which provide targeted drug delivery within the stomach or intestine. The potential biological effects of effervescence within a bioadhesive include: (1) inducing intimate contact between the drug and epithelium for a prolonged period of time (≈ 24 hours); (2) causing alteration of the epithelial monolayer; (3) increasing drug permeability; and (4) decreasing the dosing frequency. A "classical" penetration enhancer could also be combined with effervescence at a significantly lower concentration, thereby inducing an enhanced drug absorption profile without the tissue toxicities associated with high concentrations of a penetration enhancer alone.

The influence of effervescence on drug absorption and its mechanism(s) is also essential in providing a means to promote enhanced absorption of slightly permeable drugs across intestinal epithelium. These drugs include proteins and peptides, which need only slight improvement of their oral absorption profiles in order to induce positive therapeutic responses.

Chapter 2: Effervescence: Its History and Current Status

I. Effervescence History

The evolution of carbon dioxide from the chemical reaction between solubilized acid and bicarbonate components has been known for over 250 years. The popularity of effervescent dosage forms is primarily due to the reaction itself, in which the liberation of carbon dioxide bubbles provides a unique and interesting formulation for patients to prepare as well as creating a palatable saline taste masking objectionable flavors associated with certain medications (Meyer, 1897; Murphy, 1962; Taylor, 1871)

Potassium sodium tartrate, the first compound combined with effervescent technology, was formulated for use as a saline cathartic (Sendall, 1983). Towards the latter half of the 18th century, this preparation was listed in the pharmaceutical compendia as a compound effervescent powder, otherwise referred to as Seidlitz powders (Mohrle, 1985; Sendall, 1983). Seidlitz powders were the first "official" effervescent dosage form and consisted of separately wrapped acidic and bicarbonate powders, which prevented premature evolution of carbon dioxide due to atmospheric moisture. At each dosing interval, the patient emptied one packet of each powder into a glass of water, thus forming an effervescent mixture prior to ingestion. Shortly after Seidlitz powder introduction, other effervescent products began to emerge, including effervescent baths and

mercurial fumigations prepared and sold by a Paris pharmacist, George Guietand, at the start of the 19th century (Viel, 1994).

In the mid 1840's, the invention of the compressed tablet led to incorporation of the two powders within a single tablet dosage form. The tablet was dissolved in a glass of water, producing a pleasant tasting carbonated drink. In 1872, Cooper invented a lozenge which effervesced upon contact with saliva, leading to subsequent localized oral delivery of the medicament (Cooper, 1872).

Since the late 19th century, effervescent technology has lost some of the early momentum and acceptance within the drug delivery market due to the discovery of alternative dosage forms (e.g. tablets, capsules, suspensions), which revolutionized the oral drug delivery field.

Approximately 40 years ago, effervescence regained some momentum into the oral drug delivery market with the introduction of Alka-Seltzer®, a stomach distress medication. To date, Alka-Seltzer® is the number one selling effervescent medication formulated for oral drug delivery. The formulation utilizes the same principles used in the mid-19th century, in which effervescence is first generated by tablet immersion within a glass of water and then ingested.

II. Current Applications

The popularity of effervescent formulations has dramatically increased over the past few decades. To date, there are only 5 effervescent preparations included in the USP, but numerous products are continuously being marketed primarily in countries outside the United States. These include pharmaceutical products such as: digoxin, L-DOPA, antibiotics, methadone, antacids (e.g. cimetidine, ranitidine), analgesics, mouthwashes, cold medications, laxatives, sodium fluoride preparations, cough medications, and vitamin supplements (e.g. calcium). There are also additional non-pharmaceutical formulations such as: lens and denture cleansers, washing powders, flavored beverages, and surgical instrument sterilizers.

The most widely used non-pharmaceutical application is the incorporation of effervescence within flavored beverages. These products utilize the concept of dissolving carbon dioxide under pressure in water prior to bottling or addition of any ingredients. When exposed to atmospheric pressure, the CO_2 solubility decreases, and the solution becomes supersaturated, causing gas bubble formation. A modification of this concept was applied towards formulation of an effervescent aerosol delivery system in the mid-1970's, but never materialized into a marketed product.

Recently, more complex drug delivery systems incorporating effervescence have emerged. Alza's commercially available OROS® product, which delivers drugs to the gastrointestinal tract through osmotic delivery, has been reformulated to include an effervescent agent. As gastrointestinal fluid solubilizes the effervescent components, the pressure within the drug compartment increases

due to CO_2 generation. The rate of drug release is dependent upon the rate of effervescence production within the chamber and has been demonstrated to deliver drugs at a constant rate for greater than 80% of the dose within the chamber (Bassett, 1996).

Gastroinflatable delivery devices containing one or more inflatable chambers also include effervescent solid components allowing system buoyancy. As gastric fluid enters, the device fills with freshly generated CO_2 and remains floating within the stomach (Ritschel, 1991). The buoyant device is unaffected by gastric emptying, and therefore, may continuously release drug without any limiting time restraints on absorption due to gastrointestinal transit.

Currently, the innovator in development of novel technology for oral effervescent delivery is CIMA, a pharmaceutically based drug company. CIMA has patented OraSolv®, an oral tablet dosage form which incorporates a microencapsulated drug with an effervescent agent. The effervescent reaction occurs immediately as the tablet contacts saliva, enhancing tablet dissolution without water ingestion prior to release or swallowing of the microparticles. The main advantages for this system include a taste masking effect as well as ease of administration, particularly for infants and elderly who experience difficulty swallowing medications. Tempra®, a children's analgesic medication containing acetaminophen, is formulated via this technology and is scheduled for release in the latter half of 1997. Other products currently under development for use with OraSolv® technology include: antibiotics; psychotherapeutics; anti-nausea agents, and cancer therapeutics (Bassett, 1996b).

Modern effervescent delivery systems have begun to depart from earlier simplistic approaches based on tablet immersion in liquid with ingestion of the effervescent solution. While this concept is still widely utilized in a wide array of

marketed products, an enhanced awareness to the potential pharmaceutical applications for effervescence has begun to be realized. However, until a complete knowledge of the physical and biological effects produced by effervescence is known and understood, its full potential will not be completely utilized.

III. Mechanisms of Penetration Enhancement

Effervescence technology has been utilized with increased frequency. The popularity associated with the production and use of oral effervescent drug delivery systems is based primarily on two characteristic properties: (1) its ability to impart a pleasant saline taste uncommonly associated with a number of drug formulations; and (2) a buffering effect. While these two properties are important aspects of effervescence, it may also influence other physical and biological properties such as: (1) mucus layer thickness; (2) stomach motility; (3) epithelial membrane alteration; (4) drug dissolution; (5) fluid flow; (6) the gastrointestinal pH gradient; and (7) membrane hydrophobicity. Effervescent dosage forms have been demonstrated to promote rapid and enhanced oral drug absorption for a number of drug compounds in comparison to other dosage formulations. This effect may be due to one or a combination of the effervescent properties mentioned above. A brief review of these properties follows with the exclusion of mucus stripping, stomach motility, and membrane alteration, which will be discussed in subsequent chapters.

A. Dissolution

The small intestine is the major site for drug absorption due to its relatively large surface area. The "absorption window" for numerous drug compounds depends upon a relatively short small intestinal transit time of ≈ 2 to 4 hours.

Therefore, there is a limited time period for a compound to cross the epithelial barrier. One prerequisite for drug absorption is drug dissolution. If undissolved, a drug will not be absorbed, rendering it useless as a therapeutic agent. Therefore, the drug's dissolution rate from an oral dosage form will influence the rate and extent of drug absorption (Orton, 1978). Effervescent bubbling provides physical agitation, giving a well-mixed dispersion of drug particles over an extended area and creating maximum surface exposure for dissolution by the gastrointestinal fluid. Activated charcoal has been utilized in combination with effervescence for more efficient spreading of charcoal particles, thus inducing enhanced adsorption of drugs (e.g. nortriptyline, aspirin, theophylline) that need to be eliminated from the body after toxic overdose (Crome, 1977; Dawling, 1983; Helliwell, 1981).

Spreading of particles due to effervescent bubbling has been experimentally shown to promote faster drug dissolution rates. Disulfiram bioavailability was found to be 27% greater with effervescent tablet administration than with non-effervescent tablets (Andersen, 1992). This was primarily attributed to a significantly higher drug dissolution rate for the effervescent preparation. Enteric coated tablet preparations of salicylate and levodopa also showed enhanced in-vitro and in-vivo dissolution rates due to effervescent activity within the medium (Bogacz, 1987; Nishimura, 1984)

Poor water solubility is a major factor inhibiting the dissolution rate and, therefore, bioavailability of a number of therapeutic compounds. Effervescent solid dispersions of slightly soluble compounds such as prednisone, griseofulvin, and primidone, were shown to have enhanced dissolution in-vitro in comparison to non-effervescent formulations (Desai, 1989).

B. Fluid Flow

The absorption of fluid (e.g. water) across the intestinal epithelium is believed to occur through both the paracellular and transcellular pathways. Water movement across hydrophobic cellular membranes is believed to be mediated by transport through aqueous channels inserted within the membrane. Recently, water selective protein channels, aquaporins, have been identified which may support this theory (van Os, 1994). Presently, the mechanism(s) for water transport have not been conclusively elucidated and the percentage of water flow contributed by each pathway is a controversial topic at the present time. Some believe that there is an equal water flux between the cellular membrane and intercellular space while others hypothesize that there is very little water movement through the intercellular cavity (Spring, 1991).

In various animal studies (Kitazawa, 1975; Krugliak, 1989; Madara, 1987; Ochsenfahrt, 1973) water absorption from the luminal cavity across the epithelium has been shown to increase the absorption of therapeutic agents. The hypothetical mechanisms believed to explain this increase include solvent drag and an increase in solute concentration near the epithelial surface (Lennernäs, 1995).

The theory of solvent drag has been in the literature since it was first proposed by Anderson and Ussing in 1957 (Anderson, 1957). This theory proposes that when water molecules are absorbed across the epithelium, the subsequent water flow produces a streaming effect, creating a force which carries solutes through the membrane (Fine, 1994). Solvent drag may occur either through paracellular or transcellular pathways, with the prerequisite that the water and solute are

cotransported together across the membrane. Solvent drag has been shown to contribute to the increase in absorption of urea (Ochsenfahrt, 1973), benzoic acid and salicylic acid (Ochsenfahrt, 1974a), amidopyrine and antipyrene (Ochsenfahrt, 1974b), and various other drug substances (Karino, 1982; Kitazawa, 1978).

Water absorption may also contribute to an increase in passive diffusion of the solute molecule from the luminal cavity. As water is absorbed, the solute concentration near the epithelial wall within the lumen increases due to localized water loss, thereby producing an increase in the concentration gradient across the cell monolayer. The net effect is a greater proportion of the drug absorbed due to passive diffusion (Fine, 1994).

The movement of water is a passive process that is primarily caused by differences in osmolarity across the intestinal tissue. The osmolarity gradient may develop due to active ion transport across the cell epithelium, solute absorption, or by hypotonic or hypertonic conditions within the luminal cavity. A hyperosmotic solution tends to induce cell shrinkage in order to equilibrate the cell cytosol to the osmotic environment within the lumen (Noach, 1994). The intercellular space narrows with tightening of the tight junctions (Madara, 1983). Hypotonic luminal conditions, which may be induced by drinking water, produces cell swelling and induces the solvent drag effect by creating a fluid flow towards the direction of the isotonic submucosa (Noach, 1994).

Carbonation within the intestinal tract has been shown to increase the absorption of therapeutic agents. The mechanism for absorption enhancement may incorporating a fluid flow concept. The formation of carbon dioxide bubbles near the luminal surface of the epithelium will create an increased localized flow within the region. This flow may influence the surrounding fluid (i.e. water) acting

as a catalyst in producing increased water flow velocities. This may induce enhancement of water flow through the paracellular and/or transcellular pathways. In other words, a drug may be "swept" across the membrane as a result of increased water flow (i.e., solvent drag), leading to enhanced drug absorption.

CO_2 bubble production at or near the membrane surface may also be viewed as an effect producing pin-point pressure gradients across the tissue surface. If one imagines a tissue surface placed between two solutions, molecules are constantly hitting the tissue surface and bouncing away. These molecules are reflecting off the tissue surface so as to exert a pin-point pressure on the membrane based on the rate of change of momentum exerted by all molecules colliding with the surface (Hammel, 1995). However, the system is in equilibrium due to the fact that in a homogeneous solution, an equal number of collisions per unit time are occurring from the opposing solution, preventing the development of pressure gradients.

CO_2 bubbles would impart a non-equilibrium status to the system due to two effects: (1) bubbles contacting the membrane surface and (2) increased molecular velocities associated with CO_2 bubble production. These effects would not be counter balanced by the opposing solution, which therefore, would induce pressure gradients across the tissue. This will subsequently lead to increased water flow from the side through which CO_2 is bubbling in order to eliminate any imbalance (Hammel, 1995).

An alternative hypothesis to solvent drag would theorize that enhanced water flow across the membrane can lead to an increase in passive diffusion. As the pressure is increased in the lumen due to carbonation, a larger quantity of water is "forced" across the epithelium, thus creating higher concentration of drug at the

luminal surface. This would lead to greater passive absorption of the therapeutic agent.

The effect of water absorption has been shown to increase the absorption of drugs in studies based solely on data obtained from in-vivo and in-vitro animal studies (i.e., rats, rabbits, and dogs). Recently, Lennernäs, et. al.,(Lennernäs, 1995) have reported the effects of net fluid flux on intestinal absorption of drugs with in-vivo human perfusion studies. The results obtained did not correlate with previous animal studies. Studies on levadopa (Nilsson, 1994), antipyrine, atenolol, enalaprilat (Lennernäs, 1994), and terbutaline (Lennernäs, 1995) in hypotonic solutions with physiological concentrations of D-glucose (40-80 mM) did not show increases in the absorption profiles of these compounds. It was concluded that the solvent drag theory may not apply to enhancement of human drug absorption due to interspecies variation and/or unreliable experimental conditions (i.e., intestinal distention, tissue toxicity, high perfusion rates, etc.).

C. Buffer Effect

Carbonation is produced via the interaction between a bicarbonate and an acid (e.g. citric, tartaric, hydrochloric), producing carbonic acid (H_2CO_3), which subsequently proceeds to evolve carbon dioxide:

$$H^+ + HCO_3^- \rightleftharpoons H_2CO_3 \rightleftharpoons CO_2 \uparrow + H_2O$$

Effervescent formulations frequently contain sodium bicarbonate, which when solubilized, interacts with citric acid contained within the dosage form and/or hydrochloric acid present within the stomach. Alka-Seltzer®, in-vitro, has been shown to buffer 5 to 30 times the volume of hydrochloric acid solutions. The solution pH during the study rose from a range of 1.0-2.0 to 4.0-6.5 (Chen, 1984). In-vivo studies have also supported the buffering activity of Alka-Seltzer® within the stomach in which the pH rose and remained steady at pH values well above the 4.0-5.0 range (Chen, 1984).

Recently, studies have been conducted investigating the buffer activity of effervescence in combination with H_2-receptor antagonists, ranitidine and cimetidine (Atanassoff, 1995; Ormezzano, 1990; Propst, 1996; Strom, 1991). Results indicated the effervescent tablets for both drugs provided a faster onset of action than their non-effervescent counterparts. The buffering effect is not only important in terms of disease state treatment (e.g. heartburn, ulcer, aspiration pneumonitis) but also in influencing drug absorption. This is especially important after oral administration of compounds which are unstable within the acidic stomach. Delivery of these agents within an effervescent formulation would induce a localized rise in stomach pH for extended periods, providing a stable environment for the drug until transported into higher pH regions of the upper intestine.

The buffering effect may also account for enhancing the absorption rate and bioavailability of compounds having greater solubility within alkaline environments. Amoxicillin solubility is highly dependent upon pH, in which environments of pH 6 or greater leading to a rapid increase in solubility. An effervescent amoxicillin preparation was shown to have superior bioavailability over a film-coated tablet and a regular commercial tablet. The primary

explanation for the result was increased dissolution due to higher solution pH (Hespe, 1987).

Diflunisal, a poorly absorbed lipophilic salicylate, was also demonstrated to have greater bioavailability in humans. The results indicated that the effervescent formulation buffered the stomach contents towards neutrality which corresponded to enhanced absorption rates due to solubility enhancement (Nuernberg, 1989).

D. Intestinal pH Gradient

The intestinal tract epithelium is covered by a continuous layer of mucus which restricts movement of hydronium ions from the intestinal lumen cavity to the surface of epithelial cells. The barrier to hydronium ion diffusion plays an important role, especially in regions of high luminal acidity (i.e. duodenal cap), where the pH may be as low as 2.0 (Kivilaakso, 1984). However, mucus is unable to completely retard the penetration of hydronium ions due to the high rate necessary for mucus renewal in maintaining a formidable barrier.

The concept that the gastrointestinal tract mucosa secreted bicarbonate (HCO_3^-) was proposed by Shierbeck (Flemstrom, 1987). In 1898, Pavlov proposed that the gastric mucosa contained a mucosal lining which was capable of neutralizing acid within the lumen (Flemstrom, 1987). These concepts led to the theory of bicarbonate secretion by gastric and intestinal epithelium in which the mucus lining acted as a stagnant layer preventing escape of bicarbonate ions from the region. This formed an alkaline atmosphere near the mucosal surface

which created a pH gradient between the luminal cavity and the epithelial surface. The pH gradient was eventually proven to exist at the surface of gastric and small intestinal mucosa by techniques utilizing pH-sensitive microelectrodes (Flemstrom, 1987; Rechkemmer, 1986). When comparing rates of bicarbonate secretion along the duodenal segment, various human, dog, rat, and bullfrog studies (Isenberg, 1983; Konturek, 1983; Selling, 1985; Simson, 1981) have shown a higher rate at the proximal end, with decreasing rates as one moves down to the distal end. It has also been shown that the duodenal epithelium in humans secretes HCO_3^- at faster rates than in the stomach, jejunum, and ileum (Flemstrom, 1987).

There are two pathways for transport of HCO_3^- into the lumen; (1) the paracellular pathway and (2) the transcellular pathway (i.e metabolism dependent transport). The transcellular pathway utilizes movement of HCO_3^- through the cell and has been shown to exist by experiments on bullfrog duodenal segments (Flemstrom, 1980).

The metabolism dependent transport has two pathways for secretion of HCO_3^- into the lumen. The first pathway uses an electroneutral Cl^-/HCO_3^- exchange system which is stimulated by glucagon (Allen, 1993). The other pathway is independent of luminal Cl^- and is an electrogenic transport. This pathway is stimulated by protaglandins and cAMP (Allen, 1993). Entrance of HCO_3^- across the serosal membrane into the cell cytosol may occur from $NaHCO_3$ cotransport where Na^+ is transported out of the cell by the Na^+/K^+-ATPase pump (Simson, 1981).

The duodenum epithelium may also absorb carbon dioxide into the cytosol, where it reacts with a water molecule, producing a bicarbonate and ahydronium ion. Bicarbonate crosses into the lumen via membrane dependent transport and

hydronium is transported across the serosal membrane by the Na^+/H^+ pump (Allen, 1993). Paracellular transport of HCO_3^- from the serosa into the lumen is strictly a passive diffusional process. The cells that are responsible for HCO_3^- secretion into the lumen have yet to be identified, although evidence has indicated that cells located on the villus tip have a greater propensity for HCO_3^- secretion than cells located toward the distal end of the villi (Lonnerholm, 1989).

The pH of the duodenal luminal cavity stimulates HCO_3^- secretion in which the extent of secretion depends on acidity within the lumen. Rat duodenum tissue was exposed to pH solutions of 5.0 and 2.0, which increased HCO_3^- secretion by a factor of 2 and 10-fold, respectively (Flemstrom, 1983). This response is controlled by nervous reflexes, hormonal factors, and prostaglandin synthesis (Allen, 1993). Both pathways of HCO_3^- transport are activated in the presence of low pH values. Paracellular diffusion mainly occurs at relatively high luminal acidities.

The flux of bicarbonate from the tissue to the apical surface of epithelial cells leads to the formation of what is commonly referred to as a pH-microclimate at the luminal surface. Various workers have performed pH-microclimate measurements in different segments of the intestinal tract at different luminal pH's. It was concluded that the pH-microclimate along the entire intestinal tract was near neutral even when the luminal pH (2.0-7.3) was significantly altered (Rechkemmer, 1986).

The pH-microclimate may affect the extent of drug absorption across the epithelium for ionizable compounds (i.e. weak acids and bases), depending on their pK_a values. If the luminal bulk pH is 6.5 and the surface pH is 7.0, a 0.5 unit change in pH may sufficiently alter the ratio of ionized to unionized drug in such a

way as to increase or decrease the extent of drug absorption across the epithelium.

On the serosal side of the epithelium, blood circulation creates a biological pH of 7.4. Therefore a pH gradient is present across the tissue of the gastrointestinal tract. Whether or not this gradient is substantial enough to affect drug absorption across the mucosa has not been widely studied and remains controversial without a definitive answer.

The pH of the small intestinal luminal fluid ranges from 6.5 in the duodenum to 7.0-7.5 in the distal portions of the ileum. When an effervescent dosage form is transported from the stomach into the duodenum, one would expect a slight increase in luminal pH towards neutrality due to the buffering effect. Since the drug must encounter the pH-microclimate near the epithelial surface prior to absorption, the rise in luminal pH associated with effervescence should have a limited impact in terms of inducing a significant alteration of the pH gradient.

E. Membrane Hydrophobicity

The cell membrane (Figure 2.1) is a dynamic and fluid structure which encloses the cell to the extracellular environment. The membrane is composed of proteins that are randomly embedded within a phospholipid bilayer. The lipid bilayer provides the basic structure to the membrane and largely prohibits movement of polar molecules (Alberts, 1994). The lipids are amphiphilic in nature, with the majority containing a polar phosphate head group, from which,

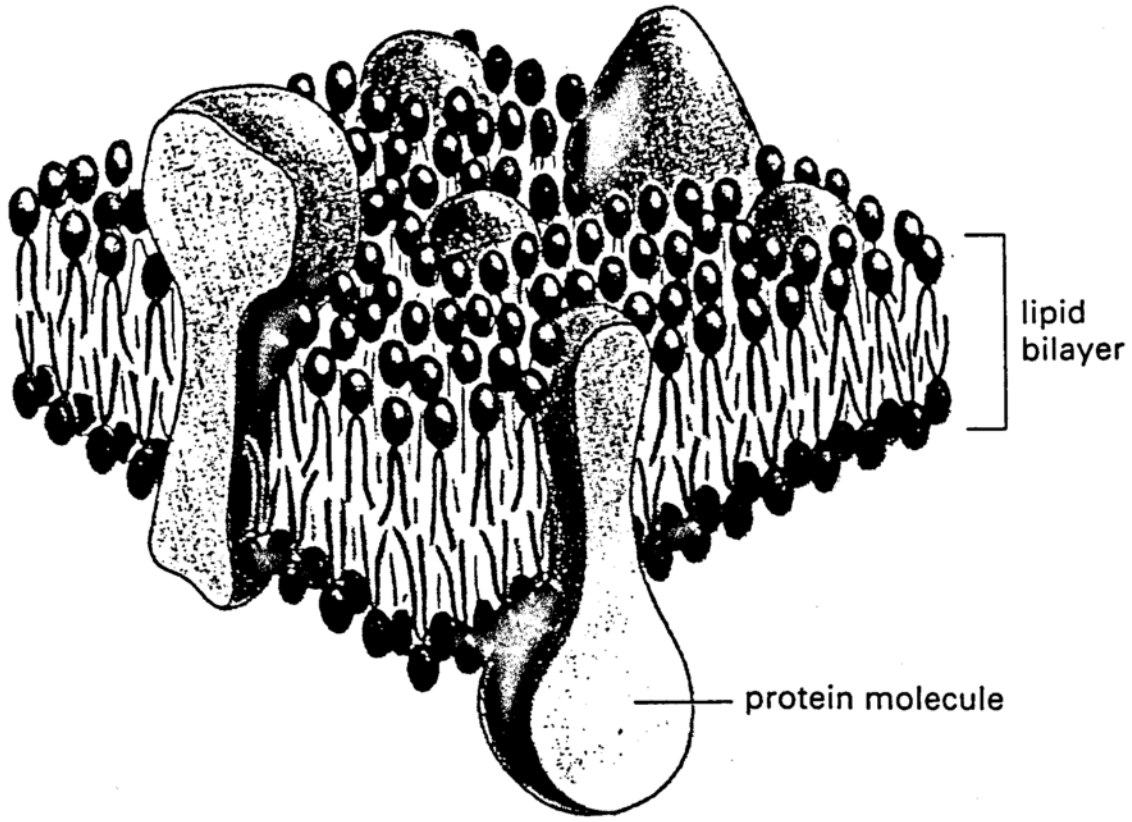

Figure 2.1: Schematic diagram depicting a three dimensional view of the cell membrane. (Reproduced from Alberts, B., et. al., 1994).

extend two hydrophobic fatty acid chains. Typically, one chain is saturated while the other contains one or more double bonds (unsaturated), which impart a characteristic kink at the terminal portion of the tail. The four major phospholipids found within the plasma membrane are: phosphatidylcholine, phosphatidylethanolamine, sphingomyelin, and phosphatidylserine. Cholesterol and carbohydrate attached lipids (i.e. glycolipids) are also found within cell membranes (Stein, 1986; Yeagle, 1985).

Proteins interact with the membrane in a number of ways (Figure 2.2). Transmembrane proteins (i.e. integral membrane proteins) span the length of the lipid bilayer and contain both hydrophobic and hydrophilic regions which interact with fatty acids within the bilayer interior or water molecules at either side of the membrane, respectively (Singer, 1990). Due to these interactions, transmembrane proteins are bound to the bilayer and cannot be easily extracted. There are also peripheral membrane proteins which do not alter the membrane structure but interact with lipids and/or proteins located intra- or extracellularly (Alberts, 1994).

Oligosaccharide chains may also attach to proteins (i.e. glycoproteins) at the cellular surface. Oligosaccharide chain extensions from proteins and lipids form a carbohydrate zone called the glycocalyx at the cell surface, which primarily functions to provide cell recognition (Alberts, 1994). The glycocalyx may also be utilized in bioadhesive drug delivery, in which interaction between polymer chains and oligosaccharides provides a strong attachment zone for drug localization and increased delivery system residence time.

Transmembrane proteins are important in terms of molecular transport across membranes by providing hydrophilic spaces (i.e. pores), enabling passive diffusion of water and electrolytes, and extracellular receptors, which generate

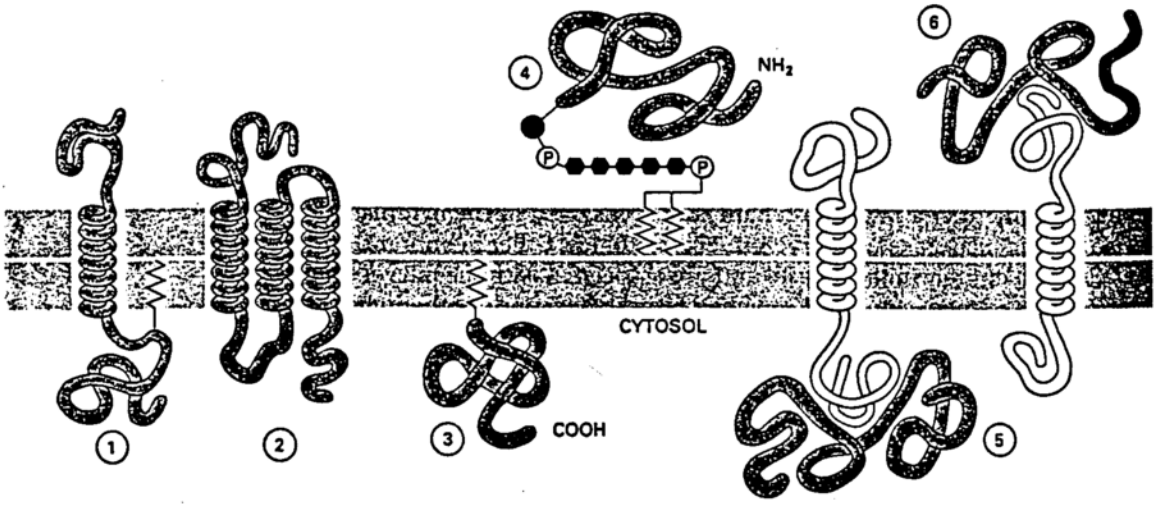

Figure 2.2: Illustration of the various ways proteins interact with the membrane lipid bilayer. Proteins may: (1) span the length of the bilayer once or (2) multiple times. Some proteins are attached to the membrane by: (3) covalent attachment to a lipid, (4) via an oligosaccharide attached to a lipid, or (5), (6) noncovalent interaction with a membrane protein. (Modified from Alberts, B., et. al., 1994).

various intracellular signals and promote molecular transport when stimulated.

The hydrophobic nature of the membrane interior creates a diffusive barrier to polar molecules which allows the cell to regulate critical concentrations of polar solutes within the cytosol. Small polar molecules (18-60 daltons), such as ions and water, are able to cross into the cytosol vial channel proteins. Non-polar solutes are typically rapidly absorbed into or diffuse across the cell membrane at significantly faster rates than their polar counterparts.

Oil/water partition coefficients ($K_{o/w}$) for a variety of gases are listed in Table 2.1. As with other solute molecules, the larger the $K_{o/w}$, the greater the potential for incorporation into the hydrophobic cell membrane regions. As shown in Table 2.1, most gases are hydrophobic, which limits the membrane as a barrier for these molecules. CO_2, which plays an important role in respiration and cellular acid-base regulation, has been shown to have high solubility and diffusion rates within lipid bilayers (Burkard, 1995; Gutknecht, 1977; Simon, 1980). CO_2 can exist in a number of different chemical forms such as HCO_3^-, CO_3^{2-}, and H_2CO_3, in which the ionic species do not easily diffuse into or across cell membranes as compared to their neutral counterparts (Gutknecht, 1977).

In a biological system, where there is a high concentration of hydrophobic gases within the extracellular environment, one would expect an increase in hydrophobicity near the membrane surface. There would also be the potential for a large quantity of the gas molecules to be absorbed within the lipid cell bilayer as well as diffusing across the bilayer into the cytosol via a concentration gradient. Due to the hydrophobic nature of the gas, partitioning of these molecules into the bilayer (Figure 2.3) would impart a greater "overall" hydrophobicity to the membrane, leading to enhanced partitioning of nonpolar drug molecules. This would lead to a faster drug absorption (i.e., a faster time to

Table 2.1: Gas partition coefficients.

Gas	Partition Coefficient (oil/water) (log $K_{o/w}$) [c,d]
Argon	5.3
Helium	1.7
Nitrogen	5.2
Oxygen	4.4 [(a)]
Carbon Dioxide	1.7 [(b)]
Krypton	9.6
Hydrogen	3.1
Nitrous oxide	17.0
Cyclopropane	35.0
Ethyl ether	3.2

(a) $K_{o/w}$ determined between erythrocyte membrane and aqueous phase, data obtained from (Fischkoff, S., et. al., 1975)

(b) Gutknecht, J., et. al., 1977

(c) 37 - 38°C, data obtained from (Altman, P.L., et.al., 1971); oil = octanol

(d) oil = octanol unless otherwise indicated

maximal drug absorption), and possibly, greater absorption profiles.

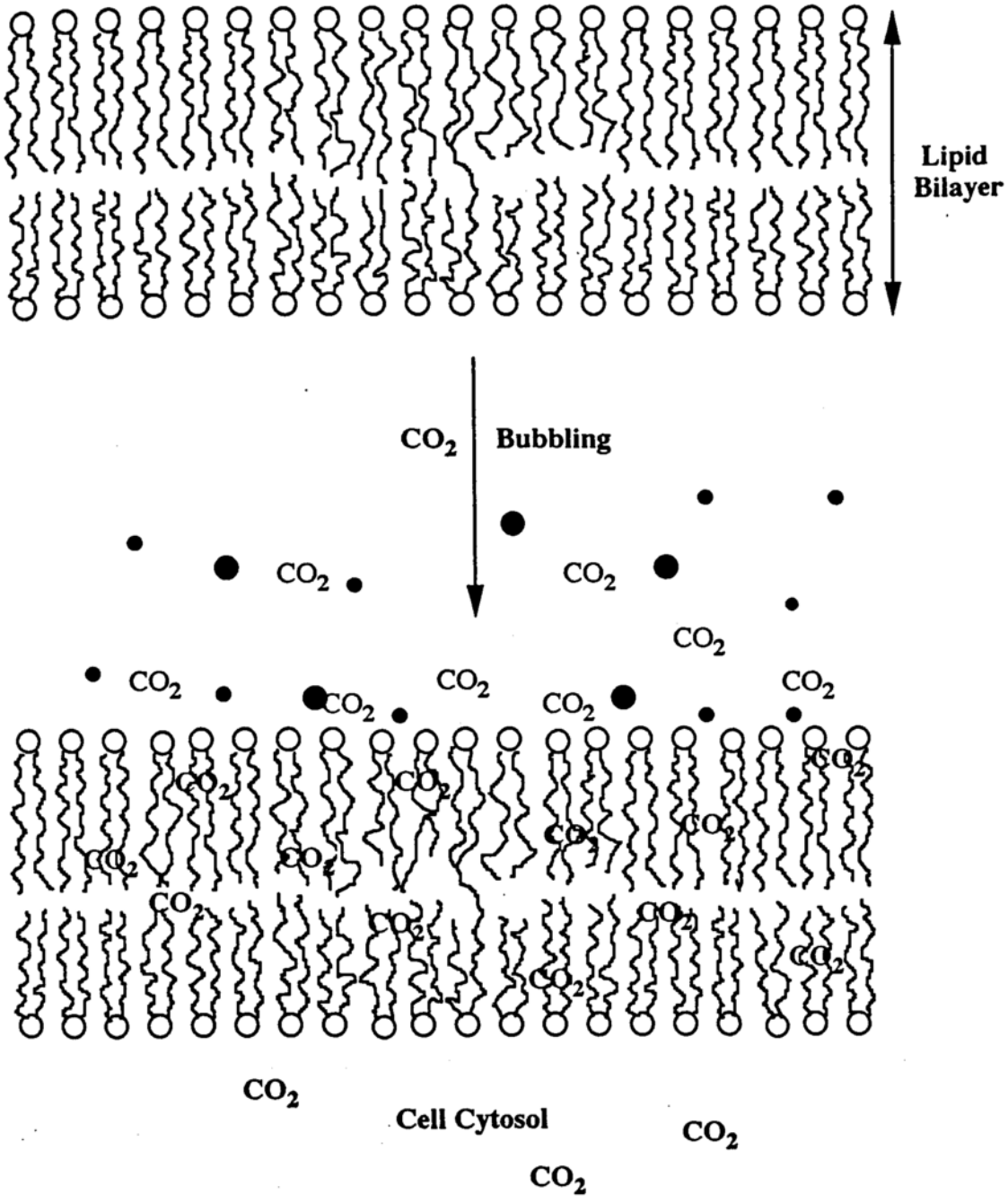

Figure 2.3: Schematic of carbon dioxide bubbles initially within the intestinal lumen with subsequent partitioning into the hydrophobic membrane bilayer. CO_2 may either: (1) dissolve within the membrane increasing the overall hydrophobicity of the membrane; (2) diffuse across the membrane into the cytosol; and/or (3) induce a hydrophobic environment near the membrane surface. CO_2 = dissolved molecule within lumen, membrane, or cytosol. ● = CO_2 gas bubble.

Chapter 3: The Influence of Effervescence on Gastrointestinal Physiological Processes

I. Stomach Emptying

Humans and other animals which consume food on a discrete basis have two patterns of gastrointestinal motility: fasted and fed (Liaw, 1990). In the fasted state, gastrointestinal motility is characterized by the Migrating Motor Complex (MMC). The MMC begins in the stomach and propagates to the terminal end of the small intestine. The MMC (Figure 3.1) is a repetitive cycle commonly organized into four phases of alternating activity and rest. Phase I is a quiescent period absent of contractions or electrical activity. Phase II is characterized by intermittent or random contractions lasting anywhere from 20 to 40 minutes. Phase III is the period of continuous peristaltic contractions of maximum frequency which clears the stomach of all residual material (i.e., the housekeeper wave), and phase IV, a transition period between phase III and phase I with decreasing contractions (Gupta, 1990). A complete MMC cycle on average ranges from 1.5 to 2 hours. The cycle may be interrupted during any phase by the conversion of the stomach from a fasted to a fed state. The fed state, induced by consumption of food and/or large volumes of liquid, is characterized by a prolonged period of continuous contractions known as "proprandial motility" and may continue for up to 8 hours depending on the type and amount of food ingested (Gupta, 1990). The stomach relaxes as food enters precipitating gradual

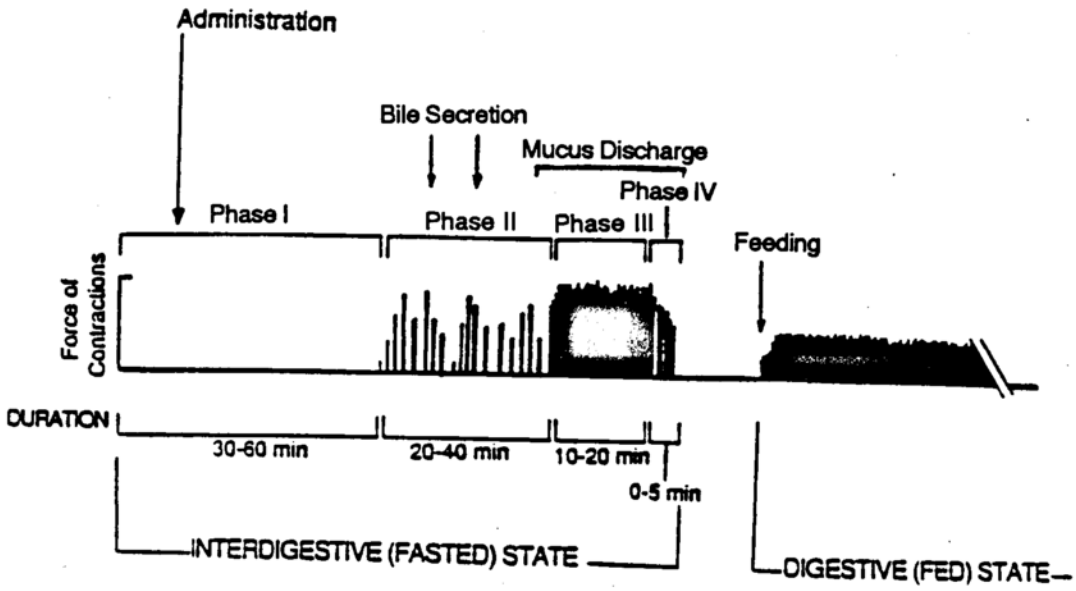

Figure 3.1: A representation of typical motility patterns in the fasted and fed state in the dog. (Reproduced from Liaw, J., et. al., 1990).

peristaltic contractions which function to move contents toward the pyloric sphinctor and to slowly break down large food particles. Food too large to empty through the pylorus is retropulsed back into the stomach body for further size reduction (Seeley, 1996).

Gastric emptying of liquids is proportional to the amount of liquid remaining in the stomach, thus it follows first order kinetics (Gupta, 1990). When liquids are administered while the stomach is in the fasted state, the MMC is affected only by large volumes. With small volumes of 100 ml or less, the gastrointestinal pressure gradient is insignificant in that the MMC will not be disrupted and emptying will mostly occur during phase II and/or phase III. When large volumes of 150 ml or more are administered, an increase in pressure (i.e. distention) within the proximal stomach is sensed. Therefore, the MMC is disrupted and immediately converts the stomach into the fed state. Liquid emptying patterns from the stomach are very important in that the absorption profile of an oral drug may be altered. For example, a drug which is highly unstable within an acidic gastric medium would see its absorption enhanced by a reduction in its gastric retention time. By converting the stomach from fasted to a fed state, a large portion of the drug would be quickly transferred into the small intestine, creating an opportunity for greater drug stability and absorption enhancement.

Effervescent formulations provide a method for conversion of the stomach to the "fed-like" state. In a recent study utilizing a cannulated dog model (Yassin, 1996), the rate of stomach discharge for small volumes (50 ml) of a carbonated solution was compared to equal volumes of control and non-carbonated solutions. The solutions were introduced into the animal's stomach while in the fasted state. The rate of discharge for the non-carbonated and control solutions were consistent with previously reported findings by Gupta and Robinson (Gupta,

1990). The non-effervescent and control solutions did not induce a pressure gradient across the gastroduodenal junction, therefore, the stomach remained in its relaxed state (phase I). The total volume discharged after 90 minutes for all solutions was 20% higher; the increase is attributed to normal gastric and pancreatic secretions. Three carbonated solutions (50 ml) with various degrees of carbonation (Table 3.1) were tested as well. Figure 3.2 illustrates the solution

---

Table 3.1: Test solutions and amounts of effervescent mixture components utilized for cannulated dog experiments. (Modified from Yassin, A.E., 1996).

Test Solution	Sodium Bicarbonate (g)	Citric Acid (g)	Water (ml)	Theoretical Molar CO_2 Concentration (M)
Water	----	----	50	----
EFF I (control)	0.656	0.500	50	----
EFF I	0.656	0.500	50	6.7×10^{-3}
EFF II (control)	1.312	1.000	50	----
EFF II	1.312	1.000	50	1.33×10^{-2}
EFF III (control)	1.968	1.500	50	----
EFF III	1.968	1.500	50	2.00×10^{-2}

---

with the lowest amount of carbonation (EFF I) had discharge rates similar to the non-carbonated water and control solutions. The other carbonated solutions, EFF II and EFF III, produced greater quantities of CO_2 and followed a completely

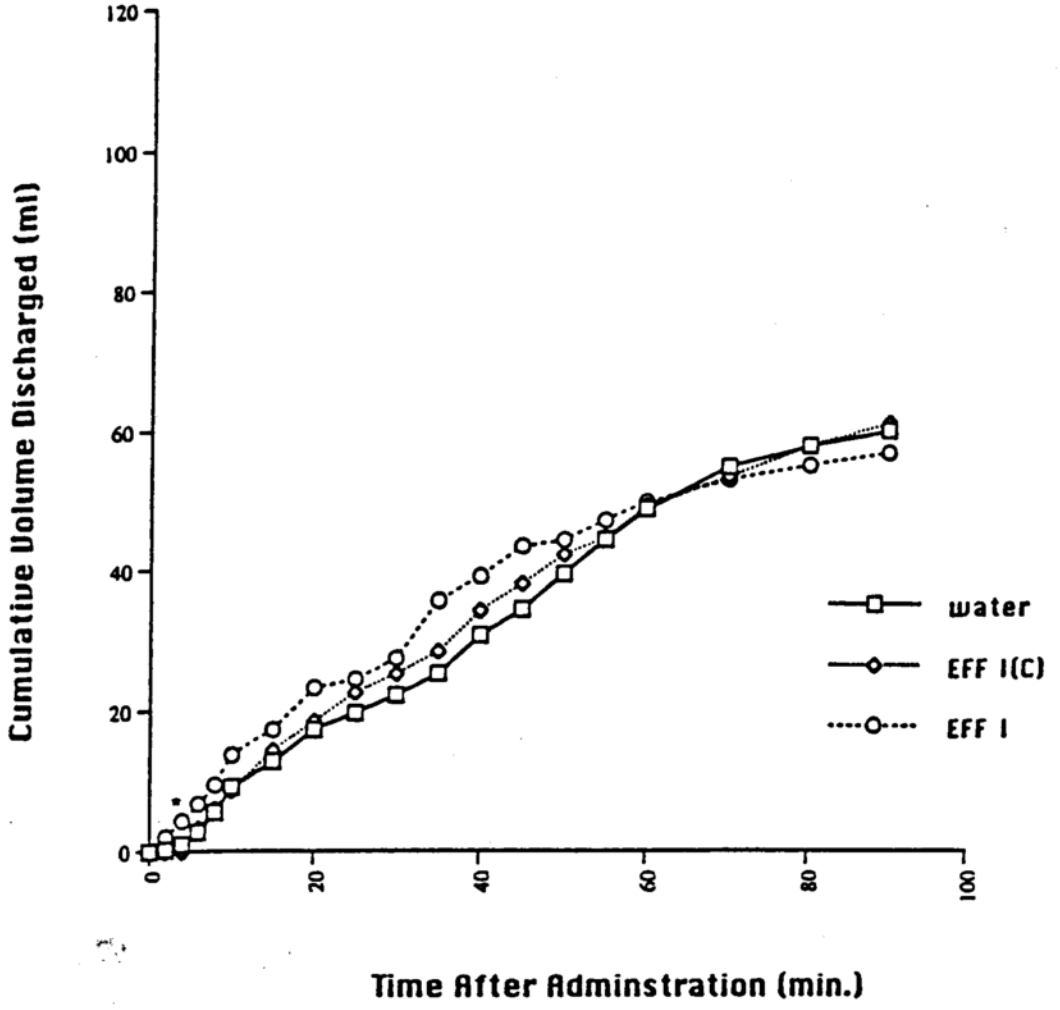

Figure 3.2: Gastric emptying of 50 ml water, EFF I, and its control solution administered during phase I in the fasted dog. * indicates significant difference ($p < 0.01$). (From Eichman, J., et. al., 1997).

different fluid discharge pattern when compared to controls (Figs. 3.3 and 3.4). Both solutions discharged immediately after administration and most of the fluid was emptied within the first 20 minutes. This pattern followed previously reported findings for large volume solutions by Hinder et. al. (Hinder, 1977) and Gupta et. al. (Gupta, 1990). The $t_{1/2}$ for EFF I, EFF II, EFF III, which is the time at which half of the administered volume is discharged, was 25.8, 7.4, and 7.2 min., respectively. When compared to the $t_{1/2}$ (35 min.) for the non-carbonated water solution and for the EFF I, EFF II, EFF III controls, 30.50, 33.00, and 27.10 min., respectively, EFF II and EFF III seemed to create enough CO_2 in order to increase the pressure within the stomach. This created a change in the motility pattern from the fasted to "fed-like" state (i.e., pseudo-fed).

Therefore, intake of small volumes of a carbonated drug solution would mimic the stomach discharge pattern for large volumes of a non-carbonated fluid. This would be useful in obtaining prompt blood levels for pediatric and geriatric patients when small fluid volumes are ingested.

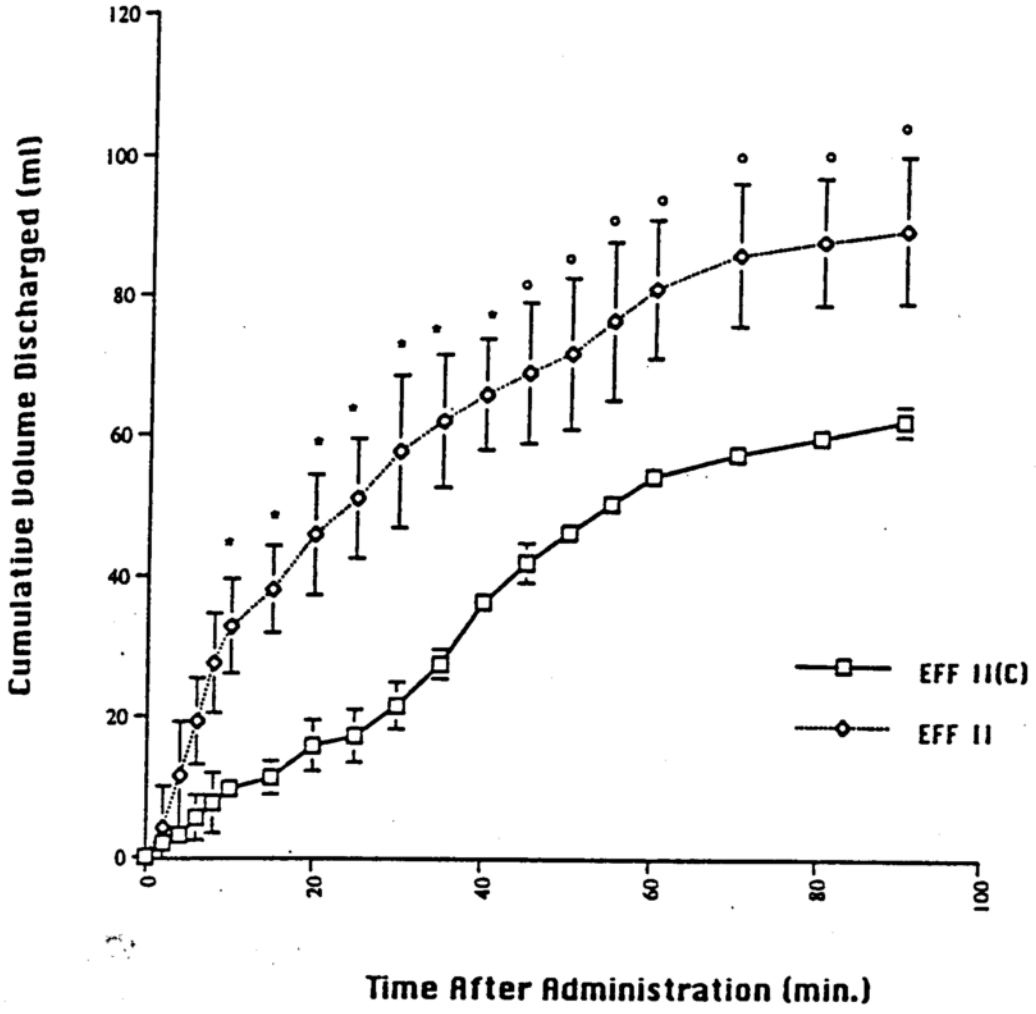

Figure 3.3: Gastric emptying of 50 ml of EFF II, and its control solution, administered during phase I in the fasted dog. * indicates significant difference at p = 0.01. ° indicates significant difference at p = 0.05. (From Eichman, J., et. al., 1997).

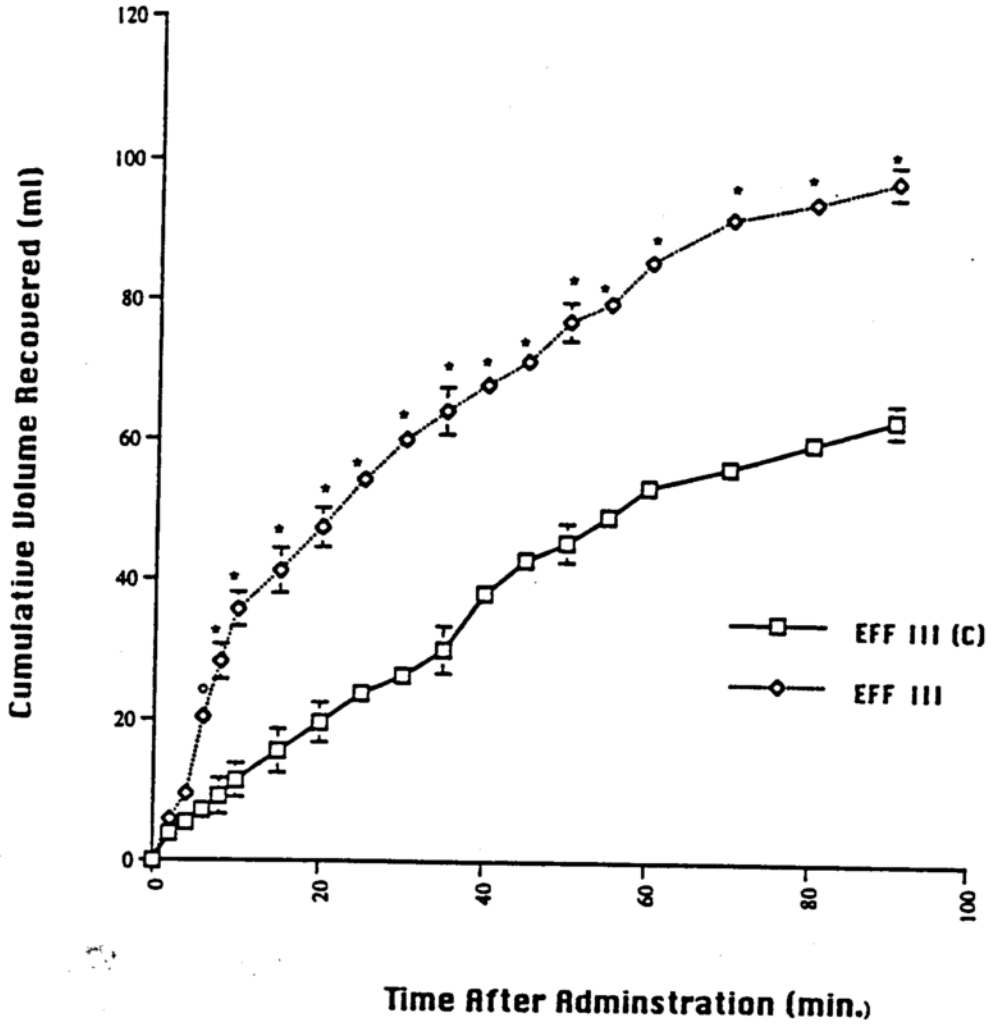

Figure 3.4: Gastric emptying of 50 ml of EFF III and its control solution, administered during phase I in the fasted dog. * indicates significant difference at p = 0.01. ° indicates significant difference at p = 0.05. (From Eichman, J., et. al., 1997)

II. Intestinal Transit

The intestinal transit rate is the primary factor governing the amount of time a dosage form has for drug release, dissolution, and absorption across a particular intestinal segment. Segmentation and propulsion (e.g. peristalsis) are the primary movements within the small intestine in which segmental contractions function to mix intestinal contents while peristaltic waves move the food and liquid down the intestinal tract at a rate of 1 to 2 cm/sec (Mayersohn, 1996). Peristaltic activity corresponds to the fasted or fed state of the stomach, such that, after meal ingestion, there is an increase in intestinal motility and secretion (Mayersohn, 1996). However, the small intestine is incapable of distinguishing between solids and liquids, which have similar transit times (Ashford, 1994). The total transit time for materials to travel from the duodenal cap to the ileo-cecal junction is ≈ 2 to 4 hours (Davis, 1986; Gruber, 1987). After expulsion from the stomach, solids and liquids rapidly move through the duodenum within 2 to 60 seconds (Parr, 1997) leaving only a brief period for absorption across the primary absorptive region of the gastrointestinal tract. Therefore, dissolution of a large percentage of drug prior to transport through the duodenum is required for significant absorption. Movement slows down through the jejunum and ileum segments, taking 2 to 4 hours, which allows an increase in absorption time but with substantially less absorptive surface area (Parr, 1997).

The ileo-cecal junction regulates the movement of material from the small to large intestine. The sphincter between the two organs is continuously kept under a mild contractive state except to when it relaxes due to an incoming peristaltic wave initiated from the upper intestine (Seeley, 1996). The relaxed sphincter

allows movement of material in only one direction, from the ileum into the large intestine.

The primary function of the colon is water and electrolyte absorption, in addition to storage of excrement prior to expulsion from the body. One may associate these functions to a rather sluggish transit time of ≈ 36 to 48 hours (Webber, 1987). There are two types of contractions within the colon; propulsive and segmental (i.e. haustrations). Propulsive contractions are weak and associated with "bowel movements" that occur 3 to 4 times daily. Segmental contractions produce bulges that give the intestine a "sac-like" appearance and serve only to mix the luminal contents (Mayersohn, 1996). Colonic transit is characterized by long periods of inactivity with only short lived bursts of activity commonly associated with food ingestion.

Due to the long duration of transit within the large intestine, drug delivery to this region has received substantial interest within the past two decades. Drugs which need prolonged absorption times to obtain therapeutic blood concentrations have been targeted to this region for possible absorption enhancement.

Effervescent technology may provide better results in delivering certain therapeutic agents dependent on intestinal transit rates. One possibility previously mentioned in Chapter 2 is the effervescent effect on drug dissolution. Since drug movement through the proximal portion of the gastrointestinal tract is quite rapid, compounds with slow dissolution rates or limited solubility will not have the potential to obtain a significant fraction of the dose absorbed across the duodenal epithelium. Enhancement of dissolution rates via effervescence production within the stomach would promote increased solubility leading to a greater fraction of drug available for rapid absorption across the duodenum.

Since effervescence converts the stomach to a "fed-like" state, there would also be a reduction in small intestinal residence time for a drug delivery system. This could be advantageous for oral peptide or protein drug delivery. The small intestine contains a high concentration of enzymes compared to that of the colon. Therefore, an increased transit rate through the small intestine would allow a greater proportion of protein to elude enzymatic degradation in addition to promoting faster absorption profiles from the colon. This concept could be applied to a number of drug compounds whose absorption and/or stability is limited within the upper gastrointestinal regions to that of the colon.

III. Mucus Stripping

Mucus is secreted as a fully hydrated viscoelastic gel which adheres to biological surfaces including; mouth, ear, eye, nose, respiratory tract, vaginal surface, and gastrointestinal tract. The primary function of mucus is to create a barrier which protects epithelial cells from chemical and physical disruption. This barrier also prevents the passage of bacterial and other harmful materials posing as potential hazards for infection and/or precipitating an immunological response. The main component of mucus creating the viscoelastic property is referred to as mucin or glycoproteins. These glycoproteins range in MW from 2×10^5 to 10×10^6 and consist of carbohydrate side chains extending from a proteinacous core (Allen, 1994). Protein cores of adjacent glycoproteins are connected by disulfide bonds, producing blocks of linked glycoprotein molecules. Noncovalent bonding, which is believed to consist of hydrogen bonds among the carbohydrate entities, hold different complexes together, creating the viscoelastic gel (Allen, 1994).

Mucus is continuously produced via secretion of a variety of sources which include; intestinal goblet cells, stomach glands (fundic, cardiac, and pyloric), and Brunner's glands within the duodenum (Allen, 1994). The major source of mucus in the gastrointestinal tract are goblet cells. Goblet cells are found in both the small and large intestines, where they increase in number from 25% of total surface cells in the duodenum to 39% in the ileum and to 60% in the colon (Allen, 1994). Mucus undergoes proteolytic decomposition by enzymes within the gastrointestinal tract. Since pepsin is capable of destroying nonglycosylated glycoprotein gel within 20 minutes, secretion of mucin glycoprotein is necessary in order to provide complete and continuous coverage of the intestinal epithelium.

Chemicals may also stimulate or inhibit mucus production. These include; acetylcholine, serotonin, atropine, and adrenergic agents among others.

The average mucus thickness lining the gastrointestinal tract in humans is 200μm, with a range anywhere from 5 to 400μm (Allen, 1994). Mucus thickness and turnover rate within the gastrointestinal tract is not uniform but varies substantially depending upon physical, enzymatic, and/or chemical perturbance of the layer.

Effervescence within the gastrointestinal tract may be viewed as a physical disruption to the mucus layer. Production of carbon dioxide gas within the stomach or intestinal lumen would create rapid bubbling near the mucus layer, potentially decreasing its thickness or completely stripping the mucus gel from the epithelium. If this occurs, one would expect intestinal goblet cells and Brunner's glands to begin secretion of mucus to compensate for the loss. In the experiment previously mentioned in the stomach emptying section, the total volume discharged after administration of 50 ml of each solution was calculated. For the control and non-carbonated solutions, the total volume discharged after 90 minutes was 20% higher and is attributed to normal gastric and pancreatic secretions. EFF I solution did not vary in total volume discharge when compared to 50 ml of water or its control solution. However, the higher carbonated solutions, EFF II and EFF III, showed a significant increase in total discharge volume, 89.74 ml and 97.40 ml respectively, when compared to a total of 60.0 ml for their control solutions (Eichman, 1997). The average solids content (Table 3.2) was also obtained after freeze-drying of 20 ml samples which were taken from total homogenate cannula discharge effluent 90 min. after administration. The mean solids content obtained from EFF II and EFF III were significantly greater than their corresponding control solutions. Again, EFF I showed insignifi-

Table 3.2: Mean weight residues after freeze drying 20.0 ml samples taken from total discharge. Modified from (Eichman, J., et. al., 1997)

Test Solution	Residue Weight (g)	Standard Deviation (±)
No Solution	0.375	0.019
EFF I (control)	0.439	0.036
EFF I	0.453	0.045
EFF II (control)	0.496	0.065
EFF II	0.673	0.041
EFF III (control)	0.542	0.053
EFF III	0.874	0.071

cant difference from its control (Eichman, 1997). These results may be explained in terms of mechanical turbulence caused by CO_2 production. The turbulence created by the bubbling action causes a thinning and/or stripping of mucus. Additionally, alteration of the mucus layer will produce stimulation of mucus and gastric secretions which may account for some of the increase in total discharge volume and weight residues seen with EFF II and EFF III.

Chapter 4: The Influence of Effervescence on Penetration Enhancement

I. Background

Effervescent dosage forms have the potential for increasing the amount of drug transversing the gastrointestinal epithelium. The first indication of a penetration enhancement effect was shown in a study examining oral caffeine absorption from cold, hot, and effervescent solutions. As indicated in Figure 4.1, the time to reach maximum (t_{max}) caffeine blood concentration (C_{max}) from the effervescent solution was faster than the other two solutions. T_{max} is a pharmacokinetic variable whose value can be obtained by equation 1. The value is independent of a given dose but is dependent on the absorption and elimination rate constants, k_a and k_e, respectively (Rowland, 1995; Shargel, 1993).

$$t_{max} = \frac{1}{k_a - k_e} \ln \left(\frac{k_a}{k_e}\right) \qquad (1)$$

Therefore, the effervescent profile indicating a shorter t_{max} must be based on an increase in the absorption rate constant. In other words, this type of profile is indicative of a decline in the barrier properties associated with the gastrointestinal epithelial monolayer. Other effervescent properties which must also be taken into

consideration when examining this outcome are its effects on mucus stripping, stomach emptying, fluid flow, and membrane hydrophobicity. Other drugs which have been demonstrated to have shorter t_{max} values within effervescent preparations include: amoxicillin, diflunisal, ranitidine, cimetidine, and ibuprofen (Hatlebakk, 1996; Hespe, 1987; Luckow, 1992; Menzel, 1993; Nuernberg, 1989; Watson, 1996). As an example, effervescent cimetidine reached an effective therapeutic plasma concentration within 11 minutes, compared to 34 minutes for a standard tablet preparation (Hatlebakk, 1996).

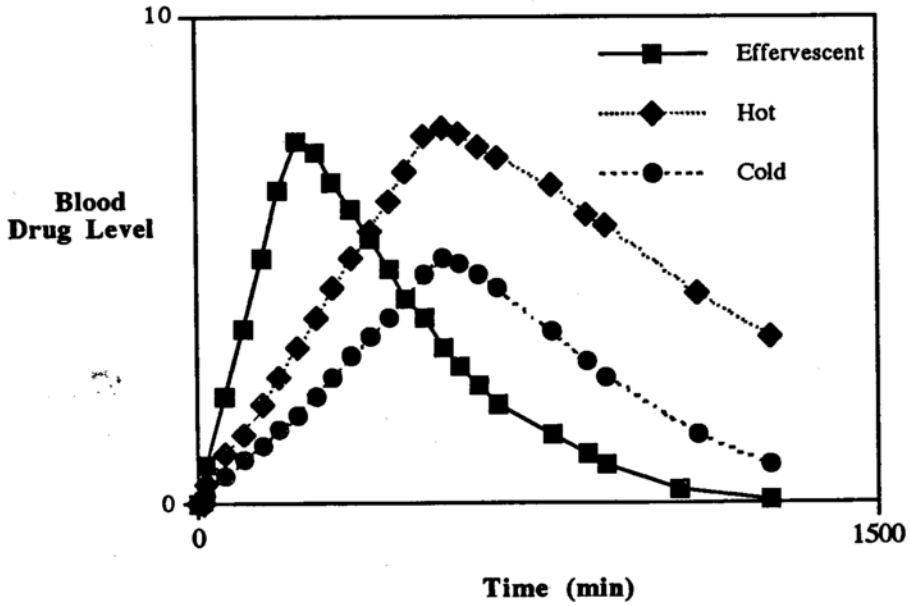

Figure 4.1: Oral caffeine absorption from a cold, hot, and effervescent solution.

Effervescent formulations have also generated superior drug concentration levels as indicated by greater area under the curve (AUC) values obtained from plasma concentration vs. time profiles than those of non-effervescent dosage forms. The AUC is related to the total amount of drug absorbed into the systemic circulation. This effect is exemplified by a study comparing the bioavailability of disulfiram (Antabuse®) after oral administration of non-effervescent and effervescent tablets. As indicated in Figure 4.2, the effervescent system demonstrated superior bioavailability with no significant difference relating to t_{max} values (Andersen, 1992). This type of profile may be attributed to contributions from a buffering effect, increase in dissolution rate, and/or alteration of the intestinal pH gradient. Examples of other drugs with similar profiles include: propoxyphene, aspirin, and paracetamol (Petersen, 1982; Wagner, 1995).

Although studies have shown differences in bioavailability and other pharmacokinetic parameters, most investigators have neglected to investigate the exact reasons for differences obtained between effervescent and non-effervescent dosage forms. Usually, the studies postulate that differences are due to an increased dissolution rate or a buffering/solubility mechanism. The following chapter will investigate the effect of effervescence on in-vitro and in-vivo drug absorption on a variety of drug compounds which differ in size, structure, and properties.

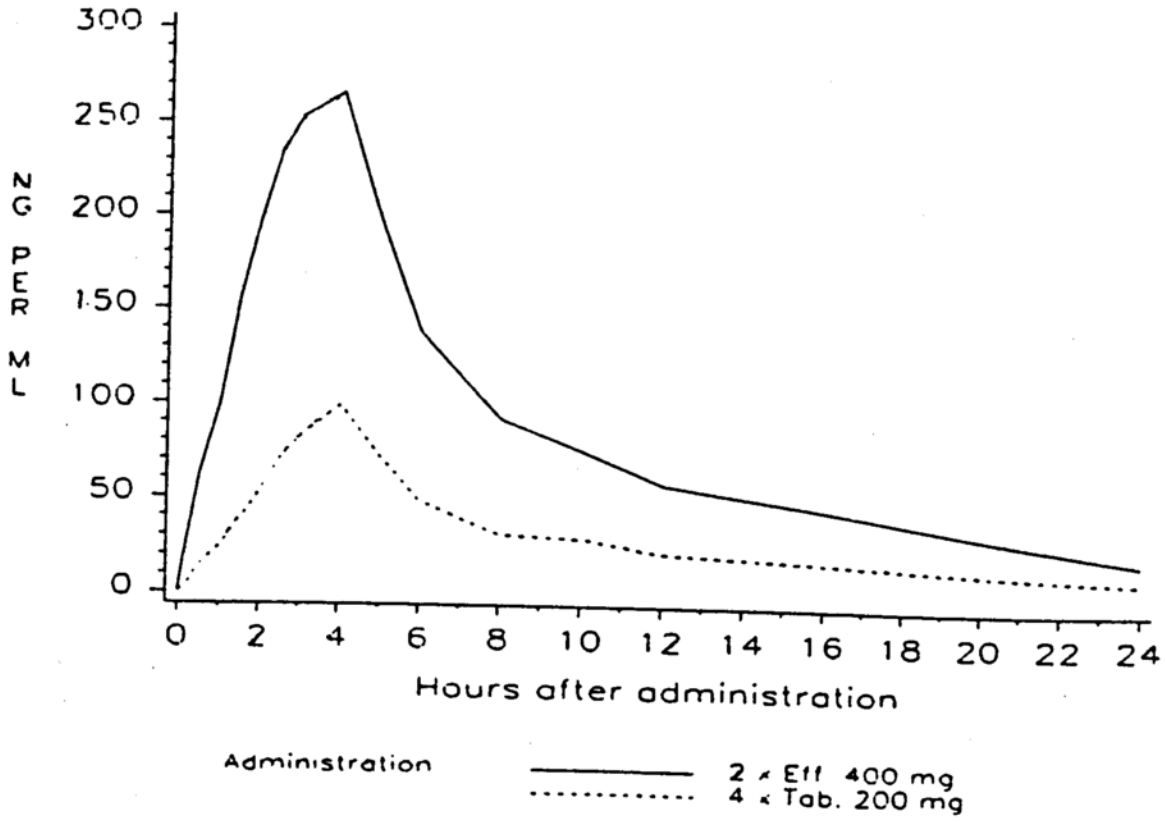

Figure 4.2: Mean serum concentrations of a disulfiram metabolite, methyl diethyldithiocarbamate (Me-DDC) after administration of Antabuse® effervescent or standard tablets. Me-DDC is commonly used as a measurement of the relative bioavailability of disulfiram. (Reproduced from Andesen, M.P., 1992)

II. Experimental

A. In-Vitro Permeability Studies

1. Materials

Unless otherwise noted, all chemicals were used as received and all solutions were prepared with distilled deionized water (DDW) which had been run through a Barnstead PCS water purification system (Sybron Corp., Boston, MA).

^{14}C-Benzoic acid (22.0 mCi/mmol), ^{3}H-polyethylene glycol (MW 900; 2.23 mCi/g), ^{3}H-polyethylene glycol (MW 4000; 2.0 mCi/g), ^{3}H-mannitol (22.5 mCi/mmol), ^{14}C-caffeine (53.3 mCi/mmol), and ^{3}H-tetracycline (1.0 mCi/mmol) were purchased from Dupont NEN Research Products (Wilmington, DE). ^{14}C-Diazepam (55.0 mCi/mmol) was purchased from Amersham Life Sciences, Inc. (Arlington Heights, IL). Benzoic acid, tetracycline, sodium phosphate monobasic, and sodium pentobarbital were obtained from Sigma Chemical Company (St. Louis, MO). Sodium phosphate dibasic was purchased from Fisher Scientific Company (Fair Lawn, NJ). Sodium chloride (NaCl), mannitol, caffeine, polyethylene glycol 900 (PEG 900) were procured from Aldrich Chemical Company, Inc. (Milwaukee, WI). Ethanol was obtained from Pharmco Products, Inc. (Brookfield, CT).

2. Solutions

Sorenson's phosphate buffer was used in all studies. Aliquots of sodium phosphate monobasic (acid stock) and sodium phosphate dibasic (alkaline stock) stock solutions were combined at a ratio of 70:30, respectively, to obtain pH 6.5 buffer. Solution pH was measured with an analog pH meter (Orion Research Inc.; Model 301; Cambridge, MA) and was adjusted to 6.5 by addition of acid or alkaline stock solution. Osmolarity was measured on a Wescor 5500 vapor pressure osmometer (Wescor, Inc.; Logan, UT) and adjusted to 300 mOsm (± 10 mOsm) with sodium chloride. Sodium phosphate buffer (pH 6.8; 300 mOsm) was prepared in a similar fashion, in which the initial mixture of acid and alkaline stock solutions was 50:50, respectively.

Separate buffer solutions containing a 0.15% (w/v) concentration of mannitol, PEG 900, PEG 4000, caffeine, tetracycline, and benzoic acid were also individually prepared by the method mentioned above

Radiolabeled ^{14}C-benzoic acid, ^{3}H-tetracycline, ^{3}H-PEG 900, and ^{3}H-PEG 4000 were received in solid form. ^{14}C-benzoic acid was dissolved in 5.0 ml DDW which led to a final stock concentration of 100 μCi/ml. ^{3}H-PEG 900 and ^{3}H-PEG 4000 were dissolved in 5.0 ml of a 3% ethanol/DDW solution, producing a 50 μCi/ml stock solution for each compound. ^{3}H-tetracycline was dissolved in 5.0 ml methanol producing a 50μCi/ml stock solution. 300 μl aliquots of tetracycline stock were pipetted into microcentrifuge tubes and placed at -20°C until needed. The other radioactive materials were obtained predissolved by the manufacturer.

3. Gastrointestinal Tissue Excision

Male Sprague-Dawley rats (Harlan Sprague-Dawley, Inc.; Madison, WI) weighing 325 - 349 g and male albino New Zealand rabbits (Bakkom's Rabbitry, Viroqua, WI) weighing between 5.0 - 5.5 lbs were maintained on an unrestricted diet with standard caging facilities and a 12 hour light/dark cycle. The rats were sacrificed by exposure to carbon dioxide. Rabbits were sacrificed by a 10 ml injection of 5% sodium pentobarbital solution into a marginal ear vein. The animal's abdominal wall was exposed and a surgical incision down the midline was performed with a scalpel. An 8 to 10 cm intestinal segment was excised and placed in ice cold saline. The epithelium was exposed via a longitudinal incision along the mesenterium, washed with ice cold saline, and mounted into the diffusion cell (see below).

4. Diffusion Cells

The diffusion cell (Figure 4.3; Jim's Instrument Manufacturing, Inc., Iowa City, IA; UW Machine Shop, Madison, WI) utilized in the experiments is a modification of the cell described by Schoenwald and originally designed for corneal permeability studies (Schoenwald, 1983). There are two acrylic cells, referred to as the donor and receiver chambers, having circular indentions which allow insertion of tissue holders between the two chambers. The tissue is impaled on stainless steel spikes imbedded within the acrylic inserts which holds the tissue firmly in place. The surface area exposed by the inserts ranges from 0.196 to 0.785 cm^2 depending on experimental conditions and amount of available tissue.

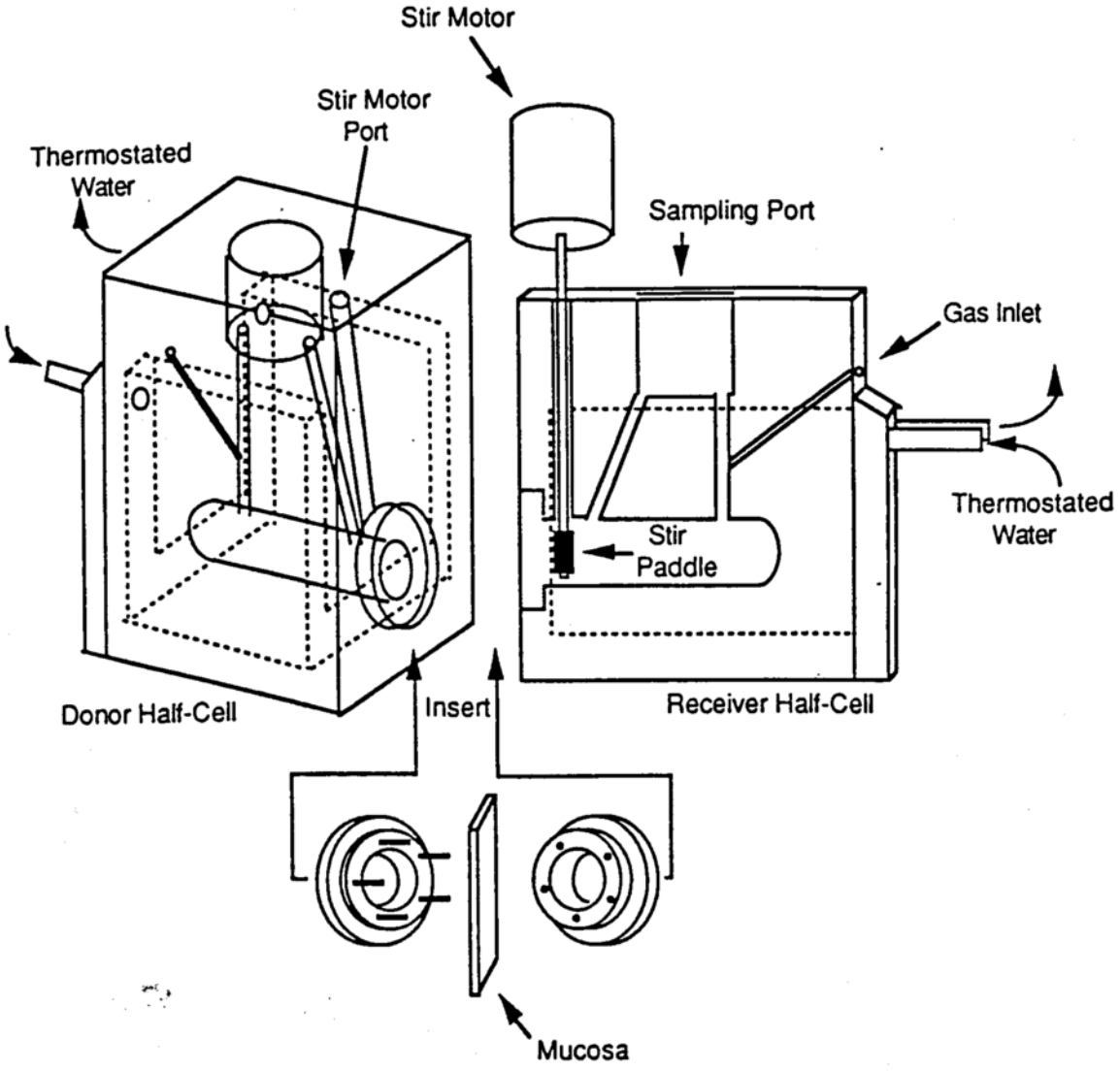

Figure 4.3: Illustration of the acrylic diffusion cell and insert used for in-vitro permeability experiments. (Reproduced from Dowty, 1991).

When placed between the cell chambers, the insert is held firmly in position by screw clamps which compress the chambers together.

The bathing buffer volume within the donor and receiver chambers may be varied from 4.0 to 7.0 ml for experimental requirements and is kept at 37°C by a circulating water jacket surrounding each chamber. Teflon washers coated with a thin layer of silicon lubricant (Dow Corning high vacuum grease) are placed between the insert and diffusion cell chambers, preventing buffer leakage. Gas bubbles (95% O_2 / 5% CO_2) or stirrers are used to mix the buffer solution within each chamber. Stirrers, connected to an electrical 9 volt motor, may be inserted through a cylindrical opening leading to a location near the tissue surface. The paddles at the end of the stirrer rotate and effectively stir the solution.

5. Drug Permeability Studies

a. Stirrers

The diffusion cell mentioned above was utilized for drug permeability studies. Rat or rabbit intestinal tissue (duodenum; ileum) was cleaned, mounted onto acrylic inserts, and placed between the chambers with the mucosal surface facing the donor chamber. 0.15% mannitol, benzoic acid, caffeine, tetracycline, PEG 900, and PEG 4000 donor buffer solutions (35 ml) were spiked with ^{3}H-mannitol (7.0 μCi), ^{14}C-benzoic acid (7.5 μCi), ^{14}C-caffeine (3.5 μCi), ^{3}H-tetracycline (11.5 μCi), ^{3}H-PEG 900 (12.0 μCi), ^{3}H-PEG 4000 (10.0 μCi), respectively. ^{14}C-Diazepam (3.5 μCi) was placed in 35 ml pure buffer. The donor and receiver solutions were prewarmed to 37°C at which time 7.0 ml of receiver buffer

(duodenum: pH 6.5; ileum: pH 6.8) was inserted into its respective chamber with a 10 ml syringe followed by placement of an equivalent amount of donor solution (duodenum: pH 6.5; ileum: pH 6.8) into the donor chamber. The tissue surface area exposed for the rat and rabbit permeability experiments were 0.196 cm^2 and 0.785 cm^2, respectively.

Electronically driven stirrers (Jim's Manufacturing, Inc., Iowa City, IA) were placed in both chambers approximately 1.0 cm from the tissue surface. The stirring rate was maintained by a control setting associated with a 9V motor (Model Rectifier Corp., Edison, NJ).

Prior to initiation of the experiment, 1.0 ml of the donor stock solution was collected and used to determine initial radioactivity concentration. At pre-designated time points, 1.0 ml of receiver solution was withdrawn from the receiver compartment and replaced with 1.0 ml of prewarmed non-radioactive buffer. At the conclusion of each experiment, 1.0 ml samples were taken from each donor chamber in order to ensure that solubility problems were not encountered. Each sample was placed into a 20 ml scintillation vial and combined with 10 ml Biosafe II scintillation counting cocktail (Research International, Mount Prospect, IL). The vial contents were shaken prior to assaying for disintegrations per minute (dpm) on a single label quench correction program utilizing the TriCarb 2000CA scintillation counter (Packard Instrument Co., Downers Grove, IL). Upon conclusion of the experiment, the cells were thoroughly cleaned with a surfactant solution, Radiacwash (Biodex Medical Systems, Inc., Shirley, NY), preventing radioactive contamination between experiments. After washing, a wipe-test was performed on each chamber to ensure radioactive and background counts were at comparable levels.

Figure A.2 (Appendix A) depicts a typical permeability plot in which the permeability coefficient, P, is calculated from the steady state slope , dC/dt, via the equation:

$$P = \frac{V}{A \times C_0} \left(\frac{dC}{dt}\right) \quad (2)$$

where V = volume (7.0 ml), A = tissue surface area (0.196 or 0.785 cm^2), and C_o = the initial concentration in the donor chamber (100%). An in depth analysis of a typical permeability plot, including discussion of the time needed for a drug to reach steady state permeability (i.e. lag time) across a membrane, is included in Appendix A.

b. Carbon Dioxide

In carbon dioxide studies, the same procedure was utilized as previously mentioned (see above) except for a few differences. First, a stirrer was placed only in the receiver chamber. In the donor chamber, the stirrer was replaced with a piece of thin rubber tubing approximately 2 mm in diameter and situated ≈ 1.0 cm from the tissue surface. The tube was slightly curved at the lower tip allowing gas bubbles to directly contact the epithelium. The tube was connected via a pipette tip to tygon tubing which was attached to two separate gas cylinders; pure CO_2 and 95% O_2 / 5% CO_2. The two gases were bubbled onto the tissue surface at a rate which did not induce solution spillage from either chamber and was kept

constant between experiments. In comparison to CO_2, very minute quantities (< 3%) of 95% O_2 / 5% CO_2 was bubbled onto the tissue preventing tissue hypoxia. The gas was bubbled onto the tissue surface at a slow enough rate so as not to alter (reduce) the system's temperature (37°C). In other words, the temperature of the gas outflowing from the cylinders quickly equilibrated to solution temperature prior to initiating tissue contact.

c. Nitrogen

The same procedure was used as mentioned under the carbon dioxide section (see above). The tubing leading to the tissue in the donor chamber was connected to a nitrogen gas tank in addition to the 95% O_2 / 5% CO_2 tank. The bubbling rates were similar to those used in the CO_2 experiments.

B. In-Vivo Absorption Studies

1. Materials

Ketamine hydrochloride was obtained from Fort Dodge Laboratories, Inc. (Fort Dodge, IA). Xylazine was purchased from Phoenix Pharmaceuticals, Inc. (St. Joseph, MO). Ethicon sterile non-absorbable surgical string (60 cm) was

procured from Johnson & Johnson (Somerville, NJ). All chemicals were used as received from the manufacturer.

2. Surgical Technique

Male Sprague-Dawley rats (Harlan Sprague-Dawley, Madison, WI) weighing 400 - 450 g were fasted for 20 to 24 hours with an unrestricted water supply prior to each study. The rats were anesthetized with a 0.4 ml intramuscular injection (IM) of ketamine (100 mg/ml) and xylazine (10 mg/ml) mixture with additional 0.1 ml IM injections every 30 to 45 minutes as necessary to maintain anesthesia. The rat's body temperature was maintained at 37°C by a heating pad and monitored with a rectal thermometer. All solutions were prewarmed to 37°C prior to each perfusion study.

After induction of anesthesia , a midline incision was performed with a scalpel blade exposing the inner organs. In experiments analyzing duodenum tissue absorption, an 8 cm duodenum segment was cannulated with tygon tubing. In ileum perfusion experiments, a 10 cm segment was cannulated ending 15 cm proximal to the ileo-cecal valve. Both cannulation procedures were performed so as to not inhibit circulation to the intestine. The intestinal segment was reinserted into the abdominal cavity and the abdominal wall was sutured with Ethicon 45 mm non-absorbable surgical suture (Johnson & Johnson, Somerville, NJ) to prevent heat loss. Saran wrap was placed securely over the abdominal region to further minimize loss of body heat. At the conclusion of the experiment, the rat was sacrificed via injection of 3.0 ml sodium pentobarbital directly into the heart.

3. Single-Pass Perfusion Studies

a. Without Carbon Dioxide

The cannulated segment was cleansed by perfusion of Sorenson's phosphate buffer (duodenum: pH 6.5; ileum: pH 6.8; 300 mOsm) for 30 min. at a controlled rate of ≈ 0.5 ml/min. by a cassette perfusion pump (Monostat, Inc., New York, NY). The drug solution, which was immediately perfused following the cleansing buffer, contained 0.15% benzoic acid in isotonic Sorenson's buffer with the addition of 5.0 μCi ^{14}C-benzoic acid and 1.0 μCi ^{3}H-polyethylene glycol (MW ≈ 4000). The non-absorbable marker, ^{3}H-PEG 4000, is used as an indicator of water flux into and from the luminal cavity and is also necessary for % absorbed calculations.

The radiolabeled solution was perfused once through the intestinal segment at a constant rate of ≈ 0.5 ml/min. with the resultant perfusate collected into polethylene tubes over 15 min. intervals. One milliliter perfusate samples were removed from the collecting tube, placed into a 20 ml scintillation vial, combined with 10.0 ml of Biosafe II scintillation cocktail, and shaken. The samples were assayed for disintegrations per minute (dpm) utilizing a dual labeled quench correcting program on the TriCarb 2000CA scintillation counter. The perfusate pH and osmolarity were monitored in separate experiments utilizing the same technique but with the exclusion of radiolabeled drugs.

b. Carbon Dioxide

The identical procedure was utilized in these experiments except that carbon dioxide was bubbled (rate ≈ 5.0 ml/min.) into the tygon tubing containing the radiolabeled solution just prior to its entry into the proximal portion of the cannulated segment.

The fraction of benzoic acid (BA) absorbed, F_A, from the perfusate was calculated by the equation:

$$F_A = 1 - \left[\left(\frac{^3H - PEG_{in}}{^3H - PEG_{out}}\right) x \left(\frac{^{14}C - BA_{out}}{^{14}C - BA_{in}}\right)\right] \qquad (3)$$

where in = inlet concentration and out = outlet concentration. Absorption, in this case, refers to the amount of benzoic acid disappearing from the perfusate due to uptake into blood and drug binding to mucus or tissue components.

There was no indication of benzoic acid or PEG binding onto any of the equipment utilized in the experiment (i.e. plastic tubing, collecting tubes, scintillation vials). Possible binding to components was determined as follows: A 1.0 ml sample of a buffer solution containing ^{3}H-PEG and ^{14}C-benzoic acid was read for initial concentration. The solution was placed in a plastic container and perfused (≈ 0.5 ml/min.) through tygon tubing into polyethylene tubes. Samples (1.0 ml) were analyzed for dpm's as to the procedure previously mentioned. Results indicated that the activity of both drug substances was the same as the initial sample and constant over time indicating the absence of drug binding.

III. Results and Discussion

A. In-Vitro Permeability Studies

1. Penetration Enhancement and Carbon Dioxide

For each experiment, the data are represented as the total amount of radioactive drug transported from the donor to the receiver chamber as a percent of total donor activity.

The purpose of these studies was to gain insight into the effect that carbonation may pose on increasing drug permeability across small intestinal tissue. In-vitro permeability studies are one of the primary methods used to determine solute flux across animal tissue.

Initial studies focusing on benzoic acid transport across rat duodenal tissue have been previously reported (Eichman, 1995). It was concluded that carbon dioxide increased benzoic acid permeability but with inconclusive results as to the mechanism(s) for this enhancement. In order to obtain a full understanding for the potential of carbonation as a penetration enhancer, additional permeability studies were required on a wide spectrum of drug compounds varying in both chemical composition and molecular weight.

The drugs utilized in permeability experiments are illustrated in Figures 4.4 and 4.5. Results of these studies are shown in Figures 4.6 through 4.31. Overall results are summarized in Table 4.1.

Each drug showed enhanced permeability across either rat or rabbit intestinal

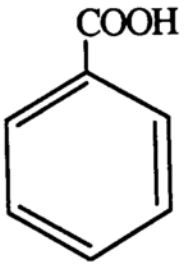

Benzoic Acid

MW = 122.1

Log Ko/w = 1.87

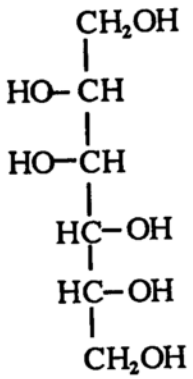

Mannitol

MW = 182.17

Log Ko/w = -3.10

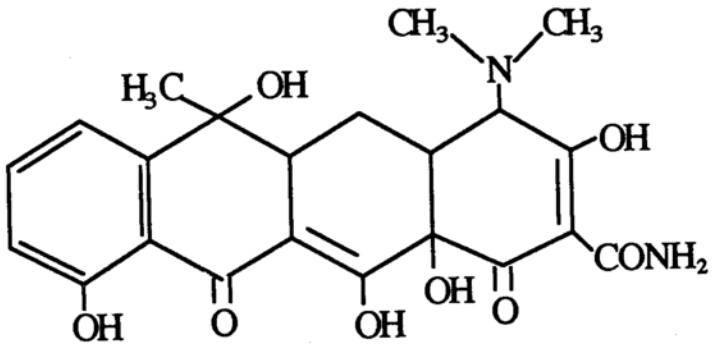

Tetracycline

MW = 444.40

Log Ko/w = -1.46

Figure 4.4: Structures of mannitol, tetracycline, and benzoic acid.

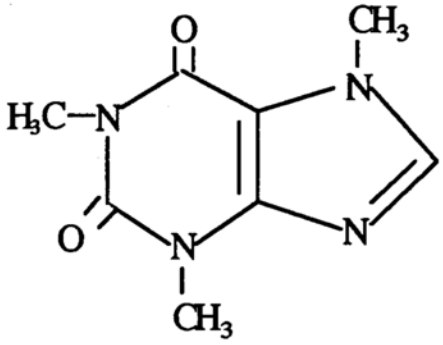

Caffeine

MW = 194.2

Log $K_{o/w}$ = 0.00

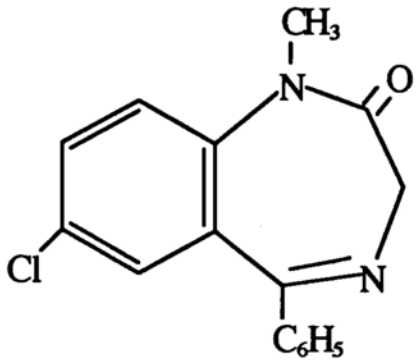

Diazepam

MW = 284.76

Log $K_{o/w}$ = 2.82

$HOCH_2CH_2O(CH_2CH_2O)_nCH_2CH_2OH$

Polyethylene Glycol

MW = 900 & 4000

PEG 900 Log $K_{o/w}$ = -3.50

PEG 4000 Log $K_{o/w}$ = -5.10

Figure 4.5: Structures of diazepam, caffeine, PEG 900, and PEG 4000.

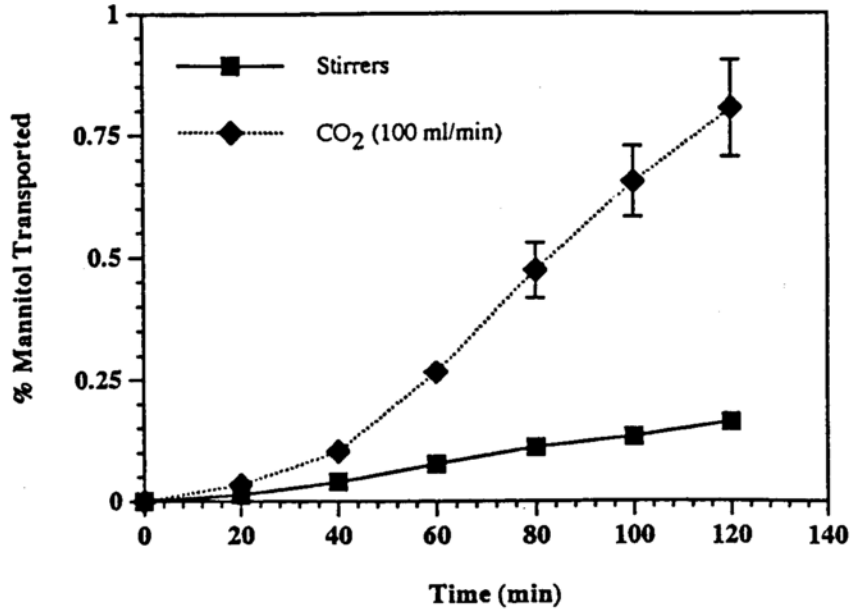

Figure 4.6: Effect of carbon dioxide bubbling on the permeability of mannitol across rabbit ileum tissue in-vitro. Error bars represent SEM of 5 to 6 experimental repetitions.

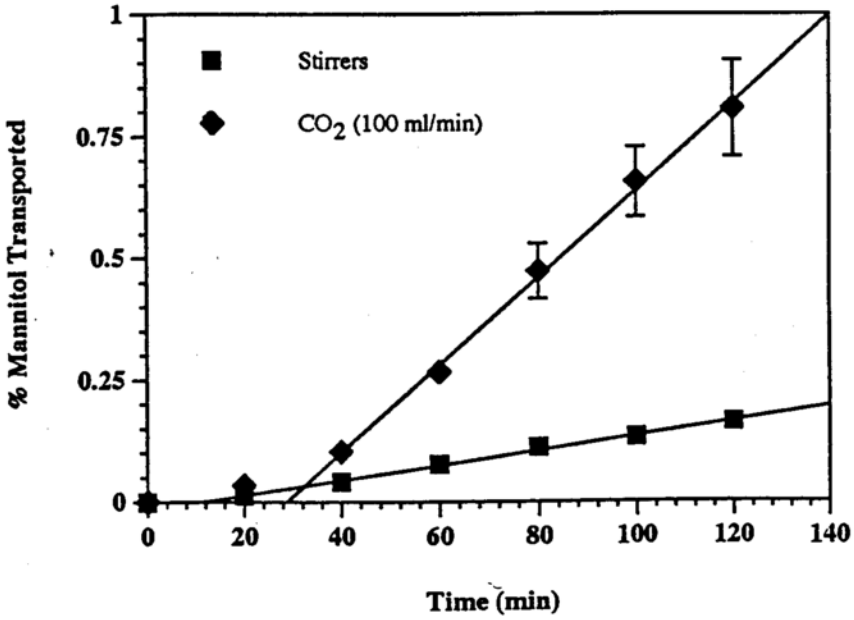

Figure 4.7: Percent mannitol transported across rabbit ileum tissue in-vitro depecting the steady state terminal slope. Number of experimental repetitions = 5-6. Error bars = SEM.

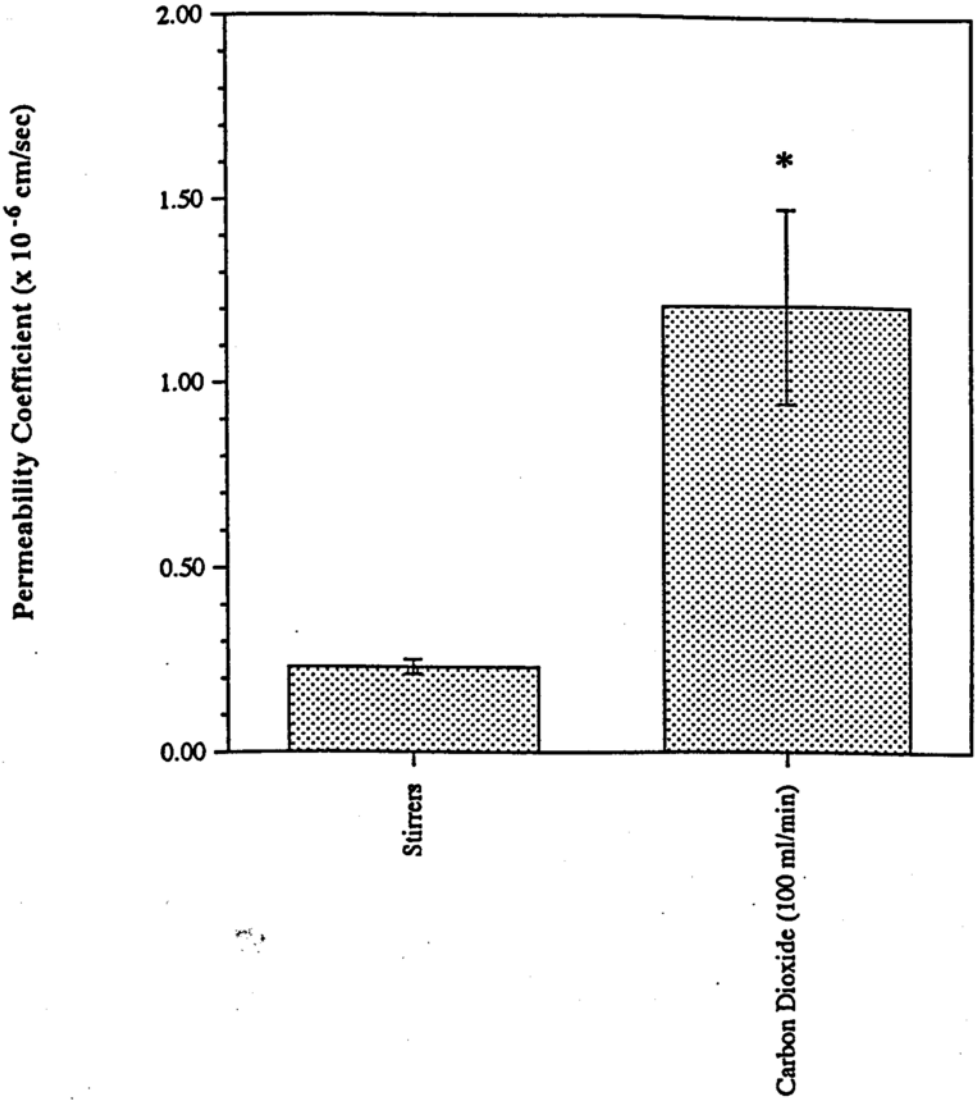

Figure 4.8: Mannitol permeability coefficients for in-vitro rabbit ileum diffusion cell studies. Error bars represent standard deviation of 5-6 experimental repetitions.
* indicates significant difference ($p < 0.0005$).

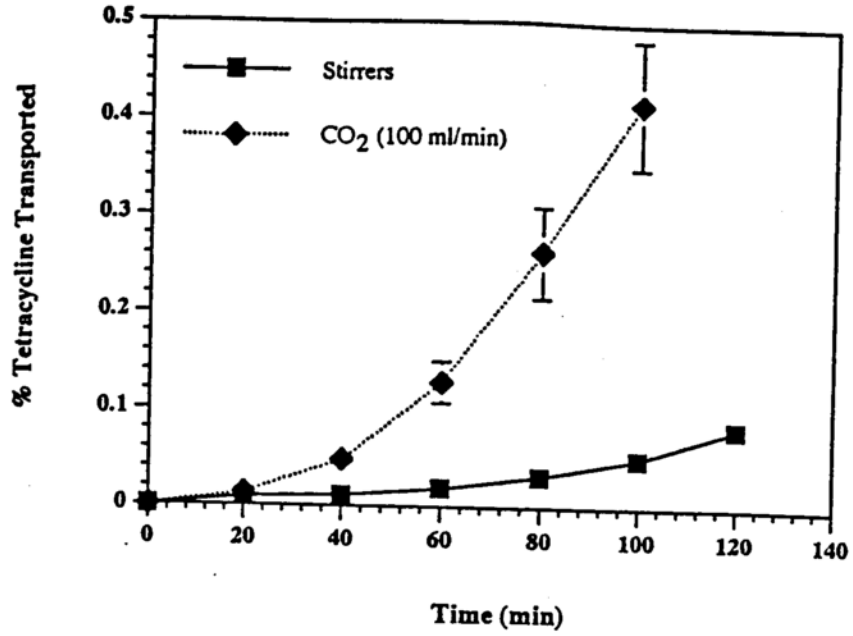

Figure 4.9: Effect of carbon dioxide bubbling on the permeability of tetracycline across rabbit ileum tissue in-vitro. Error bars represent SEM of 3 to 4 experimental repetitions.

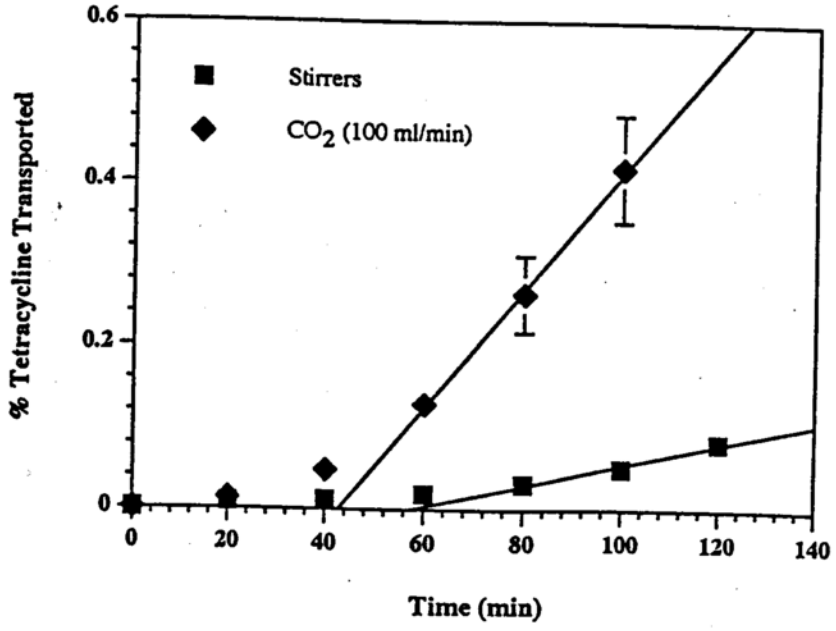

Figure 4.10: Percent tetracycline transported across rabbit ileum tissue in-vitro depicting the steady state terminal slope. Number of experimental repetitions = 3-4. Error = SEM.

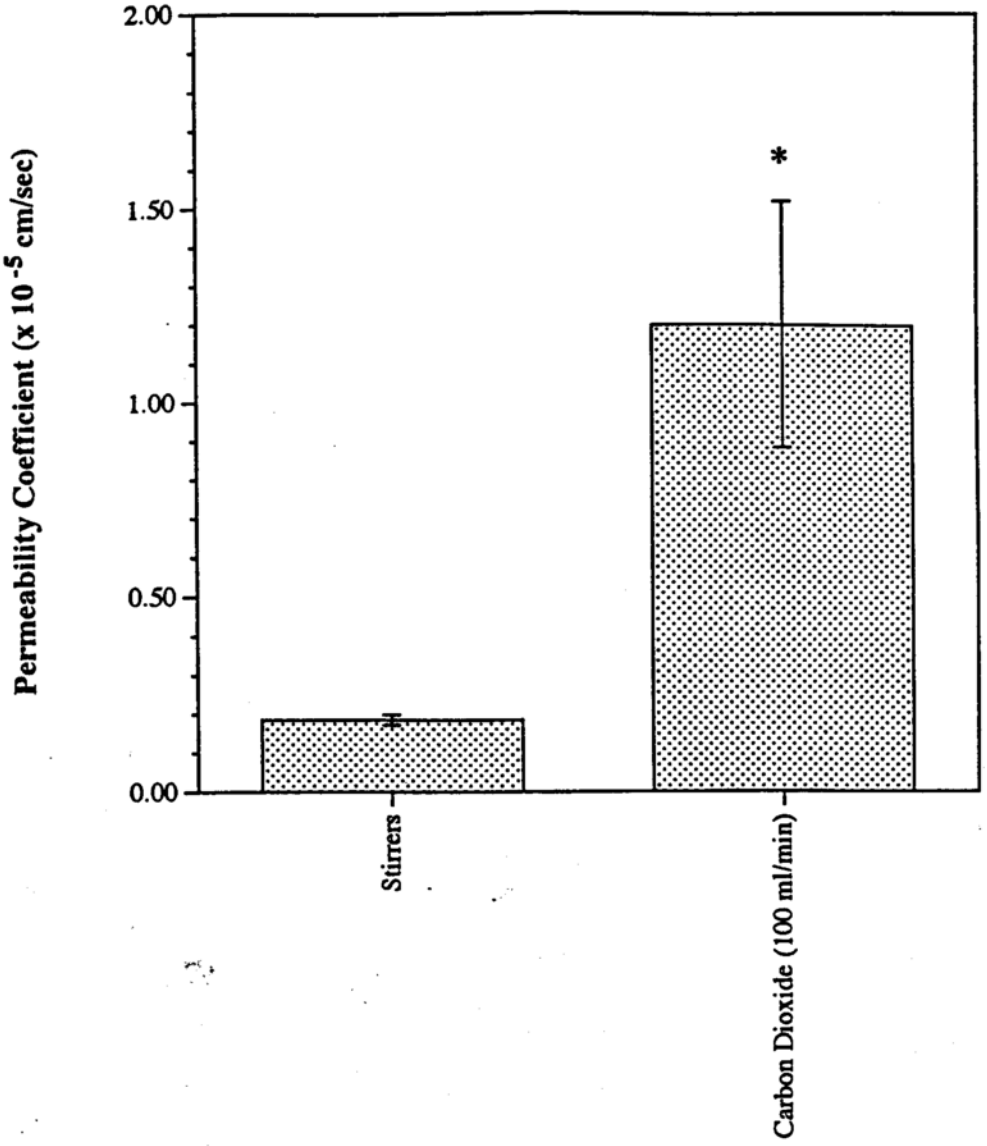

Figure 4.11: Tetracycline permeability coefficients for in-vitro rabbit ileum diffusion cell studies. Error bars represent standard deviation of 3-4 experimental repetitions. * indicates significant difference ($p < 0.002$).

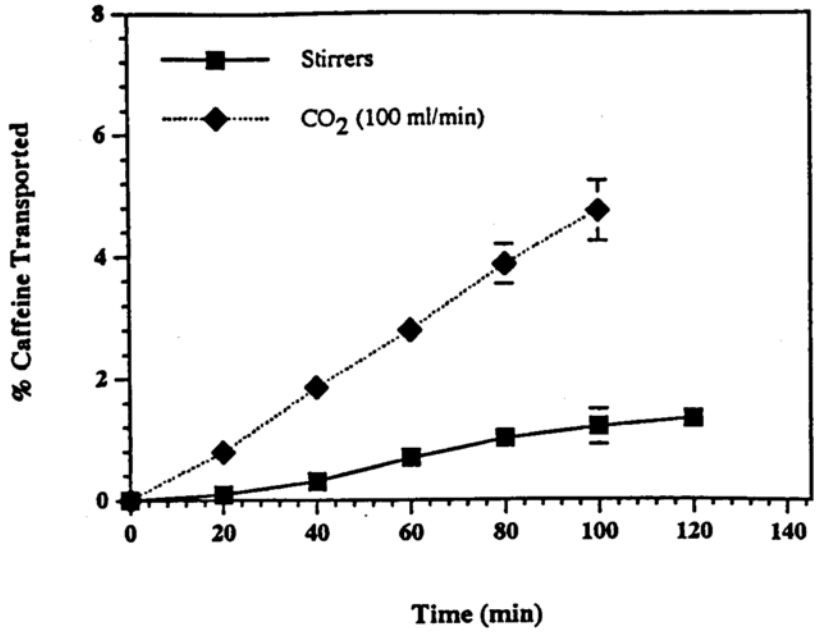

Figure 4.12: Effect of carbon dioxide bubbling on the permeability of caffeine across rabbit ileum tissue in-vitro. Error bars represent standard deviation of 4 experimental repetitions.

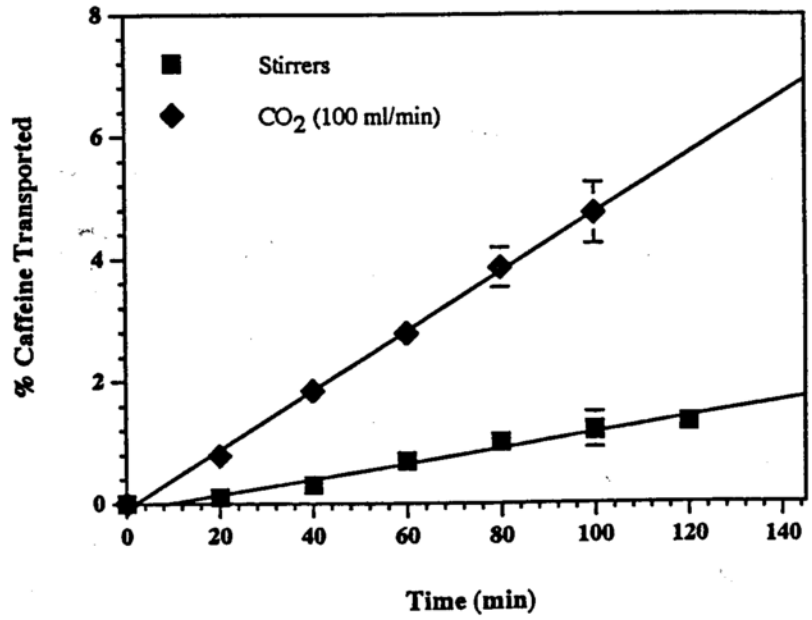

Figure 4.13: Percent caffeine transported across rabbit ileum tissue in-vitro depicting the steady state terminal slope. Number of experimental repetitions = 4. Error bars = standard deviation.

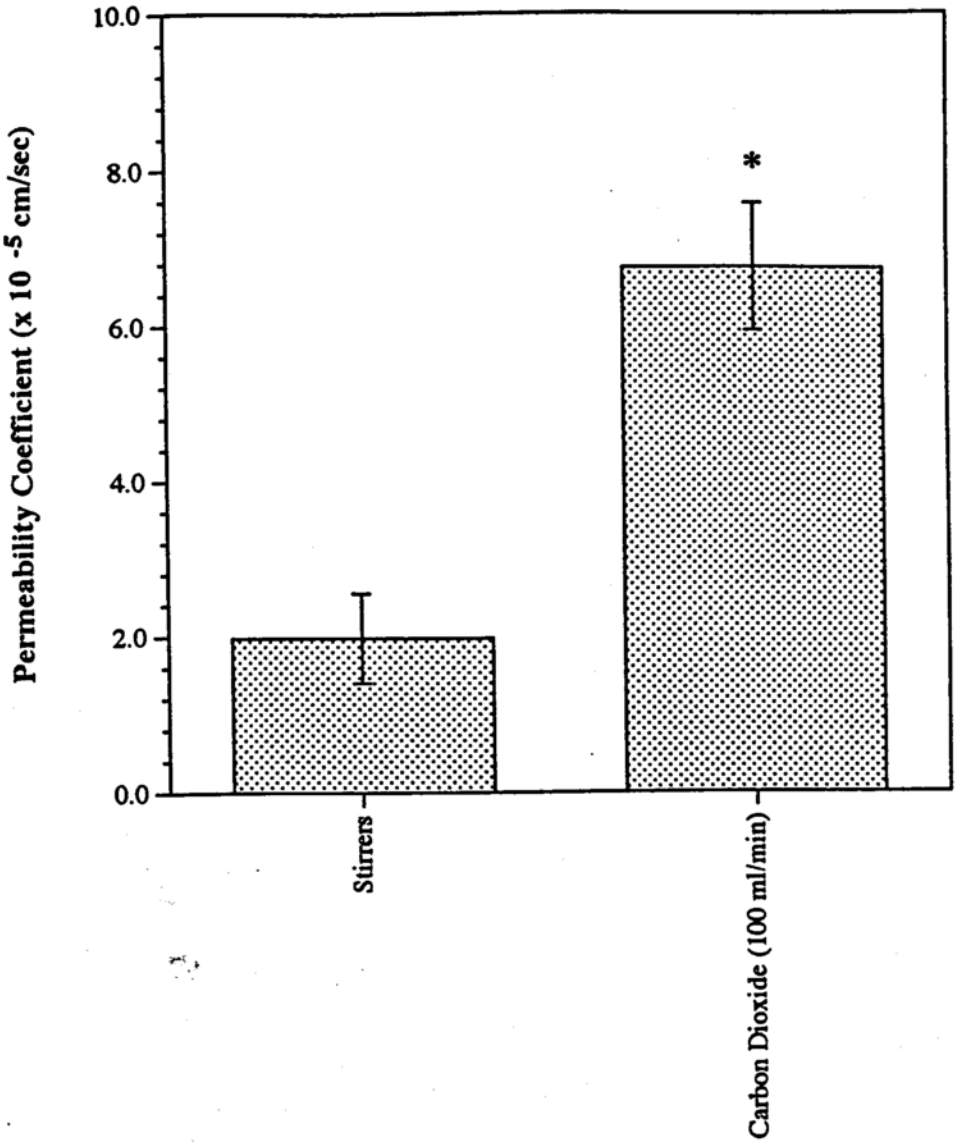

Figure 4.13: Caffeine permeability coefficients for in-vitro rabbit ileum diffusion cell studies. Error bars represent standard deviation of 4 experimental repetitions. * indicates significant difference ($p < 0.002$).

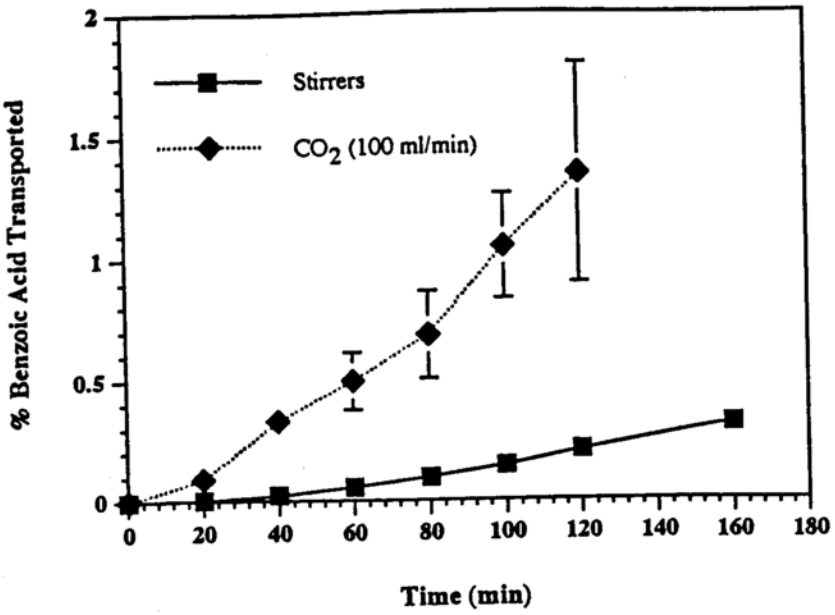

Figure 4.14: Effect of carbon dioxide bubbling on the permeability of benzoic acid across rat duodenum tissue in-vitro. Error bars represent SEM of 4-5 experimental repetitions.

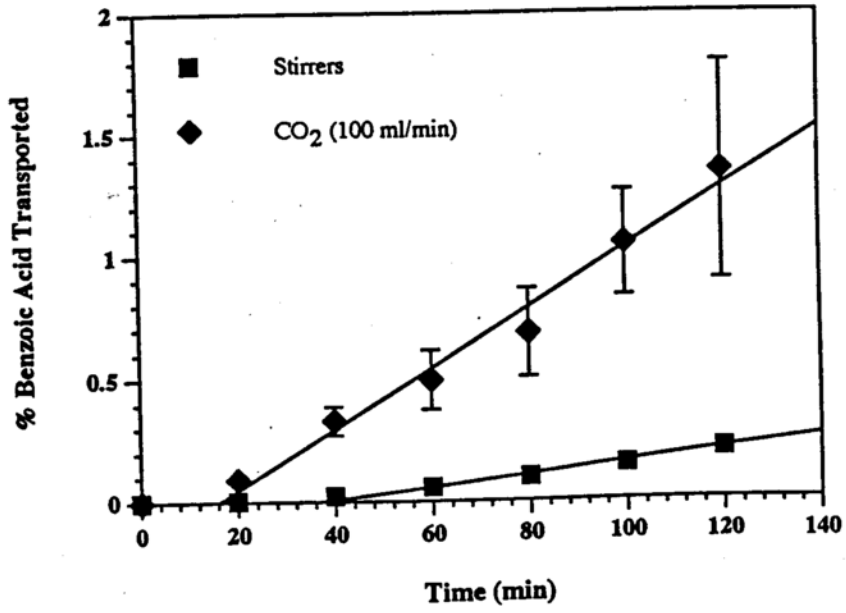

Figure 4.15: Percent benzoic acid transported across rat duodenum tissue in-vitro depictingthe steady state terminal slope. Number of experimental repetitions = 4-5. Error bars = SEM.

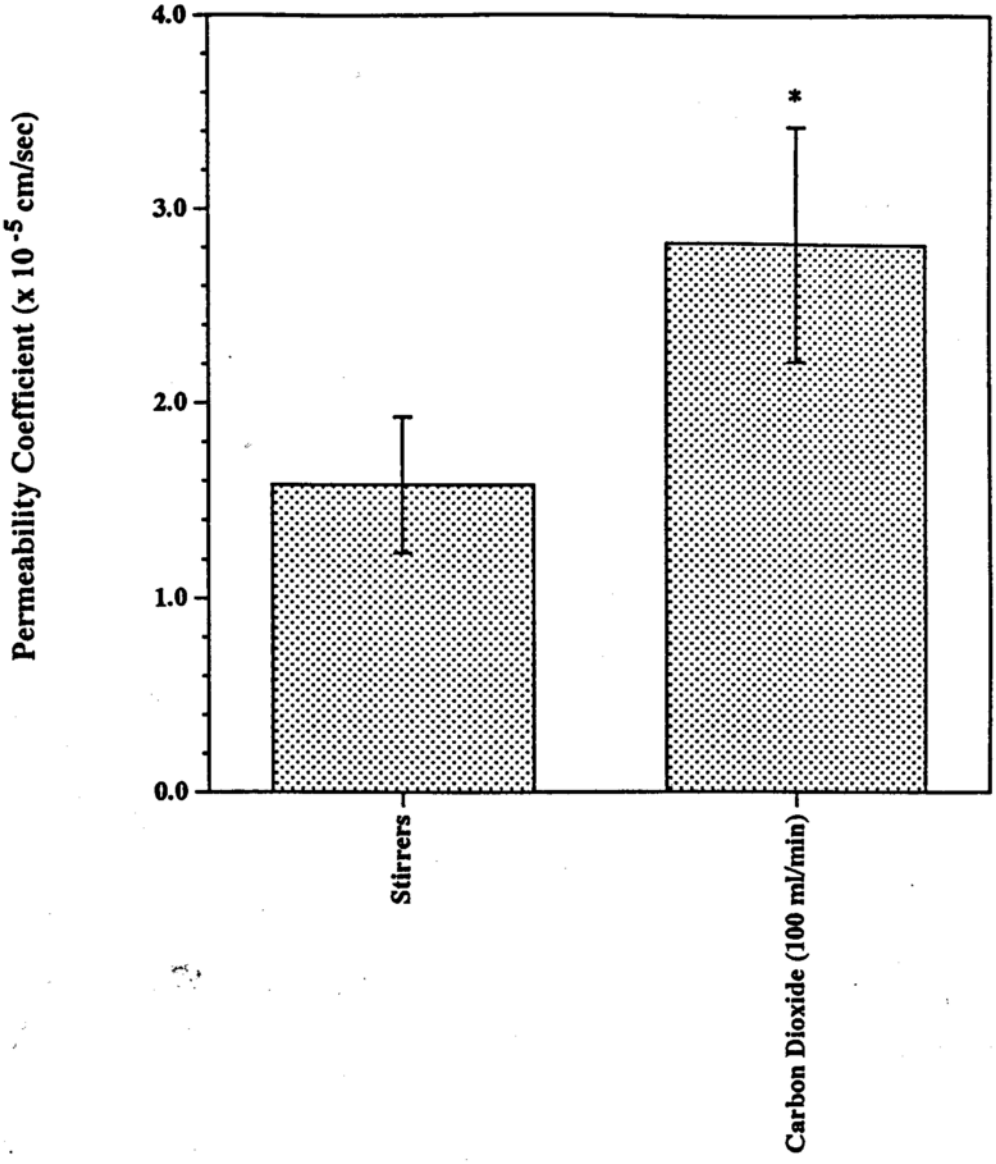

Figure 4.16: Benzoic acid permeability coefficients for in-vitro rat duodenum diffusion cell studies. Error bars represent standard deviation of 4 to 5 experimental repetitions. * indicates significant difference ($p < 0.01$).

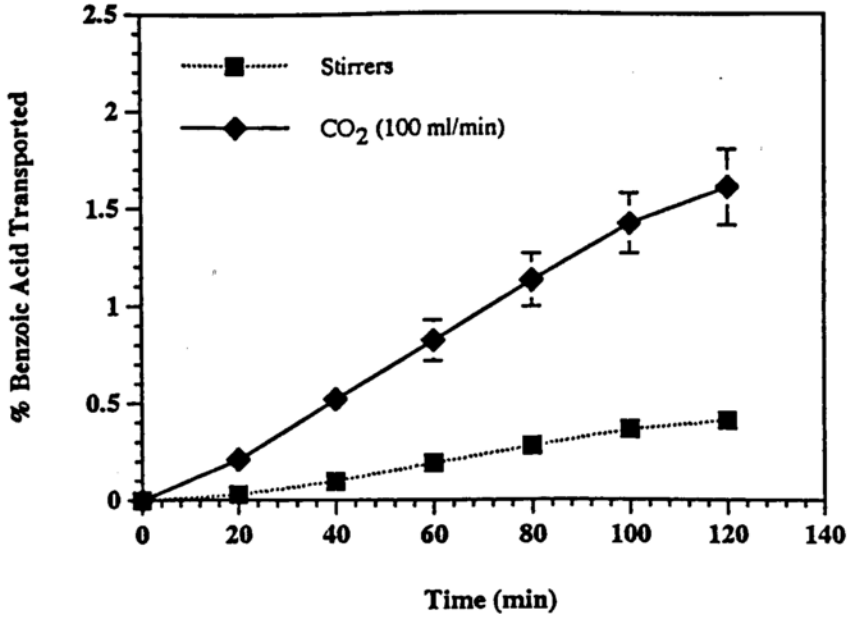

Figure 4.17: Effect of carbon dioxide bubbling on the permeability of benzoic acid across rat ileum tissue in-vitro. Error bars represent SEM of 4-6 experimental repetitions.

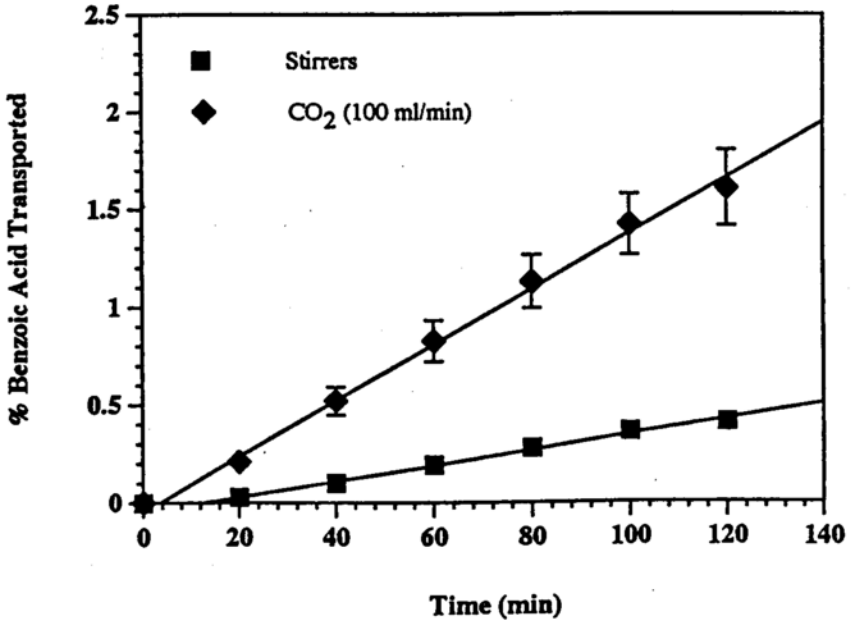

Figure 4.18: Percent benzoic acid transported across rat ileum tissue in-vitro depicting the steady state terminal slope. Number of experimental repetitions = 4-6. Error bars = SEM.

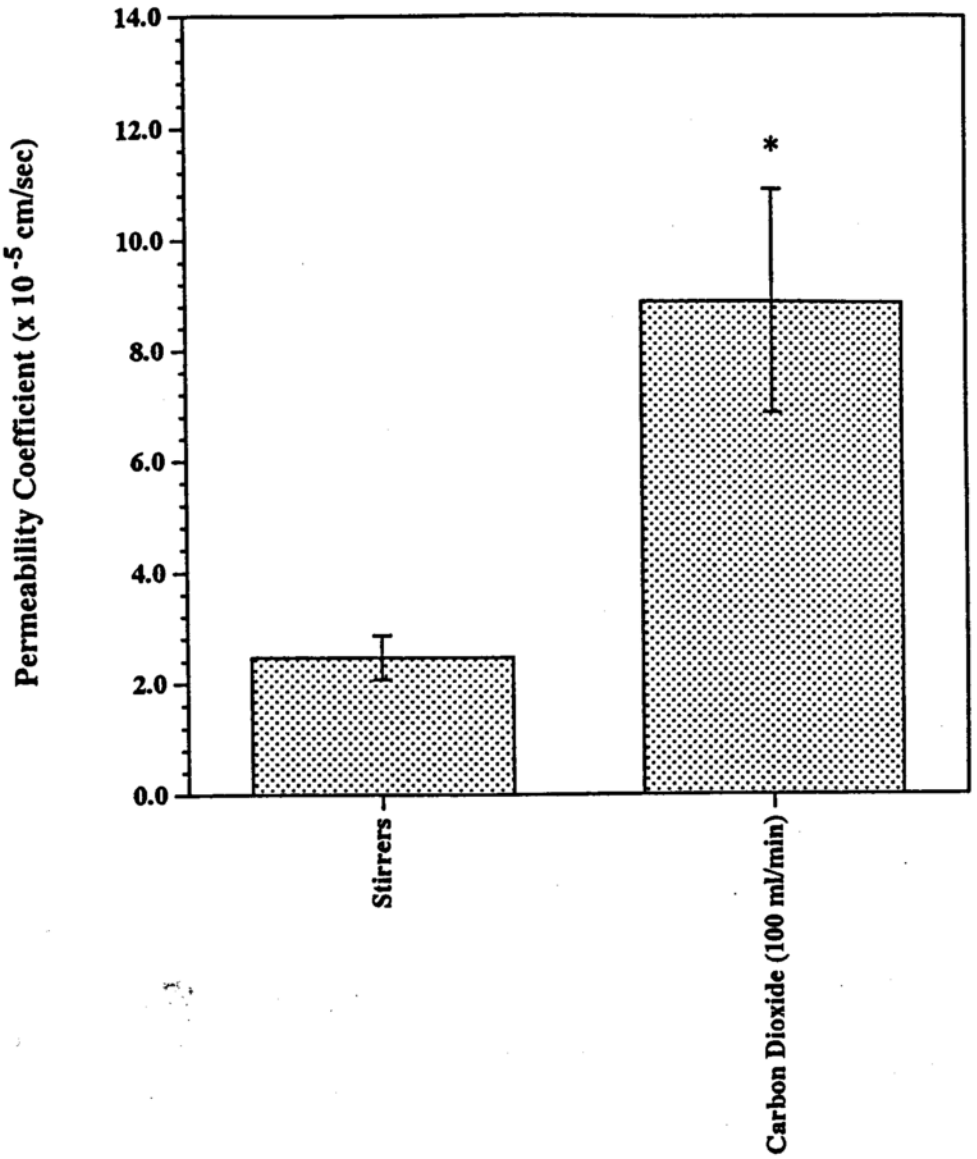

Figure 4.19: Benzoic acid permeability coefficients for in-vitro rat ileum diffusion cell studies. Error bars represent standard deviation of 4 to 6 experimental repetitions. * indicates significant difference ($p < 0.01$).

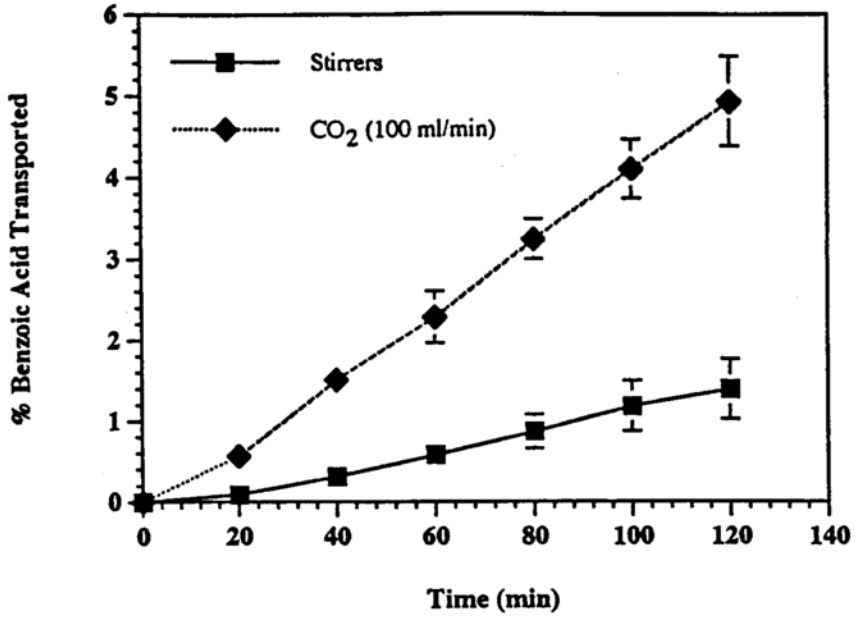

Figure 4.20: Effect of carbon dioxide bubbling on the permeability of benzoic acid across rabbit ileum tissue in-vitro. Error bars represent SEM of 3-4 experimental repetitions.

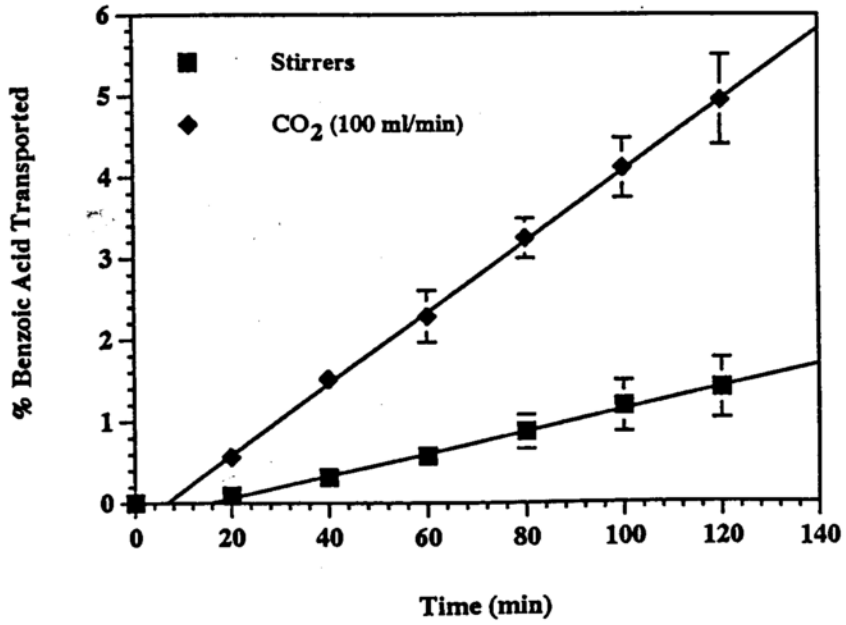

Figure 4.21: Percent benzoic acid transported across rabbit ileum tissue in-vitro depicting the steady state terminal slope. Number of experimental repetitions = 3-4. Error bars = SEM.

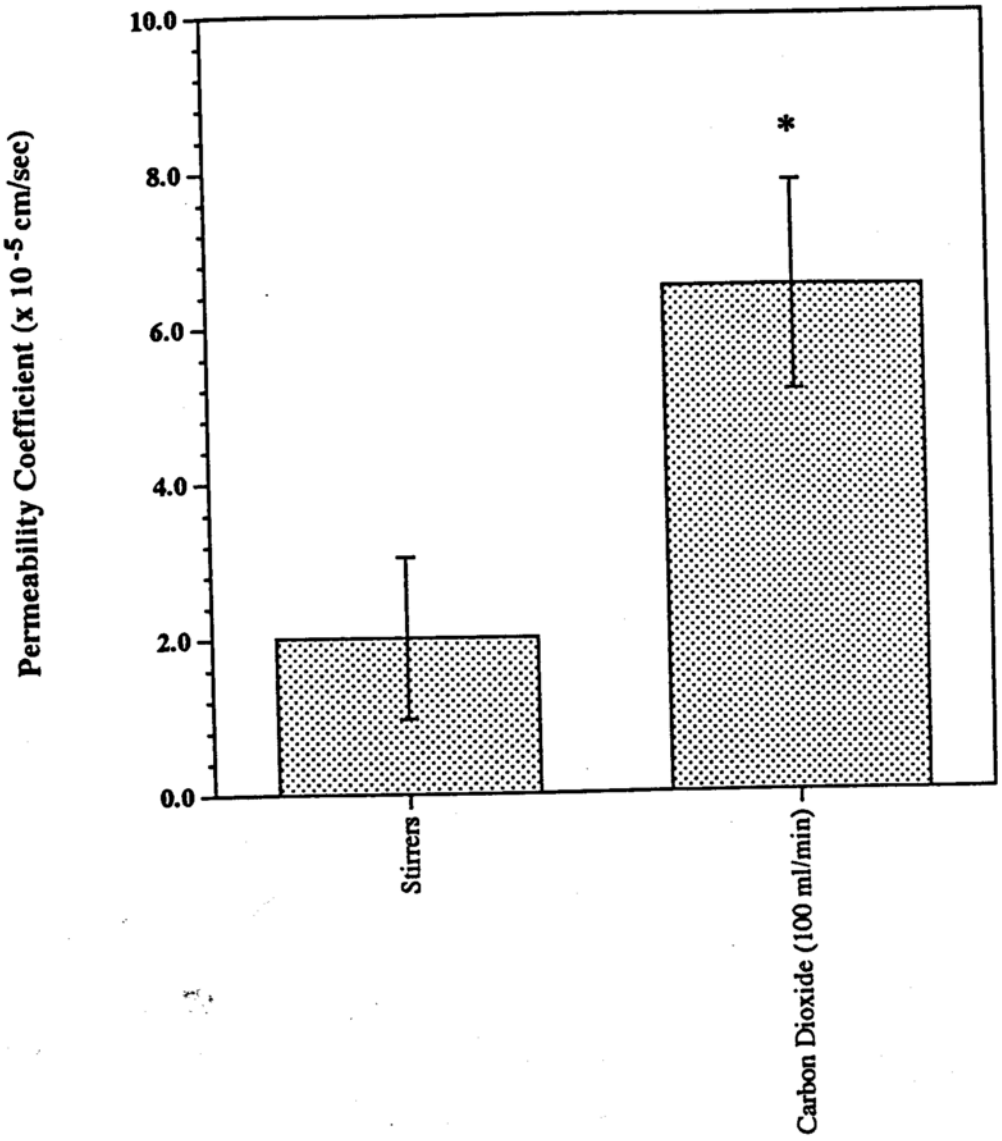

Figure 4.22: Benzoic acid permeability coefficients for in-vitro rabbit ileum diffusion cell studies. Error bars represent standard deviation of 3 to 4 experimental repetitions. * indicates significant difference ($p < 0.005$).

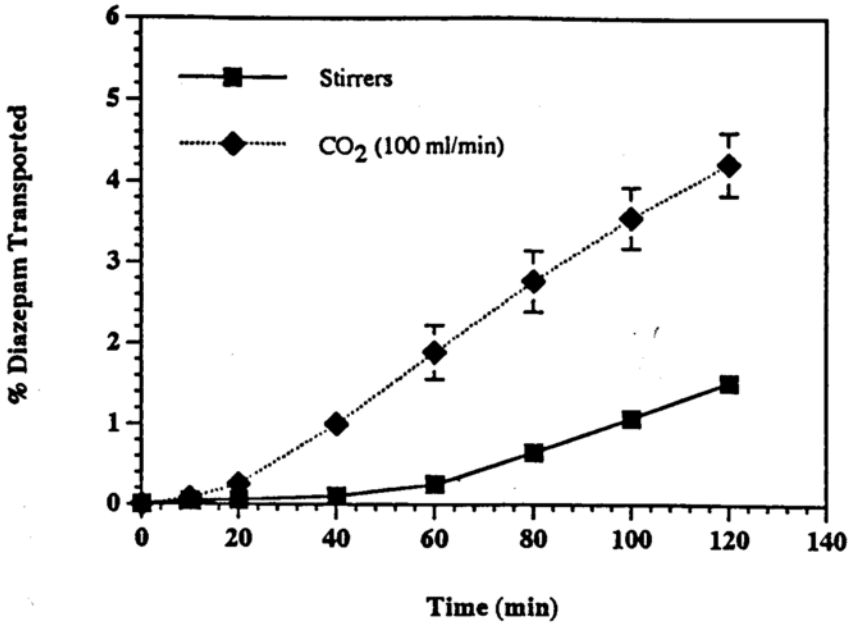

Figure 4.23: Effect of carbon dioxide bubbling on the permeability of diazepam across rabbit ileum tissue in-vitro. Error bars represent SEM of 4 to 8 experimental repetitions.

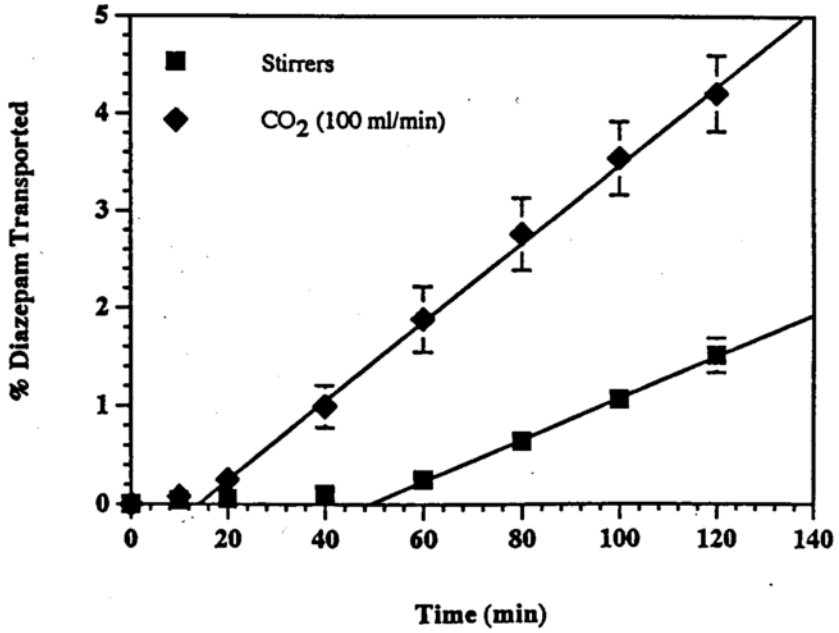

Figure 4.24: Percent diazepam transported across rabbit ileum tissue in-vitro depicting the steady state terminal slope. Number of experimental repetitions = 4-8. Error bars = SEM.

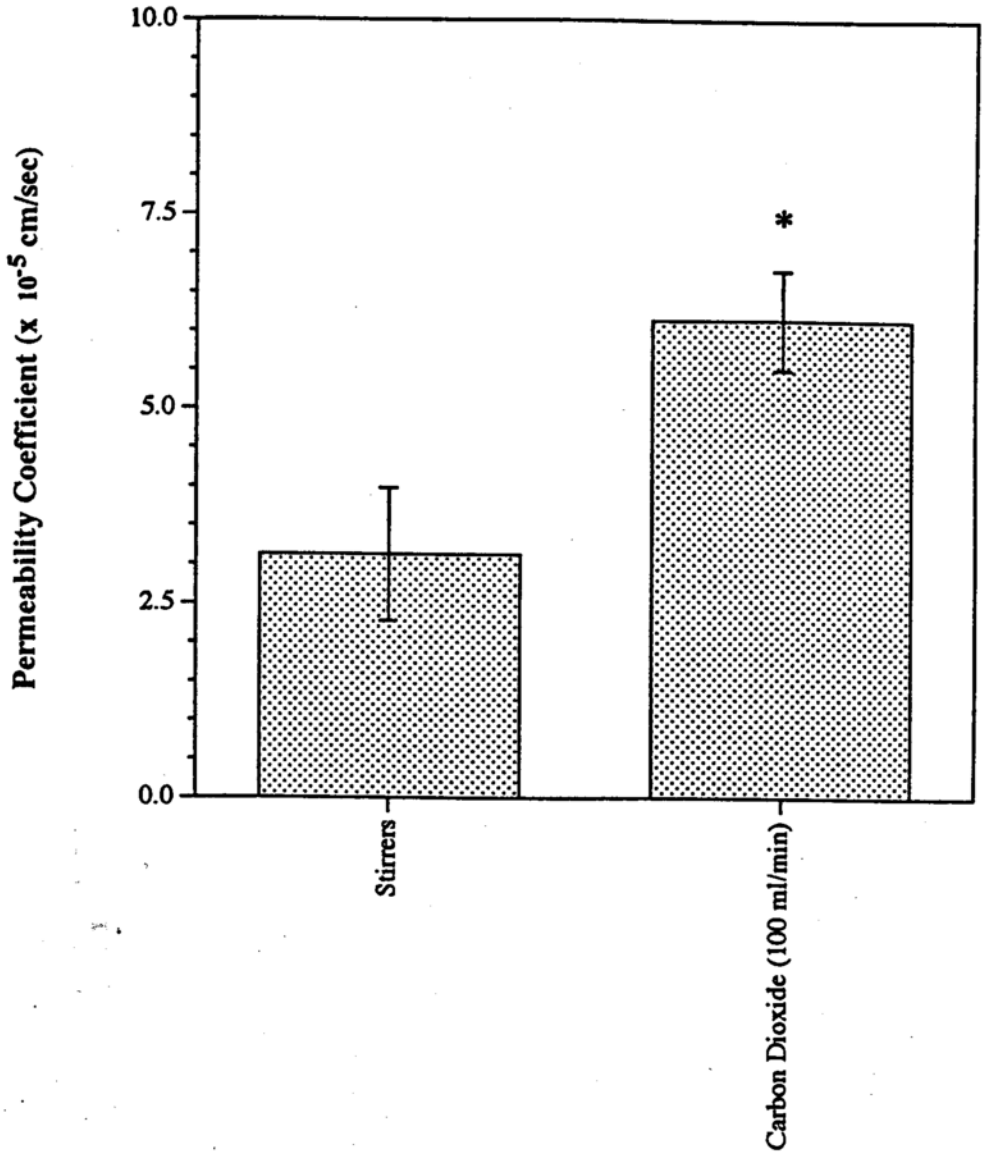

Figure 4.25: Diazepam permeability coefficients for in-vitro rabbit ileum diffusion cell studies. Error bars represent standard deviation of 4 to 8 experimental repetitions. * indicates significant difference ($p < 0.001$).

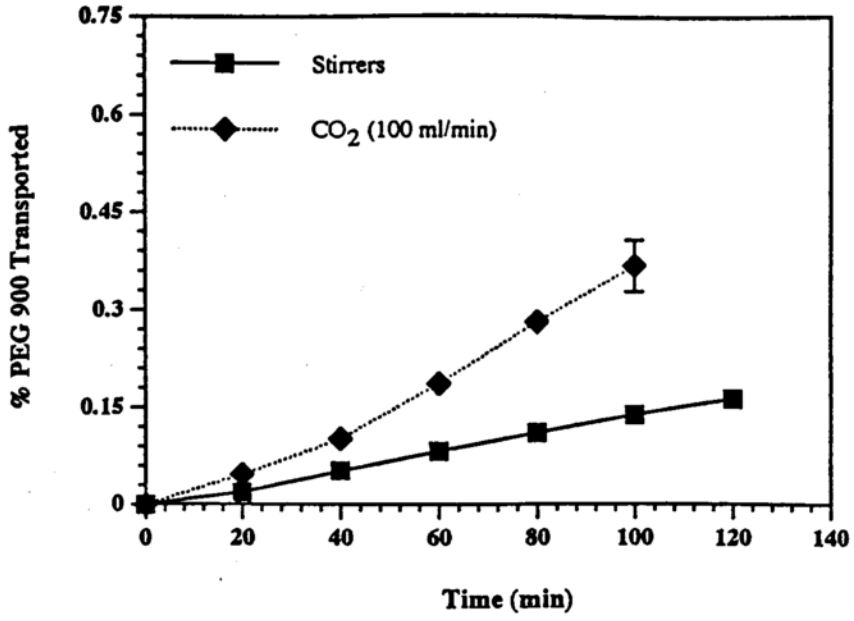

Figure 4.26: Effect of carbon dioxide bubbling on the permeability of PEG 900 across rabbit ileum tissue in-vitro. Error bars represent SEM of 3 to 5 experimental repetitions.

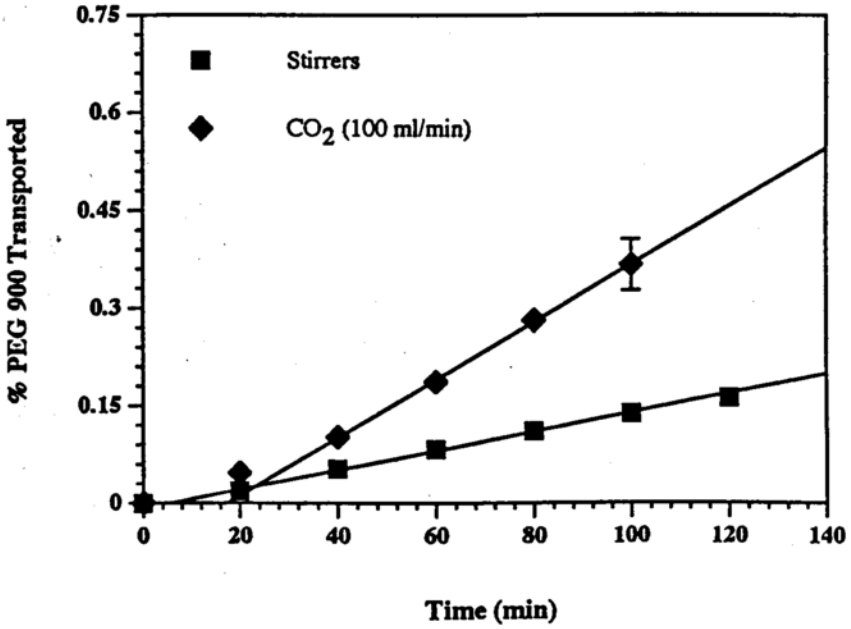

Figure 4.27: Percent PEG 900 transported across rabbit ileum tissue in-vitro depicting the steady state terminal slope. Number of experimental repetitions = 3-5. Error bars = SEM.

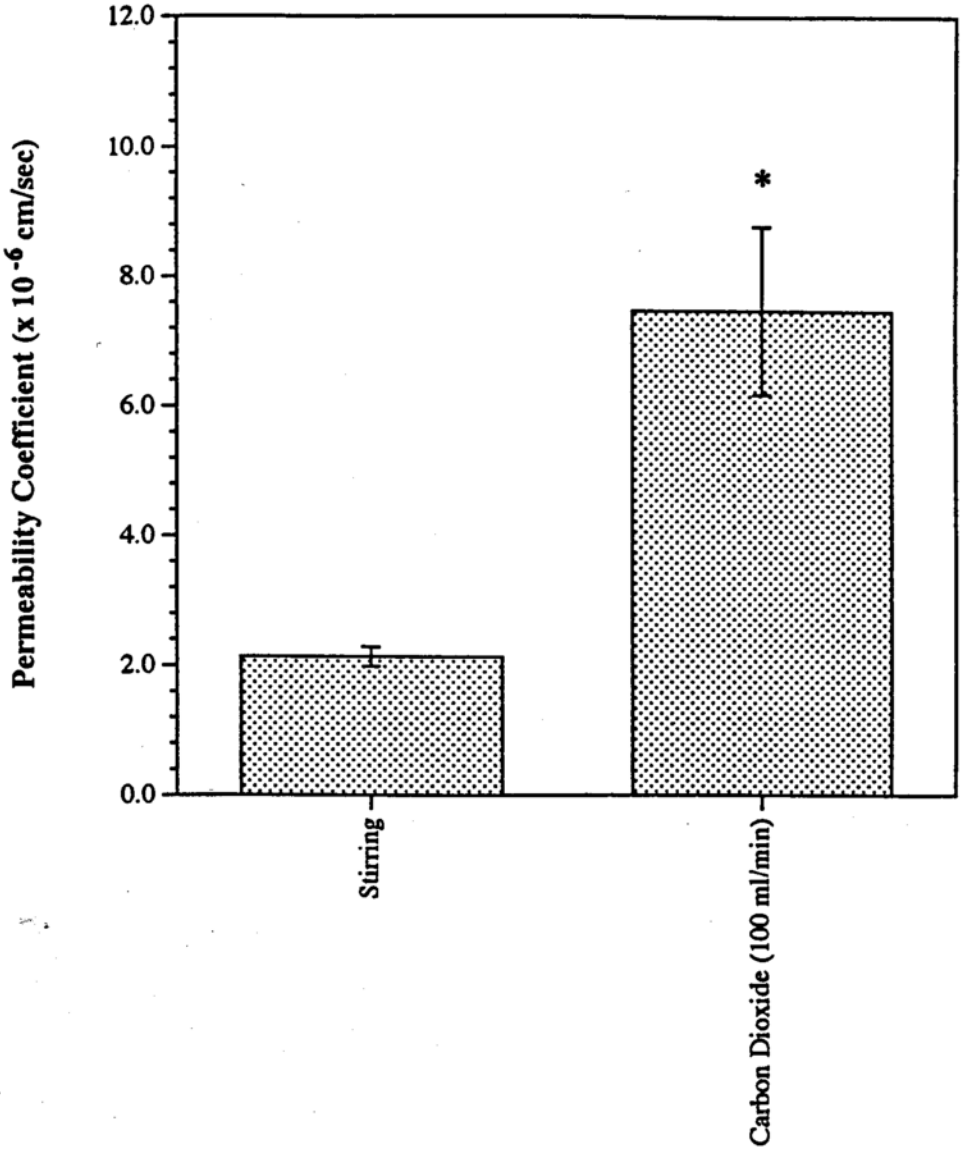

Figure 4.28: PEG 900 permeability coefficients for in-vitro rabbit ileum diffusion cell studies. Error bars represent standard deviation of 3 to 5 experimental repetitions. * indicates significant difference ($p < 0.001$).

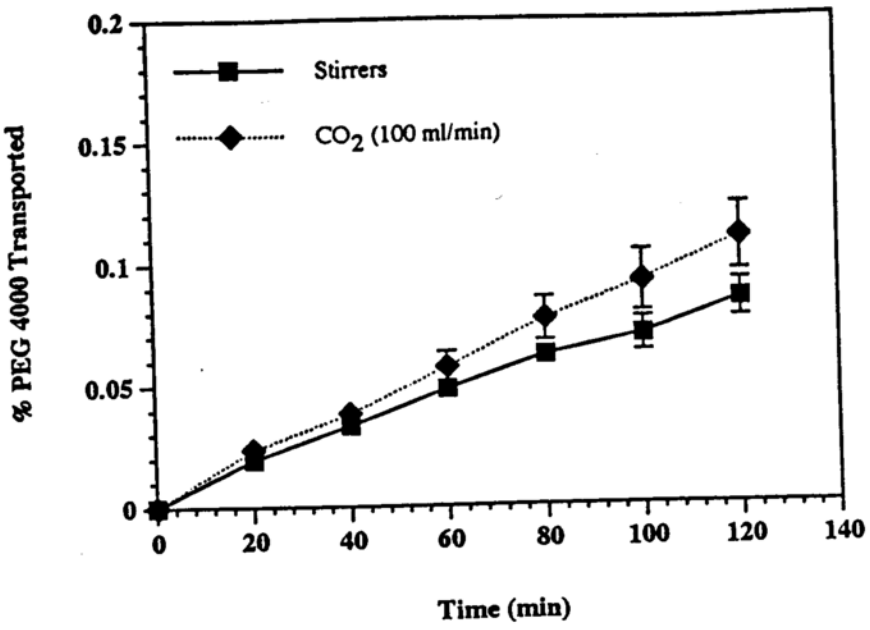

Figure 4.29: Effect of carbon dioxide bubbling on the permeability of PEG 4000 across rabbit ileum tissue in-vitro. Error bars represent SEM of 4 experimental repetitions.

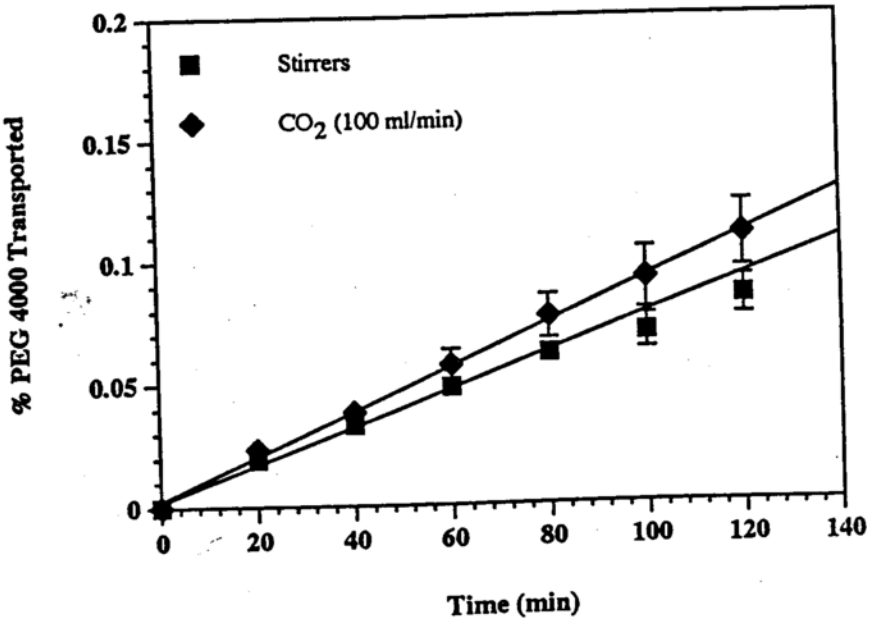

Figure 4.30: Percent PEG 4000 transported across rabbit ileum tissue in-vitro depicting the steady state terminal slope. Number of experimental repetitions = 4. Error bars = SEM.

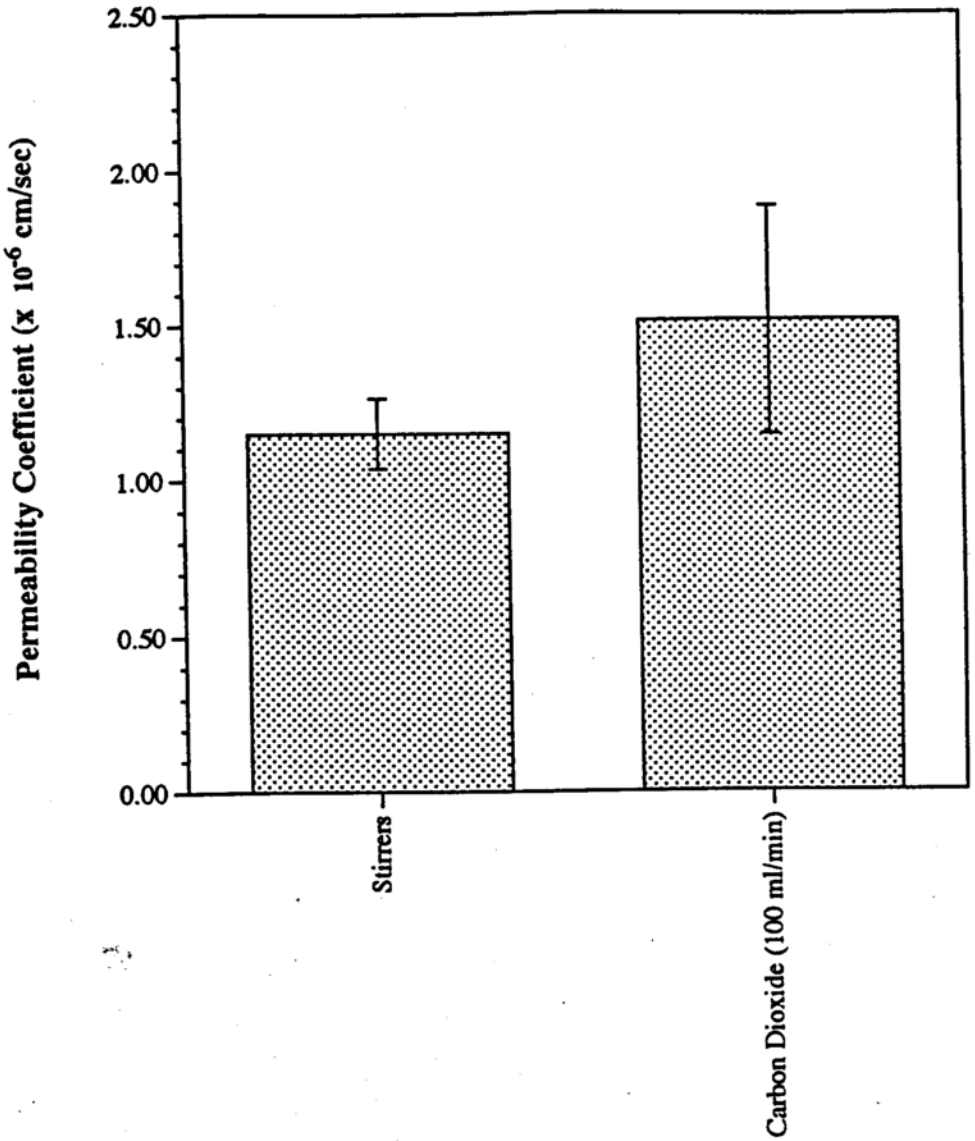

Figure 4.31: PEG 4000 permeability coefficients for in-vitro rabbit ileum diffusion cell studies. Error bars represent standard deviation of 4 experimental repetitions.

Table 4.1: Summary of results from in-vitro permeability studies utilizing rat or rabbit intestinal tissue.

Compound	Tissue	Experiment	Permeability Coefficient (x 10^{-5} cm/sec)	Standard Deviation (x 10^{-5} cm/sec)
Mannitol	Rabbit Ileum	Stirrers	0.23	0.0197
		CO_2	1.21*	0.267
Tetracycline	Rabbit Ileum	Stirrers	0.18	0.013
		CO_2	1.20*	0.317
Caffeine	Rabbit Ileum	Stirrers	1.97	0.573
		CO_2	6.74*	0.811
Benzoic Acid	Rat Duodenum	Stirrers	1.58	0.348
		CO_2	2.82*	0.605
	Rat Ileum	Stirrers	2.47	0.398
		CO_2	8.88*	2.02
	Rabbit Ileum	Stirrers	2.01	1.04
		CO_2	6.50*	1.35
Diazepam	Rabbit Ileum	Stirrers	3.12	0.849
		CO_2	6.13*	0.642
PEG 900	Rabbit Ileum	Stirrers	0.213	0.015
		CO_2	0.747*	0.130
PEG 4000	Rabbit Ileum	Stirrers	0.115	0.011
		CO_2	0.151	0.037

* denotes significant difference from stirrers (2-sample t-test, 95% confidence; p values listed with previous graphs.

tissue in the presence of carbonation as indicated by greater terminal steady state slopes in the % transport vs. time profiles when compared to stirrer experiments. The only exception was PEG 4000, the results of which will be discussed later (see Chapter 5). The experimental outcomes can be potentially explained by a number of effects induced by CO_2 as a chemical entity within the solution and/or bubble formation with subsequent tissue surface contact. The possible explanations include: (1) a change in the pH tissue gradient; (2) a buffer effect; (3) enhancement of solvent drag due to increased fluid flow; (4) thinning or complete stripping of the mucus layer; (5) a disruptive effect on the epithelial barrier; and/or (6) increased membrane hydrophobicity.

As indicated by Figure 4.32, the drugs with greater hydrophobicity; diazepam (log $K_{o/w}$ = 2.82), benzoic acid (log $K_{o/w}$ = 1.87), and caffeine (log $K_{o/w}$ = 0.00) demonstrated higher permeability coefficients with experiments utilizing stirrers and CO_2 when compared to their hydrophilic counterparts. This is expected due to the large surface area available for partitioning into the hydrophobic constituents of the cell membrane. The polar compounds: mannitol, PEG 900, PEG 4000, and tetracycline are expected to achieve lower permeability rates due to poor membrane partitioning. These compounds cross the epithelium primarily by diffusion through the paracellular space, which occupies significantly less absorptive surface area. Permeabilty coefficients obtained in stir experiments were comparable to values previously obtained in other intestinal permeability studies (Dowty, 1996).

However, when analyzing the extent of change between stirrer and carbonation permeability coefficients for individual compounds (Figure 4.33, Table 4.2), the hydrophilic drugs, mannitol and tetracycline, showed a larger increase compared with their non-polar counterparts. This may indicate that the

carbonating bubbles are inducing a structural change in the paracellular pathway, creating new or widening pre-existing aqueous pores within the cell membrane, and/or inducing a greater flux of solvent (i.e. solvent drag) across the membrane leading to substantial permeability enhancement for the hydrophilic compounds. PEG-900 and PEG-4000 are exceptions to these observations and their deviations towards less of an enhancement effect will be discussed later in greater detail (see Chapter 5).

It should also be noted that the donor and receiver solutions were monitored for pH fluctuations during the time course of similar experiments without radioactivity. Donor solution pH typically dropped 0.3 units while the pH of the receiver solution remained relatively constant during the experiments indicating relatively minor pH changes for each solution.

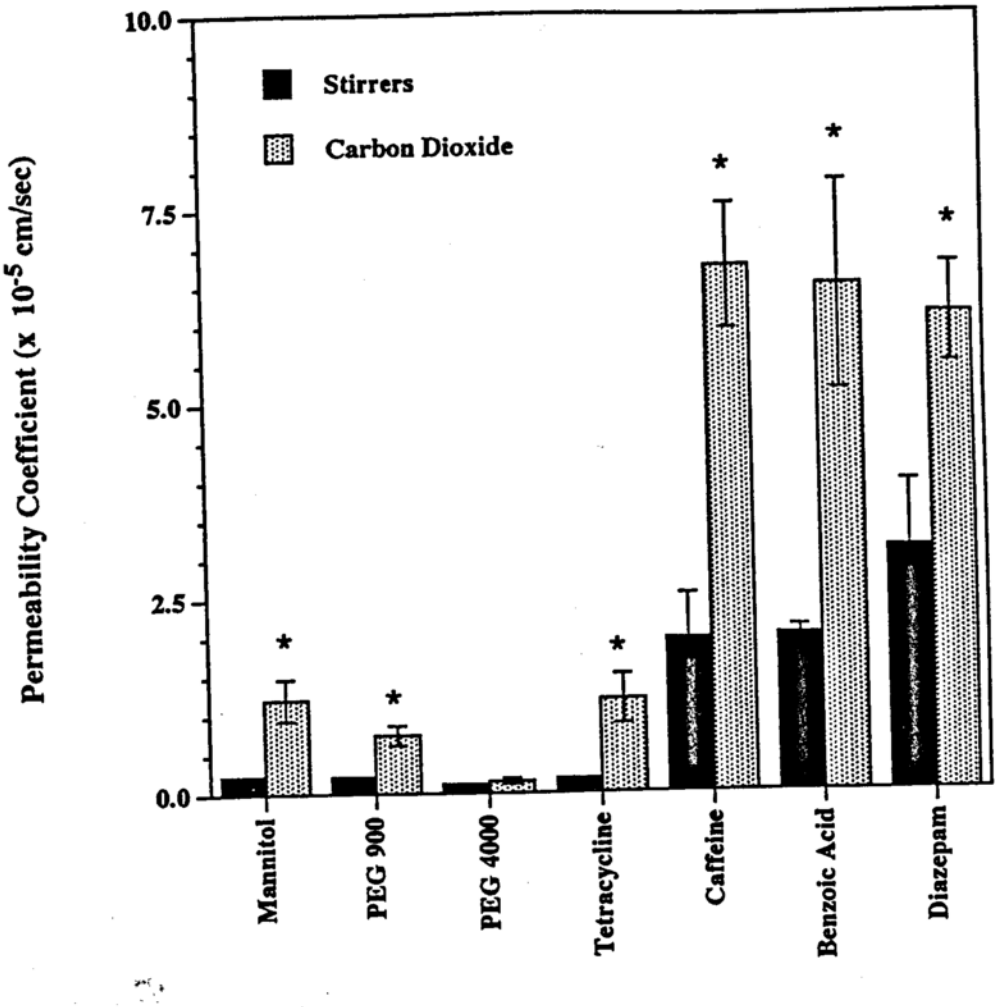

Figure 4.32: Stir and carbon dioxide permeability coefficients for compounds utilized in rabbit ileum in-vitro permeability experiments. Error bars represent standard deviation. * indicates significant difference ($p < 0.005$) between stir and carbon dioxide experiments for a drug compound.

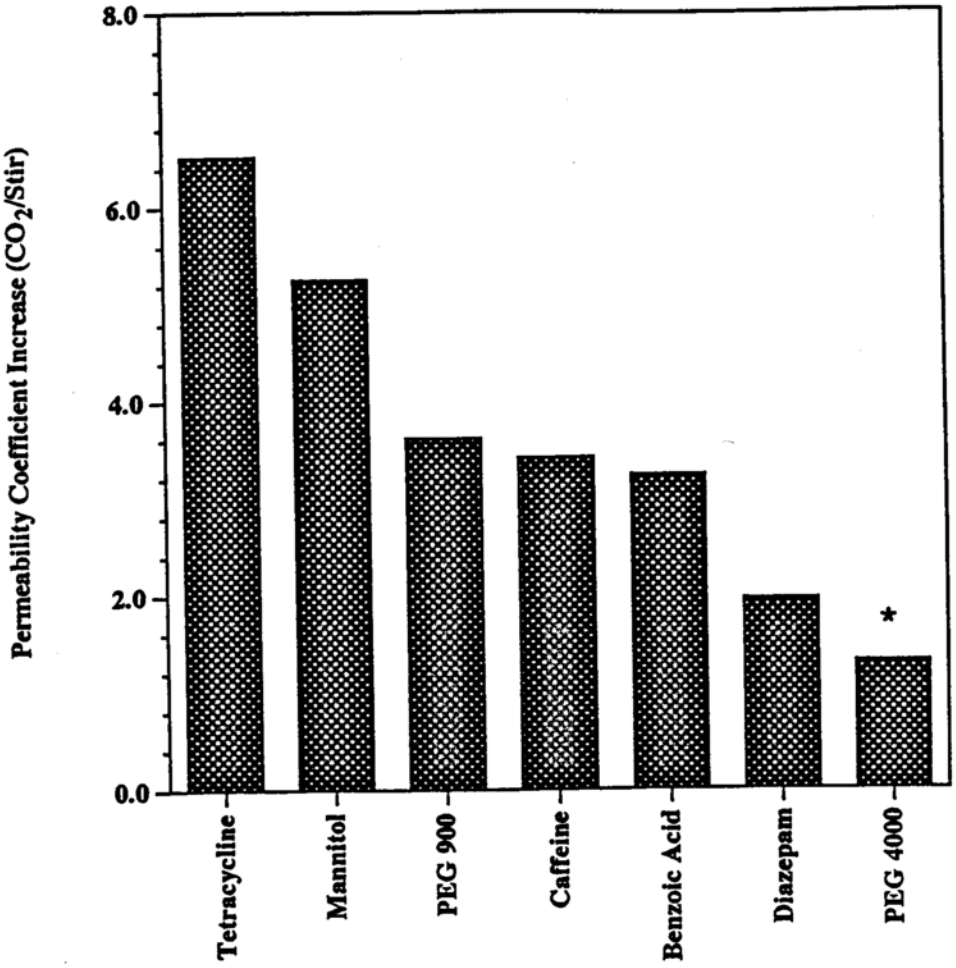

Figure 4.33: Difference in in-vitro rabbit ileum drug permeability coefficients between carbon dioxide and stirrer experiments. * indicates increase in permeability coefficient was not significantly different.

Table 4.2: Change in permeability coefficient between carbon dioxide and stir experiments for compounds utilized with in-vitro rabbit ileum permeability studies.

Compound	Change in Permeability Coefficient (CO_2/Stir)
Tetracycline	6.52
Mannitol	5.26
Caffeine	3.62
Benzoic Acid	3.23
Diazepam	1.96
PEG 900	3.62
PEG 4000	1.31*

* indicates the change was not significantly different ($p > 0.5$)

2. Nitrogen Bubbling and Drug Permeability

The influence of nitrogen bubbling onto rabbit intestinal tissue is depicted in Figures 4.34 to 4.43 with an overall summary of results listed in Table 4.3. The results indicate that nitrogen induced an equivalent enhancement effect on tetracycline, caffeine and benzoic acid permeabilities in comparison to CO_2 bubbling. What is interesting to note is the biological effects of nitrogen. Nitrogen is a hydrophobic gas like carbon dioxide, but does not influence cellular processes. Both CO_2 and nitrogen are capable of being absorbed within and across cell membranes, which could potentially impart increased hydrophobicity to the cellular membrane. It may also be possible that the gases are creating a hydrophobic micro-environment at the cell surface (see Chapter 2). Nitrogen is incapable of influencing changes in intracellular or extracellular pH, and, therefore, one may conclude that the permeability enhancement effect due to nitrogen is not the result of an alteration in solution or tissue pH. Since the magnitude of permeability enhancement is similar to that of CO_2, one may also conclude that the mechanism(s) for CO_2 enhancement do not involve issues relating to pH.

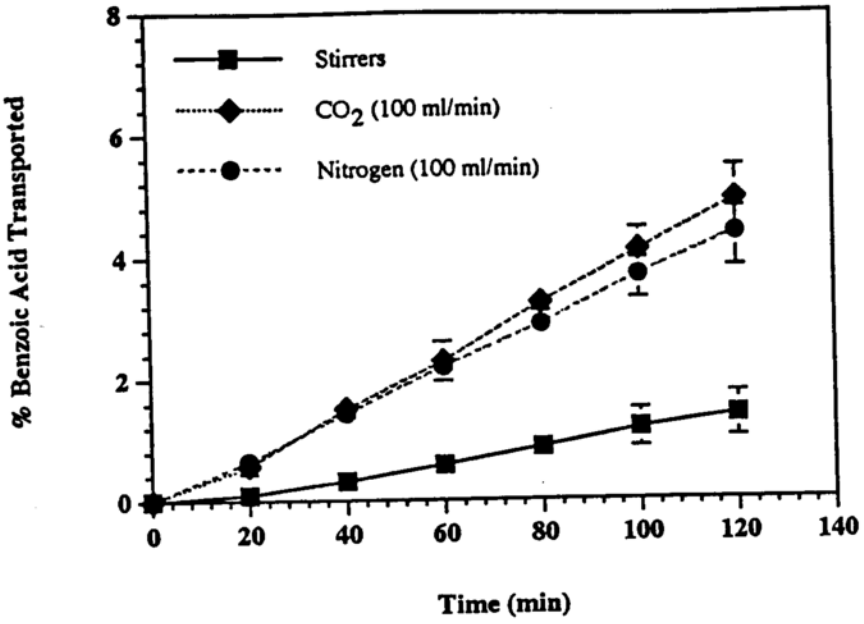

Figure 4.34: Effect of nitrogen bubbling on the permeability of benzoic acid across rabbit ileum tissue in-vitro. Error bars represent SEM of 3 to 4 experimental repetitions.

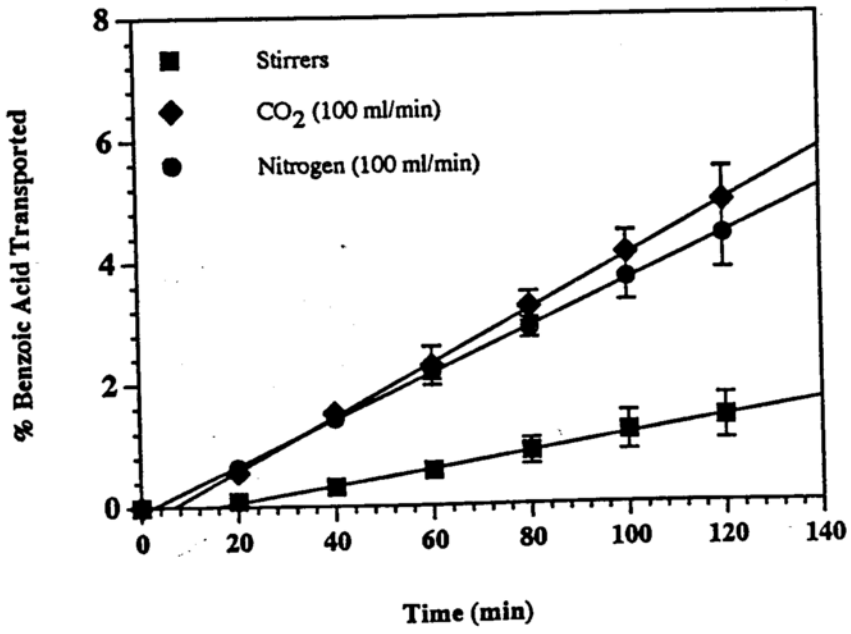

Figure 4.35: Percent benzoic acid transported across rabbit ileum tissue in-vitro depicting the steady state terminal slope. Number of experimental repetitions = 3 to 4. Error bars = SEM.

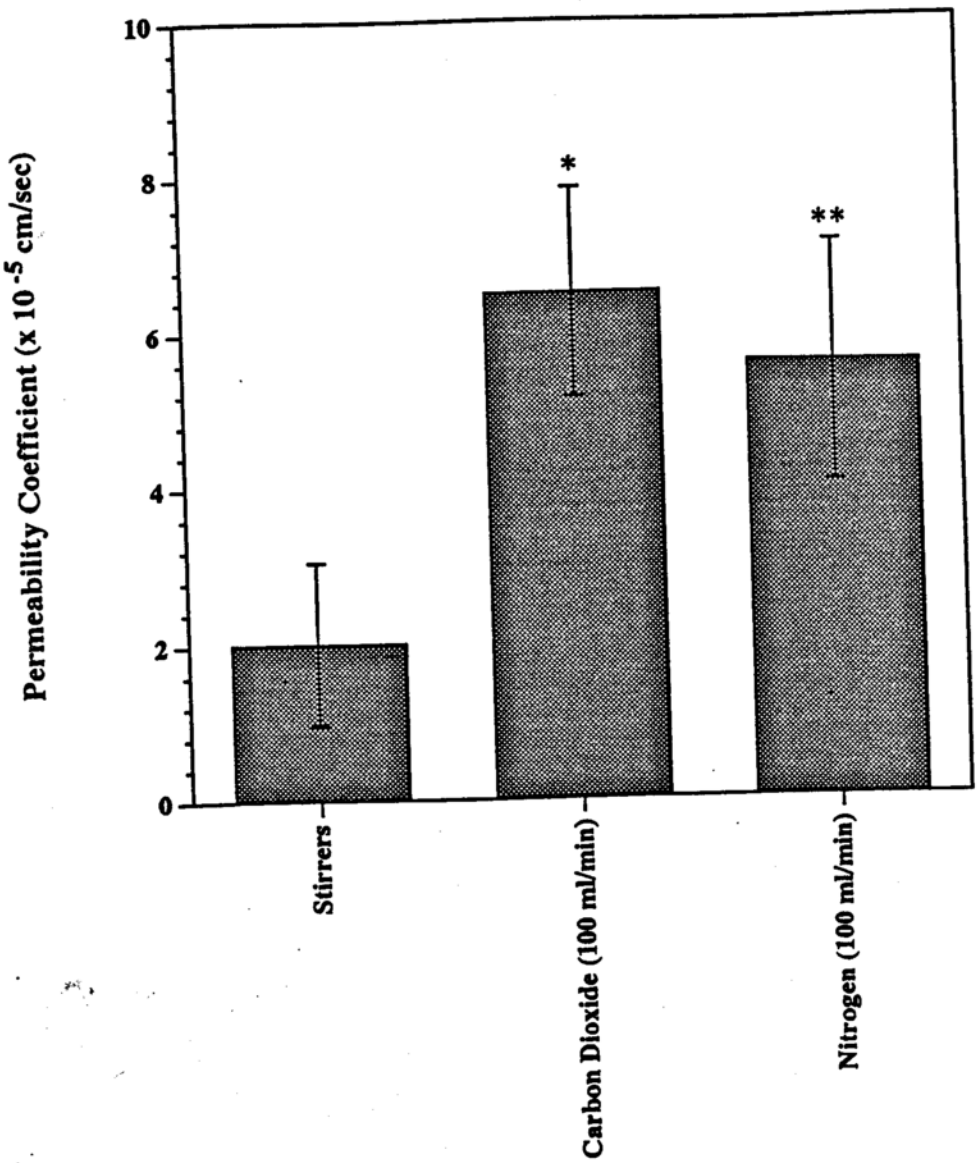

Figure 4.36: Comparison of benzoic acid in-vitro rabbit ileum permeability coefficients for nitrogen, carbon dioxide, and stirrer experiments. Error bars represent standard deviation of 3 to 4 experimental repetitions. * and ** indicate significant difference for carbon dioxide ($p < 0.005$) and nitrogen ($p < 0.02$), respectively, when compared to stirrers.

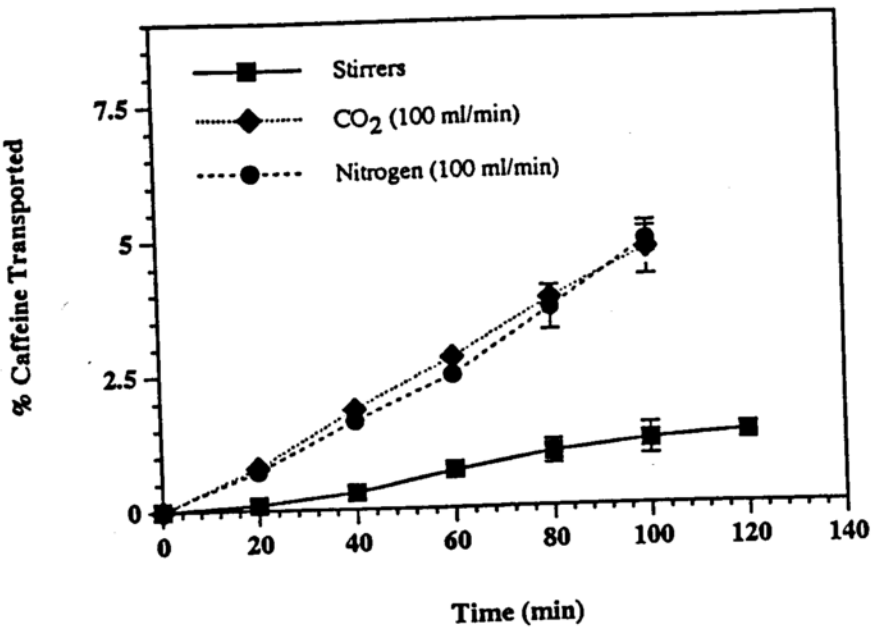

Figure 4.37: Effect of nitrogen bubbling on the permeability of caffeine across rabbit ileum tissue in-vitro. Error bars represent standard deviation of 4 experimental repetitions.

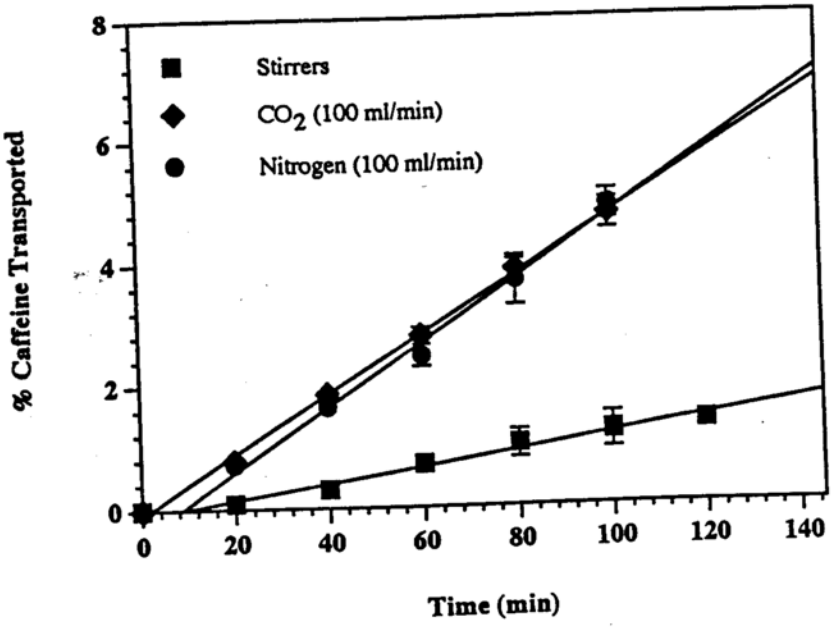

Figure 4.38: Percent caffeine transported across rabbit ileum tissue in-vitro depicting the steady state terminal slope. Number of experimental repetitions = 4. Error bars represent standard deviation.

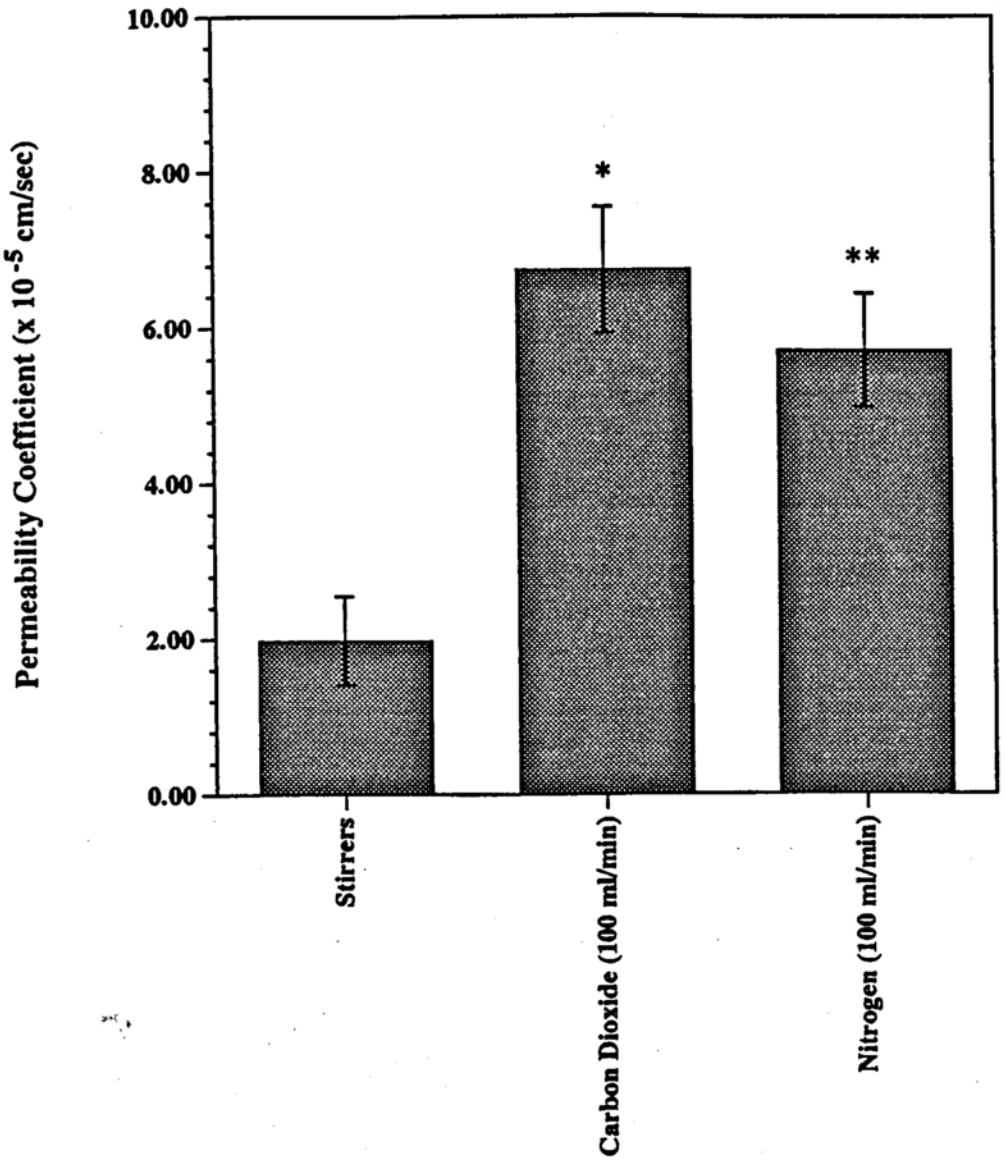

Figure 4.39: Comparison of caffeine in-vitro rabbit ileum permeability coefficients for nitrogen, carbon dioxide, and stirrer experiments. Error bars represent standard deviation of 4 experimental repetitions. * and ** indicate significant difference for carbon dioxide ($p < 0.0002$) and nitrogen ($p < 0.0005$), respectively, when compared to stirrers.

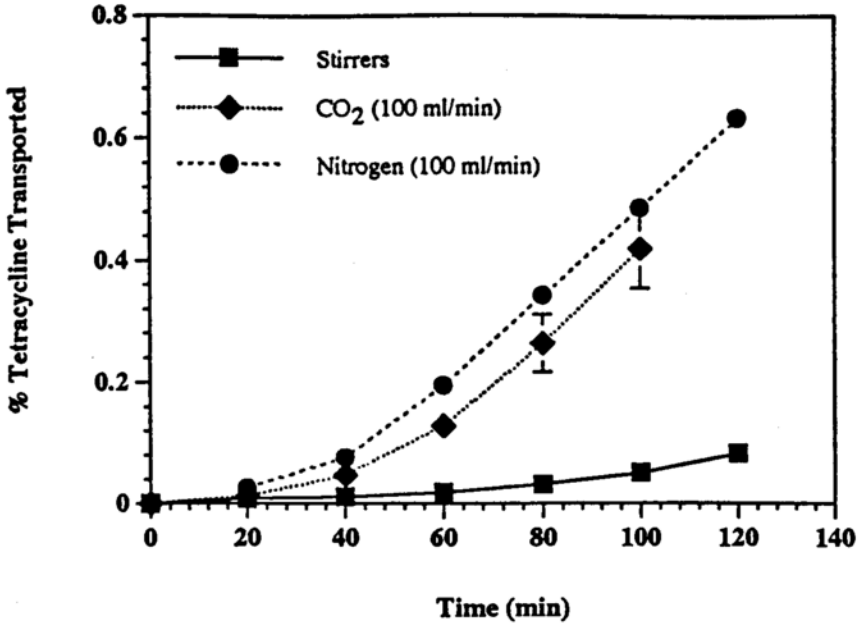

Figure 4.40: Effect of nitrogen bubbling on the permeability of tetracycline across rabbit ileum tissue in-vitro. Error bars represent SEM of 3 to 4 experimental repetitions.

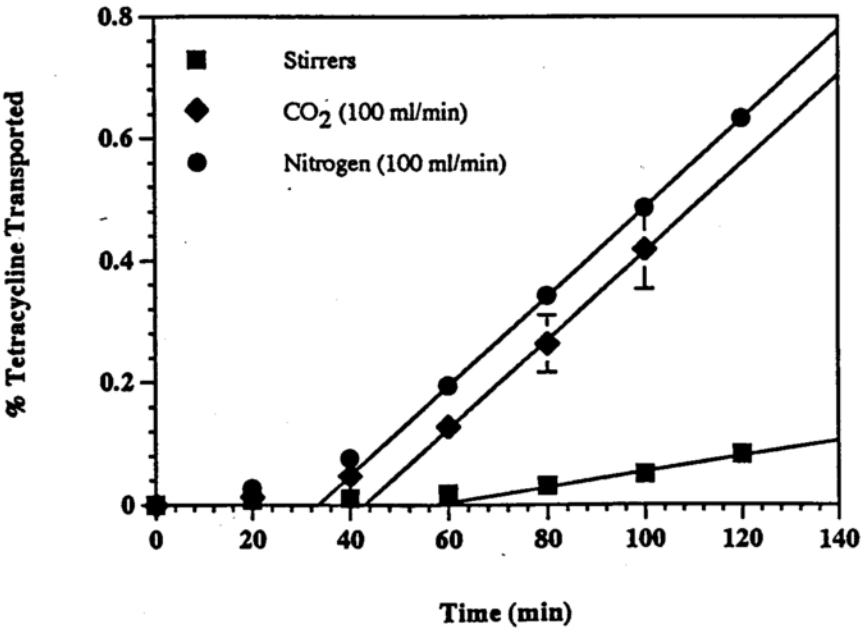

Figure 4.41: Percent tetracycline transported across rabbit ileum tissue in-vitro depicting the steady state terminal slope. Number of experimental repetitions = 3 to 4. Error bars represent SEM.

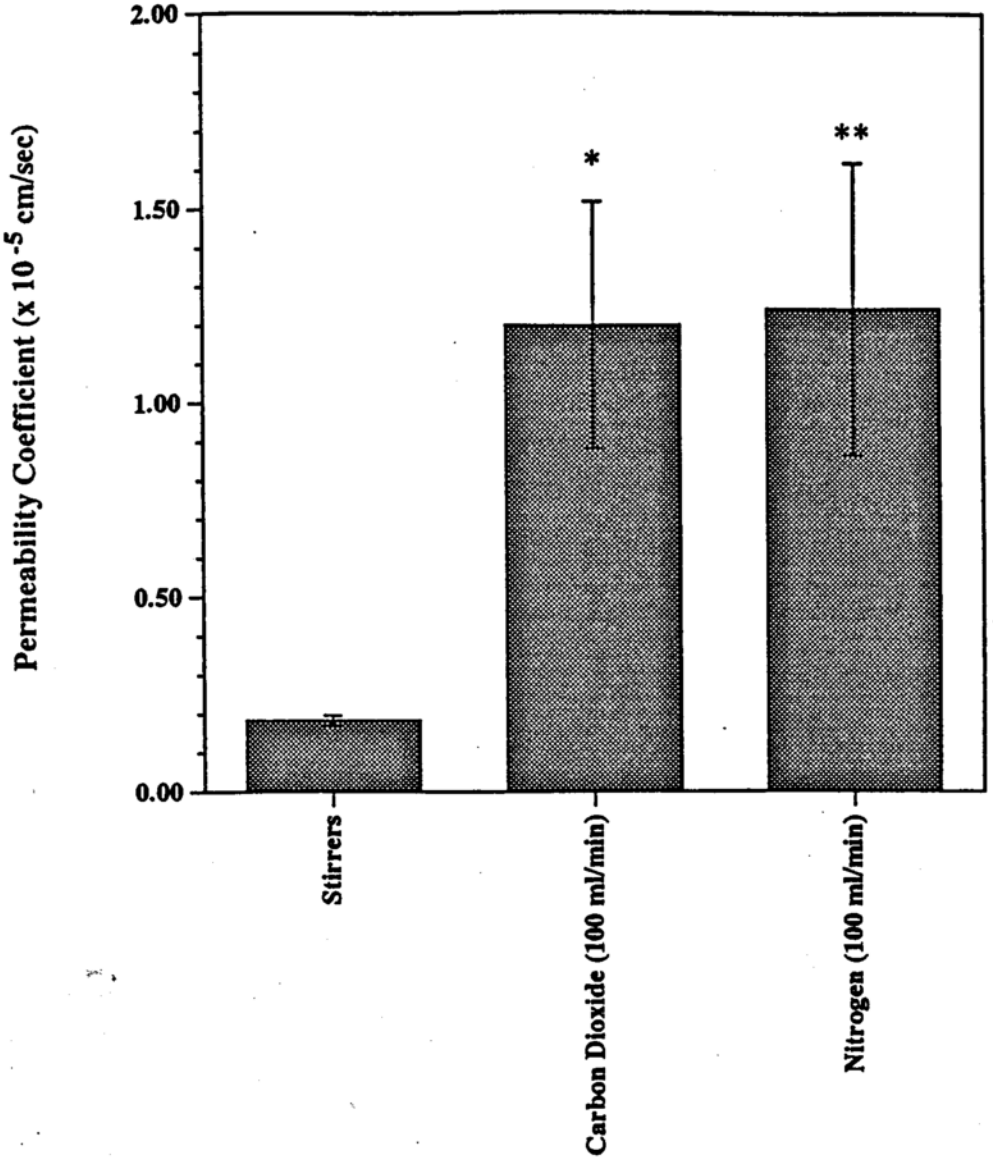

Figure 4.42: Comparison of tetracycline in-vitro rabbit ileum permeability coefficients for nitrogen, carbon dioxide, and stirrer experiments. Error bars represent standard deviation of 3 to 4 experimental repetitions. * and ** indicate significant difference for carbon dioxide ($p < 0.002$) and nitrogen ($p < 0.002$), respectively, when compared to stirrers.

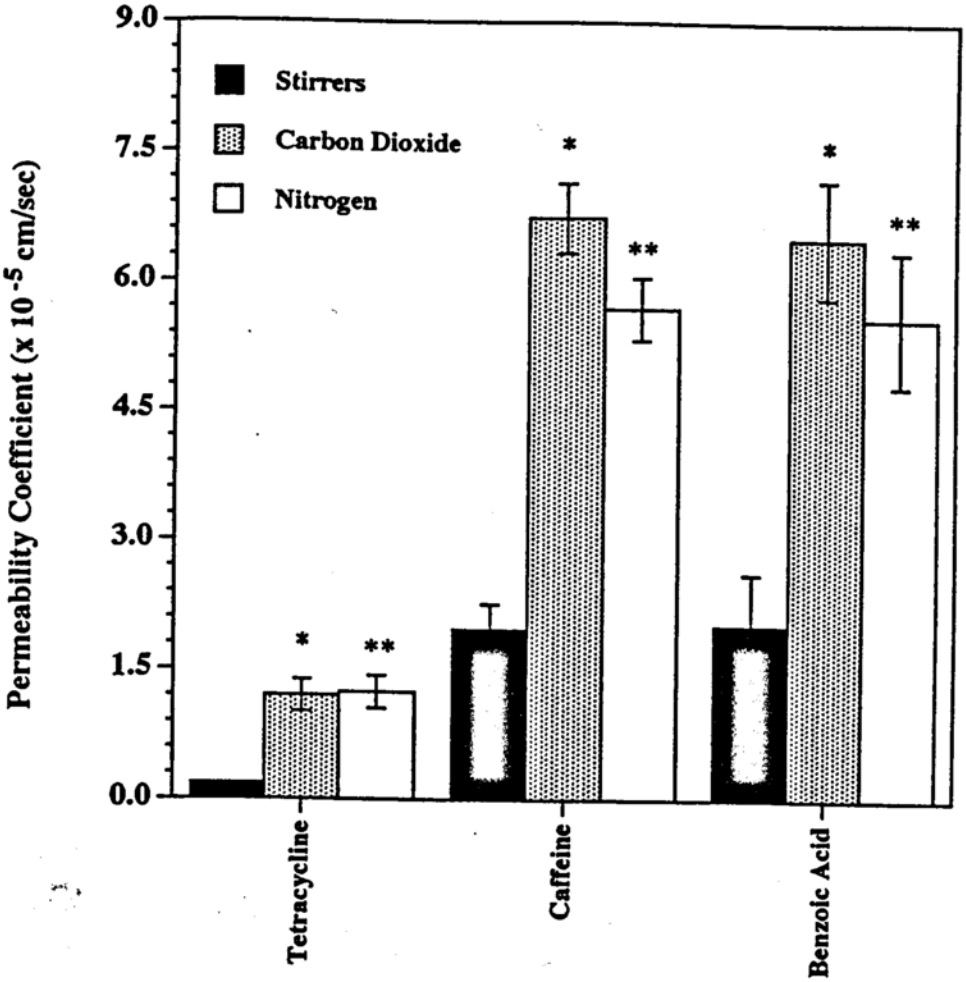

Figure 4.43: Summary of stir, carbon dioxide, and nitrogen permeability coefficients for compounds utilized in rabbit ileum in-vitro permeability studies. Error bars represent SEM. * and ** represent significant difference for carbon dioxide and nitrogen, respectively, when compared to stirrer experiments for a compound. For statistical p values, refer to previous figures or table.

Table 4.3: Effect of nitrogen bubbling on in-vitro permeability of tetracycline, caffeine, and benzoic acid across rabbit ileum tissue.

Compound	Experiment	Permeability Coefficient (x 10^{-5} cm/sec)	Standard Deviation (x 10^{-5} cm/sec)
Tetracycline	Stirrers	0.18	0.013
	CO_2	1.20	0.317
	Nitrogen	1.23	0.377
Caffeine	Stirrers	1.97	0.573
	CO_2	6.74	0.811
	Nitrogen	5.69	0.722
Benzoic Acid	Stirrers	2.01	1.04
	CO_2	6.50	1.35
	Nitrogen	5.58	1.55

3. Bubbling Rate

The rate of CO_2 bubbling onto rabbit ileum tissue was reduced by 10- and 100-fold from the initial experimental rate (100 ml/min.) to determine if there was a corresponding reduction in permeability enhancement. Figures 4.44 through 4.49 depict the effects of the bubbling rates (1, 10, and 100 ml/min.) on PEG 900 and diazepam permeability. A summary of the results is in Table 4.4.

PEG 900 permeability was not affected by a reduction in bubbling rate to 10 ml/min. Comparison of PEG 900 permeability coefficient values obtained with the 100 ml/min. and 10 ml/min. rates were found not to be significantly different ($p > 0.05$). However, a decrease in permeability was observed with further reduction in CO_2 bubbling to 1.0 ml/min. The permeability coefficient value fell to levels between that obtained for stirrer and the higher bubbling rates (10 and 100 ml/min.).

PEG 900 is a hydrophilic drug and is commonly utilized as a marker for passive diffusion through the paracellular space (Ghandehari, 1997; Ma, 1993). Since the influence of gas bubbling on permeability enhancement does not involve alterations in pH, the remaining possibilities include: (1) fluid flow; (2) stripping of the mucus layer; (3) membrane alteration; and (4) change in membrane hydrophobicity. Thinning or stripping of the mucus layer would reduce the diffusive barrier for a drug but would not influence the rate of drug permeability. The concept of fluid flow may be applicable in that an increase in solvent drag due to enhanced molecular velocities or pressure gradients could increase drug penetration across the tissue. PEG 900, as mentioned previously, is a polar drug whose flux across the cell membrane bilayer is minimal. An increase in membrane hydrophobicity would decrease the likelihood for PEG

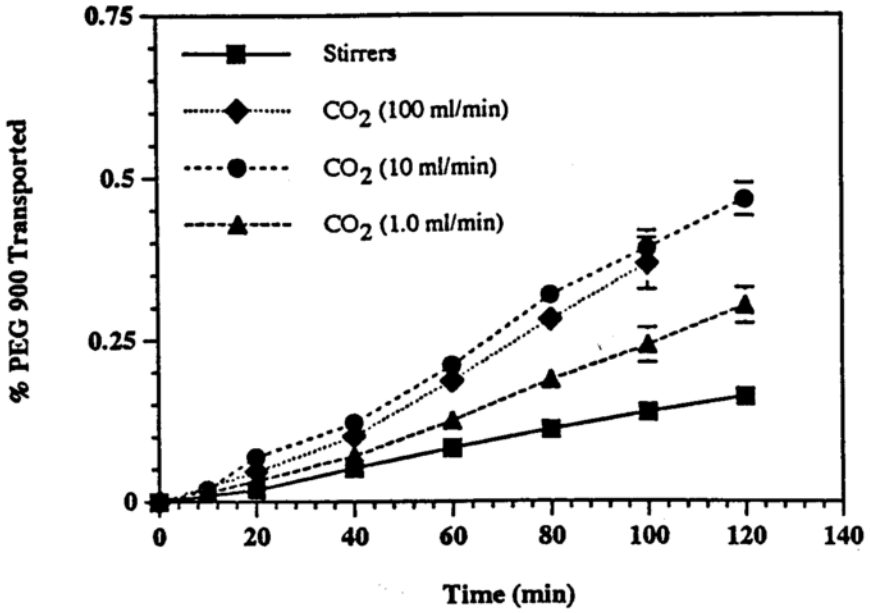

Figure 4.44: Effect of the rate of carbon dioxide bubbling on the permeability of PEG 900 across rabbit ileum tissue in-vitro. Error bars represent SEM of 3 to 5 experimental repetitions.

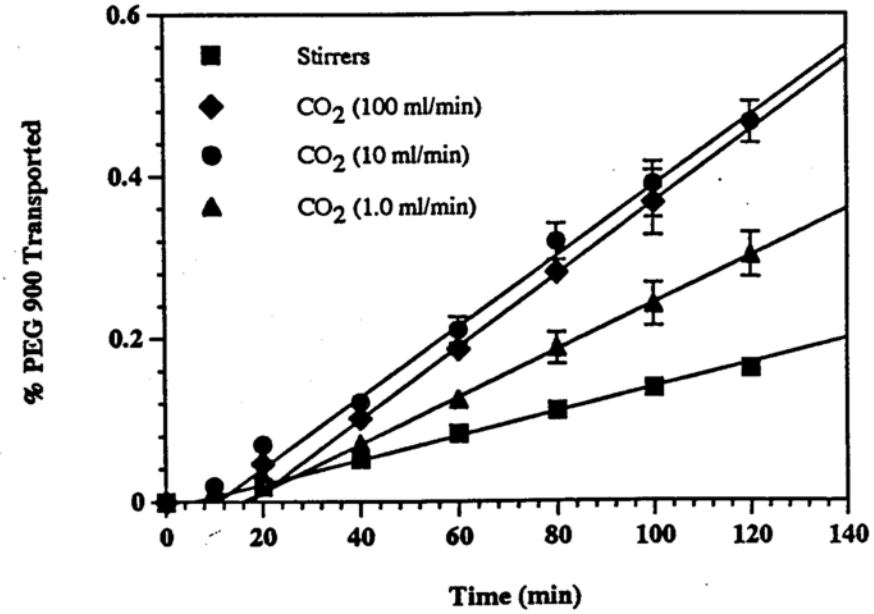

Figure 4.45: Percent PEG 900 transported across rabbit ileum tissue in-vitro as influenced by changes in carbon dioxide bubbling rate with illustration of the steady state terminal slope. Number of experimental repetitions = 3-5. Error bars = SEM.

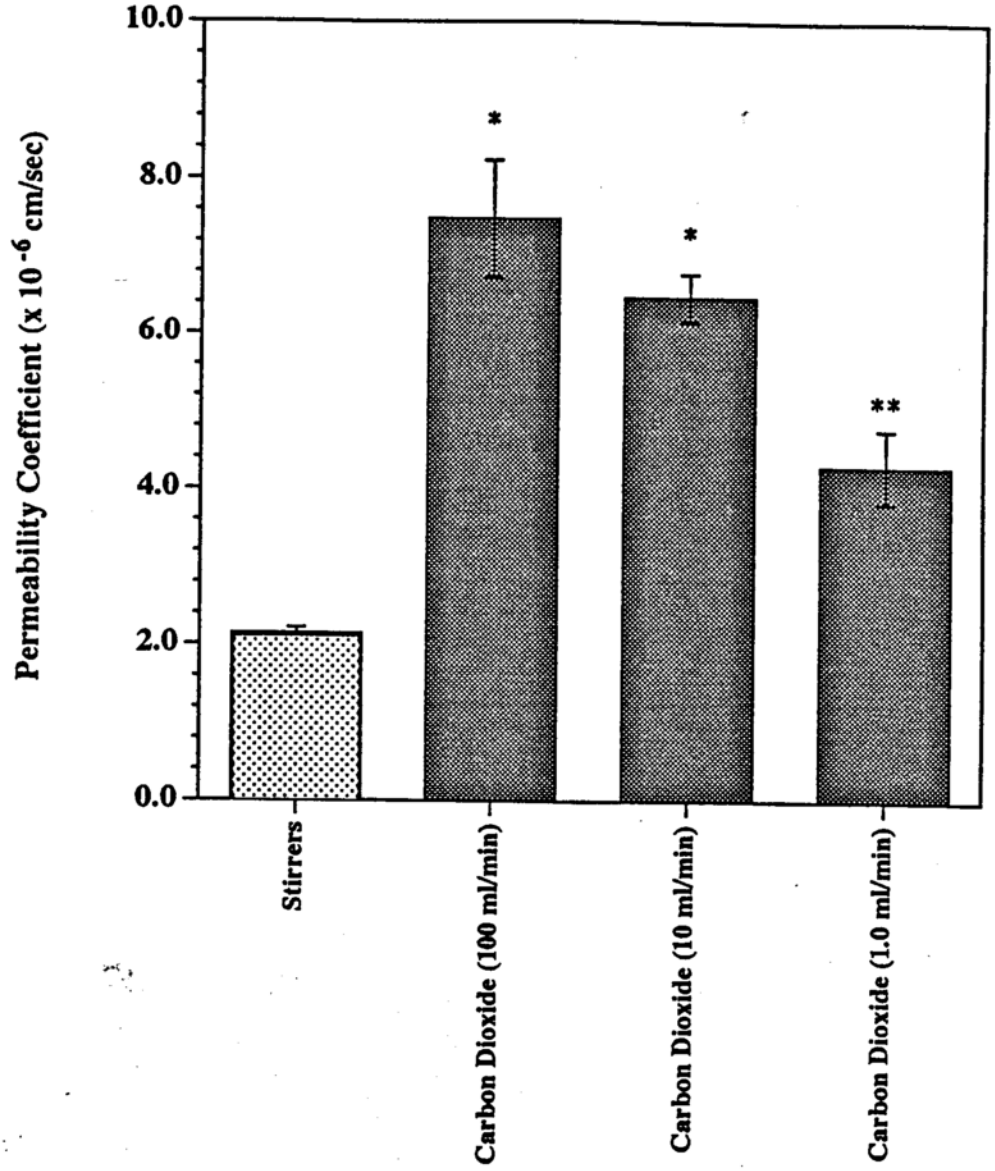

Figure 4.46: In-vitro rabbit ileum permeability coefficients for PEG 900 as influenced by the rate of carbon dioxide bubbling. Error bars represent SEM of 3 to 5 experimental repetitions. * indicates significant difference ($p < 0.006$) from stirrer experiments. ** denotes significant difference from stirrer ($p < 0.03$) and higher carbon dioxide bubbling rate ($p < 0.02$) experiments.

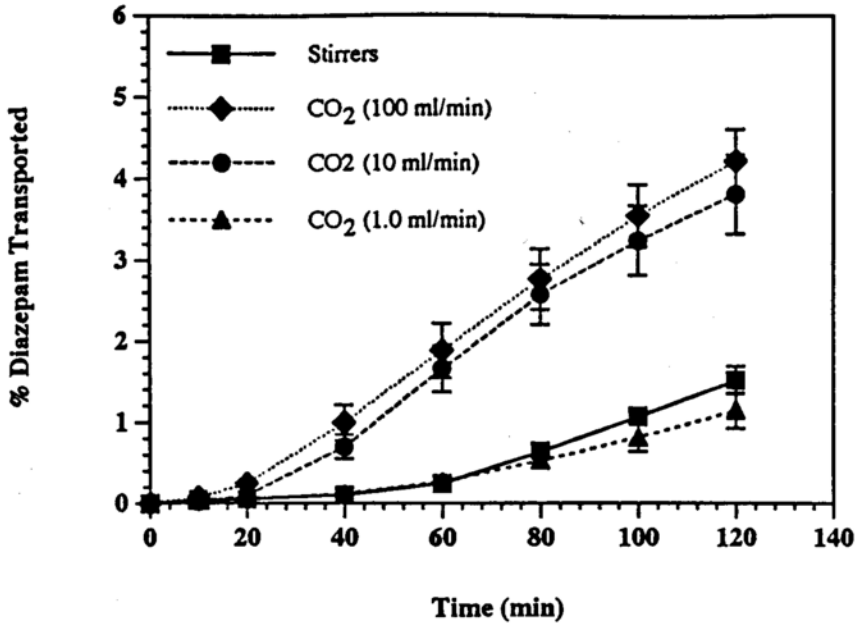

Figure 4.47: Effect of the rate of carbon dioxide bubbling on the permeability of diazepam across rabbit ileum tissue in-vitro. Error bars represent SEM of 3 to 8 experimental repetitions.

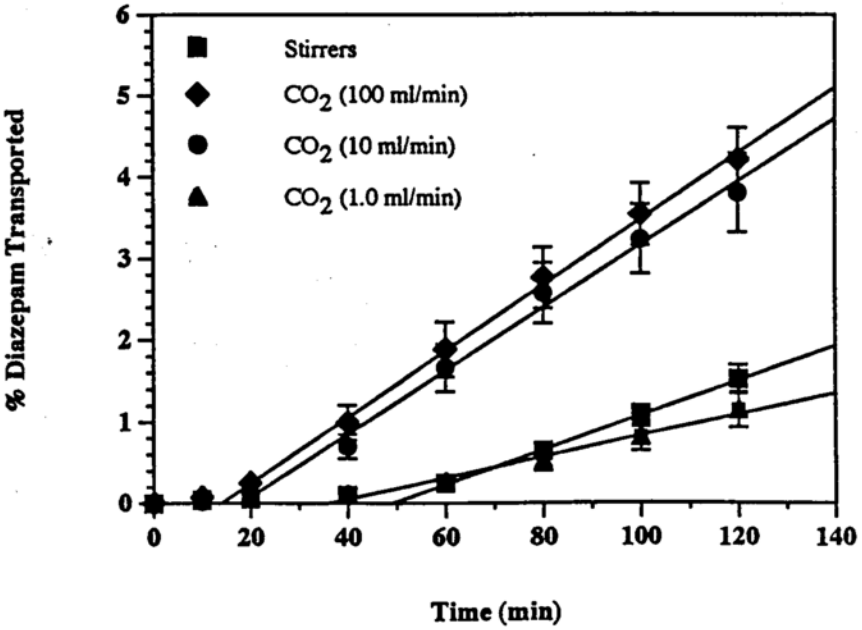

Figure 4.48: Percent diazepam transported across rabbit ileum tissue in-vitro as influenced by changes in carbon dioxide bubbling rate with illustration of the steady state terminal slope. Number of experimental repetitions = 3-8. Error bars = SEM.

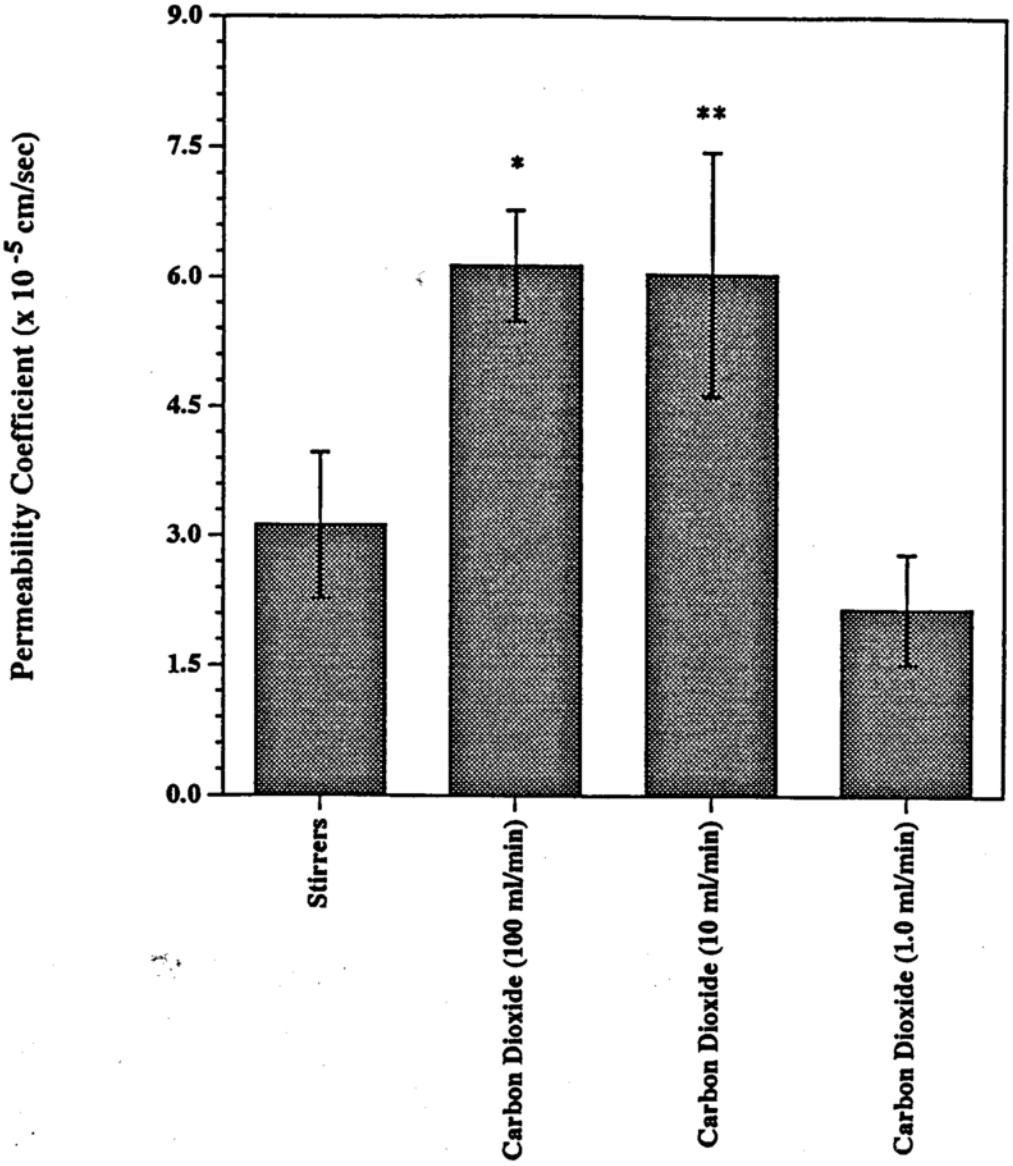

Figure 4.49: In-vitro rabbit ileum permeability coefficients for diazepam as influenced by the rate of carbon dioxide bubbling. Error bars represent standard deviation of 3 to 8 experimental repetitions. * denotes significant difference from stirrer ($p < 0.0005$) and 1.0 ml/min carbon dioxide ($p < 0.002$) experiments. ** indicates significant difference from stirrer ($p < 0.02$) and 1.0 ml/min carbon dioxide ($p < 0.01$) studies.

Table 4.4: Overall summary of the PEG 900 and diazepam permeability coefficients obtained from altering the rate of carbon dioxide bubbling onto rabbit ileum tissue.

Compound	Experiment	Permeability Coefficient (x 10^{-5} cm/sec)	Standard Deviation (x 10^{-5} cm/sec)
PEG 900	Stirrers	0.213	0.015
	CO_2 (100 ml/min)	0.747*	0.013
	CO_2 (10 ml/min)	0.646*	0.050
	CO_2 (1.0 ml/min)	0.430‡	0.094
Diazepam	Stirrers	3.12	0.849
	CO_2 (100 ml/min)	6.13(a)	0.642
	CO_2 (10 ml/min)	6.04(a)	1.400
	CO_2 (1.0 ml/min)	2.16(b)	0.641

* significant difference ($p < 0.006$) from stirrers.

‡ significant difference from stirrers ($p < 0.03$) and higher CO_2 bubbling rates ($p < 0.02$).

(a) significant difference from stirrers ($p < 0.02$).

(b) significant difference ($p < 0.01$) from higher CO_2 bubbling rates.

900 penetration into the lipid bilayer even further than compared to normal conditions. Therefore, an enhancement of membrane hydrophobicity is not a reasonable argument for the increased permeability rate for hydrophilic drugs.

The bubbles may impart a mechanical disruptive effect on the epithelial monolayer. Two effects on the epithelium are possible (see Figure 5.1). First, the tight junction, which is the rate limiting constituent of the paracellular pathway, may be disrupted (i.e. loosened), inducing an increase of its pore diameter. This would enable not only larger drug molecules to diffuse across the cell monolayer but would also enhance permeability of all hydrophilic molecules due to an increased absorptive surface area available for diffusion. Bubbling may also mechanically induce cell membrane alterations by creating aqueous pores due to protein/phospholipid leaching from the lipid bilayer and/or enlarging pre-existing membrane pores. These two mechanisms would create an environment which would allow a greater chance for hydrophilic drugs to traverse the membrane in more substantial quantity.

A reduction in PEG 900 permeability in the presence of a low CO_2 bubbling rate (1.0 ml/min.) leads to conclusions that it may be associated with a decrease in mechanical disruption imparted on the paracellular path and/or cell membrane due to lower levels of bubbling, imparting less turbulence on the epithelial surface. It may also in part be explained by reduced flow velocities and pin-point pressure gradients across the epithelium.

Diazepam permeability also was not reduced with a decrease in CO_2 bubbling to 10 ml/min. Diazepam permeability coefficient values for bubbling rates of 100 and 10 ml/min., were found not to be significantly different ($p > 0.05$). With a 100-fold rate reduction to 1.0 ml/min., diazepam permeability returned to levels equivalent to stirrer experiments.

Diazepam is used as a transcellular marker probe (Cogburn, 1991). Therefore, one would expect it to cross the epithelium by partitioning into the cell membrane with limited absorption through cellular pores or the paracellular pathway. At higher levels of CO_2 bubbling, 10 and 100 ml/min., the majority of diazepam's enhanced permeability could be accounted for as due to an increase in membrane hydrophobicity from CO_2 permeation into the membrane. The enhanced permeability could also be accounted for via increased diffusion through the disrupted epithelium (i.e. enlarged or newly created membrane pores, tight junction opening). Lipophilic drugs have the tendency to partition into hydrophobic environments rather than stay within a hydrophilic medium (e.g. water). Therefore, one would expect enhancement through the water pathways to be limited.

At the 1.0 ml/min. bubbling rate, reduction of diazepam permeability to stirrer levels is probably due to the reduced availability for CO_2 membrane incorporation. As a result, diazepam would partition into the cell membrane at similar rates to normal conditions. The possibility for enhancement due to higher fluid velocity or induction of membrane pressure gradients would also diminish due to the decreased rate of bubble production.

II. In-Vivo Perfusion Studies

Results of benzoic acid in-vivo absorption studies are shown in Figures 4.50 and 4.51. The main objective of these studies was to correlate the in-vitro CO_2 penetration enhancement effects to in-vivo animal studies. The results indicated that CO_2 induced greater benzoic acid absorption in rat duodenum and ileum tissue, verifying the findings associated with the in-vitro experiments. Under experimental conditions, in which buffer pH values were either 6.5 or 6.8, depending upon the origin of the intestinal tissue, greater than 99% of the benzoic acid molecules will be negatively charged, conferring a greater hydrophilicity to the molecule. However, the in-vitro experiments indicated a high permeability rate, which would correspond to benzoic acid still being able to partition into the cell membrane. Therefore, the mechanism(s) for enhanced benzoic acid absorption by CO_2 could be due either to an effect on the cell membrane and/or the paracellular space in addition to increased fluid flow, membrane hydrophobicity, or mucus disruption.

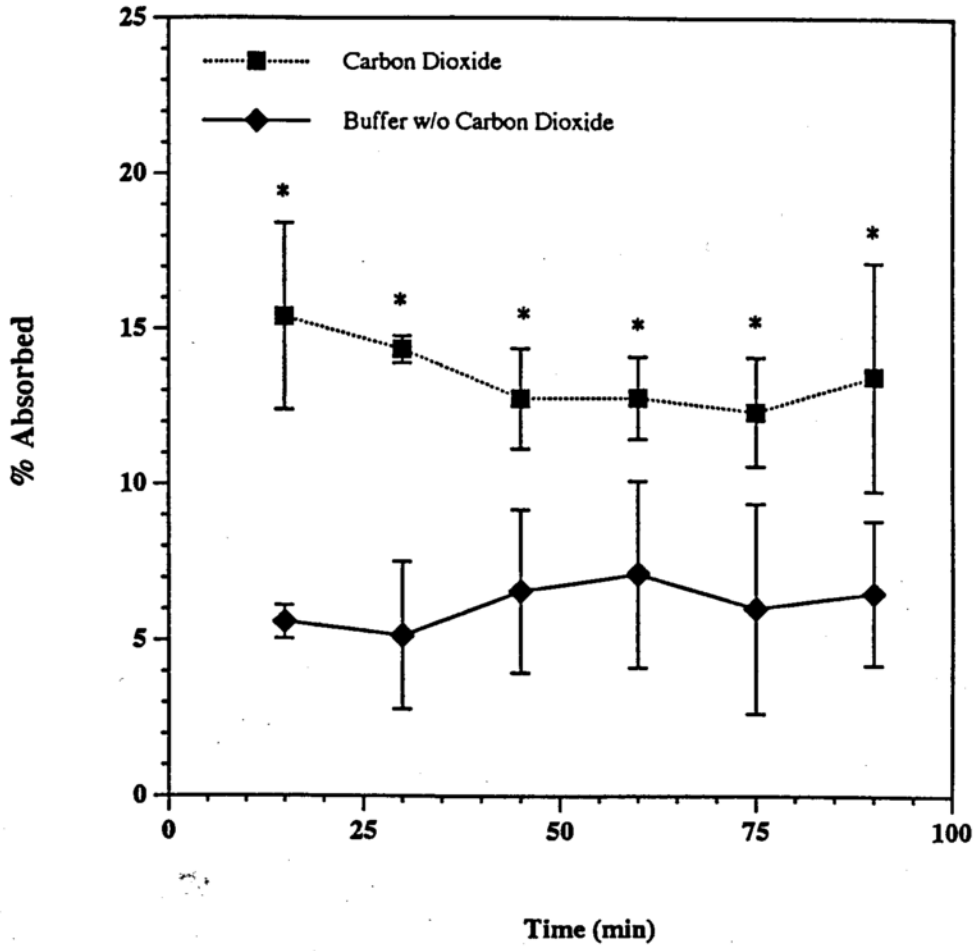

Figure 4.50: Percent benzoic acid absorbed from in-vivo single-pass perfusion of rat duodenum with and without carbon dioxide gas bubbling. Error bars represent standard deviation of 3 experimental repetitions. * denotes significant difference ($p < 0.05$). Carbon dioxide bubbling rate $\approx$ 5.0 ml/min.

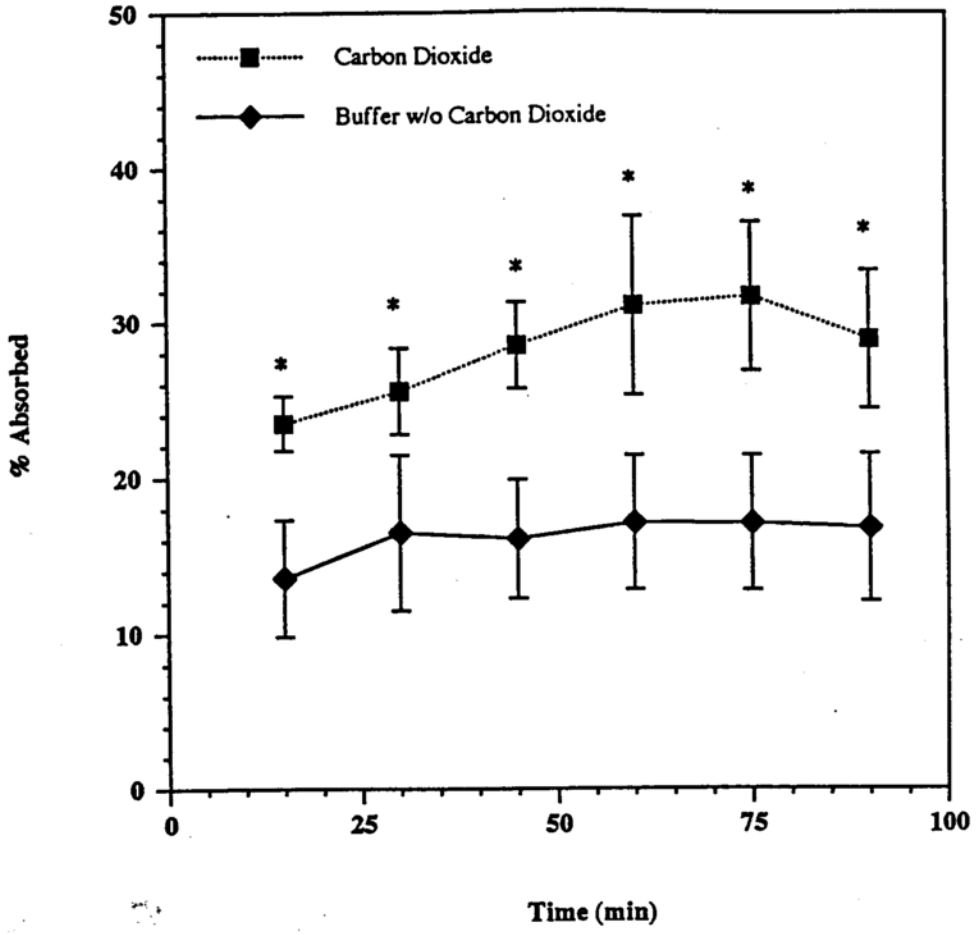

Figure 4.51: Percent benzoic acid absorbed from in-vivo single-pass perfusion of rat ileum with an without carbon dioxide gas bubbling. Error bars represent standard deviation of 4 to 7 experimental repetitions. * denotes significant difference ($p < 0.05$). Carbon dioxide bubbling rate ≈ 5.0 ml/min.

Chapter 5: Mechanistic Studies on Penetration Enhancement Through Effervescence

I. Background

The mechanisms by which absorption enhancers improve drug permeability across intestinal epithelium has been the focus of numerous studies in the past two decades. It is postulated that penetration enhancers exert their biological effect(s) in a variety of ways including: (1) reducing the mucosal layer thickness and/or viscosity; (2) tight junction alteration; (3) inducing a change in cell membrane structure; and (4) increasing the hydrophobic environment within the cellular membrane (Lee, 1991c).

The large surface area and hydrophobicity of cellular membranes create an environment in which lipophilic compounds tend to be absorbed across the intestinal epithelium without much difficulty due to rapid partitioning. The primary obstacles limiting their absorption are diffusion through the hydrophilic mucus layer and obtaining adequate drug dissolution (Rahman, 1986). Therefore, the majority of penetration enhancer studies are concerned with determining the mechanism for enhanced absorption of polar molecules, which are primarily transported via passive diffusion through the paracellular space.

Techniques used to study drug transport via the paracellular route include qualitative and quantitative methodologies. A quantitative measure of permeability alteration incurred through penetration enhancer disruption is commonly obtained by transport experiments utilizing hydrophilic marker molecules. These probes (e.g. mannitol, PEGs) have been shown to permeate

intestinal epithelium via the paracellular pathway (Krugliak, 1989; Ma, 1990; Ma, 1993). An increase in marker flux is suggestive of an effect on the paracellular pathway, but is not conclusive due to the fact that there may also be changes within the transcellular pathway as well.

Transepithelial electrical resistance (TEER) is a common technique used to provide a qualitative measure of tissue tightness in which changes in ion flux across intestinal membranes are often correlated with a structural transformation of the paracellular pathway, but may also be due to changes within the transcellular route. Numerous studies have shown that a decrease in TEER is commonly associated with increases in hydrophilic marker permeability due to changes with the intercellular space (Noach, 1993; Sawada, 1991; Tomita, 1995; Yamashita, 1985).

Another qualitative method occasionally used is histological visualization by microscopy. Electron microscopy has been utilized as a method to study alterations within the intestinal monolayer. Histological techniques are advantageous in that they provide a macroscopic view of the tissue prior to and after exposure to a penetration enhancer. However, one needs to be cautious when analyzing these pictures due to investigator subjectivity in addition to the fact that the tissue has been chemically fixed, which may lead to artificial alterations as demonstrated by Van Deurs and Luft (Van Deurs, 1979). Other types of microscopy which have been utilized include fluorescent and confocal laser scanning microscopy.

In terms of studying drug transport via the transcellular pathway, various methods are used, including cell membrane fluidity. An increase in membrane fluidity is indicative of a conformational change within the membrane bilayer. This alteration may be induced by incorporation of large molecular substances into the

bilayer or by destabilizing effects such as leaching of membrane proteins and/or phospholipids. Fluorescent spectroscopy is commonly used to measure changes in membrane fluidity through incorporation of fluorescent probes into the membrane with subsequent exposure to an absorption enhancer. An increase in fluidity is commonly associated with greater hydrophilic drug flux (LeCluyse, 1991; Morrow, 1986). Other methods utilized for determination of membrane fluidity include: Fourier infrared spectroscopy (FTIR), differential scanning calorimetry (DSC), and electron spin resonance spectroscopy (ESR). A major problem in using these techniques is that they are primarily used to investigate membrane organization within brush border membrane vesicles or cell suspensions. While these experiments are informative as to possible mechanisms for enhanced drug permeability, it is difficult to correlate these results with those one would obtain in experiments utilizing a monolayer of confluent cells.

Cell membrane integrity may also be associated with the release of proteins, intracellular enzymes, and membrane-bound enzymes. Increased levels of these molecules are indicative of the level of membrane perturbation, irritation, and damage sustained by the epithelium and have been associated with enhanced drug absorption (Hosoya, 1994; Swenson, 1994).

When investigating the mechanism(s) of drug permeability enhancement due to an absorption promoter, it is necessary to incorporate a number of experimental techniques which examine the effect on both the paracellular and transcellular pathways. Elucidation of the effects on only one pathway may potentially lead to erroneous conclusions. The potential mechanism(s) by which CO_2 bubbling may enhance drug permeability due to epithelial disruption is shown in Figure 5.1.

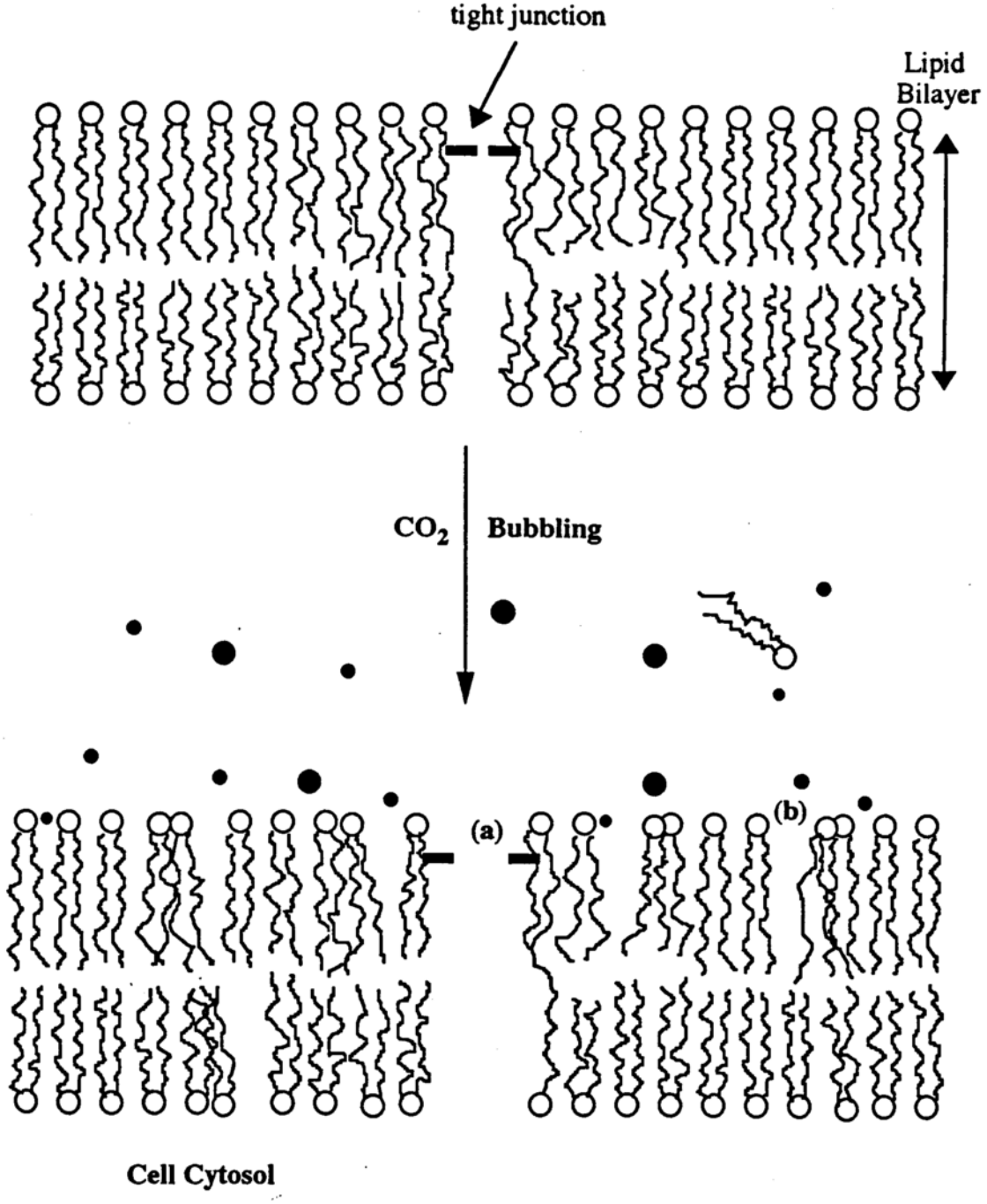

Figure 5.1: Potential mechanism(s) by which CO_2 bubbling may enhace drug permeability via intestinal epithelium disruption: (a) an opening of the tight junction and/or (b) altering the structure of the cell membrane via mechanical turbulence. • = CO_2 gas bubble.

II. Experimental

A. MTT Tissue Viability

1. Background

MTT is a water-soluble tetrazolium salt that forms a yellow solution with the addition of phosphate buffered saline, pH 6.5. In the presence of dehydrogenase enzymes, dissolved MTT is converted to an insoluble purple formazan moiety. Formazan formation occurs due to cleavage of the tetrazolium ring by dehydrogenase enzymes:

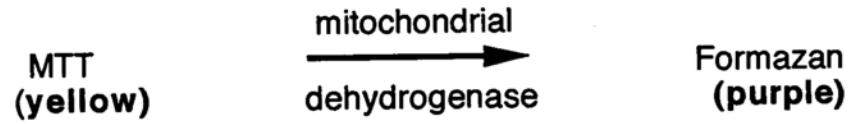

The water-insoluble purple formazan is thus solubilized using appropriate solvents (i.e. isopropanol) and the absorbance as a function of converted dye is spectrophotometrically measured at 570 nm.

Viable cells contain active mitochondrial dehydrogenase which can cause the conversion of MTT to the insoluble formazan. Non-viable cells do not contain the active enzyme, and, therefore, are unable to convert MTT to formazan. The MTT assay has been utilized as a useful technique for measurement of cell viability and cytotoxicity upon exposure to various substances (Carmichael, 1987; Grant, 1994; Lappalainen, 1994).

2. Materials

MTT (3-[4,5-Dimethylthiazol-2-yl]-2,5-diphenyltetrazolium bromide; Thiazolyl blue) was purchased from Sigma Chemical Company (St. Louis, MO). Isopropyl alcohol, 99.0%, was purchased from Spectrum Chemical Mfg. Corp. (Gardena, CA). Unless otherwise stated, all reagents were used as received.

3. Solutions

MTT stock solution (5 mg/ml) was prepared by dissolving 80 mg MTT in 16.0 ml phosphate buffered saline (pH 6.5). A fresh solution was prepared prior to the initiation of each experiment. A 0.04 N HCl/isopropanol solution was prepared by adding 0.4 ml of concentrated hydrochloric acid (10.15 N) to 100 ml isopropyl alcohol.

4. Assay Procedure

The procedure used in this section is a modification of the methodology followed by Lappalainen (Lappalainen, 1994). Rat duodenal segments were prepared for tissue mounting onto diffusion cell inserts and placed within the diffusion cell as previously described (see Chapter 4). Donor and receiver solutions and quantities (7.0 ml) were used as described in Chapter 4 under the in-vitro permeability section, except that there was no drug concentration within the donor solution. Also, stirrers were not present within the chambers. At

preselected times (10 min., 20 min., 60 min., and 120 min.) following tissue contact with the donor and receiver solutions, the tissue insert was removed from the diffusion cell. The tissue area exposed to the buffer (surface area = 0.785 cm^2) was cut from the center of the tissue holder, blotted dry, and weighed on a Mettler AE 200 balance (Mettler Instrument Corp., Hightstown, NJ). The tissue was placed within a glass test tube and 1.0 ml of MTT stock solution was added. The tube was placed in a 25.0°C water bath for 30 minutes, at which time, the tissue was removed and blotted to remove excess dye. Cold saline was used to rinse any residual dye. The tissue was placed in a clean test tube with 1.0 ml 0.04 N HCl/isopropanol solution, capped, and shaken in a 25.0°C water bath for 30 minutes. The solution was then removed, placed into a clean tube, and capped to prevent evaporation. 100 μl of the solution was removed and placed into a cuvette and subsequently diluted with 1.0 ml isopropyl alcohol. The cuvette was capped and inverted for complete mixing and scanned at 570 nm using a Hitachi U-3000 spectrophotometer (Hitachi Instruments, Inc., Naperville, IL) utilizing isopropanol as reference.

The procedure followed is the same upon tissue exposure to carbon dioxide bubbling except a tube connected to a pure CO_2 and a 95%O_2/5%CO_2 gas cylinder was placed ≈ 1.0 cm from the tissue surface in the donor chamber. CO_2 bubbling onto the epithelial surface was continuous at the rate of 100 ml/min. until time for tissue removal.

B. Membrane Perturbation/Damage

The in-vivo single-pass perfusion experimental set up previously described (see Chapter 4) was used for all membrane perturbation and damage studies.

However, these experiments utilized pure phosphate buffer (pH 6.8; ≈ 300 mOsm) without radioactivity or cold drug concentration. The buffer was perfused through a 10 cm rat ileum segment at a rate of 0.4 to 0.5 ml/min. with the and perfusate collected over pre-designated time intervals. The samples were assayed via protocols specific for each individual substance.

For positive control experiments, a 1.25% sodium deoxycholate (Sigma Chemical Co., St. Louis, MO) solution (pH 6.8; ≈ 300 mOsm) was prepared and used as the perfusate.

1. Lactate Dehydrogenase

a. Background

Lactate dehydrogenase (LDH) is a cytosolic enzyme found in a variety of body tissues (i.e. heart, liver, etc.) and also within epithelial cells lining the intestinal tract. It is permeanently located in the cytosol due to its inability to traverse or leak across the cell membrane. A variety of studies have used LDH as a biochemical marker for epithelial cell wall damage (Pujara, 1995; Swenson, 1994).

LDH catalyzes the interconversion of lactic acid to pyruvate via utilization of coenzyme NAD^+ for hydrogen transfer:

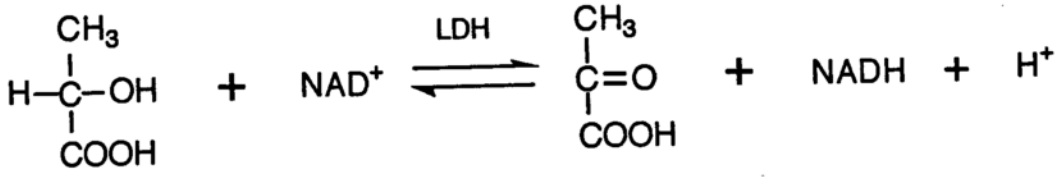

Lactate **Pyruvate**

The formation of reduced nicotinamide adenine dinucleotide (NADH) produces an increase in absorbance at 340 nm which is directly proportional to the amount of LDH activity within the sample.

b. Assay Procedure

The samples were individually assayed for lactate dehydrogenase activity following procedural guidelines outlined in the LDH enzyme kit (Sigma Chemical Company, St. Louis, MO). The samples were read utilizing a Hitachi U-3000 spectrophotometer (Hitachi Instruments, Inc., Naperville, IL) connected to a temperature controlled cuvette water bath. The assay was run at 30.0°C with distilled deionized water (DDW) as reference. One ml of LDH reagent (50 mmol/l lactate, 7 mmol/l NAD, in pH 8.9 buffer; supplied by Sigma Chemical Co.) was placed into a cuvette and warmed to 30.0°C. A 50 μl perfusate sample was added to the cuvette which was then capped and thoroughly mixed by inversion. The cuvette was placed into a prewarmed (30.0°C) cuvette compartment for 30 seconds, at which time, the absorbance was read and assigned the initial reading. The absorbance was recorded at 30 and 60 seconds past the initial reading with the 60 second absorbance reading corresponding to the final value. The difference between the initial and final values indicates the change in absorbance per minute (ΔA/min). LDH activity in units per liter was determined via the equation:

$$\text{LDH Activity (U/L)} = \frac{(\Delta A/\text{min})\,(TV)\,(1000)}{(6.22)\,(SV)\,(LP)} \qquad (4)$$

where TV = total reaction volume (1.05 ml), SV = sample volume (0.05 ml), 6.22 = mM NADH absorptivity at 340 nm, LP = lightpath (1.0 cm), and 1000 = conversion factor.

2. 5'-Nucleotidase

a. Background

5'-Nucleotidase (5'-ND) is a cell membrane-bound enzyme located within a variety of tissues including intestinal and nasal epithelium. 5'-ND denotes a group of enzymes which hydrolyze 5'-nucleotides (e.g. adenosine 5-monophosphate) to nucleosides. Arkesteijn developed an enzyme kinetic method measuring nucleoside production due to the hydrolytic activity of the enzyme on 5'-nucleotides (Arkesteijn, 1976). This method involves the following reactions:

$$\text{AMP} \xrightarrow{\text{5'-ND}} \text{Adenosine} + P_i$$

$$\text{Adenosine} \xrightarrow{\text{ADA}} \text{Inosine} + \text{Ammonia}$$

$$\text{Ammonia} + \text{2-Oxoglutarate} + \text{NADH} \xrightarrow{\text{GLDH}} \text{L-Glutamate} + \text{NAD}^+$$

in which adenosine monophosphate (AMP) is hydrolyzed to yield adenosine and inorganic phosphorus (P_i). Adenosine deaminase (ADA) deaminates adenosine to form inosine and ammonia. L-glutamate dehydrogenase (GLDH) catalyzes the reaction between ammonia and 2-oxoglutarate with NADH to form glutamate and NAD^+. Therefore, the rate of NAD^+ production results in a decrease in absorbance at 340 nm, which is directly proportional to 5'-ND activity in the sample.

b. Assay Procedure

Perfusate samples were individually assayed for 5'-ND activity following the procedures outlined in the 5'-ND diagnostic enzyme kit (Procedure No. 265-UV; Sigma Chemical Co.; St. Louis, MO).

5'-ND reagent supplied by Sigma Chemical Co. was reconstituted with 15 ml DDW leading to the following concentration of ingredients:

AMP	32. mM
NADH	0.2 mM
2-oxoglutarate	3.7 mM
GLDH	11,000 U/L
ADA	400 U/L

The perfusate samples were read on a Hitachi U-3000 spectrophotometer (Hitachi Instruments, Inc., Naperville, IL) with a temperature controlled cuvette chamber. The assay was performed at 30.0°C utilizing DDW as the reference.

Three ml of 5'-ND reagent was placed in a cuvette and brought to 30.0°C via placement in a water bath. A 20 μl perfusate sample was added to the cuvette and mixed by inversion. The cuvette was subsequently placed into the cuvette compartment for 5 minutes , at which time, the initial reading (I) was recorded. The final absorbance value (F) was recorded 5 minutes later. The difference between I and F indicated the absorbance change per minute (ΔA/min.). 5'-ND activity in units/liter (U/L) was calculated by the equation:

$$5'\text{-ND activity } (U/L) = \frac{(\Delta A/\min)(V)(1000)}{(6.22)(SV)(5)} \qquad (5)$$

where V = total reaction volume, SV = sample volume (0.02 μl), 6.22 = mM NADH absorptivity at 340 nm, 5 = conversion of ΔA/5min to ΔA/min, and 1000 = conversion factor.

3. Total Protein Release

a. Materials

A micro-protein determination kit, procedure number 690, was purchased from Sigma Chemical Co. (St. Louis, MO) and was stored at 2-6°C. NaCl was obtained from Aldrich Chemical Co. (Milwaukee, WI). Unless otherwise noted, all chemicals were used as received and solutions were prepared with distilled deionized water (DDW) run through a Barnstead PCS water purification system.

b. Solutions

The micro protein determination kit contained Biuret Reagent (cupric sulfate 0.75 mM and sodium hydroxide 94.0 mM), Folin and Ciocalteu's Reagent, protein standard (bovine albumin 10 g/dl, sodium azide 0.5% in 0.85% NaCl). 0.85% sodium chloride solution was prepared by dissolving 850 mg NaCl in 500 ml DDW.

c. Assay Procedure

The procedure utilized is a modification of the Ohnishi and Barr method and is only sensitive to final protein concentrations between 15 and 100 mg/dl (Ohnishi, 1978). A calibration curve plotting absorbance at 730 nm vs. total protein concentration (mg/dl) was obtained prior to determination of protein levels within the samples.

0.2 ml of each perfusate sample and a blank consisting of 0.85% NaCl (0.2 ml) were placed in separate prewashed test tubes. Biuret Reagent (2.2 ml) was then added to each tube. After mixing, the tubes were allowed to stand at room temperature (25°C) for 10 minutes, at which time, 0.1 ml Folin and Ciocalteu's Phenol Reagent was added to each tube and mixed. After standing at room temperature for 30 min., the absorbance for each solution was read at 730 nm using a DMS 300 Spectrophotometer (Varien Techtron, Australia). The blank was utilized as the reference and protein concentration determined from the calibration curve.

C. Paracellular Marker Permeability Studies

The materials, solutions, and procedures utilized in this section correspond to the studies previously outlined in Chapter 4 under in-vitro permeability studies.

D. Penetration Enhancer Permeability Studies

1. Materials, Solutions, and Procedure

Ethylenediaminetetraacetic acid (EDTA; Sigma Chemical Co., St. Louis, MO) was dissolved in Sorenson's phosphate buffer containing 0.15% mannitol to obtain 1.0 and 2.5 mM EDTA solutions. Solution pH was adjusted to 6.8 and made isotonic (300 mOsm) by addition of NaCl. This solution was used as the donor solution for in-vitro rabbit ileum permeability studies as previously summarized (see Chapter 4).

E. Electrophysiology

1. Electrode Preparation:

Electrodes were prepared from silver wire (1.0 mm diameter, 99.9% pure, Aldrich, Milwaukee, WI), which was cut into 6.5 cm lengths. The electrodes were

cleaned by sandpaper abrasion, placed in concentrated HCl (EM Science, Gibbstown, NJ) for 1.0 hour, and thoroughly rinsed with DDW. A layer of insoluble AgCl salt was then plated onto the wire by direct current application of ≈ 0.270 mA via a dc power supply (BK Precision, Chicago, IL) for 6 hours in 0.5 M KCl. The Ag/AgCl electrode pairs were short-circuited in 0.9% NaCl while being stored in darkness for 24 hours. Prior to and after experiments, the electrodes were tested for symmetry. Only pairs which had potential differences of 0.0 mV (Micronta digital multimeter, Radio Shack) were used.

2. Resistance Measurements:

As described in Chapter 4, rat duodenum tissue was extracted, cleaned, and mounted within a diffusion cell. The donor and receiver solutions consisted of Sorenson's phosphate buffer (pH 6.5, ≈ 300 mOsm) without inclusion of drug within the donor solution and were prepared as outlined in Chapter 4.

Two pairs of Ag/AgCl electrodes were used as sensing devices as illustrated in Figure 5.2. The inner pair of electrodes were situated ≈ 1.0 cm from the tissue surface. At pre-designated time points, current (I) was applied via a dc power supply (Hewlett Packard, Palo Alto, CA) across the membrane in a stepwise fashion from 0.0 to 15.0 μA in 5.0 μA intervals and the potential difference (V) measured. The time to complete measurement was between 20 to 30 seconds for each time point. At the completion of each time point, the resistance (R) was calculated via Ohm's Law:

$$V = I \times R \qquad (6)$$

in which the slope of V vs. I corresponds to R.

A background correction is necessary due to solution resistance between the sensing electrodes and membrane. This correction was calculated at the conclusion of each experiment in which the diffusion cell setup was used without tissue separating the donor and receiver chambers. The true membrane resistance was calculated by the difference between the two resistance values, with and without tissue, at each time point.

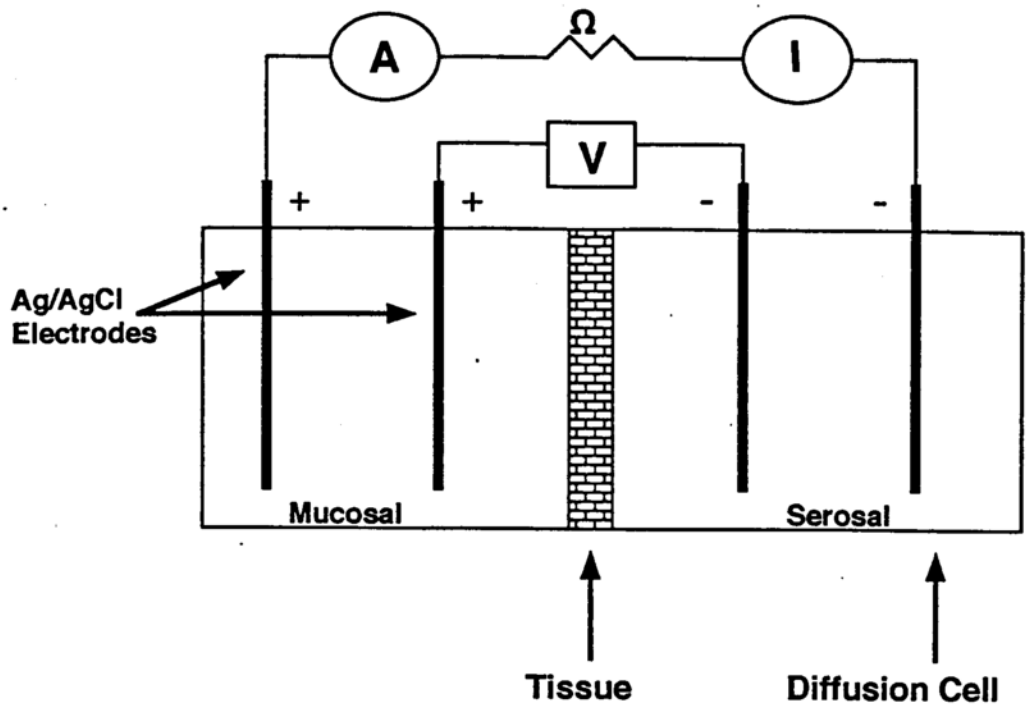

Figure 5.2: Set-up for transepithelial electrical resistance measurements of the rat duodenum. A current (I) was applied ranging from 0 to 15.0 μA (A = amps) and the potential difference (V) was recorded.

F. Tissue Recovery

1. Procedure

The procedures followed were previously outlined in Chapter 4 under in-vivo perfusion experiments. In the tissue recovery experiments, CO_2 was bubbled at a rate of 5.0 ml/min. into the proximal portion of the cannulated rat ileum segment after the 30 min. cleansing period. Initially, CO_2 was bubbled for 20 min. and then discontinued. The experiment continued without entry of CO_2 into the ileum segment. One ml samples were assayed for each time interval and the %benzoic acid (BA) absorbed calculated by equation (3).

III. Results and Discussion

A. MTT Cell Viability

MTT has been used as a measurement of cellular toxicity in a number of studies (Carmichael, 1987; Grant, 1994; Mossman, 1983). When compared to other cell viability and toxicity assays, such as lactate dehydrogenase (LDH), trypan blue, and [^{3}H] thymidine, similar results were obtained. The inter-experimental variability was also found to be the smallest for the MTT assay (Lappalainen, 1994).

As indicated by the experimental data (Figure 5.3), there is a slow decline in absorbance per gram of tissue values, indicating a decrease in cellular viability with time. This is normal and is to be expected with in-vitro experiments, since the tissue is taken from its normal biological surroundings where it is constantly nourished by blood circulation and placed within a foreign buffer. When comparing the effect of carbon dioxide and stir experiments on cellular toxicity, the initial, 10 min, 20 min, 60 min, and 120 min time point values are similar and indicate that carbon dioxide bubbling is not increasing the rate of cellular toxicity when applied to the tissue surface.

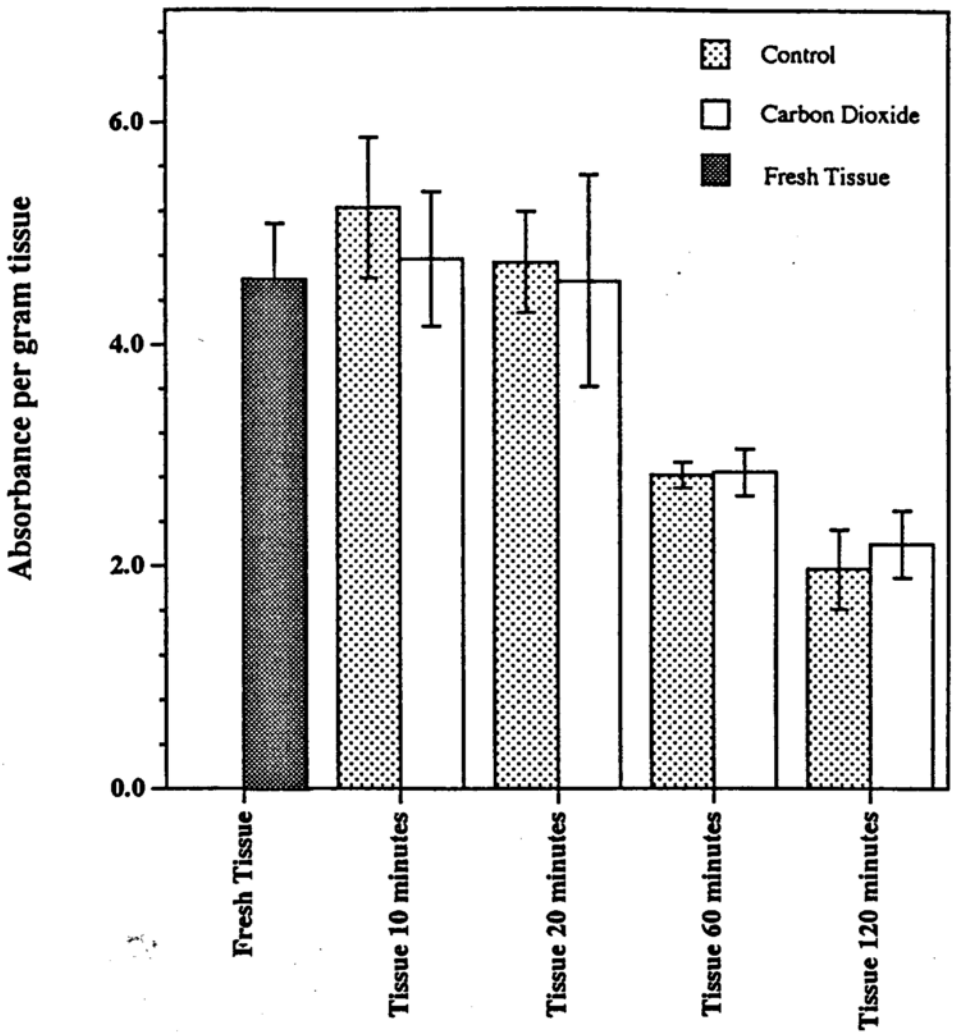

Figure 5.3: Results of the MTT cell viability assay. Error bars represent standard deviation of 3 to 9 experimental repetitions.

B. Membrane Perturbation/Damage

A variety of methods have been employed to determine the extent of epithelial cell damage or perturbation upon exposure to chemicals. Tissue microscopy has been widely used for visual examination but is costly, time consuming, and incorporates researcher subjectivity. Within the past decade, measurement of cellular enzyme or protein release has become increasingly popular as a method for determining the extent of cellular perturbations and/or damage.

Results of the enzyme/protein release experiments analyzing cell membrane disruption are shown in Figures 5.4 through 5.6. Numerical results are summarized in Tables 5.1 through 5.3.

Lactate dehydrogenase (LDH) is a cytosolic enzyme whose leakage is indicative of the extent of cell membrane porosity and/or lysis. Therefore, LDH provides a measure for cell damage (Pujara, 1995; Swenson, 1994). Previous studies have indicated that early enzyme release begins at the time when cell membrane damage is still reversible (Fredericks, 1983; Schmidt, 1987). The results obtained from the LDH activity measurements indicate significant LDH leakage into the perfusate when the epithelium was exposed to a bile salt, 1.25% sodium deoxycholate (NaDOC). Bile salts partly promote penetration enhancement across epithelial cell monolayers by damaging cell membranes through lipid and protein extraction from the bilayer (Feldman, 1973; Whitmore, 1979). The release of cytosolic enzymes is believed to be due to extensive membrane stretching and/or production of pores within the membrane allowing enzyme movement across the bilayer (Kristensen, 1994). Therefore, it can be

concluded that NaDOC is probably inducing LDH leakage through pore formation and/or membrane stretching due to removal of proteins/lipids from the membrane.

CO_2 and pure buffer experiments showed a significant reduction in LDH activity from that of 1.25% NaDOC indicating limited, if any, membrane damage. Only at the 5 min. time point was there a significant difference between control and CO_2 experiments.

Perfusate 5'-ND activity and protein concentration were higher after tissue exposure to 1.25% NaDOC then in the presence of CO_2 or pure buffer conditions. 5'-ND is a cell membrane bound enzyme whose release into the intestinal perfusate provides an indication of the level of membrane perturbation. Gradual removal of 5'-ND may disrupt the orientation of the lipid bilayer increasing membrane fluidity. Extraction of 5'-ND or other proteins from the cell membrane would create spaces within the bilayer allowing greater flexibility and movement of membrane components. Pore formation and increased membrane fluidity have been associated with increased drug flux (Lee, 1986). However, 5'-ND activity measurements did not indicate any differences between CO_2 and buffer experiments. This leads to the conclusion that CO_2 did not induce membrane perturbations causing the increase in drug flux.

The protein release assay is not only indicative of membrane perturbation but also membrane damage due to the possibility for intracellular protein leakage. Therefore, the total protein released is an additive value corresponding to both membrane and cytosolic proteins. The lack of difference between CO_2 and pure buffer experiments support the findings previously discussed for LDH and 5'-ND.

In conclusion, LDH, 5'-ND, and protein release assays provide an alternative method to quantitatively measure very subtle changes occurring within the intestinal epithelium. The combination of the three assays provide substantial

evidence as to the lack of membrane damage and/or perturbation due to CO_2 bubbling onto the tissue surface. Therefore, mechanical disruption of the transcellular pathway does not seem to play an important role for the permeation enhancement mechanism of CO_2 bubbling.

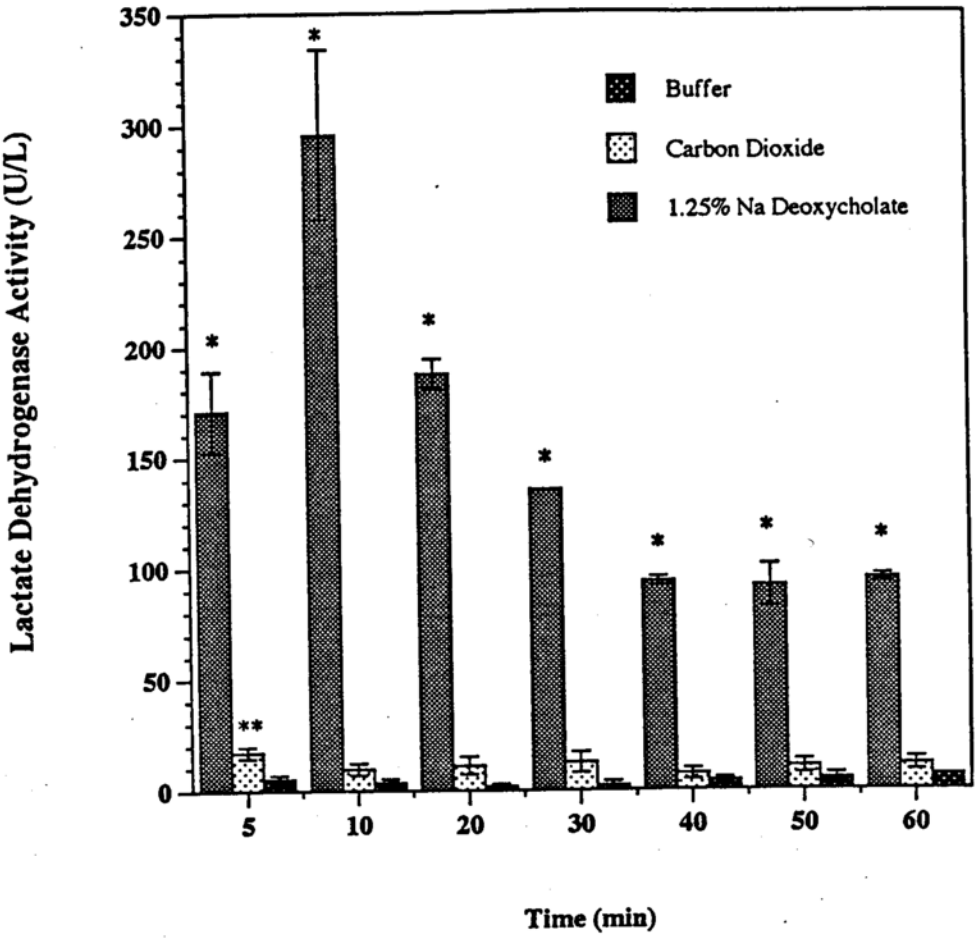

Figure 5.4: Lactate dehydrogenase enzyme activity after in-vivo single-pass perfusion of rat ileum tissue with buffer, carbon dioxide, or 1.25% sodium deoxycholate (NaDOC). Error bars represent SEM of 3 to 4 experimental repetitions. * denotes significant difference ($p < 0.02$) between NaDOC and carbon dioxide or buffer experiments. ** indicates significant difference ($p < 0.04$) from 5 min. stir value.

Table 5.1: Total lactate dehydrogenase (LDH) activity in samples from in-vivo rat single-pass perfusion studies. Perfusion rate ≈ 0.4-0.5 ml/min. CO_2 bubbling rate ≈ 5.0 ml/min.

	LDH Activity (U/L)		
Time (min)	**Buffer (± SD)**	**Carbon Dioxide (± SD)**	**1.25% NaDOC (± SD)**
5	5.53 (2.65)	17.05 (5.42)	170.9 (31.6)
10	3.99 (2.81)	9.54 (5.22)	295.7 (66.1)
20	2.08 (1.89)	11.06 (8.06)	187.7 (11.6)
30	2.33 (2.93)	12.49 (8.18)	135.6 (1.9)
40	3.96 (2.24)	7.14 (4.99)	93.8 (3.5)
50	5.27 (3.14)	10.29 (6.17)	91.8 (16.8)
60	6.10 (1.57)	11.22 (5.63)	95.1 (2.7)

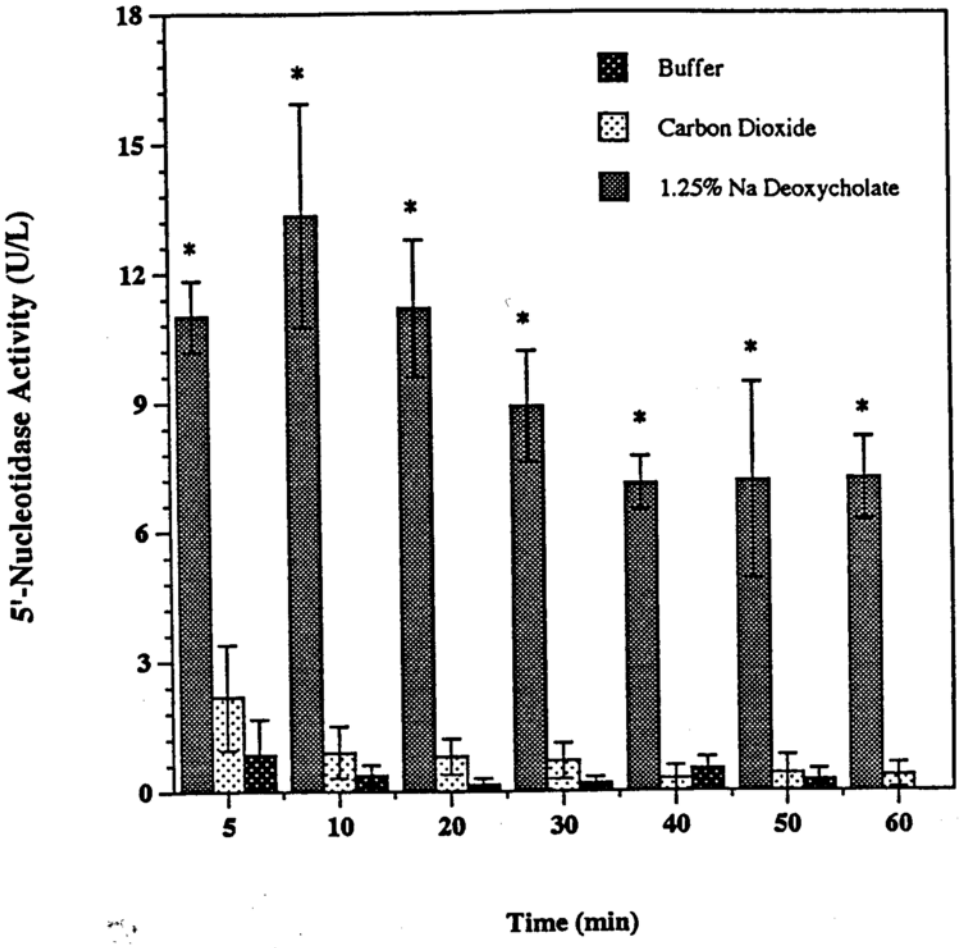

Figure 5.5: 5'-Nucleotidase enzyme activity after in-vivo single-pass perfusion of rat ileum tissue with buffer, carbon dioxide, or 1.25% sodium deoxycholate (NaDOC). Error bars represent SEM of 3 to 4 experimental repetitions. * denotes significant difference ($p < 0.01$) between NaDOC and carbon dioxide or buffer experiments.

Table 5.2: Total 5'-nucleotidase (5'-ND) activity in samples from in-vivo rat single-pass perfusion studies. Perfusion rate ≈ 0.4-0.5 ml/min. CO_2 bubbling rate ≈ 5.0 ml/min.

	5'-ND Activity (U/L)		
Time (min)	**Buffer (± SD)**	**Carbon Dioxide (± SD)**	**1.25% NaDOC (± SD)**
5	0.858 (1.39)	2.18 (2.09)	11.01 (1.44)
10	0.378 (0.42)	0.91 (1.02)	13.34 (4.48)
20	0.155 (0.27)	0.81 (0.72)	11.19 (2.73)
30	0.189 (0.24)	0.29 (0.51)	8.91 (2.21)
40	0.515 (0.47)	0.41 (0.72)	7.12 (1.08)
50	0.258 (0.47)	0.36 (0.49)	7.18 (3.95)
60	0.00 (0.00)	11.22 (5.63)	7.23 (1.68)

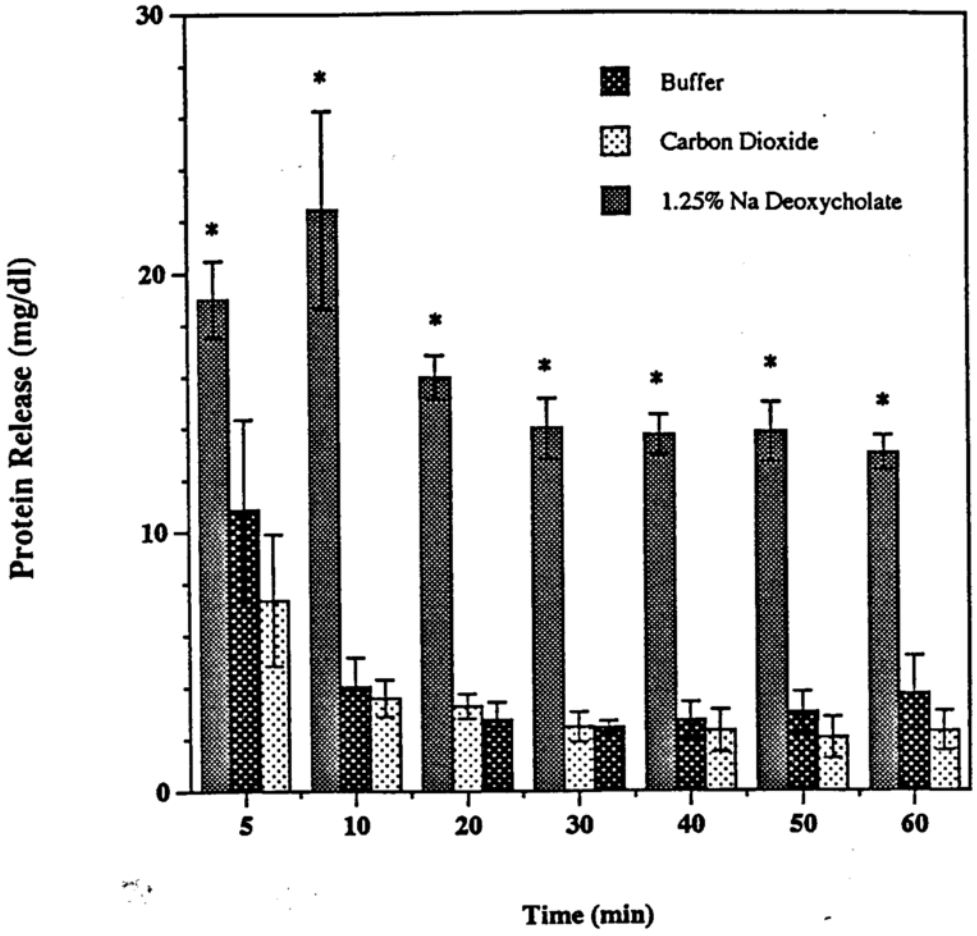

Figure 5.6: Protein release after in-vivo single-pass perfusion of rat ileum tissue with buffer, carbon dioxide, or 1.25% sodium deoxycholate (NaDOC). Error bars represent SEM of 3 to 4 experimental repetitions. * indicates significant difference ($p < 0.02$) between NaDOC and carbon dioxide or buffer experiments.

Table 5.3: Total protein release in samples from in-vivo rat single-pass perfusion studies. Perfusion rate ≈ 0.4-0.5 ml/min. CO_2 bubbling rate ≈ 5.0 ml/min.

	Total Protein Release (mg/dl)		
Time (min)	**Buffer (± SD)**	**Carbon Dioxide (± SD)**	**1.25% NaDOC (± SD)**
5	10.84 (6.03)	7.36 (5.07)	19.01 (2.54)
10	4.02 (1.96)	3.58 (1.42)	22.45 (6.57)
20	2.75 (1.15)	3.28 (0.94)	15.98 (1.47)
30	2.46 (0.43)	2.48 (1.14)	13.99 (2.03)
40	2.73 (1.22)	2.32 (1.62)	13.73 (1.35)
50	3.02 (1.40)	2.06 (1.60)	13.85 (2.02)
60	3.76 (2.49)	2.31 (1.52)	13.03 (1.15)

C. Paracellular Marker Permeability

Results depicting mannitol, PEG 900, and PEG 4000 permeability coefficients are shown in Figure 5.7. The three hydrophilic markers utilized for comparison in this study are known to traverse the intestinal epithelium by passage through the paracellular space due to their high water solubility (Krugliak, 1989; Ma, 1993). When examining the influence of CO_2 on paracellular marker permeability, a correlation between probe molecular weight and permeability coefficient is evident. Rabbit ileum permeability followed the sequence: mannitol > PEG 900 > PEG 4000, in which the smallest and largest molecular weight compounds corresponded to mannitol and PEG 4000, respectively. This is indicative of CO_2 having an effect on the paracellular pathway due to the fact that there is a reduction in probe permeability with an increase in molecular weight. This type of effect has been previously shown in experiments by Lane, et.al., (Lane, 1996) in which rat intestinal permeability for various paracellular probes ranging in molecular weight from mannitol (MW 182.17) to inulin (MW 5000) were examined in the presence of penetration enhancers which were known to induce changes to the paracellular pathway. Additionally, Nakanishi et. al. (Nakanishi, 1984) showed that the paracellular enhancing effects of EDTA on rectal permeability decreased as the MW increased.

A penetration enhancement effect on the paracellular pathway would induce a loosening of the tight junction at the apical surface, causing a subsequent increase in junctional pore diameter. This would lead to enhanced permeability for smaller MW compounds due to an increased available surface area for penetration, with subsequent reduction in overall enhancement as the MW of a

compound increased, which is characteristic of normal drug permeability. At a certain MW, a cutoff in the permeability enhancement should occur due to the fact that the enlarged pore would still obtain its barrier characteristics for molecules too large in diameter to diffuse across the tight junction. This is what is seen with CO_2 experiments, in which a reduction in permeability is observed with increased MW. The cutoff point is seen with PEG 4000 for which there is no longer any enhancement due to CO_2 effects on the tissue.

When comparing the increase in permeability to the stir experiments, there is a 5.26, 3.62, and 1.31-fold increase for mannitol, PEG 900, and PEG 4000, respectively.

Recently, it has been determined that a drug molecule's cross-sectional radius is also associated with the extent of intestinal permeability (Ghandehari, 1997; Lane, 1996). The larger the diameter, the more bulky and less permeable the drug molecule. The cross-sectional radius for mannitol, PEG 900, and PEG 4000 are 6.3, 8.3, and 15.9 Å, respectively. Therefore, experimental results also correlate very well to this parameter.

D. Penetration Enhancer Permeability Studies

The results of in-vitro mannitol transport across rabbit ileum tissue with EDTA, alone or in combination with CO_2, is shown in Figures 5.8 through 5.10 and outlined in Table 5.4. Mannitol permeability is enhanced over stir experiments by a factor of 2.79 and 4.78-fold with experiments utilizing EDTA (2.5 mM) or CO_2 (100 ml/min), respectively. In studies using the penetration enhancers in combination, mannitol permeability increased 3.43 and 1.82-fold over exper-

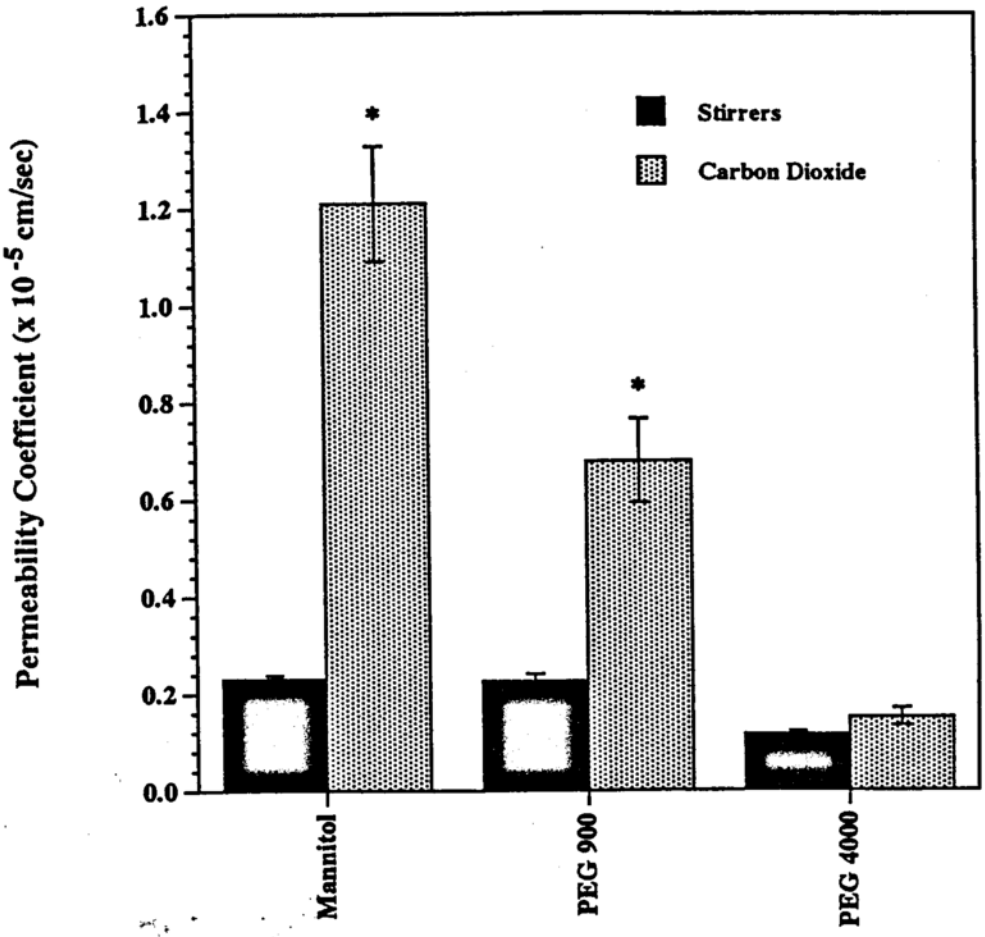

Figure 5.7: Paracellular marker permeability coefficients for in-vitro rabbit ileum permeability studies. Error bars represent SEM for 3 to 6 experimental repetitions. * denotes significant difference ($p < 0.001$).

iments involving the use of a single penetration enhancer, EDTA (2.5 mM) or CO_2, respectively. In comparison to the stirrer experiments, the combined EDTA/CO_2 experiments increased mannitol's permeability coefficient by a factor of 9.57.

The integrity of the tight junctional complex is dependent upon extracellular calcium in which a reduction in calcium ion concentration has been correlated with an opening of the intercellular space. EDTA is a chemical known to increase the permeation rate of hydrophilic drugs through the paracellular space due to calcium ion chelation within the extracellular fluid (Wang, 1993). Ranitidine, phenol red, cefmetazole, mannitol, inulin, and antipyrene are just a few examples of drugs whose permeabilities have been enhanced across intestinal tissue due to the activity of EDTA on the paracellular pathway (Gan, 1993; Shiga, 1987; Shiga, 1985; Suzuka, 1987).

Based on previous evidence as to the mechanism of EDTA, the increase in mannitol permeability caused by EDTA is associated with increased paracellular transport. Carbon dioxide also increased mannitol permeability and can also be associated with an effect on the intercellular space. The extent of mannitol permeability enhancement due to CO_2 is somewhat greater than that seen with EDTA alone and is probably due to an increased disruption of the tight junctional complex, leading to a larger pore opening.

What is also of interest is the combined effect of EDTA and CO_2 on mannitol permeability. The combination of the two penetration enhancers led to an increase in mannitol permeability in comparison to when CO_2 or EDTA were used alone. This is indicative of an effect in which the two enhancers are acting synergistically to create a greater structural change to the tight junction and/or fluid flow theories (i.e. solvent drag and tissue pressure gradients) in conjunction

with structural perturbations that are inducing higher permeability rates. 1.0mM and 2.5 mM EDTA were used in the experiments and correspond to typical concentrations utilized in penetration enhancement studies showing limited tissue toxicity. However, a variety of drugs need higher EDTA concentrations (1 to 30%) to obtain the desired absorption effect. These concentrations have been shown to be quite toxic to the epithelium (Nadai, 1972; Nakanishi, 1983; Nishihata, 1981) and would never gain approval for marketing.

The use of carbon dioxide in combination with "classical" penetration enhancers, such as EDTA, could reduce the potential for toxicity. Carbonation use has already been approved by the FDA and large quantities are ingested by the public without problems. This along with the aforementioned MTT studies (Chapter 4) indicate that CO_2 is safe and does not produce any type of harmful toxicity. By incorporating CO_2 into a dosage form with another enhancer, a reduced concentration of the latter may be used, thus possibly inducing adequate drug penetration enhancement without associated toxicities.

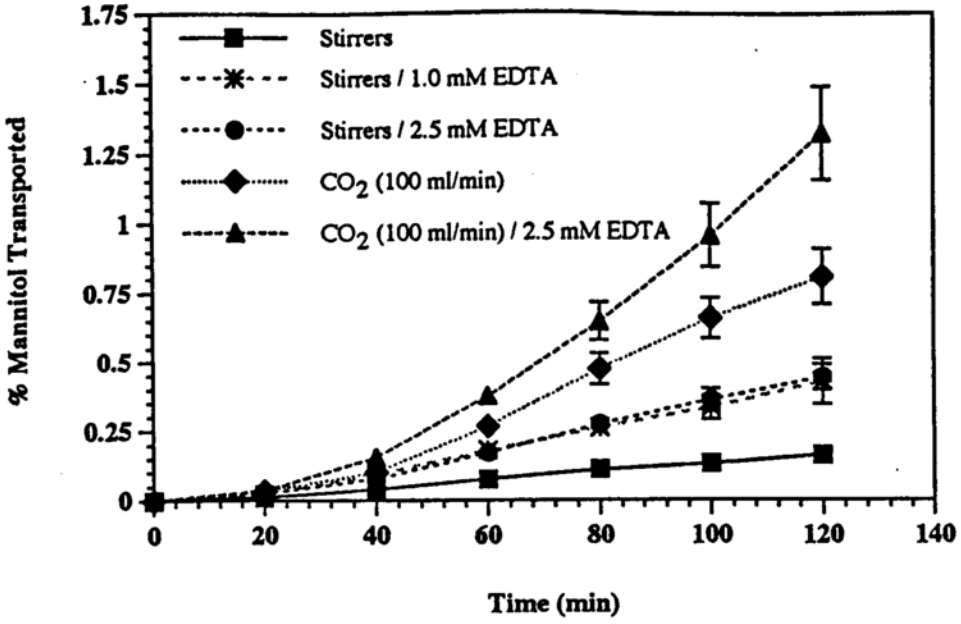

Figure 5.8: Effect of EDTA alone and in combination with carbon dioxide bubbling on the permeability of mannitol across rabbit ileum tissue in-vitro. Error bars represent SEM of 3 to 6 experimental repetitions.

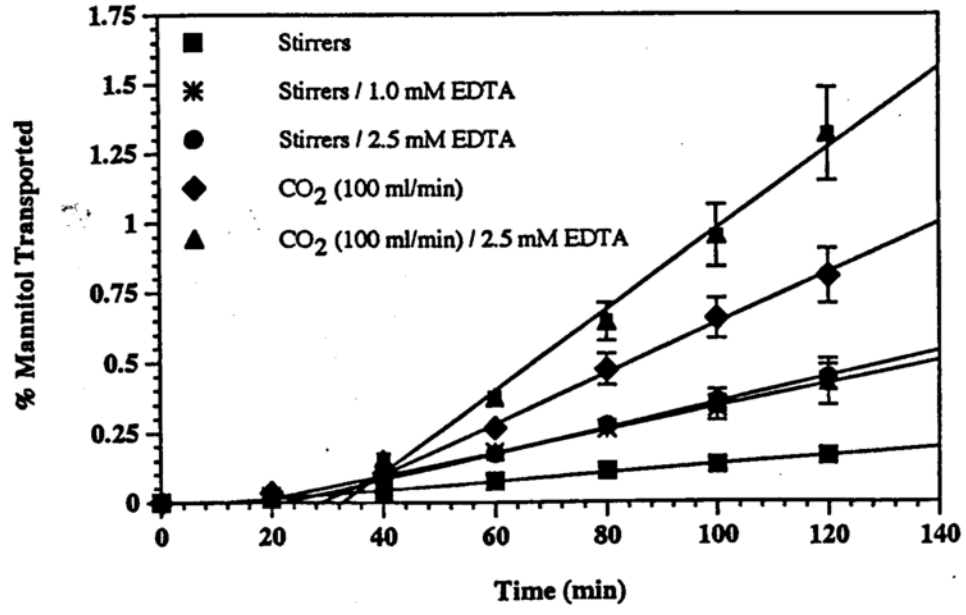

Figure 5.9: Percent mannitol transported in-vitro across rabbit ileum tissue due to EDTA or EDTA/carbon dioxide bubbling with illustration of the terminal steady state slope. Number of experimental repetitions = 3 to 6. Error bars = SEM.

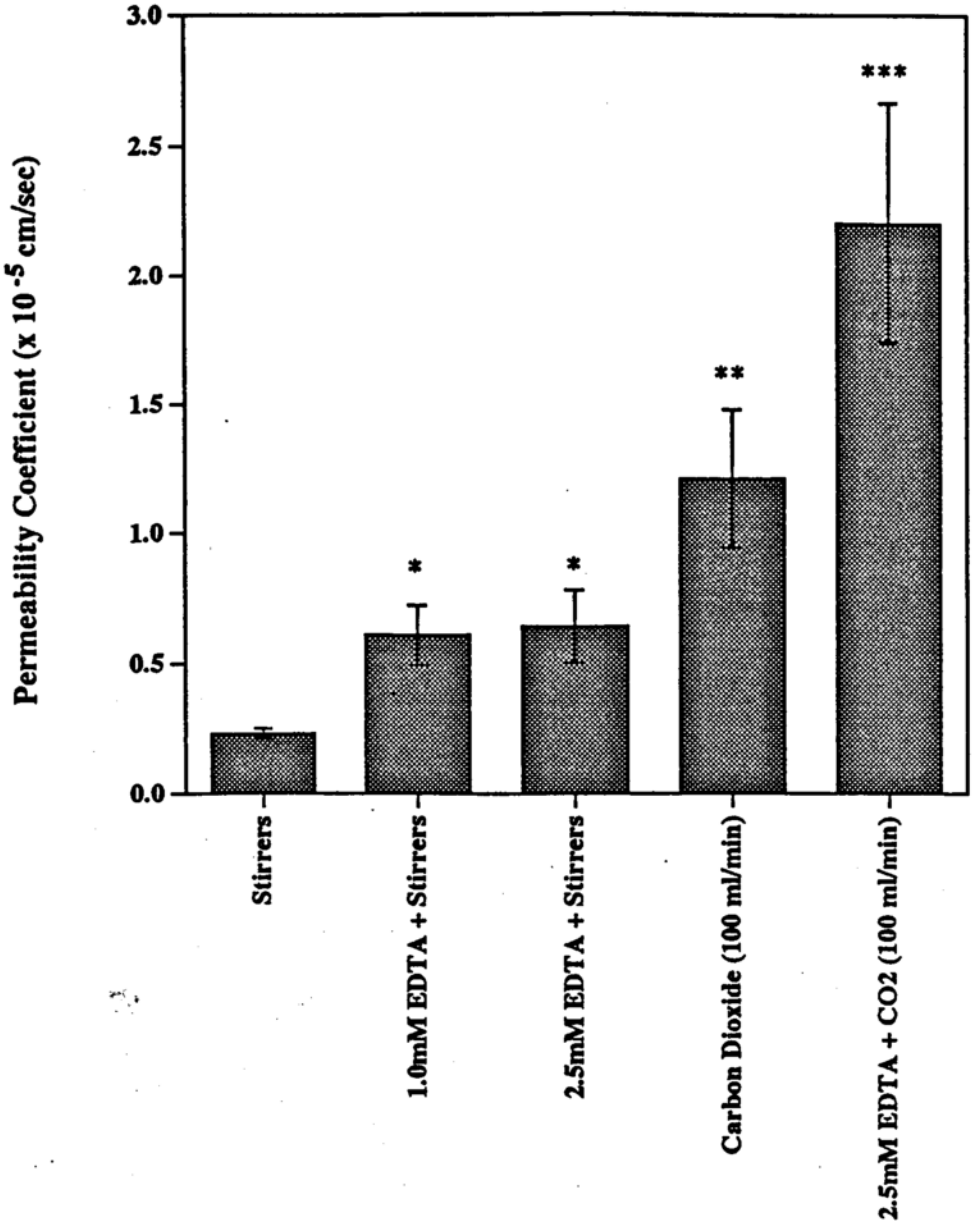

Figure 5.10: Mannitol permeability coefficients for in-vitro rabbit ileum permeability studies using EDTA alone or in combination with carbon dioxide bubbling. * denotes significantly different from stirrers ($p < 0.04$). ** indicates significant difference from 1.0 and 2.5mM EDTA/stirrers ($p < 0.01$). *** denotes significant difference from carbon dioxide ($p < 0.005$).

Table 5.4: Results of mannitol in-vitro rabbit ileum permeability studies when utilizing the"classical" penetration enhanacer EDTA alone or in combination with CO_2.

Experiment	Permeability Coefficient (x 10^{-5} cm/sec)	Standard Deviation (x 10^{-5} cm/sec)
Stirrers	0.230	0.020
Stirrers/EDTA (1.0mM)	0.608	0.114
Stirrers/EDTA (2.5mM)	0.642	0.139
CO_2 (100 ml/min)	1.21	0.267
CO_2 (100 ml/min) + EDTA (2.5mM)	2.20	0.462

E. Electrophysiology

Transepithelial electrical resistance (TEER) results in the presence and absence of CO_2 are depicted in Figure 5.11. Normal duodenum tissue area resistances have been shown to fall within the "leaky" range of 75 to 100 $\Omega \times cm^2$ as is the case with this experiment. The positive control, 2.0 mM lauroylcarnitine, is known to induce an opening of the tight junction, leading to reduced TEER values with subsequent increased hydrophilic drug flux (LeCluyse, 1993). CO_2 also caused a decrease in TEER. This is indicative that the epithelium is undergoing a morphological change in which the integrity of the tight junction and/or cell membrane is being disrupted (e.g. pores, protein leaching) creating an increase in ion flux across the tissue. According to previously mentioned results (see Membrane perturbation/damage), there is no indication of cell membrane damage or perturbation due to contact between the tissue surface and CO_2. Therefore, the only plausible explanation is a structural integrity effect on the tight junction, inducing less restriction to ion movement through the paracellular space.

This result corresponds to experiments which have shown that a decrease in intestinal TEER values corresponds to changes in tight junctional integrity in association with enhanced permeability to hydrophilic drugs (Hochman, 1994; van Hoogdalen, 1989). These findings also support the increased permeability effect of CO_2 in which the hydrophilic drugs, mannitol and tetracycline, have greater permeability enhancement in comparison to the hydrophobic drug, diazepam.

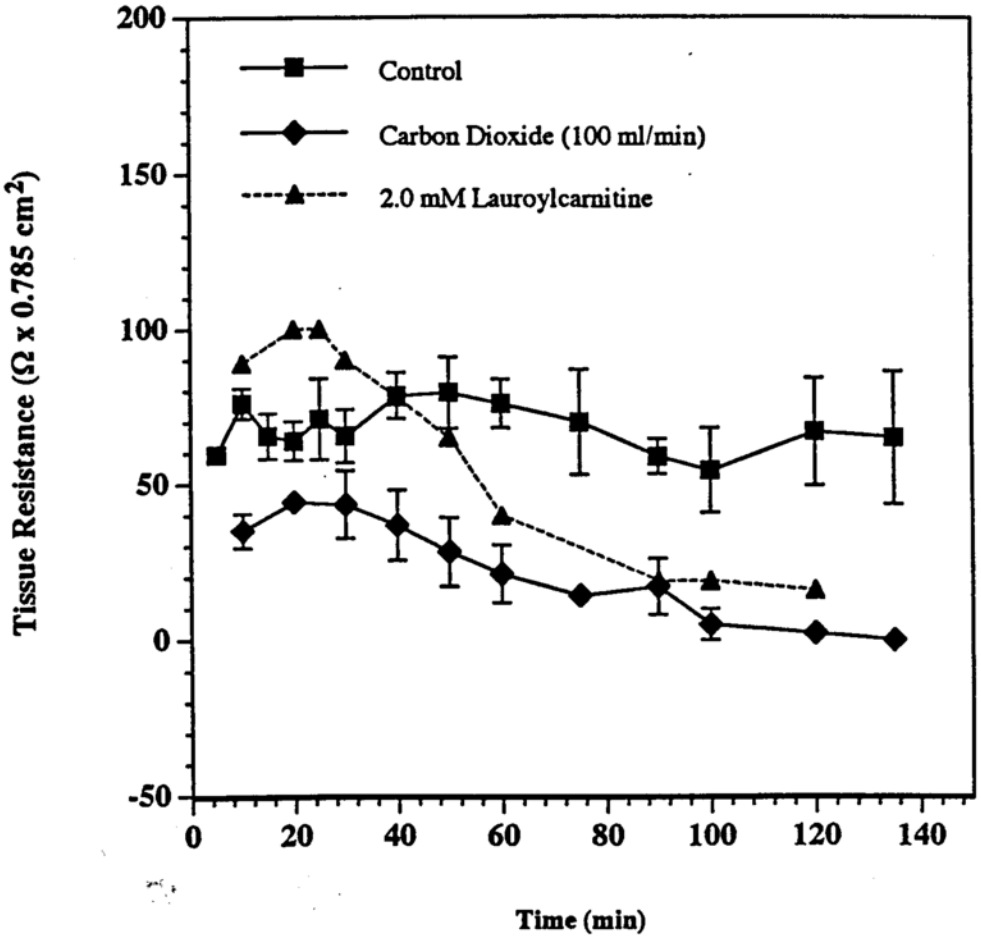

Figure 5.11: Effect of carbon dioxide bubbling on the tissue resistance of rat duodenum in-vitro. Error bars represent SEM of 4 experimental repetitions. Lauroylcarnitine data obtained from LeCluyse, et. al., 1993.

F. Tissue Recovery

An important issue in delivering therapeutic agents in combination with a penetration enhancer is safety. Most penetration enhancers influence drug permeability by altering tissue morphology, leading to a breakdown in tissue integrity. The issues of most importance concern tissue irritation, membrane damage, and the rate of damage and recovery. The rate of tissue recovery from damage imparted by an absorption enhancer is related to the extent of toxicity (Lee, 1991c). Severe damage such as sloughing of epithelial cells from the monolayer produce prolonged or irreversible recovery, while slight alterations such as transient perturbations of the membrane or tight junctional opening leads to rapid tissue recovery. A favorable enhancer is one that induces minimal toxicity with relatively fast tissue recovery rates (1-2 hours). This limits the opportunity for absorption of harmful environmental substances due to the increased membrane permeability. Therefore, it is essential to study tissue recovery rates in addition to the penetration enhancement effect.

Results of the in-vivo rat ileum tissue recovery experiments are presented in Figure 5.12. The fraction of benzoic acid absorbed from the perfusate increased when CO_2 was bubbled into the ileum segment. After discontinuation of the bubbling, a relatively rapid linear decline in absorbance to non-CO_2 experimental levels was observed. Therefore, the disruptive effect of CO_2 on the epithelium seem to be transient in nature with the epithelial barrier properties reestablished within a short period of time, 20 minutes. The results were expected due to the high use of carbonated products presently available to the public, which have never been associated with any harmful side effects. These results indicate that

carbonated drug delivery systems also could be safely used, in which tissue recovery would be rapid after discontinuation of effervescence.

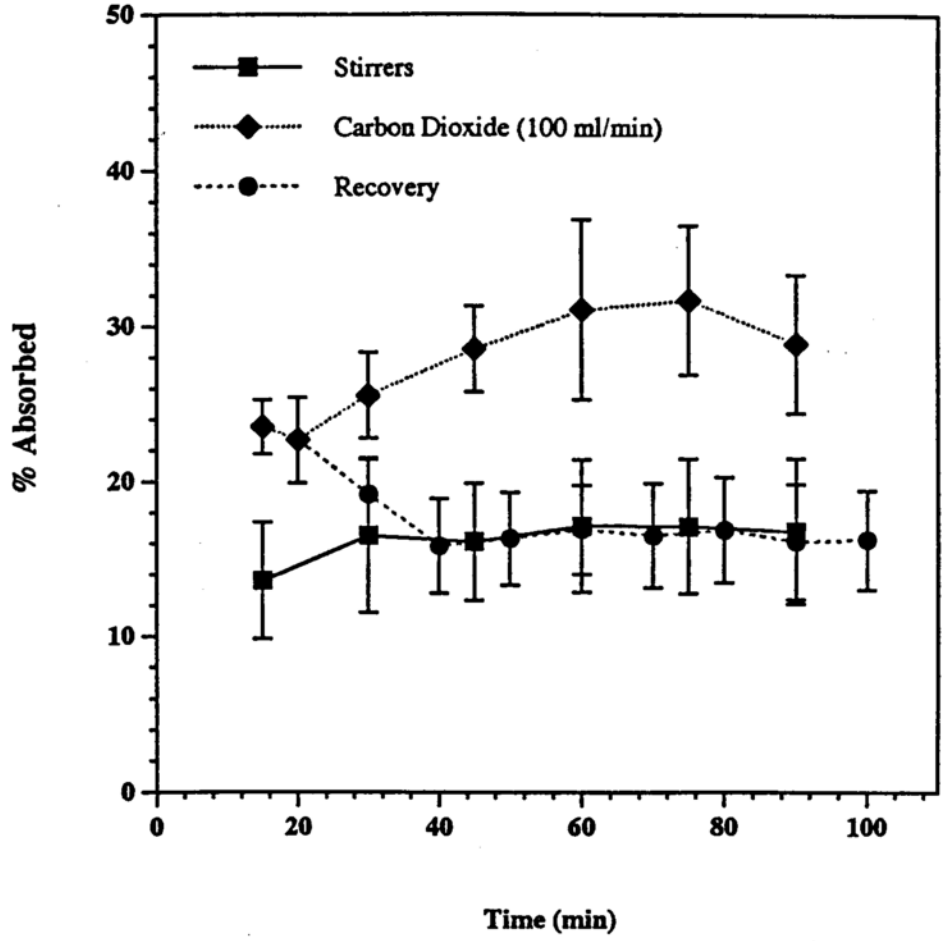

Figure 5.12: Tissue recovery as determined by percent benzoic acid absorbed from in-vivo single-pass perfusion of rat ileum. Error bars represent standard deviation of 4 experimental repetitions.

Concluding Remarks

Oral delivery is the primary administration route for therapeutic agents due to the ease, convenience, and high patient compliance rate. Interest in developing advanced oral delivery systems, which utilize local intestinal environments and/or increase drug residence time at targeted regions, has increased in the past few decades. These systems impart advantages such as increased absorption while decreasing dosing frequency for the patient. Increasing drug residence times would be advantageous for compounds exhibiting low absorption due to solubility, slow membrane permeability rates (e.g. hydrophilic drugs), and/or decreased stability due to enzymatic degradation (i.e. peptides and proteins).

The discovery and development of bioadhesive polymers, which have the ability to interact with mucus and/or epithelial components, was a significant advancement in the production of an oral vehicle that could protect, increase the residence time, and potentially enhance the absorption of orally administered drugs. However, a problem associated with bioadhesives is that the polymer primarily binds to mucus, limiting its residence time to mucus turnover (6 to 12 hours). If the polymer was bound to the epithelium, localized drug delivery could be extended to ≈ 24 hours. One of the possible solutions is to incorporate an agent that can degrade or physically move mucus from the epithelial surface.

Effervescent technology emerged two centuries ago and was utilized as a drug delivery vehicle due to its palatable saline taste. Today, it is still primarily used in this capacity, but recent discoveries have initiated a reevaluation of effervescence application to drug delivery. Studies have revealed that effervescence

encompasses a broad range of biological effects such as: (1) creating a "pseudo-fed" state in the stomach; (2) thinning or stripping the mucus layer lining the stomach and intestine; and (3) enhancing intestinal drug absorption.

The studies included within this work focused on the use of effervescence as an oral absorption enhancer. The objective(s) of the study was to gain an insight not only into the broad range of compounds whose absorption increased due to effervescence, but also to acquire a reasonable explanation as to the mechanism(s) of this enhancement.

Previous studies have unintentionally provided evidence that drugs given with effervescence showed differences in absorption profiles to those administered in conventional dosage forms (e.g. tablets, capsules, solutions). The absorption rate and/or the total amount of drug transported was occasionally greater for the effervescent rather then the conventional dosage form. The usual explanations given for this effect were arbitrarily associated with increased dissolution rates due to a buffering effect and/or mechanical turbulence. Other possible explanations that have been widely neglected include: (1) increased fluid flow; (2) thinning or stripping of mucus layer; (3) alteration in pH tissue gradient; (4) increase in membrane hydrophobicity; and (4) membrane alteration.

Results of the experiments indicated that permeability rates of a variety of drugs, ranging in molecular size, structure, and properties, increased across rat and rabbit small intestinal tissue in the presence of effervescence. Since mucus stripping would lead only to faster steady state diffusion conditions and not alter the permeability rate, this mechanism was disregarded as a potential explanation for CO_2 drug permeability enhancement.

When the rate of CO_2 bubbling onto the tissue surface was reduced 100-fold, a decrease in permeability for both PEG 900 and diazepam was encountered.

However, this reduction was greater for diazepam, a hydrophobic compound, than for PEG 900, a polar compound. The combined results of the bubbling rate and permeability experiments indicated that the permeability rates for the hydrophilic compounds were affected to a greater extent than their hydrophobic counterparts, leading to the theory that the intercellular space was being altered. This would provide an explanation for the greater enhancement effects for the polar drugs. The enhancement associated with the hydrophobic drugs could in part be due to increased flux through the paracellular route, but this effect would be limited. A better explanation would involve the theory of membrane hydrophobicity in which nonpolar CO_2 gas molecules partition into the membrane, thus creating an increased hydrophobic environment and inducing greater nonpolar drug flux.

In permeability studies using nitrogen, a similar penetration enhancement effect was noticed. Since nitrogen does not influence pH, it was concluded that CO_2 did not induce penetration enhancement due to pH alterations. Therefore, the pH buffering effect and alteration of the pH tissue gradient were ruled out as potential explanations.

Several experiments were performed to determine if mechanical activity of the bubbles were inducing a morphological change and/or toxicity to the epithelium. Enzyme (5'-ND and LDH) and protein release assays indicated insignificant membrane perturbation and/or damage due to limited leaching of these components from the cell cytosol or membrane. MTT cell viability assays did not indicate cell toxicity associated with CO_2.

Transepithelial electrical resistance (TEER) measurements indicated a reduction in tissue area resistance values in the presence of CO_2 bubbling. Since prior experiments indicated that CO_2 did not induce cell membrane

alterations (e.g. protein leaching, enzyme leakage), the decreased TEER values were associated with a morphological change in the paracellular pathway. This conclusion was further substantiated with in-vitro permeability studies utilizing hydrophilic marker probes. The markers, whose flux across intestinal tissue is primarily associated with movement through the paracellular space, showed a MW permeability dependence. The permeability enhancement effect of CO_2 decreased in association with molecular size; i.e. mannitol > PEG 900 > PEG 4000, in which PEG 4000 permeability did not show significant enhancement over the stirrer experiment. This indicated absorption enhancement via the paracellular pathway was limited to a cutoff molecular weight. In other words, the tight junctional pore diameter widened to a point at which it still acted as a barrier to larger MW compounds.

EDTA, a "classical" penetration enhancer known to increase drug permeability via tight junctional pore enlargement, was used in combination with CO_2. Results indicated that mannitol permeability across rabbit intestinal tissue was greater when the enhancers were used together than that of EDTA or CO_2 alone. This is suggestive that the two enhancers are acting synergistically to induce a greater structural change to the tight junction and leads to greater drug transport. It may also be theorized that increased fluid flow due to enhanced molecular velocities or pin-point pressure gradients formed by CO_2 bubble production could, in part, be responsible for the enhanced permeability with mannitol or other drug compounds.

Although mucus stripping does not play a role in enhancing the drug permeability rate across a membrane, it is an important biological effect produced by CO_2. Incorporation of effervescence within an oral bioadhesive delivery system could induce a situation where CO_2 generation within the intestine would

thin or strip the mucus layer to the point where the bioadhesive could intimately associate with the epithelium. This would create longer residence times for drug absorption and also provide protection for drugs susceptible to enzymatic degradation. After bioadhesive attachment, subsequent effervescent generation could act as a penetration enhancer. This action could be produced by CO_2 alone or in combination with a second "classical" penetration enhancer. As shown by experimental studies, tissue alterations induced by CO_2 recover relatively rapidly ($\approx$ 20 min.). Therefore, due to toxicity associated with "classical" enhancers and the combined penetration enhancer effect on drug permeability, a lower dose of the "classical" enhancer could be used which may provide a significant reduction in tissue toxicity.

In conclusion, effervescence has been an underutilized technology in the drug delivery field. Although it has been used as an important tool for increasing patient compliance, its biological effects have gone relatively unnoticed. Utilization of these effects may provide alternative oral delivery systems which may: (1) induce faster drug delivery system transport to a specific regions of the intestinal tract; (2) enhance residence times for gastrointestinal bioadhesives; (3) induce fast blood levels when a small volume of an effervescent solution is taken with a drug; and (4) increase absorption of drugs with limited permeability (e.g. peptides) due to effervescent penetration enhancement effects alone or in combination with a decreased concentration of a "classical" enhancer.

Appendix A: Steady State Membrane Diffusion

The complexities associated with solute diffusion across membranes with the existence of a concentration gradient has been the subject of many reviews (Cussler, 1997; Stein, 1986b).

The system of particular interest for this review is characterized by a tissue of uniform thickness placed between two aqueous solutions in which the solute molecules traverse the membrane in the direction from high to low concentration via one-dimensional simple diffusion as shown in Figure A-1.

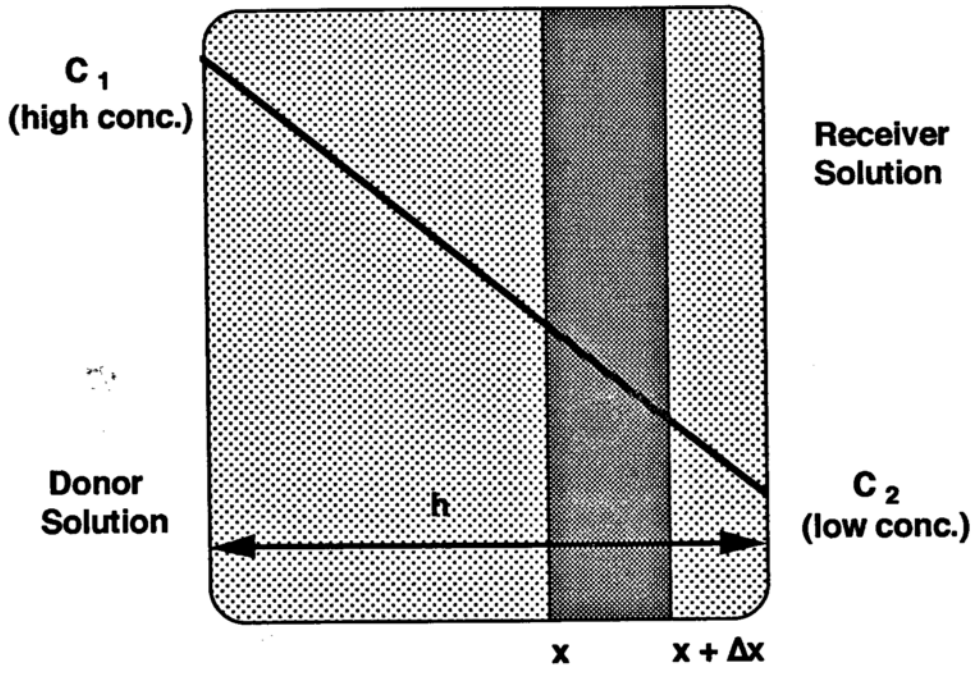

Figure A-1: Concentration profile for solute flux across a membrane from the donor to receiver solution.

The assumptions of the model include: (1) the membrane is homogeneous; (2) the system is isoosmotic, isothermal, and isobaric; (3) a linear concentration profile; (4) the activity of the solute is constant; and (5) the electrical field is constant across the membrane.

Diffusion is an entropy driven process involving random molecular movements in which solute diffusion across a concentration gradient will occur until equilibrium is reached. The mass balance of a membrane layer of thickness, Δx is:

$$\frac{dM}{dt} = A \left(j\big|_x - j\big|_{x+\Delta x} \right) \tag{8}$$

where DM/dt is the change in mass, M, with time, t. A is the layer area exposed to solute transport, and $j\big|_x$ and $j\big|_{x+\Delta x}$ are the rate of diffusion into and out of the layer, respectively. At steady state, dM/dt = 0 and equation 8 now becomes:

$$0 = A \left(j\big|_x - j\big|_{x+\Delta x} \right) \tag{9}$$

Diffusion within an isotropic medium follows Fick's first law (equation 10):

$$J = -D \frac{dC}{dx} \tag{10}$$

where D is the solute diffusion coefficient within the membrane and dC/dx is the change in solute concentration with distance. The law states that the flux of solute across a plane of tissue is proportional to the concentration differential across that plane. The negative sign indicates that solute flow is towards the direction of

lesser concentration. When substituting equation. 10 into equation. 9 and dividing by the volume of the layer, $A\Delta x$:

$$0 = D \frac{\left\langle dC/dx \Big|_{x+\Delta x} - dC/dx \Big|_{x} \right\rangle}{\Delta x} \tag{11}$$

when Δx becomes very small, equation 11 becomes the definition of the derivative where:

$$0 = D\left(\frac{d^2C}{dx^2}\right) \tag{12}$$

with the boundary conditions: $x = 0$, $C = KC_1$, and $x = h$, $C = KC_2$ where K is the partition coefficient of the solute, h is the membrane thickness, and C_1 and C_2 are the concentrations within the donor and receiver solutions, respectively. Applying the boundry conditions to equation 12:

$$J = \frac{KD(C_2 - C_1)}{h} \tag{13}$$

where the permeability coefficient, P, is defined as:

$$P = \frac{KD}{h} \tag{14}$$

Plugging equation 14 into equation 13 leads to:

$$J = P(\Delta C) \tag{15}$$

Under conditions where the receiver solution is maintained at essentially zero concentration (i.e. "sink" conditions), $C_1 >>> C_2$ and therefore equation 15 may be written as:

$$J = \frac{KD(C_1)}{h} \tag{16}$$

or

$$P = \frac{dM/dt}{AC_1} \tag{17}$$

The permeability coefficient may be obtained through a plot of the amount of drug transported across the membrane vs. time (Figure A-2) in which the terminal steady state slope, dM/dt, is determined.

Fick's second law, which can be derived from Fick's first law, may be applied to unidirectional flow experiments in which two conditions apply: (1) the concentration difference across the membrane is maintained at a constant level during the experiment; and (2) "sink" conditions exist. Utilizing the boundry conditions (Flynn, 1974; Jost, 1960): C_1 = constant, $x = 0$ for all values of t; $C = 0$, $x > 0$ at $t = 0$; and $C = 0$, $x = h$ at all t values , the concentration at any point, x, is determined by:

$$C = C_1\frac{x}{h} + \frac{2}{\pi}\sum_{n=1}^{\infty}\frac{C_1}{n}\cos(n\pi)\sin\left(\frac{n\pi x}{h}\right)e^{-n^2\pi^2Dt/h^2} \ldots\ldots \tag{18}$$

The cumulative mass of diffusant per unit area, M, that passes across the membrane at time, t, may be determined via 3 steps: (1) differentiation of equation

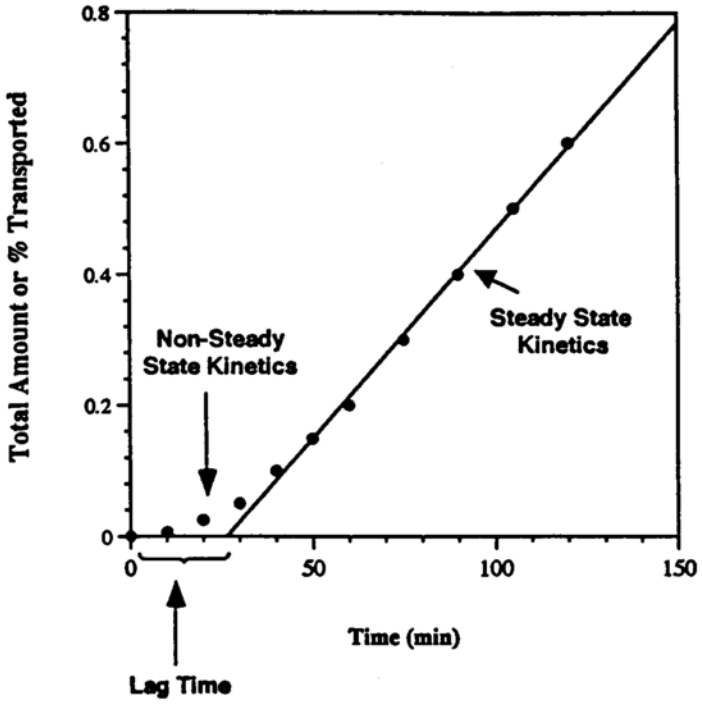

Figure A.2: A typical permeability curve showing the lag time, non-steady state (non-linear), and steady state (linear) kinetics.

18 with respect to x; (2) determining the flux, dM/dt, at x = h; and (3) integrating the equation from t = 0 to t = t. Following these three steps leads to:

$$M = \frac{DC_1 t}{h} - \frac{hC_1}{6} - \frac{2hC_1}{\pi^2} \sum_{n=1}^{\infty} \frac{(-1)^2}{n^2} e^{-n^2\pi^2 Dt/h^2} \qquad (19)$$

Taking the limit, $t \rightarrow \infty$, gives:

$$M = \frac{DC_1}{h}\left(t - \frac{h^2}{6D}\right) \qquad (20)$$

Differentiation of equation 20 results in determination of the steady state flux given by:

$$\frac{dM}{dt} = \frac{DC_1}{h} \tag{21}$$

where extrapolation of the steady state portion of the amount crossing the membrane vs. time curve leads one to obtain the x-intercept commonly referred to as the lag time, t_l. The lag time is the time it takes for a drug to obtain steady state flux across the membrane:

$$t_\ell = \frac{h^2}{6D} \tag{22}$$

As indicated by equation 22, lag time is dependent on membrane thickness and the diffusion coefficient of the drug within the membrane. Via manipulation of this equation, lag times have also been associated with a drug's partition coefficient and the resistances a drug encounters within the diffusion layers (Flynn, 1972; Flynn, 1972b).

One other general consideration to keep in mind in association with lag time determination is alterations within the membrane during an experimental procedure. If a pathway normally utilized by a solute alters in shape and/or becomes occluded, a new situation arises in which the drug's diffusional pathway (i.e. path length) will undergo a change. The average path length is adjusted via a tortuosity factor, τ, in which an increase in path length leads to increased lag times (Flynn, 1971; Flynn, 1974).

Penetration enhancers may also change lag time values due to the fact that they precipitate alterations within the epithelium. Enhancers may: (1) increase or decrease tissue thickness depending on the nature of its activity; (2) alter the hydrophobicity of membrane components; and/or (3) induce structural changes to pre-existing transport pathways. These effects will also lead to a change in the drug's diffusion coefficient within the membrane. It is difficult to predict whether an enhancer will increase or decrease the lag time of a drug , and as indicated above, the change may be due to numerous variables.

References

Ahuja, A., Khar, R. K., and Ali, J. (1997). Mucoadhesive drug delivery systems. *Drug Dev. Industrial Pharm.* **23**(5), 489-515.

Alberts, B., Bray, D., Lewis, J., Raff, M., Roberts, K., and Watson, J. D. (1994). Membrane structure. 3rd ed. *In* "Molecular Biology of the Cell" (M. Robertson, ed.), pp. 477-506. Garland Publishing, Inc., New York, NY.

Allen, A. (1994). Structure and function of gastrointestinal mucus. *In* "Physiology of the Gastrointestinal Tract" (L. R. Johnson, ed.), pp. 619-638. Raven Press, New York, NY.

Allen, A., Flemstrom, G., Garner, A., and Kivilaakso, E. (1993). Gastroduodenal mucosal protection. *Physiol. Rev.* **73**, 823-857.

Altman, P. L., and Dittmer, D. S. (1971). "Basic physical and chemical data." Respiration and Circulation (P. L. Altman and D. S. Dittmer, eds.) Federation of American Societies for Experimental Biology, Bethesda, MD.

Andersen, M. P. (1992). Lack of bioequivalence between disulfiram formulations. *Acta Psychiatr. Scand. Suppl.* **86**, 31-35.

Anderson, B., and Ussing, H. H. (1957). Solvent drag on non-electrolytes during osmotic flow through isolated toad skin and its response to anti-diuretic hormone. *Acta Physiol. Scand.* **39**, 228-239.

Arkesteijn, C. L. M. (1976). A kinetic method for serum 5'-nucleotidase using stabilized glutamate dehydrogenase. *J. Clin. Chem. Clin. Biochem.* **14**, 155.

Artursson, P., and Magnusson, C. (1990). Epithelial transport of drugs in cell culture. II: Effect of extracellular calcium concentration on the paracellular transport of drugs of different lipophilicities across monolayers of intestinal epithelial (caco-2) cells. *J. Pharm. Sci.* **79**(7), 595-600.

Artursson, P., Ungell, A. L., and Lofroth, J. E. (1993). Selective paracellular permeability in two models of intestinal absorption: cultured monolayers of human intestinal epithelial cells and rat intestinal segments. *Pharm. Res.* **10**(8), 1123-1129.

Ashford, M., Fell, J., Attwood, D., Sharma, H., and Woodhead, P. (1994). Studies on pectin formulations for colonic delivery. *J. Controlled Release* **30**, 225-232.

Ashford, M., and Fell, J. T. (1994). Targeting drugs to the colon: delivery systems for oral administration. *J. Drug Target.* **2**, 241-258.

Atanassoff, P. G., Rohling, R., Alon, E., and Brull, S. J. (1995). Effects of single-dose oral ranitidine and sodium citrate on gastric pH during and after general anaesthesia. *Can. J. Anaesth.* **42**(5), 382-386.

Atisook, P., and Madara, J. L. (1991). An oligopeptide permeates intestinal tight junctions at glucose-elicited dilatations. Implications for oligopeptide absorption. *Gastroenterology* **100**, 719-724.

Bacon, H. E., and Recio, P. M. (1962). Anatomy of colon, rectum, and anal canal. *In* "Surgical Anatomy of the Colon, Rectum, and Anal Canal", pp. 19-125. J.B. Lippincott, Co., New York, NY.

Banga, A. K. (1995). Oral Delivery of Peptide and Protein Drugs. *In* "Therapeutic Peptides and Proteins", pp. 217-244. Technomic Publishing Co., Inc., Lancaster, PA.

Bannister, H., ed. (1995). Alimentary System. 38th ed. Gray's Anatomy. New York, NY: Churchill Livingstone.

Bassett, P. (1996). Physiological Routes of Drug Administration. *In* "Drug Delivery Systems: Trends, Technologies and Market Opportunities" (S. C. DiClemente, ed.), Vol. 1, pp. 2.1-2.14. International Business Communications, Inc., Southborough, MA.

Bassett, P. (1996b). Drug Delivery Technology Companies. *In* "Drug Delivery Systems: Trends, Technologies, and Market Opportunities" (S. DiClemente, ed.), Vol. II, pp. 6.83-6.88. International Business Communications, Inc., Southborough, MA.

Bockman, D. E., and Cooper, M. D. (1973). Pinocytosis by epithelium associated with lymphoid follicles in the bursa of fabricius, appendix, and Peyer's patches. An electron microscopic study. *Am. J. Anat.* **136,** 455-478.

Bogacz, K., and Caldron, P. (1987). Enteric-coated aspirin bezoar: elevation of serum salicylate level by barium study. *Am. J. Med.* **83**(4), 783-786.

Brondsted, H., and Kopecek, J. (1992). Hydrogels for site-specific drug delivery to the colon: in vitro and in vivo degradation. *Pharm. Res.* **9**(12), 1540-1545.

Brown, A. L. (1962). Microvilli of the human jejunal epithelial cell. *J. Cell Biol.* **12,** 623-627.

Burkard, M. E., and Van Liew, H. D. (1995). Effects of physical properties of the breathing gas on decompression sickness bubbles. *J. Appl. Physiol.* **79,** 1828-1836.

Carmichael, J. (1987). Evaluation of a tetrazolium-based semiautomated colorimetric assay: assessment of chemosensitivity testing. *Cancer Res.* **47,** 936-942.

Carola, R., Harley, J. P., and Noback, C. R. (1992). The Digestive System. *In* "Human Anatomy" (K. M. Prancan and H. Gordon, eds.), pp. 595. McGraw-Hill, Inc., New York, NY.

Carr, K. E., and Tonor, P. G. (1984). Morphology of the intestinal mucosa. *In* "Pharmacology of Intestinal Permeation I" (T. Z. Csaky, ed.), pp. 1-50. Springer-Verlag, New York, NY.

Chadwick, V. S., Phillips, S. F., and Hoffman, A. F. (1977). Measurements of intestinal permeability using low molecular weight polyethylene glycols (PEG 400). *Gastroenterol.* **73,** 247-251.

Chen, C. T., Toung, J. K., Haupt, H. M., Hutchins, G. M., and Cameron, J. L. (1984). Evaluation of the efficacy of Alka-Seltzer effervescent in gastric acid neutralization. *Anesth. Analg.* **63,** 325-329.

Christensen, J. (1994). The motility of the colon. *In* "Physiology of the Gastrointestinal Tract" (L. R. Johnson, ed.) Raven Press, New York, NY.

Cogburn, J. N., Donovan, M. G., and Schasteen, C. S. (1991). A model of human small intestinal absorptive cells 1. Transport barrier. *Pharm. Res.* **8,** 210-216.

Cooper, W. T. (1872). United Kingdom.

Crome, P., Dawling, S., Braithwaite, R. A., Masters, J., and Walkey, R. (1977). Effect of activated charcoal on absorption of nortriptyline. *Lancet* **92,** 1203-1205.

Cussler, E. L. (1997). "Mass Transfer in Fluid Systems." 2nd ed. Cambridge University Press, Cambridge, UK.

Davis, S. S., Hardy, J. G., and Fara, J. W. (1986). Transit of pharmaceutical dosage forms through the small intestine. *Gut* **27,** 886-892.

Dawling, S., Chand, S., Braithwaite, R. A., and Crome, P. (1983). In vitro and in vivo evaluation of two preparations of activated charcoal as adsorbents of aspirin. *Human Toxicol.* **2,** 211-216.

DeBoer, A. G., and Breimer, D. D. (1994). GI-Tract Absorption Enhancement: general introduction and simulation of time-concentration-effect profiles of absorption enhancers. *In* "Drug Absorption Enhancement: Concepts, Possibilities, Limitations, and Trends", pp. 155-175. Harwood Academic Publishers, Switzerland.

Desai, S. R., Allen, L. V., Greenwood, R. B., Stiles, M. L., and Parker, D. (1989). Effervescent solid dispersions of prednisone, griseofulvin, and primidone. *Drug Dev. Industrial Pharm.* **15**(5), 671-689.

Dong, L., and Hoffman, A. S. (1991). A novel approach for preparation of pH-sensitive hydrogels for enteric drug delivery. *J. Controlled Rel.* **15,** 141-152.

Dowty, M. E. (1991). Transport of thyrotropin releasing hormone in rabbit buccal mucosa in-vitro. Ph.D. University of Wisconsin-Madison.

Dowty, M. E., and Dietsch, C. R. (1996). Improved prediction of in-vivo peroral absorption from in-vitro intestinal permeability using an internal standard to control for inter-rat variability. *Pharm. Res.* **13,** S-329.

Eichman, J. D. (1995). Increased drug absorption through carbonation: assessment of biological membranes. M.S. University of Wisconsin-Madison.

Eichman, J. D., and Robinson, J. R. (1997). The influence of in-vivo carbonation on GI physiological processes and drug permeability. *Eur. J. Pharm. Biopharm.* **44,** 33-38.

Evans, D. F., Pye, G., Bramley, R., Clark, A. G., and Dyson, T. J. (1988). Measurement of gastrointestinal pH profiles in normal ambulant human subjects. *Gut* **29,** 1035-1041.

Fagerholm, U., Johanson, M., and Lennernas, H. (1996). Comparison between permeability coefficients in rat and human jejunum. *Pharm. Res.* **13**(9), 1336-1342.

Feldman, S., Reinhard, M., and Wilson, C. (1973). Effect of sodium taurodeoxycholate on biological membranes: release of phosporus, phospholipid, and protein from everted rat small intestine. *J. Pharm. Sci.* **62,** 1961-1964.

Fine, K. D., Santa Ana, C. A., Porter, J. L., and Fordtran, J. S. (1994). Mechanism by which glucose stimulates the passive absorption of small solutes by the human jejunum in vivo. *Gastrenterol.* **107,** 389-395.

Fischkoff, S., and Vanderkooi, J. M. (1975). Oxygen diffusion in biological membranes determined by the fluorochrome pyrene. *J. Gen. Physiol.* **65,** 663-676.

Fix, J. A. (1996). Oral controlled release technology for peptides: status and future prospects. *Pharm. Res.* **13**(12), 1760-1764.

Flemstrom, G. (1980). Stimulation of HCO3- transport in isolated bullfrog duodenum by prostaglandins. *Am. J. Physiol.* **239,** G198-G203.

Flemstrom, G. (1987). Gastric and duodenal mucosal bicarbonate secretion. *In* "Physiology of the Gastrointestinal Tract" (L. R. Johnson, ed.), pp. 1011-1029. Raven Press, New York, NY.

Flemstrom, G., and Kivilaakso, E. (1983). Demonstration of a pH gradient at the luminal surface of rat duodenum in vivo and its dependence on mucosal alkaline secretion. *Gastroenterol.* **84,** 787-794.

Flynn, G. L., Carpenter, O. S., and Yalkowsky, S. H. (1972). Total mathematical resolution of diffusion layer control of barrier flux. *J. Pharm. Sci.* **61,** 312-314.

Flynn, G. L., and Roseman, T. J. (1971). Membrane diffusion II: influence of physical adsorption on molecular flux through heterogeneous dimethylsiloxane barriers. *J. Pharm. Sci.* **60,** 1788-1796.

Flynn, G. L., and Yalkowsky, S. H. (1972b). Correlation and prediction of mass transport across membranes I: influence of alkyl chain length on flux determining properties of barrier and diffusant. *J. Pharm. Sci.* **61,** 838-852.

Flynn, G. L., Yalkowsky, S. H., and Roseman, T. J. (1974). Mass transport phenomena and models: theoretical concepts. *J. Pharm. Sci.* **63,** 479-510.

Fredericks, W. M., Myagkaya, G. L., Bosch, K. S., Fronik, G. M., von Heen, H., Vogels, I. M. C., and James, J. (1983). The value of enzyme leakage for the protection of necrosis in liver ischemia. *Histochem.* **78,** 459-472.

Frick, H., Leonhardt, H., and Starck, D. (1991). Abdominal Viscera. *In* "Human Anatomy 2", pp. 71-176. Thieme Medical Publishers, Inc., New York, NY.

Fuiji, S., Yokohama, T., Ikegaya, K., Sato, S., and Yohoo, N. (1985). Promoting effect of the new chymotrypsin inhibitor FK-448 on the intestinal absorption of insulin in rats and dogs. *J. Pharm. Pharmacol.* **37,** 545-549.

Gan, L.-S., Hsyu, P.-H., Pritchard, J. F., and Thakker, D. (1993). Mechanism of intestinal absorption of ranitidine and ondansetron: transport across caco-2 cell monolayers. *Pharm. Res.* **10,** 1722-1725.

Ghandehari, H., Smith, P. L., Ellens, H., Yeh, P.-Y., and Kopecek, J. (1997). Size-dependent permeability of hydrophilic probes across rabbit colonic epithelium. *J. Pharm. Exp. Ther.* **280**(2), 747-753.

Goligher, J., Duthie, H., and Nixon, H. (1984). Surgical anatomy and physiology of the anus, rectum, and colon. *In* "Surgery of the Anus, Rectum, and Colon", pp. 1-47. Bailliere Tindall, East Sussex, England.

Grant, R. L., and Acosta, D. (1994). Comparative toxicity of tetracaine, proparacaine, and cocaine evaluated with primary cultures of rabbit corneal epithelial cells. *Exp. Eye Res.* **58,** 469-478.

Gray, H. (1989). Splanchnology. *In* "Gray's Anatomy" (P. L. Williams, R. Warwick, M. Dyson and L. H. Bannister, eds.), pp. 1245-1475. Churchill Livingston, New York, NY.

Gruber, P., Longer, M. A., and Robinson, J. R. (1987). Some biological issues in oral, controlled drug delivery. *Adv. Drug Del. Rev.* **1,** 1-18.

Gupta, P. K., and Robinson, J. R. (1990). Gastric emptying of liquids in the fasted dog. *Inter. J. Pharm.* **43,** 45-52.

Gutknecht, J., Bisson, M. A., and Tosteson, F. C. (1977). Diffusion of carbon dioxide through lipid bilayer membranes. *J. Gen. Physiol.* **69,** 779-794.

Haeberlin, B., and Friend, D. R. (1992). Anatomy and physiology of the gastrointestinal tract: implications for colonic drug delivery. *In* "Oral Colon-Specific Drug Delivery" (D. R. Friend, ed.), pp. 1-44. CRC Press, Boca Raton, FL.

Haeberlin, B., Rubas, W., Nowlen, H. W. I., and Friend, D. R. (1993). In-vitro evaluation of dexamethasone-B-D-glucoronide for colon-specific drug delivery. *Pharm. Res.* **10,** 1553-1562.

Hammel, H. T. (1995). Roles of colloidal molecules in Starling's hypothesis and in returning interstitial fluid to the vasa recta. *Am. J. Physiol.* **268,** H2133-H2144.

Hashida, N., Murakami, M., Yoshikawa, H., Takada, K., and Muranishi, S. (1984). Intestinal absorption of carboxyfluorescein entrapped in liposomes in comparison with its administration with lipid-surfactant mixed micelles. *J. Pharm. Dyn.* **7,** 195-203.

Hastwell, J., Lynch, S., Fox, R., Williamson, I., Skelton-stroud, P., and Mackay, M. (1994). Enhancement of human calcitonin absorption across rat colon in vivo. *Int. J. Pharm.* **101,** 115-120.

Hatlebakk, J. G., and Berstad, A. (1996). Pharmacokinetic optimisation in the treatment of gastro-oesophageal reflux disease. *Clin. Pharmacokinet.* **31,** 386-406.

Helliwell, M., and Berry, D. (1981). Theophylline absorption by effervescent activated charcoal (Medicoal). *J. Int. Med. Res.* **9,** 222-225.

Hespe, W., Verschoor, J. S. C., and Olthoff, M. (1987). Bioavailability of new formulations of amoxicillin in relation to its absorption kinetics. *Arzneim. Forsch./Drug Res.* **37,** 372-375.

Hinder, R. A., and Kelly, K. A. (1977). Canine gastric emptying of solids and liquids. *Am. J. Physiol.* **233,** E335.

Hochman, J., and Artursson, P. (1994). Mechanisms of absorption enhancement and tight junction regulation. *J. Controlled Rel.* **29,** 253-267.

Hoener, B., and Benet, L. Z. (1996). Factors Influencing Drug Absorption and Drug Availability. *In* "Modern Pharmaceutics" (G. S. Banker and C. T. Rhodes, eds.), pp. 121-153. Marcel Dekker, Inc., New York, NY.

Hole Jr., J. W. (1990). Digestive system. 5th ed. *In* "Human Anatomy and Physiology" (E. G. Jaffe, ed.), pp. 513-557. Wm. C. Brown Publishers, Dubuque, IA.

Hollander, D. (1992). The intestinal permeability barrier. A hypothesis as to its regulation and involvement in Chron's disease. *Scand. J. Gastroenterol.* **27,** 721-726.

Hosoya, K., Kubo, H., Natsume, H., Sugibayashi, K., and Morimoto, Y. (1994). Evaluation of enhancers to increase nasal absorption using ussing chamber technique. *Biol. Pharm. Bull.* **17,** 316-322.

Isenberg, J. L., Flemstrom, G., and Johansson, C. (1983). Mucosal bicarbonate secretion is significantly greater in the proximal versus distal duodenum in the in vivo rat. *In* "Mechanisms of Mucosal Protection in the Upper Gastrointestinal Tract" (A. Allen, G. Flemstrom, A. Garner, W. Silen and L. A. Turnberg, eds.), pp. 175-180. Raven Press, New York, NY.

Jost, W. (1960). "Diffusion in Solids, Liquids, Gases." Academic Press, Inc., New York, NY.

Junqueira, L. C., Carneiro, J., and Kelly, R. O. (1989). Digestive tract. *In* "Basic Histology" (C. Langan, ed.), pp. 282-310. Appleton and Lange, Norwalk, CT.

Karino, A., Masahiro, H., Awazu, S., and Hanano, M. (1982). Solvent drag effect in drug intestinal absorption. II. Studies on drug absorption clearance and water influx. *J. Pharm. Dyn.* **5,** 670-677.

Keljo, D. J., and Hamilton, J. R. (1983). Quantitative determination of amcromolecular transport rate across intestinal Peyer's patches. *Am. J. Physiol.* **244,** G637-G644.

Kim, Y.-H., Bae, Y. H., and Kim, S. W. (1994). pH/Temperature-sensitive polymers for macromolecular drug loading and release. *J. Controlled Rel.* **28,** 143-152.

Kitazawa, S., Ito, H., Johno, I., Takahashi, T., and Takenaka, H. (1978). Generality in effects of transmucosal fluid movement and glucose on drug absorption from the rat small intestine. *Chem. Pharm. Bull.* **26,** 915-924.

Kitazawa, S., Ito, H., and Sekaki, H. (1975). Transmucosal fluid movement and its effect on drug absorption. *Chem. Pharm. Bull.* **23,** 1856-1865.

Kivilaakso, E., and Flemstrom, G. (1984). HCO3- secretion and surface pH gradient in rat duodenum exposed to luminal acid. *Scand. J. Gastroenterol. Suppl.* **19,** 51-54.

Kleinman, R. E., and Walker, W. A. (1989). The development of barrier function of the gastrointestinal tract. *Acta Paediatr. Scand. Suppl.* **351,** 34-37.

Knuth, K., Amiji, M., and Robinson, J. R. (1993). Hydrogel delivery systems for vaginal and oral applications: formulation and biological considerations. *Adv. Drug Del. Rev.* **11,** 137-167.

Konturek, S. J., Tasler, J., Bilski, J., and Kania, J. (1983). Prostaglandins and alkaline secretion from oxuntic, antral, and duodenal mucosa of the dog. *Am. J. Physiol.* **245,** G539-G546.

Kopecek, J., Kopeckova, P., Brondsted, H., Rathi, R., Rihova, B., Yeh, P.-Y., and Ikesue, K. (1992). Polymers for colon-specific drug delivery. *J. Controlled Rel.* **19,** 121-130.

Kristensen, R. (1994). Mechanisms of cell damage and enzyme release. *Danish Med. Bull.* **41,** 423-433.

Krugliak, P., Hollander, D., and Ma, T. Y. (1989). Mechanisms of polyethylene glycol 400 permeability in perfused rat intestine. *Gastroenterol.* **97,** 1164-1170.

Lane, M. E., O'Driscoll, C. M., and Corrigan, O. I. (1996). The relationship between rat intestinal permeability and hydrophilic probe size. *Pharm. Res.* **13**(10), 1554-1558.

Lappalainen, K., Jaaskelainen, I., Syrjanen, K., Urtti, A., and Syrjanen, S. (1994). Comparison of cell proliferation and toxicity assays using two cationic liposomes. *Pharm. Res.* **11,** 1127-1131.

LeCluyse, E. L., Appel, L. E., and Sutton, S. C. (1991). Relationship between drug absorption enhancing activity and membrane perturbing effects of acylcarnitines. *Pharm. Res.* **8,** 84-87.

LeCluyse, E. L., Sutton, S. C., and Fix, J.A. (1993). In-vitro effects of long-chain acylcarnitines on the permeability, transepithelial electrical resistance and morphology of rat colonic mucosa. *J. Pharm. Exp. Ther.* **265,** 955-962.

Lee, V. H. L. (1986). Enzymatic barriers to peptide and protein absorption and the use of penetration enhancers to modify absorption. *In* "Delivery Systems for Peptide Drugs" (S. S. Davis, L. Illum and E. Tomlinson, eds.), pp. 87. Plenum Press, New York, NY.

Lee, V. H. L. (1990). Protease inhibitors and penetration enhancers as approaches to modify peptide absorption. *J. Controlled Release* **13,** 213-223.

Lee, V. H. L. (1991b). Protease inhibitors and penetration enhancers as approaches to modify peptide absorption. *J. Controlled Release* **13,** 213-223.

Lee, V. H. L., Dodda-Kashi, S., Grass, G. M., and Rubas, W. (1991a). Oral Route of Peptide and Protein Drug Delivery. *In* "Peptide and Protein Drug Delivery" (V. H. L. Lee, ed.), pp. 691-738. Marcel Dekker, Inc., New York, NY.

Lee, V. H. L., Yamamoto, A., and Kompella, U. B. (1991c). Mucosal penetration enhancers for facilitation of peptide and protein drug absorption. *Crit. Rev. Ther. Drug Carrier Syst.* **8,** 91-192.

Lehr, C.-M., Bouwstra, J. A., deBoer, A. G., Verhoef, J. C., Breimer, D. D., and Junginger, H. E. (1992). Intestinal Bioadhesive Drug Delivery Systems. *In* "Drug Targeting and Delivery: concepts in dosage form design" (H. E. Junginger, ed.), pp. 92-100. Ellis Horwood, New York, NY.

Lennernäs, H. (1995). Does fluid flow across intestinal mucosa affect quantitative oral drug absorption? Is it time for a reevaluation? *Pharm. Res.* **12**(1573-1582).

Lennernäs, H., Ahrenstedt, O., and Ungell, A.-L. (1994). Intestinal drug absorption during induced net water absorption in man; a mechanistic study using antipyrine, atenolol and enalaprilat. *Br. J. Clin. Pharmacol.* **37,** 589-596.

Lennernäs, H., Nylander, S., and Ungell, A.-L. (1997). Jejunal permeability: a comparison between the ussing chamber technique and the single-pass perfusion in humans. *Pharm. Res.* **14**(5), 667-671.

Liaw, J., Rubenstein, A., and Robinson, J. R. (1990). Bioavailability study of Theo-Dur tablets in the fasted cannulated dog. *Inter. J. Pharm.* **59,** 105-114.

Lindner, H. H. (1989). The Stomach. *In* "Clinical Anatomy" (H. H. Lindner, ed.), pp. 326-339. Appleton and Lange, Norwalk, CT.

Loehry, C. A., Kingham, J., and Baker, J. (1973). Small intestinal permeability in animals and man. *Gut* **11,** 683-688.

Lonnerholm, G., Knutson, L., Wistrand, P. J., and Flemstrom, G. (1989). Carbonic anhydrase in the normal rat stomach and duodenum and after treatment with omeprazole and ranitidine. *Acta Physiol. Scand.* **136,** 253-262.

Luckow, V., Krammer, R., and Traub, R. (1992). Vergleichende bioverfugbarkeitsuntersuchung zweier verschiedener ibuprofen-granulate. *Arzneim.Forsch/Drug Res.* **42,** 1339-1342.

Ma, T. Y., Hollander, D., Bhalla, D., Nguyen, H., and Krugliak, P. (1992). IEC-18, a nontransformed small intestinal cell linefor studying epithelial permeability. *J. Lab Clin. Med.* **120,** 329-341.

Ma, T. Y., Hollander, D., Krugliak, P., and Katz, K. (1990). PEG 400, a hydrophilic probe for measuring intestinal permeability. *Gastroenterol.* **98,** 39-46.

Ma, T. Y., Hollander, D., Riga, R., and Bhalla, D. (1993). Autoradiographic determination of permeation pathway of permeability probes across intestinal and tracheal epithelial. *J. Lab Clin. Med.* **122,** 590-600.

Madara, J. L. (1983). Increases in guinea pig small intestinal transepithelial resistance induced by osmotic loads are accompanied by rapid alterations in absorptive-cell tight-junction structure. *J. Cell Biol.* **97,** 125-136.

Madara, J. L., and Dharnsathaphorn, K. (1985). Occluding junction structure-function relationships in a cultured epithelial monolayer. *J. Cell Biol.* **101,** 2124-2133.

Madara, J. L., and Pappenheimer, J. R. (1987). Structural basis for physiological regulation of paracellular pathways in intestinal epithelia. *J. Membrane Biol.* **100,** 149-164.

Madara, J. L., and Trier, J. S. (1994). The functional morphology of the mucosa of the small intestine. *In* "Physiology of the Gastrointestinal Tract" (L. R. Johnson, ed.), pp. 1577-1622. Raven Press, New York, NY.

Marieb, E. N., and Mallatt, J. (1997). The Digestive System. *In* "Human Anatomy" (J. Schmid, ed.), pp. 561-599. Benjamin/Cummings, Menlo Park, CA.

Martin, G. P., Marriott, C., and Kellaway, I. W. (1989). Direct effect of bile salts and phospholipids on the physical properties of mucus. *Gut* **19,** 103-107.

Martinez-Palomo, A., and Erlij, D. (1975). Structure of tight junctions in epithelia with different permeability. *Proc. Nat. Acad. Sci.* **11,** 4487-4491.

Mayersohn, M. (1996). Principles of Drug Absorption. 3rd ed. *In* "Modern Pharmaceutics" (G. S. Banker, ed.), pp. 21-72. Marcel Dekker, Inc., New York, NY.

McMinn, R. M. H., and Hobdell, M. H. (1974). Small intestine. *In* "Functional Anatomy of the Digestive System", pp. 151-168. Sir Isaac Pitman and Sons, Ltd., Nairobi, Kenya.

Menzel, V. S., Geiblinger, G., and Brune, K. (1993). Frei verkaufliche analgetika im vergleich. *Deutsche Apotheker Zeitung* **133,** 17-20.

Meyer, W. M. (1897). U.S. Patent.

Mohrle, R. (1985). *Pharm Tech Conference.*

Morrow, J. S., and Anderson, R. A. (1986). Shaping the too fluid bilayer. *Lab Invest.* **54,** 237-240.

Mossman, T. (1983). Rapid colorimetric assay for cellular growth and survival: application to proliferation and cytotoxicity assays. *J. Immunol. Methods* **65,** 55-64.

Mrsny, R. J. (1992). Drug absorption in the colon: a critical review. *In* "Oral Colon-Specific Drug Delivery" (D. R. Friend, ed.), pp. 45-84. CRC Press, Boca Raton, FL.

Munck, B. G., and Rasmussen, S. N. (1977). Paracellular permeability of extracellular space markers across rat jejunum in vitro. Indication of transepithelial fluid circuit. *J. Physiol. (Lond.)* **271,** 473-488.

Muranishi, S. (1985). Modification of intestinal absorption of drugs b lipoidal adjuvants. *Pharm. Res.*, 108-118.

Muranishi, S. (1990). Absorption enhancers. *Crit. Rev. Ther. Drug Carrier Syst.* **7,** 1-33.

Muranishi, S. (1991). *Capsugel Symposia Series, Greenwood, SC.*

Muranishi, S., Muranushi, N., and Sczaki, H. (1979). Improvement of absolute bioavailability of normally poorly absorbed drugs: inducement of the intestinal absorption of streptomycin and gentamycin by lipid-bile salt mixed micelles in rat and rabbit. *Int. J. Pharm.* **2,** 101-111.

Murphy, D. R. (1962). U.S. Patent.

Nadai, T., Kondo, R., Tatematsu, A., and Sezaki, H. (1972). Drug-induced histological changes and its consequences on the permeability of the small intestinal mucosa. I. EDTA, tetracycline and sodium laurylsulfate. *Chem. Pharm. Bull.* **20,** 1139-1144.

Nakanishi, K., Masada, M., and Nadai, T. (1983). Effect of pharmaceutical adjuvants on the rectal permeability of drugs. III. Effect of repeated administration and recovery of the permeability. *Chem. Phar. Bull.* **31,** 4161-4166.

Nakanishi, K., Masada, M., and Nadai, T. (1984). Effect of pharmaceutical adjuvants on the rectal permeability to drugs. IV. Effect of pharmaceutical adjuvants on the rectal permeability to macromolecular compounds in the rat. *Chem. Pharm. Bull.* **32,** 1628-1632.

Nilsson, D., Fagerholm, U., and Lennernas, H. (1994). The influence of net water absorption on the permeability of antipyrine and levodopa in the human jejunum. *Pharm. Res.* **11,** 1540-1544.

Nishihata, T., Rytting, J. H., and Huguchi, T. (1981). Effects of salicylate on rectal absorption of theophylline. *J. Pharm. Sci.* **70,** 71-75.

Nishimura, K., Sasahara, K., Arai, M., Nitanai, T., Ikegami, Y., Morioka, T., and Nakajima, E. (1984). Dosage form design for improvement of bioavailability of levodopa VI: formulation of effervescent enteric-coated tablets. *J. Pharm. Sci.* **73**(7), 942-946.

Noach, A. B. J., Kurosaki, Y., Blom-Roosemalen, M. C. M., de Boer, A. G., and Breimer, D. D. (1993). Cell-polarity dependent effect of chelation on the paracellular permeability of confluent caco-2 cell monolayers. *Inter. J. Pharm.* **90,** 229-237.

Noach, A. B. J., Sakai, M., Blom-Roosemalen, M. C. M., de Jonge, H. R., de Boer, A. G., and Breimer, D. D. (1994). Effect of anisotonic conditions on the transport of hydrophilic model compounds across monolayers of colonic cell lines. *J. Pharmacol. Exper. Ther.* **270,** 1373-1380.

Nuernberg, B., and Brune, K. (1989). Buffering the stomach content enhances the absorption of diflunisal in man. *Biopharm. Drug Disposition* **10,** 377-387.

Ochsenfahrt, H., and Winne, D. (1973). The contribution of solvent drag to the intestinal absorption of tritiated water and urea from the jejunum of the rat. *Naunyn-Schmiedeberg's Arch. Pharmacol.* **279,** 133-152.

Ochsenfahrt, H., and Winne, D. (1974a). The contribution of solvent drag to the intestinal absorption of the acidic drugs benzoic acid and salicylic acid from the jejunum of the rat. *Naunyn-Schmiedeberg's Arch. Pharmacol.* **281,** 197-217.

Ochsenfahrt, H., and Winne, D. (1974b). The contribution of solvent drag to the intestinal absorption of the basic drugs amidopyrine and antipyrine from the jejunum of the rat. *Naunyn-Schmiedeberg's Arch. Pharmacol.* **281,** 175-196.

Ohnishi, S. T., and Barr, J. K. (1978). A simplified method of quantitating proteins using the biuret and phenol reagents. *Anal. Biochem.* **86,** 193.

Ormezzano, X., Francois, T. P., Viaud, J.-Y., Bukowski, J.-G., Bourgeonneau, M.-C., Cottron, D., Ganansia, M.-F., Gregoire, F. M., Grinand, M. R., and Wessel, P. E. (1990). Aspiration pneumonitis prophylaxis in obstetric anaesthesia: comparison of effervescent cimetidine-sodium citrate mixture and sodium citrate. *Br. J. Anaesth.* **64,** 503-506.

Orton, R. (1978). Ergotamine tartrate levels using radioimmunoassay. *In* "Current Concepts in Migrane Research" (R. Green, ed.), pp. 79-84. Raven Press, New York, NY.

Pappenheimer, J. R. (1987). Physiological regulation of transepithelial impedance in the intestinal mucosa of rats and hamsters. *J. Membr. Biol.* **100,** 137-148.

Parr, A. (1997). *39th Annual International Industrial Pharmaceutical Research and Development Conference, Merrimac, WI.*

Pellicciari, R., Garzon-Aburbeh, A., Natalini, B., and Marinozzi, M. (1993). Brush-border-enzyme-mediated intestine-specific drug delivery. Amino acid prodrugs of 5-aminosalicylic acid. *J. Med. Chem.* **36,** 4201-4207.

Petersen, T., Husted, S. E., Pedersen, A. K., and Geday, E. (1982). Systemic availability of acetylsalicylic acid in human subjects after oral ingestion of three different formulations. *Acta Pharmacol. et Toxicol.* **51,** 285-291.

Powell, D. W. (1981). Barrier function of epithelia. *Am. J. Physiol.* **241G,** G275-G288.

Propst, A., Propst, T., and Judmaier, G. (1996). Comparison of the effects of ranitidine effervescent tablets and magnesium hydroxide-aluminum oxide on intragastric acidity. *Arzneim. Forsch.* **46,** 621-624.

Pujara, C. P., Shao, Z., Duncan, M. R., and Mitra, A. K. (1995). Effects of formulation variables on nasal epithelial cell integrity: biochemical marker evaluations. *Inter. J. Pharm.* **114,** 197-203.

Rahman, A., Barrowman, J. A., and Rahimtula, A. (1986). The influence of bile on the bioavailability of polynuclear aromatic hydrocarbons from the rat intestine. *Can. J. Physiol. Pharmacol.* **64,** 1214-1218.

Ranade, V. V. (1991). Drug Delivery Systems 5A. Oral Drug Delivery. *J. Clin. Pharmacol.* **31,** 2-16.

Ranade, V. V., and Hollinger, M. A. (1996). Oral Drug Delivery. *In* "Drug Delivery Systems" (V. V. Ranade and M. A. Hollinger, eds.), pp. 127-173. CRC Press, New York, NY.

Rechkemmer, G., Wahl, M., Kuschinsky, W., and von Engelhardt, W. (1986). pH microclimate at the luminal surface of the intestinal mucosa of guinea pig and rat. *Pflugers Arch.* **407,** 33-40.

Ritschel, W. A. (1991). Targeting in the gastrointestinal tract: new approaches. *Meth. Find. Exp. Clin. Pharmacol.* **13**(5), 313-336.

Rowland, M., and Tozer, T. N. (1995). Estimation of absorption kinetics from plasma concentration data. 3rd ed. *In* "Clinical Pharmacokinetics: Concepts and Applications" (D. Balado, ed.), pp. 478-482. Williams & Wilkins, Baltimore, MD.

Rubas, W., Cromwell, M. E. M., Shahrokh, Z., Villagran, J., Nguyen, T.-N., Wellton, M., Nguyen, T.-H., and Mrsny, R. (1996). Flux measurements across Caco-2 monolayers may predict transport in human large intestinal tissue. *J. Pharm. Sci.* **85**(2), 165-169.

Rubas, W., and Grass, G. (1991). Gastrointestinal lymphatic absorption of peptides and proteins. *Adv. Drug Del. Rev.* **7,** 15-69.

Rubin, C. E., and Saunders, D. R. (1987). The small bowel. *In* "The Gut" (R. F. Barreras, ed.), pp. 86-137. University of Wisconsin, Madison, WI.

Sawada, T., Ogawa, T., Tomita, M., Hayashi, M., and Awazu, S. (1991). Role of paracellular pathway in nonelectrolyte permeation across rat colon epithelium enhanced by sodium caprate and sodium caprylate. *Pharm. Res.* **8,** 1365-1371.

Schmidt, E., and Schmidt, F. W. (1987). Enzyme release. *J. Clin. Chem. Clin. Biochem.* **25,** 525-540.

Schoenwald, R. D., and Ward, R. L. (1978). Relationship between steroid permeability across excised rabbit cornea and octanol/water partition coefficients. *J. Pharm. Sci.* **67**(6), 786-788.

Seeley, R. R., Stephens, J. D., and Tate, P. (1996). The Digestive System. 2nd ed. *In* "Essentials of Anatomy and Physiology" (J. M. Smith, ed.), pp. 425-429. Mosby-Year Book, Inc., St. Louis, MO.

Selling, J. A., Hogan, D. L., Koss, M. A., and Isenberg, J. I. (1985). Human proximal versus distal duodenal bicarbonate secretion: effect of endogenous prostaglandin synthesis. *Gastroenterol.* **88,** 1388.

Sendall, F. E. J., Staniforth, J. N., Rees, J. E., and Leatham, M. J. (1983). Effervescent tablets. *Pharm. J.* **230,** 289-294.

Shargel, L. (1993). Pharmacokinetics of drug absorption. 3rd ed. *In* "Applied Biopharmaceutics and Pharmacokinetics" (C. L. Mehalik, ed.), pp. 169-192. Appleton & Lange, Norwalk, CT.

Shiga, M., Hayashi, M., Horie, T., and Awazu, S. (1987). Difference in the promotion mechanism of the colonic absorption of antipyrene, phenol-red and cefmetazole. *J. Pharm. Pharmacol.* **39,** 118.

Shiga, M., Muraoka, T., Hirasawa, T., Hayashi, M., and Awazu, S. (1985). The promotion of rectal drug absorption by water absorption. *J. Pharm. Pharmacol.* **37,** 446.

Simon, S. A., and Gutknecht, J. (1980). Solubility of carbon dioxide in lipid bilayer membranes and organic solvents. *Biochim. Biophys. Acta* **596,** 352-358.

Simson, J. N. L., Merhav, A., and Silen, W. (1981). Alkaline secretion by amphibian duodenum. III. Effects of DBcAMP, theophylline and prostaglandins. *Am. J. Physiol.* **241,** G528-G536.

Singer, S. J. (1990). The structure and insertion of integral proteins in membranes. *Ann. Rev. Cell Biol.* **6,** 247-296.

Smith, P. L., Wall, D. A., Gochoco, C. H., and Wilson, G. W. (1992). Routes of delivery: Case studies (5) oral absorption of peptides and proteins. *Adv. Drug Del. Rev.* **8,** 253-290.

Spring, K. R. (1991). Mechanism of Fluid Transport by Epithelia. *In* "The Gastrointestinal System" (B. B. Rauner, ed.), pp. 195-207. American Physiological Society, Bethesda, MD.

Stein, W. D. (1986). Physical Basis of Movement across Cell Membranes. *In* "Transport and Diffusion across Cell Membranes", pp. 1-68. Academic Press, Inc., New York, NY.

Stein, W. D. (1986b). "Transport and Diffusion Across Cell Membranes." Academic Press, Inc., New York, NY.

Stewart, H. C. (1990). Drug Absorption, Action and Disposition. 18th ed. *In* "Remington's Pharmaceutical Sciences" (A. R. Gennaro, ed.), pp. 697-724. Mack Publishing Co., Easton, PA.

Stratford, R. E., Jr., and Lee, V. H. L. (1985). Aminopeptidase activity in albino rabbit extraocular tissues relative to the small intestine. *J. Pharm. Sci.* **74,** 731-734.

Stratford, R. E., Jr., and Lee, V. H. L. (1986). Aminopeptidase activity in homogenates of various absorptive mucosae in the albino rabbit: implications in peptide delivery. *Int. J. Pharm.* **30,** 73-82.

Strom, M., Madsen, S., and Norlander. (1991). Intragastric pH rise with effervescent citrate-cimetidine. *Lancet* **337,** 433.

Suzuka, T., Furuya, A., Kamada, A., and Nishihata, T. (1987). Effect of phenothiazines, disodium ethylenediaminetetraacetic acid and diethyl maleate on in vitro rat colonic transport of cefmetazole and inulin. *J. Pharmacobiodyn.* **10,** 63-71.

Swenson, E. S., Milisen, W. B., and Curatolo, W. (1994). Intestinal permeability enhancement: efficacy, acute local toxicity, and reversibility. *Pharm. Res.* **11,** 1132-1142.

Taylor, A. S. (1871). U.S. Patent.

Thompson, D. O. (1997). Cyclodextrins-enabling excipients: their present and future use in pharmaceuticals. *Crit. Rev. Ther. Drug Carrier Syst.* **14**(1), 1-104.

Tomita, M., Hayashi, M., and Awazu, S. (1995). Absorption-enhancing mechanism of sodium caprate and decanoylcarnitine in caco-2 cells. *J. Pharmacol. Exp. Ther.* **272,** 739-743.

Van de Graaff, K. M., and Fox, S. I. (1995). Digestive System. 4th ed. *In* "Concepts of Human Anatomy and Physiology" (H. Wheatley, ed.), pp. 764-810. WCB Publishers, Dubuque, IA.

Van Deurs, B., and Luft, J. H. (1979). Effects of gluteraldehyde fixation on the structure of tight junctions. *J. Ultrastruc.* **68,** 160-172.

Van Elburg, R. M., Uil, J. J., De Monchy, J. G. R., and Heymans, H. S. A. (1992). Intestinal permeability in pediatric gastroenterology. *Scand. J. Gastroenterol. Suppl.* **27,** 19-24.

van Hoogdalen, E. J., deBoer, A. G., and Breimer, D. D. (1989). Intestinal drug absorption enhancement: an overview. *Pharm. Ther.* **44,** 407-443.

van Os, C. H., Deen, P. M. T., and Dempster, J. A. (1994). Aquaporins: water selective channels in biological membranes. Molecular structure and tissue distribution. *Biochim. Biophys. Acta* **1197,** 291-309.

Viel, C. (1994). Effervescent baths and mercurial fumigations of Guietand, a Paris, pharmacist. *Revue D'Histoire de la Pharmacie* **41,** 149-154.

Wagner, J. G. (1995). "Fundamentals of Clinical Pharmacokinetics." Drug Intelligence Publications, Inc., Hamilton, IL.

Wang, L., Toledo-Velasquez, D., Schwegler-Berry, D., Ma, J. K. H., and Rojanasakul, Y. (1993). Transport and hydrolysis of enkephalins in cultured alveolar epithelial monolayers. *Pharm. Res.* **10,** 1662-1667.

Wang, W. (1996). Oral protein drug delivery. *J. Drug Targeting* **4**(4), 195-232.

Watson, R. G. P., Johnston, B. T., Tham, T. C. K., and Kersey, K. (1996). Effervescent and standard formulations of ranitidine - a comparison of their pharmacokinetics and pharmacology. *Aliment Pharmacol. Ther.* **10,** 913-918.

Webber, J., and Ducrotte, P. (1987). Colonic motility in health and disease. *Dig. Dis.* **5,** 1-12.

Whitmore, D. A., Brooks, L. G., and Wheeler, K. P. J. (1979). Relative effects of different surfactants on intestinal absorption and release of proteins and phospholipids from the tissue. *J. Pharm. Pharmacol.* **31,** 277-283.

Woodley, J. F. (1992). Peptidase enzymes of the gastrointestinal tract: barriers to peptide delivery, but potential for controlled release. *Proc. Int. Symp. Controlled Rel. Bioact. Mater.* **19,** 2-3.

Yamamato, A., Taniguchi, T., Rikyuu, K., Tsuji, T., Fujita, T., Murakami, M., and Muranishi, S. (1994). Effects of various protease inhibitors on the intestinal absorption and degradation of insulin in rats. *Pharm. Res.* **11,** 1496-1500.

Yamashita, S., Saitoh, H., Nakanishi, K., Masada, M., Nadai, T., and Kimura, T. (1985). Characterization of enhanced intestinal permeability; electrophysiological study on the effects of diclofenac and ethylenediaminetetraacetic acid. *J. Pharm. Pharmacol.* **37,** 512-513.

Yassin, A. E. B. (1996). Optimization of the biological availability of certain medicament. Ph.D. thesis. Al-Azhar University.

Yeagle, P. L. (1985). Cholesterol and the cell membrane. *Biochim. Biophys. Acta.* **822,** 267-287.